ЖУРНАЛ
ПРИКЛАДНОЙ ХИМИИ

JOURNAL OF APPLIED CHEMISTRY OF THE USSR

(ZHURNAL PRIKLADNOI KHIMY)

IN ENGLISH TRANSLATION

VOL. 30

NO. 1

CONSULTANTS BUREAU, INC.

227 WEST 17TH STREET, NEW YORK 11, N. Y.

an agency for the interpretation of international knowledge

4 MORE RUSSIAN JOURNALS NOW IN ENGLISH TRANSLATION

DOKLADY SECTIONS

PHYSICAL CHEMISTRY, BIOCHEMISTRY
GEOLOGICAL SCIENCES, APPLIED PHYSICS

IMMEDIATELY AVAILABLE — SUBSCRIPTIONS BEGIN WITH THE 1957 VOLUMES

Doklady (Proceedings of the Academy of Sciences of the USSR) contains concise reports by leading Soviet scientists. It offers a comprehensive survey of the most advanced Soviet research.

Physical Chemistry—Approx. 500 pages per year. Includes all reports on chemical kinetics, interface phenomena, electrochemistry, absorption spectra, and related subjects.
Single issues, $35.00 — 6 issues per year, $160.00

Biochemistry—Approx. 150 pages per year. Covers plant and animal biochemistry.
Single issues, $15.00 — 6 issues per year, $65.00

Geological Sciences—Approx. 750 pages per year. Covers geology, hydrogeology, mineralogy, petrography, and geophysics.
Single issues, $40.00 — 6 issues per year, $200.00

Applied Physics—Approx. 600 pages per year. Includes all reports on crystallography, electrotechnics, hydraulics, hydromechanics, mechanics, theory of elasticity, and related subjects.
Single issues, $40.00 — 6 issues per year, $200.00

Individual articles are $5.00 each — Tables of Contents on request

Cover-to-cover translations by **bilingual scientists,** including all diagrams, photographs, and tabular material. Journals are staple bound in durable paper covers; clear multilith reproduction from IBM "cold type." Doklady is published in 36 issues annually—Consultants Bureau's English translation is published in 6. Issues are mailed to subscribers immediately upon publication.

For free catalogs of our current Russian translations, including 28 Soviet journals, write to Dept. S, specifying field of interest.

CONSULTANTS BUREAU, INC.

227 WEST 17th STREET, NEW YORK 11, N. Y. — U.S.A.

Telephone: ALgonquin 5-0713 • Cable Address: CONBUREAU, NEW YORK

JOURNAL OF APPLIED CHEMISTRY OF THE USSR

(ZHURNAL PRIKLADNOI KHIMII)

Volume XXX, No. 1

January, 1957

(A Publication of the Academy of Sciences of the USSR)

IN ENGLISH TRANSLATION

Copyright, 1958

CONSULTANTS BUREAU, INC.

227 West 17th Street

New York 11, N.Y.

Printed in the United States

	Domestic	Foreign
Annual Subscription	$60.00	$65.00
Annual Subscription for non-profit research or academic institutions	20.00	25.00
Single Issue	7.50	

Note: The sale of photostatic copies of any portion of this copyright translation is expressly prohibited by the copyright owners.

SIGNIFICANCE OF ABBREVIATIONS MOST FREQUENTLY ENCOUNTERED IN SOVIET PERIODICALS

FIAN	Phys. Inst. Acad. Sci. USSR.
GDI	Water Power Inst.
GITI	State Sci.-Tech. Press
GITTL	State Tech. and Theor. Lit. Press
GONTI	State United Sci.-Tech. Press
Gosenergoizdat	State Power Press
Goskhimizdat	State Chem. Press
GOST	All-Union State Standard
GTTI	State Tech. and Theor. Lit. Press
IL	Foreign Lit. Press
ISN (Izd. Sov. Nauk)	Soviet Science Press
Izd. AN SSSR	Acad. Sci. USSR Press
Izd. MGU	Moscow State Univ. Press
LEIIZhT	Leningrad Power Inst. of Railroad Engineering
LET	Leningrad Elec. Engr. School
LETI	Leningrad Electrotechnical Inst.
LETIIZhT	Leningrad Electrical Engineering Research Inst. of Railroad Engr.
Mashgiz	State Sci.-Tech. Press for Machine Construction Lit.
MEP	Ministry of Electrical Industry
MES	Ministry of Electrical Power Plants
MESEP	Ministry of Electrical Power Plants and the Electrical Industry
MGU	Moscow State Univ.
MKhTI	Moscow Inst. Chem. Tech.
MOPI	Moscow Regional Pedagogical Inst.
MSP	Ministry of Industrial Construction
NII ZVUKSZAPIOI	Scientific Research Inst. of Sound Recording
NIKFI	Sci. Inst. of Modern Motion Picture Photography
ONTI	United Sci.-Tech. Press
OTI	Division of Technical Information
OTN	Div. Tech. Sci.
Stroiizdat	Construction Press
TOE	Association of Power Engineers
TsKTI	Central Research Inst. for Boilers and Turbines
TsNIEL	Central Scientific Research Elec. Engr. Lab.
TsNIEL-MES	Central Scientific Research Elec. Engr. Lab.—Ministry of Electric Power Plants
TsVTI	Central Office of Economic Information
UF	Ural Branch
VIESKh	All-Union Inst. of Rural Elec. Power Stations
VNIIM	All-Union Scientific Research Inst. of Meteorology
VNIIZhDT	All-Union Scientific Research Inst. of Railroad Engineering
VTI	All-Union Thermotech. Inst.
VZEI	All-Union Power Correspondence Inst.

Note: Abbreviations not on this list and not explained in the translation have been transliterated, no further information about their significance being available to us. — Publisher.

HYDROMETALLURGICAL PROCESSES AT HIGH PRESSURES*

F. A. Forward** and J. Halpern***

Hydrometallurgical processes have long been used in the treatment of certain ores. Well-known examples of such processes are the cyanidation of gold and silver, acid and carbonate leaching of uranium and vanadium, and the Baeyer process for extraction of aluminum oxide from bauxite by means of caustic soda solutions. Hydrometallurgical processes are, in general, used with low-grade ores which cannot be treated directly by other chemical methods and which are not readily amenable to mechanical concentration.

The older hydrometallurgical processes, such as those mentioned above, are still being widely used. In recent years, however, there has been a markedly increasing interest in hydrometallurgical treatment of ores, reflected in intensive development of research in this field and in the development and application of certain new hydrometallurgical processes of industrial interest [1-7]. Among the factors which have assisted in the development of this trend are: 1) the great attention paid to the utilization of low-grade ores which are not easily amenable to other methods of treatment; 2) the development of the production of new flocculating agents which have helped to overcome settling and filtration problems, highly important in the technology of hydrometallurgical processes; 3) the development of radically new techniques, such as ion exchange and solvent extraction of valuable metals for recovery; and 4) the introduction into hydrometallurgical practice of high-temperature and high-pressure techniques, with the aid of which entirely new results and considerable improvements in existing hydrometallurgical processes can be achieved. The present paper is mainly concerned with this last question and with a review of the recent achievements in the hydrometallurgical field, including high-pressure techniques. The obvious advantages provided by such techniques include:

1. The possibility of the use of temperatures above the normal boiling points of solutions.

2. The creation of favorable shifts in thermodynamic equilibria and especially in the kinetics of many reactions, and the use of conditions which increase productivity and make possible numerous processes which do not take place at ordinary temperatures and pressures.

3. By increase of partial pressures it is possible to obtain high concentrations of gaseous or highly volatile reagents in aqueous solutions, ensuring their efficient utilization. Hydrometallurgical processes often involve oxidation and reduction reactions in aqueous solutions, and owing to the introduction of high-pressure techniques such reactions can now be carried out with the use of atmospheric oxygen or gaseous hydrogen, respectively. Thus, these gases, and also certain volatile substances such as ammonia, have become valuable metallurgical reagents.

---

* This paper is to be published in February of this year in London in the Bulletin of the Institution of Mining and Metallurgy.

** Professor and Head, Department of Mining and Metallurgy, University of British Columbia, Vancouver, Canada.

*** Professor in the Department of Mining and Metallurgy, University of British Columbia, Vancouver, Canada.

Because of the advantages which the use of high temperatures and pressures confer, these conditions have long been used in a number of other branches of the chemical industry, particularly those concerned with the production and processing of organic compounds. However, their value in hydrometallurgical processes has been recognized, and their extensive application in this field commenced, only recently.

Thermodynamic and Kinetic Factors which Influence Hydrometallurgical Processes

With the aid of thermodynamics it is possible to define equilibrium in a chemical system and to predict the direction in which the equilibrium will shift with variations of such conditions as temperature, pressure, concentration, etc. In general, an increase in the concentrations or partial pressures of the reactants shifts the equilibrium in the forward direction, while an increase in the concentrations of the reaction products has the opposite effect. If the reactants or reaction products are gases or highly volatile compounds, the influence of pressure on the thermodynamics of the process becomes obvious.

The thermodynamics of a large number of systems of interest in hydrometallurgy have been studied by Pourbaix and his associates and graphically represented by them in the form of "potential—pH" diagrams. Such diagrams have been published for the metals: copper, iron, chromium [8, 9], silver [10, 11], zinc [12], lead [13], aluminum, arsenic, gold, beryllium, cadmium, cobalt, mercury, selenium, tin, titanium, thallium [14], and sulfur [15]. In addition to other data, these diagrams show under what conditions various oxidation and reduction reactions can be effected with the use of gaseous oxygen or hydrogen respectively, and the extent to which these reactions become more favorable thermodynamically with increasing pressure.

Since reaction rates at elevated temperatures are usually high and equilibria are established rapidly, pyrometallurgical processes are most often limited by thermodynamic conditions. On the other hand, hydrometallurgical operations, and especially leaching reactions, are carried out in conditions which are extremely favorable from the thermodynamic standpoint (i.e, there is a large release of free energy in the desired process) and the limitations arise mainly from the kinetic aspects. In particular, if the thermodynamic conditions of several alternative reactions, leading to the formation of different products, do not differ appreciably, then the formation of a particular product is often determined by kinetic factors. The kinetics of a reaction and its mechanism are closely associated and therefore, an understanding of the latter is of great practical and theoretical importance. Unfortunately, such understanding has been achieved only for very few hydrometallurgical systems.

Most hydrometallurgical processes, irrespective of whether they involve leaching or precipitation, included heterogeneous reactions at a solid—liquid interface; and, apart from a few special cases, such reactions determine the rate of the process. Most of the heterogeneous reactions of interest in such processes consist of the following consecutive stages:

1. Absorption of gaseous reactants (if present) by the solution.
2. Transport of the dissolved reactants from the bulk of the solution to the solid—solution interface.
3. Reaction on the surface (including adsorption and desorption stages).
4. Transport of the soluble desorbed products into the bulk of the solution.

The slowest step in this sequence determines the rate of the process as a whole.

The absorption of a gaseous reactant by a liquid is usually rapid in semiworks conditions, but, as the reaction vessel is increased in size, and the ratio of the gas—liquid interface area to the liquid volume is correspondingly reduced, absorption may become the rate-limiting process., At least one industrial process is known where this is the case, namely the ammonia leaching of a nickel sulfide concentrate with the use of gaseous oxygen for oxidation of sulfides in aqueous suspension [16]. In general, such an effect is favored by a high rate and by high gas requirements in the reaction.

An increase of the rate of gas absorption can be effected by: 1) an increase of the partial pressure of the gas, 2) an increase of the gas— liquid interface area relative to the liquid volume, and 3) an increase of the effeciency of agitation. Increase of temperature usually has no appreciable effect.

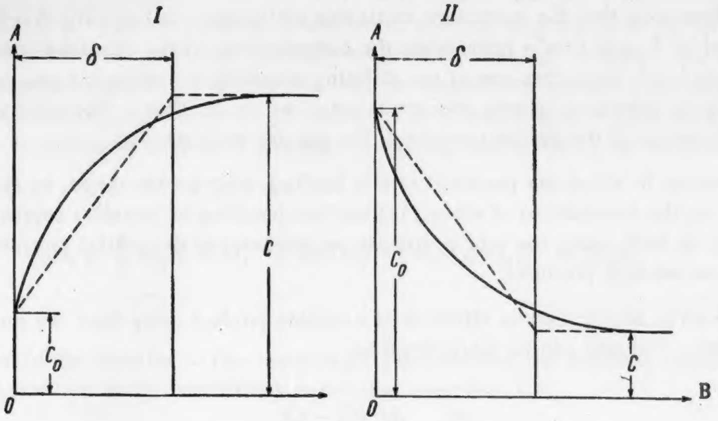

Fig. 1. Solution concentration of a diffusing substance near a reacting solid surface.
I) Diffusion of reactant to surface, II) diffusion of product from surface.
A) Concentration of diffusing components, B) distance from solid surface, C) volume concentration of solution, δ) thickness of diffusion layer.

The rate of a process is more often determined by transport of a dissolved reactant to the surface (stage 2) or of a dissolved product away from the surface into the bulk of the solution (stage 4). The essential characteristics of such systems are given in Fig. 1, which shows the variation of the concentration of a given component in the solution as a function of the distance from the surface. The rate of transport to (or from) the surface is determined by the diffusion of the particular component across a diffusion layer of thickness δ, immediately adjacent to the surface where it is consumed (or formed). Within this layer the concentration of the diffusing component can be represented, as a first approximation, as a linear function of the distance (corresponding to the broken line in Fig. 1.), while on the solution side the concentration is essentially constant and equal to that of the bulk of the solution.

On the basis of this approximate model, the rate at which a dissolved substance diffuses to a solid surface (where it is consumed in the reaction) may be represented by:

$$\frac{dn}{dt} = \frac{DA\,(C - C_0)}{\delta}, \tag{1}$$

where n is the amount of diffusing component passing through the diffusion layer in time t, D is the diffusion coefficient (usually of the order of $2 \cdot 10^{-5}\,cm^2/sec.$ [17]; this value increases only slightly with temperature). A is the area of the diffusion layer (i.e., of the surface), C is the bulk solution concentration.

Thus, the diffusion rate reaches a limiting value

$$\frac{dn}{dt} = \frac{DAC}{\delta}, \tag{2}$$

when the solution at the interface is completely free (as the result of the reaction) from the diffusing com-

ponent, and hence, $C_0 = 0$. This represents and upper limit of the reaction rate.

For a given system, the thickness of the diffusion layer δ depends primarily on the agitation. Its value usually lies between 0.05 cm in an unstirred system to 0.001 cm in a system which is vigorously stirred [18]. These values show that the maximum attainable (diffusion-limited) rate of a heterogeneous reaction is of the order of 10^{-1} mole/cm^2 • hour, when the concentration of the dissolved reactant is 1 mole/liter, or about 10^{-4} mole/cm^2• hour when one of the diffusing reactants is a dissolved gas, such as O_2 or H_2, the concentration of which under atmospheric pressure is only 10^{-3} mole/liter. The advantages which follow in such cases from an increase of the partial pressure of the gas are quite evident.

Examples of systems in which the practical rate is limited, over a wide range, by diffusion of a dissolved gas (i.e., O_2) are the cyanidation of silver [11] and the leaching of metallic copper by aqueous ammonia solution [19]. In both cases, the rate is directly proportional to the partial pressure of gaseous oxygen and it is advantageous to use high pressures.

The rate is less often determined by diffusion of a soluble product away from the surface, but such cases have been described [20]. The rate can be represented by

$$\frac{dn}{dt} = \frac{AD\,(C_0 - C)}{\delta}, \qquad (3)$$

where the symbols have the same meanings as in Equation (1). C_0, and therefore the diffusion rate, can increase until the saturation limit of one of the products is reached, when its precipitation commences. In such cases, an increase of the pressure of a gaseous reactant (or of the temperature) is rarely advantageous, and may even lead to passivation of the surface by deposition of a precipitate, as in reactions of corrosion of iron [21] and of copper—gold alloys [22].

Several criteria have been proposed for distinguishing diffusion-controlled reactions from reactions which depend on the chemistry of the process [23]. In contrast to the latter type, the rates of diffusion-controlled reactions are usually characterized by a clearly defined dependence on agitation and a low temperature coefficient (usually corresponding to an apparent activation energy between 1 and 4 kcal/mole).

Stage 3 (the stage which includes adsorption, chemical reaction at the surface, and desorption) varies greatly from system to system and cannot be considered in general terms as was done in the case of diffusion. The complications which may arise include the formation of insoluble by-products such as oxides during leaching. For example, in the ammonia leaching of pentlandite (see later) nickel dissolves in the form of nickel ammine sulfate, while iron remains in the form of a hydrated ferric oxide deposit, through which the reactants and the reaction products must diffuse to sustain the reaction [16]. Such diffusion, which is usually much slower than the previously considered liquid diffusion, (even if the solid layer is fairly porous) may become rate-determining.

The above and other features of the kinetics and mechanisms of hydrometallurgical reactions are most conveniently considered, for individual systems. The physicochemical factors (including thermodynamics and kinetics) which influence numerous diverse reactions and processes of interest in hydrometallurgy have recently been reviewed [24]. A further discussion of some of these systems is given below, special emphasis being laid on practical aspects.

Chemical Aspects of Pressure Hydrometallurgy and Descriptions of some Specific Processes

1. Leaching Processes

Leaching of oxides. One of the oldest and best-known examples of the use of high pressures in hydrometallurgy is the Baeyer process, in which bauxite is leached out with a relatively concentrated caustic soda solution [25]. In this case, autoclave conditions are used to ensure the attainment of very high temperatures (150-170°C) necessary to convert aluminum oxide into a soluble state.

Pressure digestion at high temperatures has also been used for treatment of other oxidized ores, for example, in the extraction of uranium and vanadium from carnotite ores [26], and of tungsten from scheelite

ores [27, 28]. In both these processes, carbonate solutions are used for leaching, and neither involves the use of oxygen or other gaseous reagents.

Pressure leaching of pitchblende. Only the sexivalent form of uranium is soluble in carbonate solution [as the complex $UO_2(CO)_3^{4-}$]. Thus, in contrast to carnotite, primary uranium minerals such as pitchblende and uraninite, in which uranium is present in partially reduced form (U_3O_8) cannot be dissolved directly by carbonate solutions. However, recently a process has been developed and applied industrially in Canada [4, 29, 30], for pressure leaching, applicable to pitchblende, in which gaseous oxygen (or air) is used to oxidize the uranium and make it soluble in carbonate solution. Leaching is effected by the reaction

$$U_3O_8 + \frac{1}{2}O_2 + 3CO_3^{2-} + 6HCO_3^- \rightarrow 3UO_2(CO_3)_3^{4-} + 3H_2O. \quad (4)$$

An examination of the kinetics of this reaction [31] showed that the leaching rate is determined by the chemical oxidation of uranium at the pitchblende—solution interface, i.e.,

$$U_3O_8 + \frac{1}{2}O_2 \rightarrow 3UO_3, \quad (5)$$

followed by rapid dissolution of UO_3. The rate increases appreciably with increase of partial oxygen pressure (Fig. 2) and temperature (Fig. 3). Thus, intensification of the process requires the highest feasible temperature and pressure. In practice, a temperature of 100-110° C and a partial pressure of oxygen of about one atmosphere are used [30], in conjunction with a leaching solution containing 5% Na_2CO_3 and 2% $NaHCO_3$. In these conditions, over 90% of the uranium is extracted from most pitchblendes in 2-6 hours. To prevent a lowering of the yield through hydrolytic precipitation of insoluble uranates, excessively high temperatures should be avoided, and relatively high $NaHCO_3$ concentrations maintained in the solution. In the treatment of carnotite ores by this process, high yields of vanadium as well as uranium can be obtained by preliminary roasting of the ore in presence of calcium sulfate [32].

If sulfides, such as pyrite, are present in the ore, they may be oxidized during leaching, leading to neutralization of the carbonate, i.e.,

$$2FeS_2 + 7\frac{1}{2}O_2 + 8Na_2CO_3 + 7H_2O \rightarrow 2Fe(OH)_3 + 4Na_2SO_4 + 8NaHCO_3. \quad (6)$$

If reagent consumption becomes excessive for this reason, the prior removal of sulfides from the ore may be economically justified [29].

The results of laboratory experiments and a description of a continuous pilot plant (40-50 tons per day) for testing the possibility of using the carbonate pressure leach process (and also the hydrogen precipitation process to be described later) for treatment of Yugoslavian uranium ores were recently published [33].

Leaching of metals. Some hydrometallurgical processes consist of direct leaching of a metal. An important and widely applied example is the cyanidation process in which metallic gold and metallic silver are dissolved in an aqueous cyanide solution. Oxidation is effected by dissolved air, oxygen being first reduced to hydrogen peroxide and ultimately to water:

$$2Ag + O_2 + 4CN^- + 2H_2O \rightarrow 2Ag(CN)_2^- + H_2O_2 + 2OH^-, \quad (7)$$

$$2Ag + H_2O_2 + 4CN^- \rightarrow 2Ag(CN)_2^- + 2OH^-. \quad (8)$$

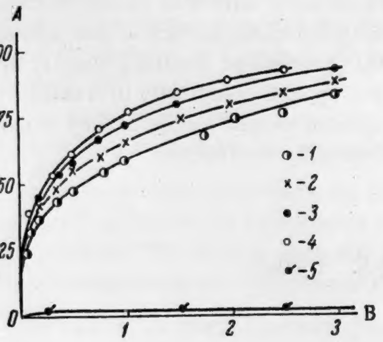

Fig. 2. Effect of oxygen partial pressure on the rate of leaching of a pitchblende ore with 5% Na_2CO_3 solution at 100°. A) Extraction of U_3O_8 (in %), B) time (hours).
Oxygen pressures (in atm.): 1) 0.5, 2) 1.0, 3) 2.0, 4) 4.0, 5) 0.0.

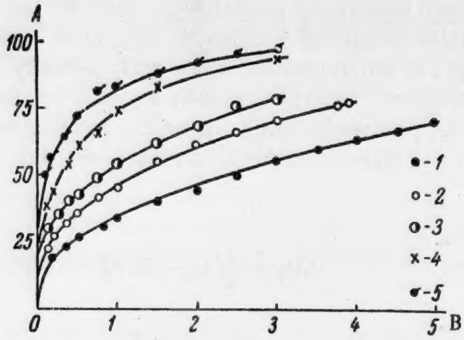

Fig. 3. Effect of temperature on the rate of leaching of a pitchblende ore with 5% Na_2CO_3 solution under 2 atm. oxygen pressure.
A) Extraction of U_3O_8 (in %), B) time (hours)
Temperature (°C): 1) 61, 2) 71, 3) 81, 4) 100, 5) 115.

(Similar equations represent the dissolution of gold).

The reaction is usually effected at atmospheric pressure and temperature. Various kinetic and electrochemical investigations [11, 34, 35] have shown that at not very low cyanide concentrations the dissolution rate of gold or silver is determined by diffusion of dissolved oxygen to the metal surface, even under very vigorous agitation conditions. Cyanidation of both gold and silver has been studied under autoclave conditions, [11, 36, 37] and it was shown that the rate increases in direct proportion to the partial pressure of oxygen up to relatively high pressures. However, it is doubtful whether the use of autoclaves in such cases is economically justified.

Similar considerations apply to the leaching of metallic copper by aqueous ammonia solutions

$$Cu + \frac{1}{2} O_2 + 2NH_3 + 2NH_4^+ \rightarrow Cu(NH_3)_4^{2+} + H_2O. \qquad (9)$$

This reaction, which is of some hydrometallurgical interest, has recently been studied under autoclave conditions [19]. In practice, its rate is limited by transport of dissolved oxygen to the copper surface, and it may be raised by an increase of the oxygen partial pressure, as shown in Fig. 4. At high pressures the rate ceases to increase and attains a constant value which is independent of the oxygen concentration, but which depends on the ammonia (and ammonium salt) concentration. In this region the rate is limited by the rate of chemical action of NH_3 and (NH_4^+) on the oxidized copper surface.

It has been reported that various precious metals, including gold, platinum, palladium, iridium, and rhodium, can be dissolved in aqueous hydrochloric acid at high temperatures and oxygen pressures [38, 39].

Leaching of sulfides. It has been found that numerous sulfide minerals, including FeS_2, FeS, FeS ·NiS, CuS, ZnS, PbS and MoS_2, can be oxidized fairly rapidly when treated with water or aqueous solutions of H_2SO_4, NH_3, NaOH, etc., under oxygen pressure at elevated temperatures. Recent work in this field is discussed below, special attention being paid to hydrometallurgical systems of industrial interest.

Ammonia leaching of concentrates. A process has recently been developed and applied on the industrial scale in Canada for treatment of Ni — Cu — Co sulfide concentrates by ammonia leaching [1, 2, 3, 16, 40, 41]. The process is applied to the treatment of a flotation concentrate of the following approximate composition (in wt. %): Ni 12-16, Cu 1-2, Fe 30-40, Co 0.5, S 28-34, insoluble residue 20 (no precious metals). Nickel is present mainly as pentlandite [(Ni, Fe)S], copper as chalcopyrite ($CuFeS_2$) and iron as pyrrhotite (FeS) and pyrite (FeS_2).

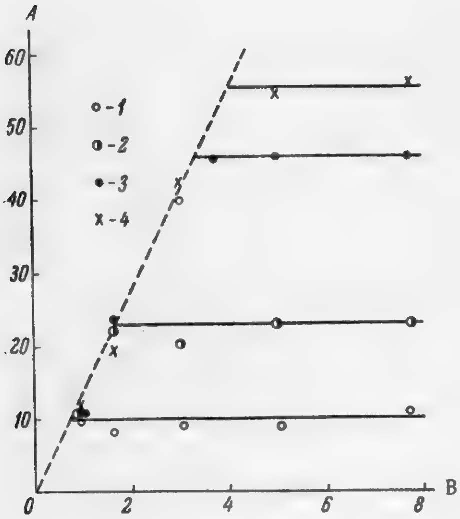

Fig. 4. Effect of oxygen partial pressure on the solution rate of copper in aqueous ammonia at 20°.
A) Solution rate (in mg Cu/cm²· hour), B) oxygen pressure (atm). NH_3 contents (in moles/liter): 1) 0.26, 2) 0.52, 3) 0.74, 4) 1.00.

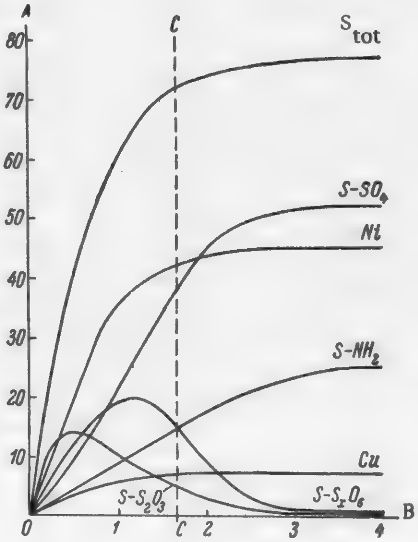

Fig. 5. Leaching of Ni — Cu — Co sulfide concentrate with aqueous ammonia solution under oxygen pressure. Variation of the concentration of copper, nickel, and sulfur compounds during leaching.
A) Concentration in solution (g/liter), B) time (hours).
The line C — C represents the final solution concentration.

The concentrate is mixed with water and ammonia and subjected to countercurrent leaching in two stages in continuously operating autoclaves in which a solution is formed containing ammine compounds of nickel, cobalt, and copper, free ammonia, and a number of ammonium salts, including the thiosulfate ($S_{S_2O_3}$), thionates ($S_{S_xO_6}$), sulfamate (S_{NH_2}), and sulfate (S_{SO_4}). It is highly probable that the following consecutive reactions play an important role in the leach:

$$NiS \cdot FeS + 3FeS + 7O_2 + 10NH_3 + 4H_2O \rightarrow [Ni(NH_3)_6]SO_4 + + 2Fe_2O_3 \cdot H_2O + 2(NH_4)_2S_2O_3, \quad (10)$$

$$2(NH_4)_2S_2O_3 + 2O_2 \rightarrow (NH_4)_2S_3O_6 + (NH_4)_2SO_4, \quad (11)$$

$$(NH_4)_2S_3O_6 + 2O_2 + 4NH_3 + H_2O \rightarrow NH_4SO_3NH_2 + 2(NH_4)_2SO_4. \quad (12)$$

The variation of the composition of the leach liquor during the leaching process is shown in Fig. 5. At the end of the leach, the following extracts are obtained [41] (in %): nickel 90, copper 89, cobalt 45,

sulfur 75. In practice the two-stage countercurrent leach is carried out to give a final solution composition represented by the line C—C.

It seems probable that in the early stages of leaching, the leaching rate is limited by absorption of gaseous oxygen by the solution, while in the subsequent stages the rate is limited by diffusion of oxygen through the iron oxide film around the sulfide particles (Fig. 6). A detailed study has been made of the chemistry of this process and of the influence of different variables — temperature, oxygen pressure, ammonia concentration, agitation, etc. — on the leaching rate and the yields; the results have been published [16].

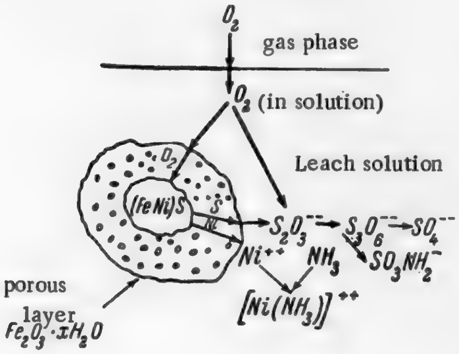

Fig. 6. Diagrammatic representation of a leaching pentlandite particle.

As already stated, the leaching operation is so regulated as to yield a rich solution containing considerable amounts of thiosulfate and polythionates. In the subsequent operation, this solution is boiled to reduce the ammonia content and to cause decomposition of thiosulfate and polythionates, which react with the copper and precipitate it as sulfide. The remaining traces of copper are removed under autoclave conditions by addition of a small amount of H_2S. The final copper-free solution, containing about 45 g/liter of nickel and 0.8 g/liter of cobalt, is purified by heating in an autoclave to 175-200°C under oxygen pressure: 1) to oxidize residual thiosulfate and thionates to sulfate, 2) to oxidize traces of ferrous ions to iron in the ferric state, which is then hydrolyzed and precipitated, and 3) to hydrolyze the sulfamate to sulfate. The clarified solution is then treated with hydrogen in an autoclave as described below, to precipitate metallic nickel and cobalt in powder form, and the spent liquor is evaporated to yield ammonium sulfate.

Acid digestion of sulfides. Sulfide minerals can also be digested by gaseous oxygen under pressure in an neutral or acid medium, to yield mainly metal sulfates, sulfuric acid, and in some cases, elemental sulfur [5, 7, 42-46]. The oxidation reactions are usually slower than reactions in an alkaline medium, and correspondingly higher temperatures and pressures are required. The base metals such as uranium, nickel, cobalt, copper, etc., usually dissolve under these conditions, while iron tends to hydrolyze and to be precipitated as ferric oxides or basic ferric sulfates.

The acid digestion of iron sulfides has recently been investigated. Pyrrhotite reacts with oxygen at temperatures between 100 and 125° C, under moderately high oxygen pressures and solution pH below 1.5 to give a good yield of elemental sulfur:

$$2FeS + 3O_2 \rightarrow 2Fe_2O_3 + 2S^\circ. \tag{13}$$

Only about 10-15% of the sulfur is oxidized to sulfate. On the other hand, pyrite under the same conditions is oxidized almost exclusively to sulfate:

$$2FeS_2 + 7\frac{1}{2}O_2 + 4H_2O \rightarrow Fe_2O_3 + 4H_2SO_4, \tag{14}$$

unless it is first subjected to heat treatment for conversion into FeS and S.

The reason for the difference in the behavior of these two minerals (which is also observed when chlorine is used instead of oxygen as the oxidizing agent [47]) is not clear. The process is of potential industrial interest for the extraction of elemental sulfur from iron sulfides; moreover, the large amounts of sulfuric acid formed in situ can be used for leaching of other valuable metals.

This process has been used on the industrial scale for the treatment of cobalt—nickel—copper ores in the United States [6]. The ores are mixed with water and digested in an autoclave under oxygen pressure at about 200°C. This treatment leads to rapid dissolution of the metals — cobalt, nickel, copper — in the sulfuric acid formed by oxidation of sulfides, particularly pyrite. The iron salts formed are largely precipitated as insoluble oxides or basic sulfates. Thus, this method is an alternative to the ammonia pressure leach process descrived above.

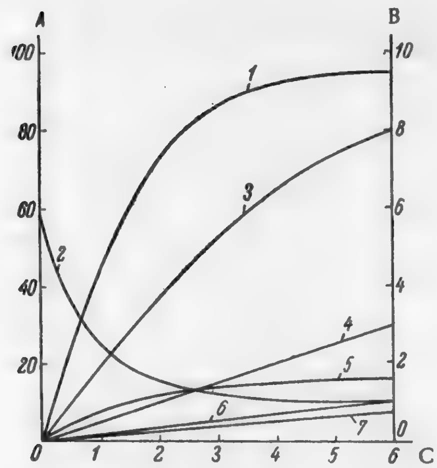

Fig. 7. Leaching of a sulfidic uranium ore (0.17% U_3O_8, 4.4% S) under an oxygen pressure of 1 atm. at 130°.
A) Degree of U_3O_8 extraction (in %), Curve 1; B) pH of solution, Curve 2, or concentration (in g/liter), Curves : 3) SO_4^{--} (−2); 4) Fe^{++}, 5) U_3O_8, 6) Al^{+++}, 7) SiO_2, C) time (hours).

Acid formation in situ has also been used in the leaching of uranium from sulfidic uranium ores [5]. The ore, which sometimes contains only 2% of sulfur (preferably in the form of pyrite) is digested in an autoclave at 120-150° C under an oxygen pressure of 0.5-1 atm. The course of a typical leach by means of this process is shown in Fig. 7. The pyrite is oxidized to give sulfuric acid, and uranium (together with small variable amounts of iron, aluminum, and silica) is dissolved. Most of the liberated iron is oxidized to the trivalent state and precipitated in the form of oxides and basic salts. The combination of high temperatures and oxidizing conditions leads to rapid decomposition of such uranium minerals as pitchblende

$$U_3O_8 + \frac{1}{2}O_2 + 3H_2SO_4 \rightarrow 3UO_2SO_4 + 3H_2O, \qquad (15)$$

and uranium yields of 90-95% are usually reached in 6 hours or less. The hydrolysis reactions serve to buffer the solution at a relatively low acidity (pH ≈ 1) and to maintain a relatively low concentration of dissolved iron, which facilitates subsequent treatment of the solution after leaching to recover uranium. Additional advantages of this process over the usual acid leaching are: 1) considerably lower reagent costs (since only air and water are required for leaching), 2) considerably shorter retention times, and 3) higher uranium yields, especially with ores containing refractory uranium minerals, which are only decomposed with difficulty at lower temperatures.

The experiments described above were performed with Canadian ores. Laboratory experiments have been recently described [46, 48] on the application of this method to the treatment of Australian uranium ores. Somewhat higher temperatures (140-200 °C and pressures were used, with correspondingly shorter retention times (1-2 hours).

Various applications of pressure leaching. The digestion of various other sulfide minerals, including ZnS[43, 44, 49, 50], PbS [43, 44, 51, 52], and MoS_2 [53] in aqueous solutions under oxygen pressure has also been studied. Although these reactions are still of no industrial interest, studies of them are important, as they shed light on the mechanism of sulfide oxidation and on the factors which determine the rate of this oxidation.

Special interest attaches to PbS, as its oxidation in an alkaline medium leads exclusively to sulfate formation [51], while elemental sulfur is obtained in a neutral or acid medium, such as ammonium acetate [52].

Oxidation of pyrite in aqueous alkali solution leads to formation of sodium sulfate and insoluble iron oxides [54]. It has been reported that this oxidation procedure can be used in place of high temperature roasting for pretreatment of refractory sulfidic gold ores, leading to higher gold recoveries in the subsequent cyanidation [55].

A pressure-leaching process for low-grade manganese ores has also been described recently [56]. The ore is first leached with aqueous SO_2 solution when most of the MnO_2 is converted into soluble manganese sulfate with simultaneous formation of some MnS_2O_6. Subsequent digestion of the slurry in an autoclave at high temperature under oxygen pressure leads to oxidation of MnS_2O_6:

$$MnS_2O_6 + \frac{1}{2} O_2 + H_2O \rightarrow MnSO_4 + H_2SO_4 \qquad (16)$$

and to an increase of the total manganese yield. The leach solution is then evaporated to crystallize $MnSO_4$, which is sintered to yield an MnO_2 product and SO_2 (the latter is recycled).

2. Pressure Precipitation Processes

High pressure and high temperature techniques have also been used for purification of leach solutions and for separation and recovery of metals by precipitation and replacement.

Hydrolysis reactions. As the temperature of an aqueous solution is raised, there is a tendency for many metal ions to be hydrolyzed and precipitated as oxides and basic salts. An outstanding example is Fe^{3+}, which probably reacts as follows:

$$2Fe^{3+} + 3H_2O \rightarrow Fe_2O_3 + 6H^+, \qquad (17)$$

$$Fe^{3+} + H_2O + SO_4^{2-} \rightarrow Fe(OH)SO_4 + H^+ . \qquad (18)$$

As the result of reactions similar to the above, ferric iron is completely precipitated at temperatures above 130°C, even from solutions with pH $\cong$ 1. The important role of these reactions in the acid pressure leaching of sulfide ores has already been noted.

Ferrous salts are not hydrolyzed so easily, but they can be oxidized in presence of oxygen to ferric salts

$$2Fe^{2+} + \frac{1}{2} O_2 + 2H^+ \rightarrow 2Fe^{3+} + H_2O. \qquad (19)$$

At room temperature this reaction proceeds relatively slowly in acid solutions, but its rate increases with temperature and oxygen pressure [57].

Other metals which may be hydrolytically precipitated from sulfuric acid solutions at high temperatures include titanium, copper, cobalt, nickel, aluminum, and chromium, but the chemistry of these reactions is not clear. The hydrolytic precipitation of uranium (in the form of sodium uranate) from carbonate solutions at high temperatures has also been described [58].

Such reaction may find application either for the recovery of metals from leach solutions, or for preliminary purification of the solution to remove undesirable impurities.

Another hydrolytic reaction under high pressure, in which no precipitation occurs, but which is nevertheless of hydrometallurgical interest, is the conversion of ammonium sulfamate to ammonium sulfate at 200°C in the leach liquors from ammonia leaching of sulfides [3].

Precipitation of sulfides. The efficiency of precipitation of metals as sulfides by hydrogen sulfide, for example CuS, from aqueous solutions can be increased considerably if the process is performed in an autoclave at temperatures above 100° C. This shortens the time for complete precipitation and also decreases the excess of H_2S required [16].

At high temperatures (≈200°) replacement precipitation of metal sulfides from solution can be effected by digestion with other (more soluble) metal sulfides [7, 16]:

$$Cu^{2+} + FeS \rightarrow CuS + Fe^{2+}. \quad (20)$$

Precipitation of copper sulfide by the action of heat on ammoniacal solutions containing thiosulfate and polythionates has already been mentioned [16].

Precipitation of metals by reduction with hydrogen. Although individual examples of the replacement of metals such as silver and mercury by hydrogen in aqueous solutions of their salts were known as early as 1859 [59], the first systematic and extensive studies of these reactions, especially at high temperatures and pressures, are due mainly to Ipatyev and his co-workers. Between 1909 and 1931, they published the results of numerous experiments in which they succeeded in precipitating the following metals from aqueous solutions: copper, nickel, cobalt, lead, bismuth, arsenic, antimony, tin, platinum, iridium, and mercury [60-78]. In some cases, precipitates of oxides, basic sulfates, or other compounds of the metals were obtained instead of (or together with) the metals, as the result of reduction and/or hydrolysis reactions [79-83]. Subsequent investigations, also conducted in Russia, mainly by Tronev and his associates, deal with the hydrogenation of aqueous solutions of salts of precious metals and the precipitation of silver, gold, palladium, platinum, rhodium, and iridium [84-88]. It was shown that this process may be used for separation of the metals of the platinum group by selective precipitation [89]. These authors also studied the hydrogen reduction of cobalt, copper, and nickel from solutions of their complex salts [90]. More recently, investigations in this field have been made in the United States and Canada, leading to the development of new industrial processes [91, 92].

Precipitation of nickel and cobalt. Precipitation of metallic nickel by hydrogen reduction of ammoniacal nickel sulfate solution, is applied on the industrial scale in Canada in conjunction with the ammonia pressure leach process described earlier [1, 41, 91, 93]. The reaction proceeds very successfully in a solution in which the ratio of NH_3 to Ni^{++} is close to two and most of the nickel is present as the diammine complex $Ni(NH_3)_2^{++}$, i.e.,

$$Ni(NH_3)_2^{++} + H_2 \rightarrow Ni^{\circ} + 2NH_4^{+}. \quad (21)$$

If a higher initial ratio of NH_3 to Ni^{++} is used, higher nickel ammine complexes are formed (especially as the reaction proceeds and excess NH_3 is liberated), the reduction of which by hydrogen is less favorable both from the thermodynamic and from the kinetic standpoints, than reduction of the diammine. A lower initial ratio leads to liberation of free H^+, which has an unfavorable influence on the thermodynamics of the process.

In the conditions usually employed (150-200° C and up to 30 atm. H_2) the reaction apparently does not proceed homogeneously in solution, but only on the surface of the metallic nickel already formed. This reflects the well-known ability of metallic nickel to activate hydrogen heterogeneously — a property responsible for its catalytic activity in many hydrogenation reactions. Thus, nickel is the ideal metal for reduction by hydrogen, having an autocatalytic effect on the reaction. In order to induce the reduction reaction, it is necessary either to add some metallic nickel powder or, (as is done in practice) to add a suitable catalyst, such as a ferrous salt, which induces nucleation, i.e., the formation of highly disperse nickel particles. Such particles serve as centers for the subsequent growth, and can be recycled in the system until they reach the desired size (usually about 50 μ). The growth of these particles has been studied [93] and it was found that after the first growth stages the number of particles becomes fairly constant and that the reaction rate at any subsequent instant is directly proportional to the total surface area of the nickel particles present. The rate also increases with increase of temperature and the partial pressure of hydrogen.

The leach solutions in present use in production contain about 50 g nickel and 1 g cobalt per liter. Treatment for 30 minutes with hydrogen under 30 atm. pressure at ≈ 175 °C results in preferential precipitation of nickel (Fig. 8) until its concentration decreases to about 1 g per liter, while all the cobalt still remains in solution. The precipitated nickel is then separated from the solution, the nickel and cobalt remaining in the solution are treated with H_2S, and the resulting sulfide precipitate is again leached under pressure, precipitated, and reduced with hydrogen for separate recovery of cobalt and nickel. The barren liquor is evaporated to yield ammonium sulfate fertilizer.

The reduction precipitation of metallic cobalt from ammoniacal cobalt sulfate solutions probably occurs similarly to the precipitation of nickel (cobalt is also a catalyst for heterogeneous hydrogenation). By appropriate adjustment of the conditions in order to utilize a number of thermodynamic and kinetic factors, it is possible to achieve a high degree of separation of nickel and cobalt by selective precipitation with hydrogen in separate stages from solutions containing both metals [94]. It has recently been reported that reduction of cobalt can be catalyzed by colloidally dispersed graphite and by dissolved hydroquinones [95]. It is suggested by the kinetics that the function of the catalyst consists of activation of the hydrogen, enabling it to form an active hydrogen-containing intermediate compound ($Co^{II} \cdot H_2$), which decomposes to form metallic cobalt.

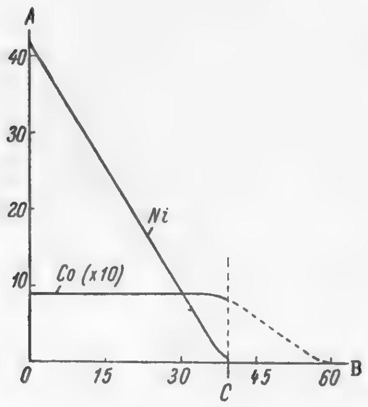

Fig. 8. Precipitation of metallic cobalt and nickel from aqueous ammonia solution by hydrogen reduction.
A) Solution concentration (in g/liter), B) time (min.). C) Point corresponding to nickel precipitation.

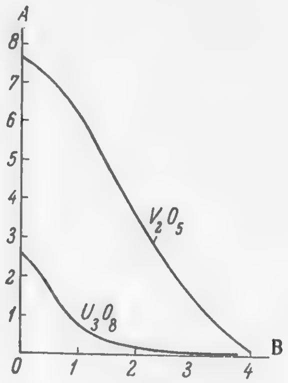

Fig. 9. Precipitation of uranium and vanadium oxides from carbonate solutions by hydrogen reduction (temperature 150° C, H_2 pressure 13 atm., 5 g nickel powder per liter).
A) Concentration of U_3O_8 or V_2O_5 (in g/liter), B) time (hours).

<u>Precipitation of copper</u>. Metallic copper can also be precipitated by reduction of its aqueous salt solutions with hydrogen (or carbon monoxide), but it differs from nickel and cobalt in two important aspects.

1) Thermodynamically, salts of bivalent copper are much more easily reduced than nickel or cobalt salts and therefore, metallic copper can be precipitated by hydrogen both from ammoniacal and from acid solutions.

2) In contrast to nickel and cobalt salts, bivalent copper salts in certain conditions can react homogeneously with hydrogen in aqueous solutions, and therefore the presence of a catalyst to initiate reduction is not necessary. The homogeneous reaction proceeds rapidly above 100°C, and its rate is directly proportional to the Cu^{++} and H_2 concentrations. In the light of recent kinetic investigations [96], it seems probable that the total reduction of copper

$$Cu^{++} + H_2 \rightarrow Cu^{\circ} + 2H^+ \tag{22}$$

passes through the following consecutive stages, the first being rate-determining:

$$Cu^{++} + H_2 \rightarrow CuH^+ + H^+ \quad \text{(slow)} \tag{23}$$

$$CuH^+ + Cu^{++} \rightarrow 2Cu^+ + H^+ \quad \text{(fast)} \tag{24}$$

$$2Cu^+ \rightarrow Cu^{\circ} + Cu^{++} \quad \text{(fast)} \tag{25}$$

At high pH values (for example, in acetate-buffered solutions) the disproportionation stage [25] is replaced by another reaction [68, 97], which leads to the formation of cuprous oxide instead of metallic copper, especially at low temperatures:

$$2Cu^+ + 2OH^- \rightarrow Cu_2O + H_2O. \tag{26}$$

Complex compounds of Cu^{++} with certain anions, such as sulfate, chloride, acetate, etc., react more rapidly with hydrogen than the uncomplexed Cu^{++} ion, while complexes of the ammine type react more slowly [98]. Because of their ability to activate hydrogen, copper salts can also act as homogeneous catalysts for the hydrogenation of other substances in aqueous solution (for example, Cr^{VI}).

Among the few other metal ions which share with copper the ability of reacting homogeneously with hydrogen in aqueous solution, are Ag^+ [99], Hg^{++}, and Hg_2^{++} [100].

Precipitation of uranium and vanadium oxides. The reduction of uranium compounds to metallic uranium by hydrogen is thermodynamically possible only at very high temperatures. However, reduction of sexivalent uranium to the quadrivalent state is thermodynamically favorable, and can be used for precipitation of UO_2 from carbonate solutions containing sexivalent uranium salts [4, 33, 58].

$$UO_2(CO_3)_3^{4-} + H_2 \rightarrow UO_2 + 2HCO_3^- + CO_3^{2-}. \tag{27}$$

The reaction only proceeds in presence of a hydrogenation catalyst, such as finely divided metallic nickel, and the rate is directly proportional to the amount of catalyst present and the hydrogen partial pressure. Satisfactory precipitation rates are obtained at 150°C, 13 atm. H_2, and with 5 g/liter of nickel powder as catalyst (Fig. 9). The advantages of this method include: 1) very low reagent consumption, 2) efficient and complete extraction of uranium, 3) short retention times, 4) the production of high-grade uranium oxide in the reaction, and 5) applicability to all carbonate solutions, including those of very low initial uranium content. The leach solutions are not changed substantially during the precipitation, and are well suited for repeated use.

Vanadates [101] can also be reduced by hydrogen in carbonate solution (in presence of a catalyst), vanadium being precipitated as the lower oxide V_2O_3 :

$$2VO_3^- + 2H_2 + 2HCO_3^- \rightarrow V_2O_3 + 2CO_3^{2-} + 3H_2O. \tag{28}$$

The kinetics of the process is similar to the kinetics of UO_2 precipitation reaction. When both metals are present in the same solution (as in the solutions obtained by carbonate leaching of carnotite ores) they are precipitated simultaneously (Fig. 9). In such cases, the product obtained directly from the autoclave consists of

a mixture of uranium and vanadium oxides and unchanged powdered nickel catalyst. The latter is removed by a magnetic method and recycled. The uranium and vanadium oxides can be separated and obtained as high-grade products by a relatively simple fusion process [4].

Experimental and Technological Aspects of Pressure Hydrometallurgy

Laboratory experiments. The thermodynamics and kinetics of most hydrometallurgical reactions, especially at high temperatures and pressures, are still not completely understood, and their course is therefore difficult to predict. Before a new process can be put into industrial operation, it is usually necessary to test it thoroughly on a laboratory and pilot plant scale. In these early development stages, careful planning of the equipment and test procedures is extremely important.

In most of the pressure leaching and precipitation experiments carried out in our laboratory, mechanically stirred cylindrical stainless steel autoclaves of relatively simple design [11, 19], from one to three gallons, (from 4.5. to 13.6 liters) in capacity have been used. If the solutions were strongly corrosive, the liners and internal parts of the equipment were made from titanium. Equipment of this type is now available on the industrial scale. There has also been a description [102] of another laboratory autoclave of somewhat more complex design, which can operate at higher pressures, and which has also been used for hydrometallurgical studies. Experience has shown convincingly that for hydrometallurgical studies, it is necessary to ensure vigorous agitation in the autoclave (this was not taken into consideration in many earlier studies of high-pressure reactions); mechanical stirring by impellers rotating at relatively high speeds is much more efficient than shaking or rocking. In addition to ensuring adequate temperature and pressure control, it is important to provide a sampling device so that samples can be withdrawn for analysis periodically during a reaction. Standard analytical methods can generally be used for following the course of the reactions.

The laboratory investigations should provide for a detailed and systematic study of all the chemical and physical factors which influence the process, such as grind, pulp density, reagent concentrations, temperature, pressure, catalysts, reaction time, etc., and each of these factors should be varied independently over the widest possible range. Useful data can often be obtained in studies of a reaction under conditions far removed from those to be used in practice. For example, in studies of the leaching of a solid, it is often preferable (when possible) to use large specimens, the surface area of which can be accurately determined and kept constant during the experiment, rather than a pulp of finely divided material, the surface area of which, and its variations during leaching, are very uncertain [51-53].

Corrosion and materials of construction. Although at high temperatures corrosion and erosion effects are more pronounced, they are rarely serious enough to present an insurmountable obstacle to the industrial application of hydrometallurgical processes such as those described in this paper. It should be noted in this connection, that at high temperatures and pressures it is often possible to use milder and hence, less corrosive leaching solutions (i.e., weaker acids) than at ordinary temperatures, as leaching reactions are then more rapid and efficient, as, for example, in the leaching of uranium. Moreover, because of the greatly reduced retention time, the leaching equipment can usually be considerably smaller, so that it is possible to use more expensive corrosion-resistant materials for its construction.

If relatively noncorrosive solutions are used, as in the carbonate leaching of uranium ores at 110° and 5 atm. air pressure, the equipment (including autoclaves) can be made from ordinary mild steel [30]. With more corrosive solutions, such as ammonia, stainless steel should be used [41]. It has been found that austenitic stainless steels, type 316 (molybdenum-stabilized) and type 321 (titanium-stabilized) have good resistance to sulfuric acid solutions (pH 1-2) at temperatures up to 150°C. If the process is carried out at higher temperatures or lower pH, corrosion problems become more serious and equipment lined with titanium or acid-resistant brick should be used.

Technological aspects. It is quite evident from the above discussion of the fundamental aspects of the use of superatmospheric pressure techniques at high temperatures in hydrometallurgical processes, that to ensure the optimum results, the operating units must be designed to provide the necessary conditions of temperature, pressure, agitation, and retention times specific for each type of treated material and for every reaction, whether it is leaching, hydrolysis, or precipitation of metals, or their oxides, salts, or other compounds. However, if the desired chemical and physical operating conditions for a given reaction have been established by proper tests in the laboratory and pilot plant, their application on the industrial scale becomes essentially the

problem of utilizing conventional chemical engineering principles and techniques for providing the necessary operating units and controls.

There are 2 types of processes in the field of chemical technology: a) those in which the starting materials are largely similar in composition, but which give rise to an infinite variety of end products, and b) those in which the starting materials are infinitely varied, but which produce a relatively small number of products of simple composition. Processes of the first group are used in branches of industry based on coal, coke, natural gas, petroleum, salt, water, air, sulfur, cellulose, and limestone, which give rise to numerous inorganic and organic compounds, explosives, acids, etc. If high-pressure processes are used in these branches of industry, as a rule they involve liquids and gases, and only rarely solids. The second group of processes is used in branches of industry based on processing of metallic minerals which occur in various concentrations in different locations, and which have chemical compositions, physical forms and associations unique for each case, and often differing appreciably within each site. The production of metals conforming to technical specifications from such minerals, is usually considered to be among the functions of the primary metallurgical industry. The processes of this industry almost invariably involve reactions with solid materials, and at some stage or other, liquids and gases, often at high temperatures. Pressures exceeding atmospheric by more than one atmosphere are only rarely used.

For treatment of minerals and production of metals by hydrometallurgical processes at elevated temperatures and pressures, the conditions generally adopted in the types of processes described above must be modified to some extent, and the technology must be adapted to suit the specific requirements of high pressure and temperature operation. The chemist must have a good mastery of the concepts of reactions at the solid—liquid interface, of diffusion in solids, of the peculiarities of mineral particles, and metallic surfaces; the metallurgist must learn to take into account the factors involved in diffusion in solutions, in reactions at the gas—liquid interface, the influence of pressure and concentration, and of catalysts in the liquid and gas phases, etc.

From the engineering standpoint, the efficient development of these processes demands only that the problems should be solved with a full understanding of all the chemical and physical factors involved and an appreciation of the character of minerals and metals, with recognition of the fact that the high pressure operations to be used, apply not only to solids, but also to liquids and gases. If these aspects are accepted, the technological problems of plant design reduce to planning efficient handling of materials and production control techniques.

The most important details which should be taken into account in design and operation are described below.

Preparation of the material for treatment. As the solids to be leached must be suspended in a liquid pulp, it is important that they should be finely ground; they should usually all pass a 100 mesh sieve (Tyler). In some cases, as in the utilization of artificial pyrrhotite for sulfur production [45], it is necessary to decompose the mineral, in this instance pyrite, thermally, before introduction into the autoclave. Sometimes [32] it may also be advantageous to roast the ore before leaching, to improve its physical properties or to adjust its chemical composition. If metal scrap, metal powders [41], or metal plates are to be leached, the reaction rate greatly depends on the surface area of the metal. In general, it should be noted that the preparation of the material for treatment largely reduces to maximum, economically advantageous comminution of the solid material which, in the case of minerals, will not prevent homogeneous suspension in a liquid pulp.

Autoclave charging. Continuous operation of pressure vessels has certain advantages, and therefore it is desirable to use charging equipment which will pump the suspension into an autoclave working under high pressure, and which can be operated at various rates. Diaphragm pumps of various types are well suited for this purpose; these operate stably at pressures up to 50 kg/cm^2 with pulps containing up to 50% solids. For processes at 7 kg/cm^2 or less, where water balance is not particularly important, good results have been obtained with centrifugal sand pumps [30], operating in series, if necessary. If only liquids are involved, as in charging solutions into precipitation autoclaves, at pressures of 21-35 kg/cm^2, multistage centrifugal pumps are satisfactory.

The feed rate can be controlled by variation of the pump stroke length, alteration of speed, or in some cases, by throttling the pump inlet or outlet.

Thus, continuous charging presents no serious problems.

Pressure vessel design. In designing pressure vessels for continuous operation in which a suspended ore or metal powder is to be agitated, consideration must be given to such factors as pressure, process temperature, solution composition, amount, and nature of the solids present, etc., which will vary considerably with the type of process.

One type of vessel, the horizontal cylinder, described by Nashner [41] and by Mancantelli [30], with or without internal partitions, has, according to one report, proved unstable in operation, but is completely satisfactory for a number of leaching and precipitation properties. At temperatures below 120°C in weak acid solutions, or for use with alkaline solutions, the vessel and the internal mechanisms can be made of basic (mild) steel clad with stainless steel. At higher temperatures, and for strongly acid solutions, good results are obtained with brick-lined stainless steel vessels, although titanium must be used for the agitators and other fittings.

In such a vessel, the agitator drive shaft enters the vessel through a seal of the mechanical type in the lid. The seal can operate under pressures up to 35 kg/cm^2 for many months without appreciable leakages of gas or vapor, and can be easily repaired or replaced.

Provision can be made for introduction of gases — air, ammonia, hydrogen, hydrogen sulfide, CO_2, etc. — either into the vapor phase of the autoclave or through pipes leading into the liquid through the upper or lower part of the vessel.

The vessel dimensions depend on the individual requirements. For example, vessels of 3.3 m internal diameter and 13.2 m long with vertical mechanical agitators have been used [41].

Agitation of the pulp, which is extremely important in all leaching and metal precipitation operations, is satisfactorily effected by numerous types of impeller. Strangely enough, corrosion or erosion of correctly designed agitators present no special problems. The blades can operate for a year or more without any damage or loss of efficiency and do not require more than the ordinary maintenance.

Another type of autoclave which has given promising results is a vertical tower in which the liquid slurry is charged at the bottom and discharged at the top. Agitation is effected by introduction of steam or air at the bottom of the tower with the slurry. As the tower does not contain any moving parts or obstructions, maintenace costs are low. Units of this type may be used with high-acid solutions, and in high temperature processes, as the towers can be easily lined with acid-resisting brick or other materials.

Heat transfer. In many leaching operations, heat is liberated by oxidation of sulfides, while in others, steam must be added to maintain working temperatures, and in yet others, especially in metal precipitation, the solutions must be heated without dilution by live steam.

Therefore, heat transfer must be taken into account in most pressure leaching and precipitation operations. Provision must be made for addition or removal of heat through the vessel walls or internal coils, or flash cooling may be used. Gases leaving the vessels may have to be scrubbed or condensed; some vessels may have to be insulated and heat exchangers of one type or another may have to be employed. Necessary units for special uses can be easily designed and operated, according to the usual chemical engineering practice. A flash heat exchanger installation has been described by Mancantelli and Woodward [30].

Pressure vessel discharge. The charging of pulps into pressure vessels involves no difficulties at pressures up to 35 kg/cm^2, but discharging presents a much more complex problem, since the discharge pulp may be hot, strongly acid, or abrasive. For operations at lower pressures, (about 7 kg/cm^2) it is easy to provide a throttling or intermittent action valve. In such cases, it is usually possible to cool the pulp in a heat exchanger to a temperature at which rubber valve parts can be used. At higher temperatures and pressures (about 35-42 kg/cm^2) erosion and corrosion of discharge valves present a more serious problem. Units have been designed, however, which give satisfactory performance, but this involves high maintenance costs and rapid wear of valve parts.

To ensure continuous operation, the discharge valves in horizontal autoclaves are actuated by automatic level controllers in the final compartments of the autoclave. The discharge valves of tower leaching units can be regulated similarly.

Gas removal presents no problem, but it is sometimes necessary to provide condensers or scrubbing units for recovery of vapors or soluble gases.

Separation of solid and liquid phases. In pressure leaching and precipitation plants, separation of the liquid and solid phases can be effected by any of the usual methods such as settling, thickening, or filtration. Dissolved gases do not interfere, as they are removed by expansion when the heated solutions or pulps are discharged to atmospheric pressure. Conventional evaporation and crystallization units with centrifugal separators can be used if required.

Automatic control. One of the advantages of the continuous autoclave process is that the units and reactions can be controlled by automatic devices. Temperatures, feed and discharge rates, pressures, gas mixtures, and many other factors involved in pressure processes can be measured, and therefore, controlled by means of suitable electrical or mechanical devices. As a result, the operator is relieved of much of the care and responsibility which so often falls on the operator in a metallurgical plant.

It is evident that samples must be taken from time to time, analyses must be periodically checked, and the proper operation of the control mechanisms must be watched.

Ancillary units. In addition to the usual complement of workshops, power units, etc., pressure operations usually require other ancillary services.

These include compressors for air and other gases, some of which must operate at pressures up to 56 kg/cm ^{2}, and high-pressure steam is also required. If hydrogen precipitation is used, a source of hydrogen must be provided. Simple units are available for producing hydrogen from propane relatively cheaply. A source of hydrogen sulfide may sometimes be needed; this gas can be made simply and cheaply from H_2 and molten sulfur in a compact unit.

It must be stated in conclusion, that although in recent years much information has been obtained on the chemistry of pressure processes in hydrometallurgy, much remains to be studied. The study of basic process principles offers a wide field for scientific research. The present development of technology is such that it may be reasonably supposed that operations in ranges up to 35 kg/cm^2 and 300° C. are technically feasible and that equipment exists or can be designed which will operate economically and satisfactorily for prolonged periods.

LITERATURE CITED

[1] F.A. Forward, Trans. Can. Inst. Mining Met. 56, 363 (1953).

[2] F.A. Forward, Mining Congress J. 40 (5), 49 (1954).

[3] F.A. Forward, Proc. 27-th Congr. Ind. Chem. 2, 320 (1954).

[4] F.A. Forward and J. Halpern, Trans. Am. Inst. Mining Met. Eng. 200, 1408 (1954).

[5] F.A. Forward and J. Halpern, Trans. Am. Inst. Mining Met. Eng. 203, 463 (1955).

[6] J. A. O'Connor, Chem. Eng. 59, 164 (1952).

[7] P.M.J. Gray, Rev. Pure Appl. Chem. (Australia) 5, 194 (1955).

[8] M. Pourbaix, Thermodynamics of Dilute Aqueous Solutions (Edward Arnold and Co., London 1949).

[9] M. Pourbaix, Corrosion, 5, 121 (1949).

[10] P. Delahay, M. Pourbaix and P. Van Rysselberghe, J. Electrochem. Soc. 98, 65 (1951).

[11] G.A. Deitz and J. Halpern, Trans. Am. Inst. Mining Met. Eng. 197, 1109 (1953).

[12] P. Delahay, M. Pourbaix and P. Van Rysselberghe, J. Electrochem. Soc. 98, 101 (1951).

[13] P. Delahay, M. Pourbaix and P. Van Rysselberghe, J. Electrochem. Soc. 98, 57 (1951).

[14] P. Delahay, M. Pourbaix and P. Van Rysselberghe, Compt. rend. Reunion 1951, 15.

[15] G. Valensi, Compt. rend. Reunion, 1950, 51.

[16] F.A. Forward and V. N. Mackow, Trans. Am. Inst. Mining Met. Eng. 203, 457 (1955).

[17] R.A. Robinson and R.H. Stokes. Electrolyte Solutions (Butterworth Publications, London, 1955), 494-495.

[18] G. Kortum and J.O. Bockris, Textbook of Electrochemistry (Elsevier Publishing Co., Amsterdam, 1955), II, 403-405.

[19] J. Halpern, J. Electrochem. Soc. 100, 421 (1953).

[20] B.C.-Y. Lu and W. F. Graydon, J. Am. Chem. Soc. 77, 6136 (1955).

[21] E. Groesbeck and L.J. Waldron, Proc. Am. Soc. Testing Materials 31, 11, 279 (1931).

[22] J.I. Fischer and J. Halpern, J. Electrochem. Soc. 103, 282 (1956).

[23] H.W. Salzberg, H. Knoetgen and A.M. Molless, J. Electrochem. 98, 31 (1951).

[24] J. Halpern, Some Aspects of the Physical Chemistry of Hydrometallurgy, Am. Inst. Mining Met. Eng., Annual Meeting (New York, 1956).

[25] D.M. Liddell, Handbook of Nonferrous Metallurgy (McGraw Hill. Co., New York, 1945) II, 8.

[26] W.F. Blecker, U. S. Patent 1,438,357 (1922).

[27] H.C. McKinley, T.W. Holmes and L.E. Sausa, Eng. Mining J. 152, 76 (1951).

[28] F.W. Wessel, Treatment of Low-Grade Scheelite Ores, Am. Inst. Mining Met. Eng., Annual Meeting (New York 1956).

[29] F.A. Forward and J. Halpern, Trans. Can. Inst. Mining Met. 56, 344 (1953).

[30] R.W. Mancantelli and J.R. Woodward, Trans. Am. Inst. Mining Met. Eng. 202, 557 (1955).

[31] E. Peters and J. Halpern, Trans. Can. Inst. Mining Met. 56, 350 (1953).

[32] J. Halpern, F.A. Forward and A.H. Ross, Effect of Roasting on the Recovery of Uranium and Vanadium Ores by Carbonate Leaching, Am. Inst. Mining Met. Eng., Annual Meeting, New York (1956).

[33] B. Bunji, International Conference on the Peaceful Uses of Atomic Energy (Geneva, 1955), 8 (P), 965.

[34] H.A. White, J. Chem. Met. Chem. S. Africa 20, 1 (1919).

[35] V. Kudryk and H.H. Kellogg, Trans. Am. Inst. Mining Met. Eng. 200, 541 (1954).

[36] V.G. Tronev and S.M. Bondin, Proc. Acad. Sci. USSR 16, 281 (1937).

[37] V.G. Tronev and S.M. Bondin, Proc. Acad. Sci. USSR 16, 313 (1937).

[38] V.G. Tronev, Proc. Acad. Sci. USSR 15, 558 (1937).

[39] V.G. Tronev and S.M. Bondin, Ann. Sector Platinum, Inst. Gen. Chem. 15, 113 (1938).

[40] C.F. Brenthel, Z. Erzbergbau u. Metallhütten 8 (9) (1955).

[41] S. Nashner, Trans. Can. Inst. Mining Met. 58, 212 (1955).

[42] P.M.J. Gray, Research (London) 7, 432 (1954).

[43] H. Neuhans and F. Pawlek, Z. Erzbergbau u. Mettalhütten 6, 41-44 (1953).

[44] G. Bjorling, Metall. 8, 781 (1954).

[45] K.W. Downes and R.W. Bruce, Trans. Can. Inst. Mining Met. 58, 77 (1955).

[46] P.M.J. Gray, Trans. Can. Inst. Mining Met. 65, 55 (1955).

[47] M. Sherman and J.D.H. Strickland, Dissolution of Sulfide Ores in Acid Chlorine Solutions, Trans. Am. Inst. Mining Met. Eng., Annual Meeting, New York (1956).

[48] P.M.J. Gray, International Conference on the Peaceful Uses of Atomic Energy, (Geneva, 1955) 8, 986.

[49] V.G. Tronev and S.M. Bondin, Proc. Acad. Sci. USSR 23, 541 (1939).

[50] O.E. Zvyagintsev and V.G. Tronev, Proc. Acad. Sci. USSR 23, 537 (1939).

[51] J.E. Andersen, J. Halpern and C.S. Samis, Trans. Am. Inst. Mining Met. Eng. 197, 554 (1953).

[52] D.P. Seraphim, Oxidation of Galena in Ammonium Acetate Solutions under Oxygen Pressure, Thesis (University British Columbia, Vancouver, Canada, 1952).

[53] W.H. Dresher, M.E. Wadsworth and W.M. Fassell, Jr., A Kinetic Study of the Leaching of Molybdenite, Am. Inst. Mining Met. Eng., Annual Meeting, New York (1956).

[54] J.E. Stenhouse and W.M. Armstrong, Trans. Can. Inst. Mining Met. 55, 48 (1952).

[55] R. Carter and C.S. Samis, Trans. Can. Inst. Mining Met. 55, 130 (1952).

[56] L.N. Allen, Jr., Chem. Eng. Progr. 50, 9 (1954).

[57] K.A. Kobe and W. Dickey, Ind. Eng. Chem. 37, 429 (1945).

[58] F.A. Forward and J. Halpern, Trans. Can. Inst. Mining Met. 56, 355 (1955).

[59] M.N. Beketoff, Compt. rend., 48, 442 (1859).

[60] V. Verkhovsky and V. Ipatyev, J. Russ. Phys. Chem. Soc. 41, 769 (1909).

[61] V. Ipatyev and V. Verkhovsky, Ber. 44, 1755 (1911).

[62] V. Ipatyev, J. Russ. Phys. Chem. Soc. 43, 1746 (1911).

[63] V. Ipatyev and V. Zvyagintsev, J. Russ. Phys. Chem. Soc. 44, 1712 (1912).

[64] V. Ipatyev and A.N. Starynkevich, Bull. Russ. Acad. Sci. 1918, 119.

[65] V. Ipatyev and A. Andreevsky, Compt. rend. 183, 51 (1926).

[66] V. Ipatyev, Ber. 59B, 1412 (1926).

[67] V. Ipatyev and V.I. Micolaev, J. Russ. Phys. Chem. Soc. 60, 331 (1928).

[68] V. Ipatyev and V. Ipatyev, Jr., Ber. 60B, 1982 (1927).

[69] V. Ipatyev and A. Andreevskii, Compt. rend., 185, 357 (1927); Bull. Soc. Chim. 41, 1466 (1927).

[70] V. Ipatyev, Ber. 61B (1928).

[71] V. Ipatyev and V. Ipatyev, Jr., Ber. 62B, 386 (1929).

[72] V. Ipatyev and O. E. Zvyagintsev, J. Russ. Phys. Chem. Soc. 61, 823 (1929); Ber. 62B, 386 (1929).

[73] V. Ipatyev, G. A. Razuvaev and V. Malionovskii, Ber. 166, 2812 (1930).

[74] V. V. Ipatyev, Jr., M. N. Platonova and V. S. Malionovskii, Ber. 64B, 1959 (1931).

[75] V. V. Ipatyev, Jr. and V. I. Tikhomirov, Ber. 64B, 1951 (1931).

[76] V. V. Ipatyev, Jr., and V. P. Teodorovich, J. Gen. Chem. 1, 729 (1931).

[77] V. V. Ipatyev, Jr., Ber. 64B, 2725 (1931).

[78] V. V. Ipatyev, Jr., I. R. Molkentin and V. P. Teodorovitch, Ber. 64B, 1964 (1931).

[79] V. Ipatyev and A. K. Starynkevich, J. Russ. Phys. Chem. Soc. 46, 172 (1914); J. Soc. Chem. Ind. 33, 1205 (1914).

[80] V. Ipatyev and B. A. Mouromtsev, Ber. 60 B, 1980 (1927).

[81] V. Ipatyev and A. Kisselev, Ber. 59B, 1418 (1926).

[82] V. Ipatyev and N. Kondyrev, Ber. 59B, 1421 (1926).

[83] V. Ipatyev and V. Nikolaev, Ber. 59B, 1423 (1926).

[84] V. V. Ipatyev, Jr. and V. G. Tronev, Proc. Acad. Sci. USSR 1, 622 (1935).

[85] V. G. Tronev, Bull. Acad. Sci. USSR, Chem. Ser. (1937), 331.

[86] V. G. Tronev, Proc. Acad. Sci. USSR 16, 317 (1937).

[87] V. G. Tronev and V. V. Chulkov, Proc. Acad. Sci. USSR 57, 269 (1947).

[88] V. G. Tronev and S. M. Bondin, Bull. Sector Platinum, Inst. Gen. Chem. 22, 187, 194 (1948).

[89] V. V. Ipatyev, Jr., and V. G. Tronev, Proc. Acad. Sci. USSR 29 (1935).

[90] V. G. Tronev, S. M. Bondin, and A. L. Khrenova, Bull. Sector Platinum, Inst. Gen. Chem. 22, 194 (1948).

[91] F. A. Forward, Bull. Inst. Metals 82 (5) 113 (1954).

[92] F. A. Schaufelberger, Metal Precipitation from Salt Solution by Hydrogen Reduction, Am. Inst. Mining Met. Engrs., Annual Meeting (Chicago, 1955).

[93] V. N. Mackiw, W. C. Lin and W. Kunda. Reduction of Nickel by Hydrogen from Ammoniacal Nickel Sulfate Solutions. Am. Inst. Mining Met. Eng., Annual Meeting, New York (1956).

[94] F. A. Schaufelberger and T. K. Roy, Trans. Inst. Mining Met. 64, 375 (1955).

[95] T. M. Kaneko and M. E. Wadsworth, J. Phys. Chem. 60, 457 (1956).

[96] E. Peters and J. Halpern, J. Phys. Chem. 59, 793 (1955).

[97] R. G. Dakers and J. Halpern, Can. J. Chem. 32, 969 (1954).

[98] E. Peters and J. Halpern, Can. J. Chem. 33, 356 (1955); 34, 554 (1956).

[99] A. H. Webster and J. Halpern, J. Phys. Chem. 60, 280 (1956).

[100] G. J. Korinek and J. Halpern, J. Phys. Chem. 60, 285 (1956).

[101] R. N. O'Brien, F. A. Forward and J. Halpern, Trans. Can. Inst. Mining Met. 56, 359 (1953).

[102] W. H. Dresher, T. M. Kaneko, W. M. Fassell and M. S. Wadsworth, Ind. Eng. Chem. 47, 1681 (1955).

[103] U. S. Patent 2,740,707.

PHYSICOCHEMICAL ANALYSIS OF THE ACID CONVERSION OF APATITE

III. USE OF KINETIC DATA ON THE SOLUBILITY OF APATITE FOR CALCULATION OF THE OPTIMUM CONDITIONS FOR DOUBLE SUPERPHOSPHATE PRODUCTION

K. S. Krasnov

The Ivanovo Institute of Chemical Technology

The present paper consists of an attempt to utilize data on the kinetics of the dissolution of apatite in solutions of the system $CaO - P_2O_5 - H_2O$ [1, 2] to explain certain peculiarities of the chemical process and to provide a theoretical basis for the selection of the optimum concentration of the original phosphoric acid in the production of double superphosphate.

The Scientific Research Institute for Fertilizers and Insectofungicides has carried out extensive investigations of this process and established the optimum temperatures for the process and the optimum phosphoric acid concentrations [3-8]. Several investigations of the same problem have also been reported abroad [9-11].

These researches have shown that: 1) artificial increase of the temperature of the reactants in the mixer does not accelerate decomposition of the apatite; 2) the phosphate mineral cannot be decomposed satisfactorily by an acid containing less than 40-45% P_2O_5; 3) the optimum concentration of the original acid is 54-56.5% P_2O_5 (74.5-78% H_3PO_4).

The experiments were carried out with various types of raw materials (apatite, phosphorites, thermal process H_3PO_4, wet process acid, etc).

The purpose of the present work is to provide a theoretical generalization of the established facts on the basis of the mechanism, common to all the processes studied, of the decomposition of apatite by saturated solutions in the system $CaO - P_2O_5 - H_2O$.

For this purpose, we shall use Chepelevetsky's method [6, 12, 13] of graphical physicochemical analysis of a slowly reacting condensed system, such as double superphosphate.

The latter is obtained by the action of phosphoric acid on fluor apatite according to the reaction

$$Ca_5(PO_4)_3F + 7H_3PO_4 = 5Ca(H_2PO_4)_2 + HF. \qquad (I)$$

The crystallization of monocalcium phosphate proceeds rapidly, the reaction mass "sets" and subsequent decomposition is extremely slow; the system can be regarded as a quasi-equilibrium system. Therefore, as has been shown by Chepelevetsky, from its physicochemical aspects, this reaction can be represented by the solubility diagram for the three-component system $CaO - P_2O_5 - H_2O$ [$Ca(H_2PO_4)_2 - H_3PO_4 - H_2O$]. The formation of HF may be neglected, and in calculations fluor apatite may be replaced by hydroxyl apatite $Ca_5(PO_4)_3OH$[6, 13]. Chepelevetsky's calculation method, based on the introduction of auxiliary variable degree of neutralization of the first hydrogen ion of phosphoric acid in the water–acid–salt phase complex is given below.

The figure shows the solubility isotherms for the system, based on Elmore and Farr's data [14].

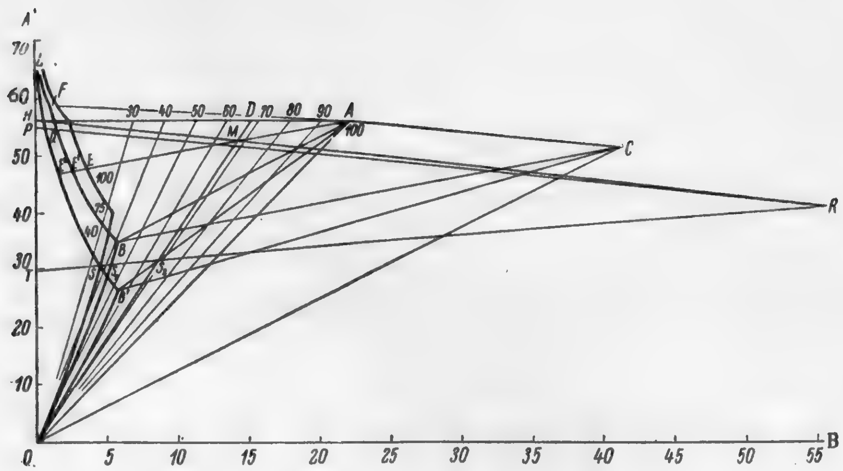

Solubility isotherms for the system $CaO-P_2O_5-H_2O$.
A') P_2O_5 concentration (in %), B") CaO concentration (in %).

OBFL, the 75° isotherm, consists of three branches, each corresponding to a solution in equilibrium with a definite solid phase: OB with $CaHPO_4$, BF with $Ca(H_2PO_4)_2 \cdot H_2O$, FL with $Ca(H_2PO_4)_2$. The point A corresponds to the composition $Ca(H_2PO_4)_2 \cdot H_2O$, the point C to $CaHPO_4$, and R to hydroxyl apatite. The triangle FAB is the crystallization surface of $Ca(H_2PO_4)_2 \cdot H_2O$, OCB is the crystallization surface of $CaHPO_4$, the triangle ABC is the surface for the joint crystallization of $Ca(H_2PO_4)_2 \cdot H_2O$ and $CaHPO_4$.

The composition of the phase complex varies continuously during decomposition of the apatite. (The phase complex is taken to mean the principal components of the system, without the unreacted part of the apatite and HF, that is, water, acid, and salt.)

The figurative point for the phase complex is thereby, shifted to the right, along the "solution path," the straight line joining the figurative point for the acid, for example, H, with the figurative point for apatite R.

The position of the figurative point at any given instant is determined by means of the network of paths of equal degrees of neutralization of the first H^+ ion of the acid, which radiate from the coordinate origin.

The degree of neutralization Z is connected with the decomposition coefficient of apatite K (which may be determined by the conventional methods of analytical chemistry) by the relationship

$$Z = \frac{333\ A \cdot K}{A \cdot K + 72.5\ n}\ , \qquad (1)$$

where A is the P_2O_5 content in the apatite concentrate (in %), and n is the number of kg of H_3PO_4 per 100 kg of apatite.

For the stoichiometric ratio (n = 126.2 kg H_3PO_4) and A = 39.4% we have:

$$Z = \frac{333\ K}{K + 232.5}\ . \qquad (2)$$

After determining K for a given instant, we calculate Z from Formula (2) and use the graph to determine the position of the figurative point for the phase complex at the given instant as the point of intersection of the corresponding neutralization path, for example, OD; with the solution path, for example, HR. This gives the point M.

From the position of the point M we find for each instant of decomposition:

a) Composition of the liquid phase of the complex. Through the point A, corresponding to solid monocalcium phosphate, and the point M, a crystallization path is drawn to its intersection with the solubility isotherm at the point E'. The point E' determines the composition of the liquid phase at 75°, the point E" at 40°, etc. (the tie line rule).

b) The liquid phase – salt ratio. The ratio of the crystallization path segments AM/ME' is equal to the liquid phase–salt ratio in the complex. The fraction α of monocalcium phosphate crystals in the decomposed part of the complex is equal to the ratio ME'/AE' (lever rule).

c) The ratio S/L of the solid and liquid phases by weight (with allowance for the undecomposed apatite). The value of α can be used for calculation of S/L by means of an equation proposed by Chepelevetsky [12].

The method is described in more detail in Chepelevetsky's publications [6, 12, 13] and in Viktorov's book [15].

We shall use this calculation method and our data on the kinetics of apatite in the system $CaO-P_2O_5-H_2O$ for an analysis of the experimental facts referred to above, which require explanation.

Effect of temperature on the decomposition of apatite in the mixing process. Temperature variations in the range 20-60° (40-100° according to other sources) do not cause an increase in the degree of conversion of chamber superphosphate.* This requires explanation, as the increase of the reactivity of phosphoric acid with temperature is well known. We shall provide an explanation for this experimental fact.

As can be easily shown, when apatite is decomposed by the stoichiometric amount of phosphoric acid, the liquid phase is an acid solution saturated with monocalcium phosphate; its composition varies during the decomposition along the curve FB and can be determined for any instant as described above.

Let us take an original acid containing 55% P_2O_5 at 75°. We draw the solution path of apatite in this acid, PR, in the diagram. This cuts the 75° isotherm at the point Q. This point corresponds to a definite apatite decomposition coefficient, determined by means of the neutralization-path network and equal to 5.4%. This is reached in the first stages of the reaction. On further decomposition, the figurative point of the phase complex shifts to the right along the path PR, passing through the crystallization surface FAB of monocalcium phosphate. This means that at $K \geq 5.4\%$, crystallization of $Ca(H_2PO_4)_2 \cdot H_2O$ takes place during decomposition of apatite, while the liquid phase consists of an acid solution saturated with monocalcium phosphate.

The decomposition rate of apatite according to Equation (I), other conditions being equal, is determined by the hydrogen ion concentration C_{H^+} in the solution, which is a mixture of a weak acid and its salt. The value of C_{H^+} can be calculated from solubility data for the ternary system $CaO-P_2O_5-H_2O[Ca(H_2PO_4)_2-H_3PO_4-H_2O]$ by means of the usual formulas.

In the calculation, allowance was made for the variation of the first dissociation constant of H_3PO_4 with temperature, calculated with the aid of the formula

$$\log Ka = -\frac{1264.51}{T} - 0.01859T + 7.6601 \text{ [16]}. \tag{3}$$

The calculated values of C_{H^+} for saturated solutions at 40, 75, and 100°, and the ratios of C_{H^+} values for pairs of temperatures are given in the table. This table also gives the temperature coefficients of the rate of reaction between apatite and H^+ ions of phosphoric acid for the corresponding temperature intervals, determined experimentally (Column 7) and calculated from experimental data (Column 8). The temperature coefficient is taken to be the ratio of the rate constants at the corresponding temperatures, k_{t_1}/k_{t_2}.

* Here and subsequently, the term "superphosphate" instead of "double superphosphate" is used. The chamber decomposition of apatite is termed the first stage of the process, and decomposition during curing, the second.

A comparison of the data in Columns 2, 3, and 4 shows that as the temperature increases, the concentration of H^+ ions of a saturated solution with a definite P_2O_5 content falls sharply. The most important solutions in superphosphate production contain from 40 to 60% P_2O_5. The calculations were performed for these solutions only. Let us consider the data in Column 5, which relate to them.

Hydrogen Ion Concentrations in Saturated Solutions in the Ternary System $CaO-P_2O_5-H_2O$ at Various Temperatures

P_2O_5 content in solution (%)	Hydrogen ion concentration of solution: $C_{H^+} \cdot 10^3$ mole/liter at temperatures (°C)			Ratios of hydrogen ion concentrations at two temperatures		Temperature coefficient of reaction rate of apatite with the ions	
	40°	75°	100°	$\frac{C_{H+40°}}{C_{H+75°}}$	$\frac{C_{H+75°}}{C_{H+100°}}$	$\frac{k_{75}}{k_{40}}$	$\frac{k_{100}}{k_{75}}$
40	58	18.3	7.8	3.16	2.54	2.82	2.12
45	95	30.2	13.9	3.14	2.27	3.01	2.20
50	148	51.0	21.0	2.90	2.42	3.20	2.28
55	209	79.0	33.6	2.55	2.35	3.27	2.32
60	255	133	65.4	1.91	2.04	3.34	2.32

Increase of temperature from 40 to 75° for a 40% solution decreases C_{H^+} by a factor of 3.16, and for a 50% solution, by a factor of 2.9. At the same time the rate of reaction between H^+ ions and apatite, calculated per gram-ion, increases by factors of 2.82 and 3.20 respectively (Column 7). The combined result of these two effects is that when the temperature is raised from 40 to 75°, the decomposition is slowed down by a factor of 1.12 for a 40% solution, and accelerated by a factor of 1.1 for a 50% solution, so that increase of temperature will not have any significant effect on the decomposition rate of apatite in the chamber.

Let us also compare the data in Columns 6 and 8. Here, as the temperature is increased from 75 to 100°, the reaction is retarded by a factor of 1.03 for a solution with 45% P_2O_5, by a factor of 1.06 for a 50% solution, and 1.01 for a 55% solution, so that there will no be any change in the decomposition rate.

Thus, the resultant effect of two opposing factors due to increase of temperature – acceleration of the reaction between H^+ ions and apatite, and a simultaneous decrease of the H^+ ion concentration in the solution – is that the decomposition rate of apatite in the ternary system $CaO-P_2O_5-H_2O$ is practically independent of the temperature.

This accounts for the experimental fact, established by Voskresensky, Milovanova, and Remen [8], and also by others, that the temperature of the reactants has no significant effect on the chamber decomposition of apatite. This explanation suggests that acceleration of the chamber decomposition of apatite cannot be achieved by an increase of temperature.

Basis for the selection of the optimum initial phosphoric acid concentration. It was shown earlier that the decomposition of the bulk of the apatite in the chamber is effected by saturated solutions in the system $CaO-P_2O_5-H_2O$. Investigation of the kinetics of the reaction of apatite with these solutions showed that the maximum rate is attained when the solution contains 47% P_2O_5 (at 100°) or 46% P_2O_5 (at 75°) and the amounts of CaO and H_2O corresponding to saturation [1, 2].

The process should be so conducted, that at the end of the first (chamber) stage of the process, when a decomposition coefficient of 60% is reached, the liquid phase should contain the above amounts of P_2O_5, which would favor the most rapid decomposition of the residual apatite during the cure.

The choice of the optimum H_3PO_4 concentration depends on the answer to the following question: what should be the initial phosphoric acid concentration in order that when a decomposition coefficient of 60% is reached the liquid phase in the chamber superphosphate should contain 47% P_2O_5 at 100° (46% at 75°)? (these temperatures were chosen owing to the exothermic nature of the process).

We make use of the diagram. With the aid of the neutralization path network, we find the path OD corresponding to $K_{decomp.}$ = 60% (according to Equation (2), Z = 68.5% for this case). On the 100° isotherm we find the point E, the ordinate of which corresponds to 47% P_2O_5. This is the point for the composition of the liquid phase which can be formed at $K_{decomp.}$ = 60% if we have an optimum initial acid concentration. By joining it with point A, we find the crystallization path of monocalcium phosphate. Intersection of AE with OD gives the point M. The point M is the figurative point for the decomposed phase complex when $K_{decomp.}$ = = 60% and the liquid phase contains 47% P_2O_5.

To find the initial phosphoric acid concentration corresponding to these conditions, we draw a straight line through the apatite composition point R and the point M, to its intersection with the ordinate axis at the point H. RH is the solution path of apatite in H_3PO_4. The ordinate of the point H = 55% P_2O_5. This is the required optimum initial H_3PO_4 concentration. If the chamber temperature is 75° , a similar calculation gives 55% P_2O_5.

Consequently, general data on the kinetics of apatite decomposition in the system $CaO-P_2O_5-H_2O$ leads to the conclusion that the optimum initial phosphoric acid concentration corresponds to 55% P_2O_5.

This is confirmed by experimental data on the production of double superphosphate from apatite (Voskresensky, Milovanova, and Remen [8]; P_2O_5 = 54-55% and phosphorite (Bridger and co-workers [10, 11]; P_2O_5 = 54.5-56.7).

Decomposition of phosphate by acid of moderate concentration and nonsetting slurries. A number of authors here and abroad have studied the possibility of attaining high phosphate decomposition coefficients by prolonged stirring; nonsetting slurries were prepared with acid of moderate concentration (about 30% P_2O_5), which can be stirred for up to 6-8 hours instead of the usual 3-5 minutes.

Despite this long time of stirring, the decomposition coefficient remains very low, about 30%. According to Marshall's data [9], when fluor apatite is decomposed by an acid containing 34% P_2O_5 (47% H_3PO_4), $K_{decomp.}$ = 23% is reached during the mixing; for phosphorite $K_{decomp.}$ = 41% is reached after ten minutes and 45% after two hours of stirring, so that the duration of stirring has little effect on the decomposition.

Despite the fact that the acid is taken in the stoichiometric quantity, and even higher, the process does not go any further.

This paradox may be explained by a graphical analysis of the process (see diagram). The original acid with 30% P_2O_5 is represented by the point T on the ordinate axis. We join it to R, thus constructing the path TR for the solution of apatite in this acid.

The figurative point for the decomposed phase complex is shifted to the right along TR during decomposition and meets the 100° isotherm at the point S. By using the neutralization path network and Equation (2) we find that at the point S, $K_{decomp.}$ = 27%. The liquid phase at the point S is a solution saturated with dicalcium phosphate $CaHPO_4$. The diagram shows that at 75° $K_{decomp.}$ = 35 is reached at the point S_1 and the liquid phase is also saturated with $CaHPO_4$.

As was shown previously [1, 2], such a liquid phase hardly acts on apatite because of formation of $CaHPO_4$ films on the apatite grains. The maximum film thickness does not exceed 10μ.

According to sedimentation analysis data, an apatite flotation concentrate contains 37% of grains with diameter less than 44μ [17]. According to the "double thickness" rule, when impermeable films are formed, grains of diameter equal to or less than half the thickness of the film can be completely dissolved. In our case, these are grains less than 20μ in diameter. Allowing for porosity of the film, the diameter can be doubled and it can be assumed that in a nonsetting slurry in which the liquid phase is in equilibrium with $CaHPO_4$ grains less than 40μ in diameter are dissolved. About 40% of such grains is present. The others dissolve only partially, and further decomposition stops.

Therefore, when acid with 30% P_2O_5 is used at 100°, when $K_{decomp.}$ = 27% is reached (or 35% P_2O_5 at 75°) further decomposition will cease owing to formation of impermeable $CaHPO_4$ films in the apatite grains. Graphical analysis shows that at 40° such films will appear when the liquid phase is saturated with $CaHPO_4$ and $Ca(H_2PO_4)_2 \cdot H_2O$ simultaneously, at $K_{decomp.}$ = 60% (point S_2 in the triangle AB'C). In practice, decomposition will be arrested in this case at much lower decompositions. At $K_{decomp.}$ = 60%, the degree of neutralization of

the first hydrogen ion of the acid is 68%. However, as was shown by Chepelevetsky, in an acid of 20% P_2O_5 at 20°, the decomposition rate is only 1/20 of the initial rate even at 50% neutralization [6]. This also applies to other P_2O_5 contents and other temperatures.

For a 30% neutralization of the first H^+ ion of the acid, the decomposition rate is not more than 1/5 of the initial value [18]. In such a case, the reaction may cease long before $K_{decomp.}$ = 60% is reached; namely, when the acid is 30-50% neutralized of when $K_{decomp.}$ = 24-40% is reached, as is confirmed in practice.

The above analysis of phosphate decomposition by acid of moderate concentration reveals the causes of the failure of attempts to reach high decomposition coefficients with the use of nonsetting slurries.

The causes are as follows: a) the high degree of neutralization of the acid in the liquid phase formed during decomposition, so that the process is arrested in the first stage; b) during the cure, the decomposition finally stops as the result of formation of impermeable $CaHPO_4$ films.

It must be emphasized that the above results, obtained by interpretation of kinetic data by means of the solubility diagram do not in themselves finally settle the question of the optimum conditions for double superphosphate production or explain all the peculiarities of the process, which is a complex topochemical reaction. Diverse heterogeneous processes which occur in the solid product of the reaction between the acid and apatite must be taken into consideration.

In conclusion, I express my deep gratitude to E. B. Brutskus and M. L. Chepelevetsky for joint discussions of this paper and for their valuable comments.

SUMMARY

Solubility data for the system $CaO-P_2O_5-H_2O$ and data on the kinetics of apatite decomposition in saturated solutions of this system have been used to calculate the optimum conditions for double superphosphate production.

The negligible influence of temperature on the chamber decomposition of apatite during mixing is explained by the fact that the decomposition rate of apatite in solutions in the system $CaO-P_2O_5-H_2O$ is practically independent of the temperature (this is the result of two opposing factors which follow from an increase of temperature: increased reaction of H^+ ions with apatite, and a simultaneous decrease of the H^+ ion concentration in the solution).

There are two reasons for the failure of attempts to attain high decomposition coefficients with the use of nonsetting slurries:

a) The high degree of neutralization of the acid in the liquid phase formed during decomposition, so that the process is arrested in the first stage;

b) During the cure, the decomposition finally stops as the result of formation of impermeable $CaHPO_4$ films on the apatite grains.

The optimum phosphoric acid concentration is 54-55% P_2O_5.

LITERATURE CITED

[1] K. S. Krasnov, J. Appl. Chem. 26, 1114 (1953)(T. p. 1057).*

[2] K. S. Krasnov, J. Appl. Chem. 28, 12, 1275 (1955)(T. p. 1233).*

[3] Trans. Sci. Inst. Fertilizers and Insectofungicides (State Chem. Press, 1932) 109.

[4] Chemical Industry in the Struggle for the Harvest (State Chem. Tech. Press, 1934).

[5] Trans. Sci. Inst. Fertilizers and Insectofungicides (Chem. Theoret. Press, 1935), 132.

[6] M. L. Chepelevetsky, "Physicochemical investigations in the field of acid conversion of phosphates," Trans. Sci. Inst. Fertilizers and Insectofungicides (Chem. Theoret. Press, 1937), 137.

[7] N. N. Postnikov, I. I. Orlov, and N. I. Kryuchkov, J. Chem. Ind. 14, 729 (1937).

[8] Trans. Sci. Inst. Fertilizers and Insectofungicides (State Chem. Press, 1940), 153.

* T. p. = C. B. Translation pagination.

[9] H. Marshall, L. Rader and K. Jacob, Ind. Eng. Chem. 25, 11, 1253 (1933).

[10] G. Bridger, R. Burt and W. Cerf, Ind. Eng. Chem. 37, 9, 829 (1945).

[11] G. Bridger, G. Willson and R. Burt, Ind. Eng. Chem. 39, 10, 1265 (1947).

[12] M. L. Chepelevetsky, Dissertation (VAKhZ, Moscow 1947).

[13] M. L. Chepelevetsky, Ann. Sector Phys. Chem. Anal. 19, 326 (1949).

[14] K. Elmore, T. Farr, Ind. Eng. Chem. 32, 4, 580 (1940).

[15] M. M. Viktorov, Graphical Calculations in Mineral Technology (State Chem. Press, 1954).

[16] H. Harned and B. Owen, Physical Chemistry of Electrolytic Solutions (Foreign Lit. Press, Moscow, 1952).

[17] L. B. Grinshpan and M. I. Kobrin, J. Chem. Ind. 3, 1 (1950).

[18] G. S. Krasnov, Dissertation (Odessa State University 1950).

Received May 31, 1955

PHENOMENA AT THE INTERPHASE IN BOILING SOLUTIONS

V. G. Gleim and I. K. Shelomov

Department of Chemistry, the Rostov-on-Don Institute of Railroad Transport Engineers

The main laws which govern the ejection of droplet moisture from boiling solutions were considered in a series of previous papers from this department [1, 2]. The present paper deals with an investigation of the composition of the liquid phase in the vapor phase and therefore, with an examination of the problem of the so-called selectivity of carry-over.

Composition of the Liquid Phase Carried Away From the Surface of a Boiling Solution

To determine the possible composition of a drop generated into the vapor space by the evaporation surface of a boiling liquid, we consider the following cycle. 1) The drop is detached from the solution surface. The total energy expenditure in the process is denoted by $-E_1$. 2) The concentrations of the drop and solutions are equalized, yielding work +A. 3) The drop is introduced into the solution. The energy obtained in the process is denoted by $+E_2$.

The energy balance of this cycle will have the form

$$E_2 - E_1 + A = 0.$$

Let us consider limiting cases of the above cycle.

1) Let the cycle be performed reversibly, with the drop detachment process lasting an infinitely long time. Then the excess of electrolyte in the newly forming surface layer should diffuse into the solution. Diffusion into the drop should lead (because $V_{drop} \ll V_{solution}$) to the spontaneous formation of a concentration gradient between the drop and the solution. This would evidently contradict the principle that equilibrium can only be disturbed from outside, as the drop still forms a part of the solution.

If we regard the introduction of a drop into the solution also as a reversible process, the same processes would occur, but in the opposite direction.

Returning to the energy balance of this cycle, as shown above, we have, in virtue of its reversibility,

$$E_1 = E_2 \text{ and therefore, } A = 0. \qquad (2)$$

It follows that the concentration distributions in the surface layer and the bulk are identical for the drop and the main mass of the solution, or

$$C^{surface}_{drop} = C^{surface}_{soln}$$
$$C^{volume}_{drop} = C^{volume}_{soln} \qquad (3)$$

To characterize the composition of the drop and solution, we introduce the concept of average drop concentration ($C^{av}_{1\ drop}$).

This concentration can evidently be represented as follows:

$$C_{1\,drop}^{av} = C_{drop}^{surface} X_{drop} + C_{drop}^{volume}(1 - X_{drop}), \qquad (4)$$

where X_{drop} is the fraction of surface layer in the drop.

The average concentration of the solution is evidently equal to its volume concentration.

2) Let the cycle be performed irreversibly, with the drop detachment process lasting an infinitesimally short time.

Since we are considering a limiting case, the value of the work will reach a maximum.

In virtue of the irreversibility of the cycle, $E_1 > E_2$ and $A_{max} = E_1 - E_2 > 0$.

In the case under consideration, the concentrations do not have time to be completely equalized. If we do not consider entrapment of the surface layer, which is discussed later, then the average concentration in the drop will be equal to the concentration of the region of solution in which it is formed. This is a consequence of the impossibility of the spontaneous formation of a concentration gradient in the region where the drop is detached before its instantaneous formation.

Electrolyte diffuses from the surface into the detached drop until equilibrium is established.

It is evident that the surface and volume concentrations in this drop are greater than their corresponding solution concentrations, i.e.,

$$\begin{aligned} C_{drop}^{surface} &> C_{soln}^{surface} \\ C_{drop}^{volume} &> C_{soln}^{volume} \end{aligned} \qquad (5)$$

These values are connected by the relationship

$$C_{2\,drop}^{av} = C_{drop}^{surface} X_{drop} + C_{drop}^{volume}(1 - X_{drop}) = C_{soln}^{volume}, \qquad (6)$$

where $C_{2\,drop}^{av}$ is the average concentration in the drop.

The connection between the average drop concentrations in the two cases considered (C_{1drop}^{av} and C_{2drop}^{av}) is given by the following equation

$$A_{max} = RT \ln \frac{C_{2\,drop}^{av}}{C_{1\,drop}^{av}}$$

or, taking Equation (6) into consideration,

$$C_{1drop}^{av} = C_{soln}^{volume} e^{-\frac{A_{max}}{RT}}. \qquad (7)$$

As already stated, both these are limiting cases. Obviously, in reality the detachment of the drop occurs over a certain finite time interval. Partial equalization of the drop and solution concentration occurs during this time.

In this case, the work of equalization is less than the maximum value, i.e., $A_{max} > A > 0$.

The relationship between the average drop concentrations for the first of the above cases and the real process, analogously to Equation (7), will be

$$C^{av}_{1\,drop} = C^{av}_{drop}\, e^{-\frac{A}{RT}}, \tag{8}$$

where C^{av}_{drop} is the average concentration of a real drop.

To determine the relationship between the volume concentration of the solution and the average concentration of the drops formed from it during boiling, we use Equations (7) and (8)

$$C^{av}_{drop} = C^{volume}_{soln}\, e^{-\frac{A_{max} - A}{RT}}. \tag{9}$$

Therefore,

$$C^{av}_{1\,drop} \leq C^{av}_{drop} \leq C^{volume}_{soln}. \tag{10}$$

From Equation (4) it follows that

$$C^{av}_{1\,drop} \geq C^{surface}_{drop}, \text{ but } C^{surface}_{drop} = C^{surface}_{soln},$$

and hence,

$$C^{surface}_{soln} \leq C^{av}_{drop} \leq C^{volume}_{soln}, \tag{11}$$

that is, the average drop concentration lies between the surface and volume concentrations of the solution.

Relationship Between the Average Composition and the Size of a Drop

The volume fraction of the surface layer in the drop is

$$x_{drop} = \frac{S\delta}{V},$$

where S is the surface area of the drop, V is its volume, and δ is the thickness of the surface layer, or

$$x_{drop} = \frac{3\delta}{r}, \tag{12}$$

where r is the drop radius.

In accordance with Equation (4),

$$C^{av}_{1\,drop} = \frac{3\delta}{r} C^{surface}_{drop} + \left(1 - \frac{3\delta}{r}\right) C^{volume}_{drop}.$$

The thickness of the surface layer can be taken [3] as 10^{-7} to 10^{-8} cm.

Consequently, even for radii of the order of 10^{-5} cm the influence of the surface layer in the drop is practically negligible. Therefore, it can be assumed that

$$C^{av}_{1\,drop} = C^{volume}_{drop} = C^{volume}_{soln}.$$

From Equation (10),

$$C_{drop}^{av} = C_{soln}^{volume} \,.$$

Thus, the average concentration of a drop (for all drops $r \geq 10^{-5}$cm) does not differ from the volume concentration of the solution.

For drops with radius of the order of 10^{-6} cm, the influence of the surface layer will always be less than 10%.

Relationship Between the Composition of the Surface Layer and the Volume Composition of the Boiling Liquid

As was shown by Rebinder [3], water in solutions of inorganic salts is a powerful surface-active agent. Therefore, in the dilute solution region, strong adsorption of water on the surface is to be expected. The contents of inorganic components in the surface solution may be considerably lower than in an equal volume of the bulk solution. These concentrations should tend to become more or less equal with increase of temperature. Differences in negative salt adsorption are too small to alter the relationship between the inorganic content of the surface layer and that of the bulk of the solution.

To verify these views for a number of solutions important from the point of view of boiler chemistry, we studied the surface tensions of such systems.

The measurements were performed over the 20 to 90° temperature range by determination of maximum bubble pressure [3].

The temperatures were recorded to the nearest 0.05°. The results are given in Tables 1 and 2, and in the figure.

TABLE 1

Solution Concentration 1 molar %

Temperature (°C)	σ_{NaCl}	σ_{NaOH}	$\sigma_{Na_2SO_4}$	$\sigma_{Na_2CO_3}$	σ_{MgSO_4}
20	74	74.3	74.4	74.2	74.1
30	72.5	72.7	72.9	72.7	72.6
40	70.8	71.1	71.1	71.2	71
50	69.2	69.5	69.7	69.6	69.4
60	67.4	67.7	67.9	67.7	67.4
70	65.7	66.0	66.0	65.9	65.8
80	64.4	64.4	64.3	64.3	64.1
90	62.3	62.3	62.5	62.4	62.0

TABLE 2

Solution Concentration 2 molar %

Temperature (°C)	σ_{NaCl}	σ_{NaOH}	$\sigma_{Na_2SO_4}$	$\sigma_{Na_2CO_3}$	σ_{MgSO_4}
20	74.8	75.5	75.5	75.6	75.2
30	73.2	74	74.4	74	73.7
40	71.6	72.2	72.7	72.3	72.1
50	70	70.8	71.1	70.8	70.4
60	68.2	69.1	69.4	69.0	68.6
70	66.5	66.9	67.7	67.1	67.0
80	64.8	65.5	65.8	65.4	65.1
90	63.0	63.6	64.0	63.5	63.3

Examination of the above data shows that the differences of surface tension of the salt solutions studied are not great for equal molar % concentrations. This gives reason to believe that desorption of salts from the surface will not be selective in character, and all salts will be desorbed to approximately the same extent.

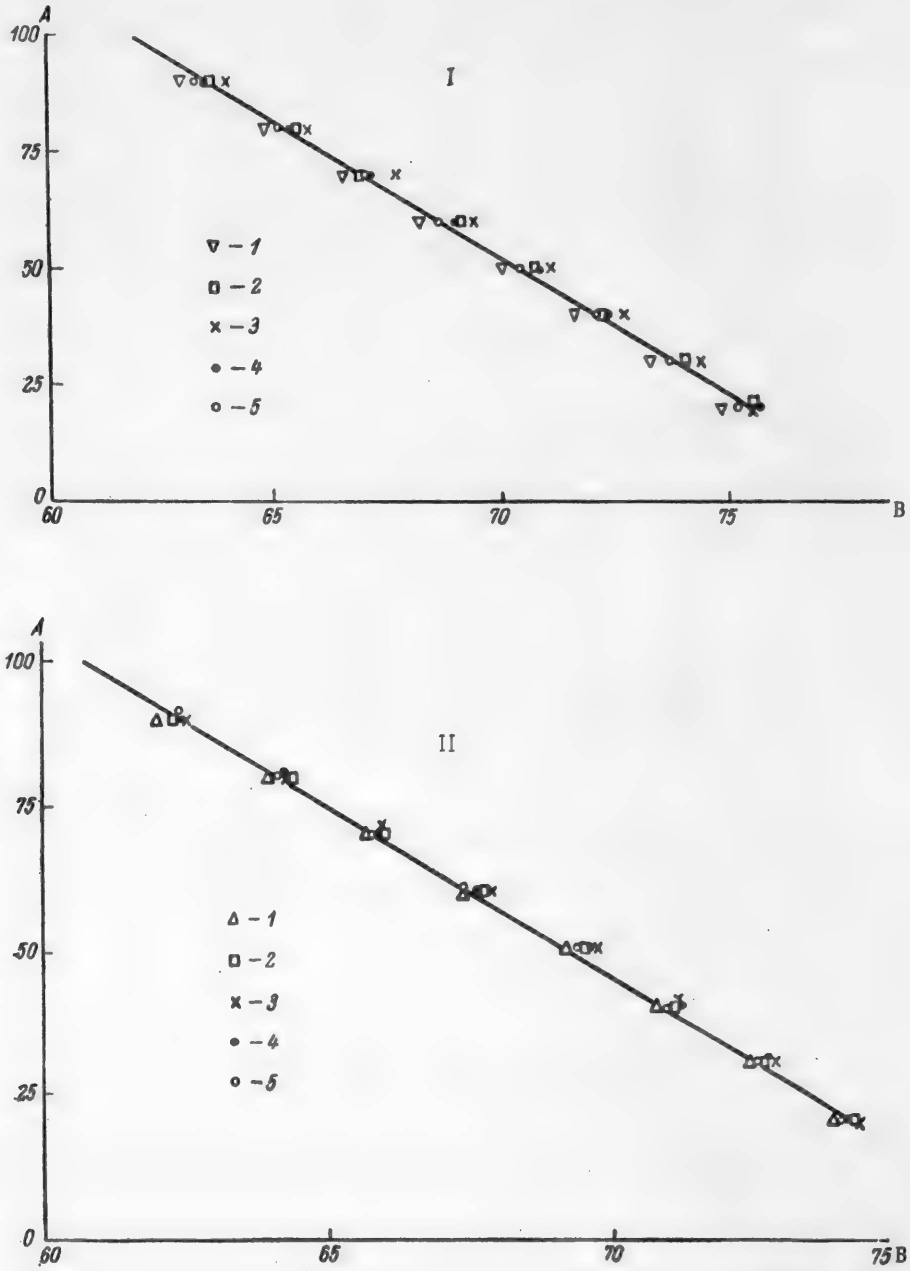

Surface tension of some electrolyte solutions as a function of temperature.
A) Temperature (°C); B) surface tension (in ergs/cm^2).
Electrolyte concentrations (in molar %) : I) 1, II) 2.
Electrolytes: 1) NaCl, 2) NaOH, 3) Na_2SO_4, 4) Na_2CO_3, 5) $MgSO_4$.

Thus, although the surface layer will be impoverished by loss of salts, the proportions of the concentrations of these salts in the surface layer will remain constant.

Tables 3 and 4 show differences between the surface tension of water and the surface tensions of solutions.

TABLE 3

Solution Concentration 1 molar %

Temperature (°C)	σ_{H_2O}	$\Delta\sigma_{NaCl}$	$\Delta\sigma_{NaOH}$	$\Delta\sigma_{Na_2SO_4}$	$\Delta\sigma_{Na_2CO_3}$	$\Delta\sigma_{MgSO_4}$
20	72.75	1.25	1.56	1.65	1.45	1.35
30	71.18	1.32	1.52	1.72	1.72	1.42
40	69.56	1.24	1.54	1.54	1.64	1.44
50	67.91	1.29	1.59	1.79	1.69	1.49
60	66.18	1.22	1.52	1.72	1.52	1.22
70	64.12	1.28	1.58	1.58	1.48	1.38
80	62.61	1.79	1.79	1.69	1.69	1.49
90	60.75	1.55	1.55	1.75	1.65	1.25

TABLE 4

Solution Concentration 2 molar %

Temperature (°C)	σ_{H_2O}	$\Delta\sigma_{NaCl}$	$\Delta\sigma_{NaOH}$	$\Delta\sigma_{Na_2SO_4}$	$\Delta\sigma_{Na_2CO_3}$	$\Delta\sigma_{MgSO}$
20	72.75	2.05	2.75	2.75	2.85	2.45
30	71.18	2.02	2.82	3.22	2.82	2.52
40	69.56	2.04	2.64	3.14	2.74	2.54
50	67.91	2.09	2.89	3.19	2.89	2.49
60	66.18	2.02	2.92	3.22	2.82	2.42
70	64.42	2.08	2.48	3.28	2.68	2.58
80	62.61	2.19	2.89	3.19	2.79	2.49
90	60.75	2.25	2.85	3.25	2.75	2.55

It follows from these results that $\sigma_S - \sigma_{H_2O} = \text{const}$, where σ_S is the surface tension of solution and σ_{H_2O} is the surface tension of water, so that $\Delta\sigma$ is independent of the temperature.

The deviations from this rule observed at 80-90° can be attributed to experimental error, which increases at these temperatures for a number of reasons.

Differentiation with respect to temperature gives

$$\frac{\partial\sigma_S}{\partial T} - \frac{\partial\sigma_{H_2O}}{\partial T} = 0 \quad \text{or} \quad \frac{\partial\sigma_S}{\partial T} = \frac{\partial\sigma_{H_2O}}{\partial T}.$$

Denoting by σ_S' the surface tension of the solution at some fixed temperature T_1, we have $\sigma_S = \sigma_S' + \frac{\partial\sigma_S}{\partial T}(T - T_1)$ or $\sigma_S = \sigma_S' + \frac{\partial\sigma_{H_2O}}{\partial T}(T - T_1)$.

Evidently the term $\frac{\partial\sigma_{H_2O}}{\partial T}(T - T_1)$ is independent of the concentration. Differentiation with respect to concentration gives $\frac{\partial\sigma_S}{\partial C} = \frac{\partial\sigma_S'}{\partial C} \neq f(T)$.

Consequently, the temperature coefficient of surface tension of a solution does not depend on the nature of the electrolyte or the composition, and is always equal to the temperature coefficient of surface tension of water. Surface activity, being a function of the composition and nature of the substance, is independent of the temperature.

However, if $\partial\sigma/\partial C \neq f(T)$, adsorption will be inversely proportional to the temperature, i.e., the concentration difference between the surface and the volume of the solution will vary inversely with the temperature.

Since the concentrations in the surface layer are proportional to the surface activities of the components, it is evident that the proportions of the components will remain constant at all temperatures. It is, therefore, permissible to extrapolate to high temperatures, the data obtained at room temperature.

It follows from all the foregoing that adsorption effects cannot have any significant influence on the composition of even very small drops ($r \sim 10^{-6}$).

SUMMARY

1. Selective carry-over of salts by a liquid phase from a boiling solution is thermodynamically impossible.

2. The composition of the surface layer approaches the composition of the boiler water with increase of temperature (in direct proportion to the temperature).

3. The proportions between the inorganic salt concentrations in the surface layer are similar to those in the solution and are independent of the temperature.

These results are obviously not applicable to colloids and suspensions, as such systems are not in thermodynamic equilibrium.

The question of colloids and suspensions requires a special study.

LITERATURE CITED

[1] V. G. Gleim, J. Appl. Chem. 26, No. 11 (1953).

[2] V. G. Gleim, J. Appl. Chem. 28, No. 1. (1955).

[3] P. A. Rebinder, "Properties and structure of surface layers in solutions," in Symposium: Molecular Forces and Their Electrical Nature (1929).

Received January 20, 1956

HYDRODYNAMICS OF EMERSION

II. HYDRODYNAMIC CONDITIONS IN THE ASCENT OF A GAS THROUGH A LIQUID LAYER

R. A. Melikyan *

Processes based on the ascent of gases through liquid layers have been described in various terms — bubbling, foam process, bead conditions, etc. However, these terms and the processes which they represent have not been thermodynamically defined. Therefore, classification of processes observed in practice involves enormous difficulties; moreover, in absence of defining criteria, such a classification is meaningless.

This can be illustrated by the following example: as is known, Pozin, Mukhlenov, et al. [1-3] found on the basis of experimental data obtained in studies of mass and heat transfer in processes of mass ascent of gas bubbles through liquids that, in addition to bubbling, there is a special hydrodynamic regime which they term the foam process. Kuzminykh, Akselrod, et al. [4] consider that a new term (foam) should not be artificially introduced, as this may be a special case of bubbling conditions existing in plates within a definite range of gas speeds. The same case has been termed the streaming regime by Akselrod and Dilman [5] only because during their experiments, the gas entered the liquid layer in the form of a stream.

It is seen that the same process has been given three different names, and at present it is difficult to establish which of them corresponds to reality and what hydrodynamic regime is to be described by a given term.

The purpose of the present communication is to fill this gap by an examination of the possible hydrodynamic regimes in the ascent of a gas in a liquid layer.

The hydrodynamic character of the process which takes place in the ascent of a gas through a liquid layer is determined by the gas content of the mixed layer.

At low gas contents, irrespective of the method by which the gas is introduced, free ascent of individual bubbles through the liquid layer always occurs. In this instance, even if the gas is introduced in the form of a stream, the latter immediately divides into individual bubbles if the inertia force of the gas jet does not exceed the hydrostatic pressure of the liquid layer.

This hydrodynamic regime is generally termed the bubbling process for mass ascent of bubbles, and the bead regime for the emersion of single bubbles.

In the previous communication [6] the free ascent of bubbles through a liquid layer was considered; it was established that it comprises a complex hydrodynamic process which occurs by means of three coexisting streams: 1) the stream of ascending bubbles, 2) the stream of descending liquid, and 3) the stream of ascending gas–liquid mixture.

In the mass ascent of gas bubbles the hydrodynamical picture is made more complicated because the process is accompanied by coalescence of small and disintegration of large bubbles [7].

Moreover, the values [5] and profiles [6] of the speeds of the main streams vary considerably with the gas feed rate (bubble concentration), the initial height of the liquid payer, and the bubble size.

* K. T. Oganesyan participated in the experimental work.

Independently of the above complications, in these conditions each of the main streams has a certain average speed. This does not reflect the true magnitude of the displacement of all the material particles of the gas or liquid in the given stream, since the velocity profiles of the streams are complex in nature. However, it is possible to use average resultant values for these stream velocities.

In this process the volume displacement in unit time is the same in all three streams [6], and its value depends on the amount of incoming gas.

We can therefore write:

$$w_s = \frac{v_{sec}}{F_g}, \tag{1}$$

$$w_1 = \frac{v_{sec}}{F - F_g}; \tag{2}$$

$$w_m = \frac{v_{sec}}{F}; \tag{3}$$

where v_{sec} is the volume of gas entering per second; F is the cross section of the vessel; F_g is the cross section of the vessel occupied by the gas; w_s is the resultant average speed of bubble ascent; w_1 is the average speed of the descending liquid stream; w_m is the average speed of ascent of the gas–liquid mixture. By combining Equations (1), (2), and (3), we have

$$w_1 = \frac{w_m}{1 - \frac{w_m}{w_s}} \tag{4}$$

Equation (4) shows that the free ascent regime does not extend beyond the $\frac{w_m}{w_s} < 1$ region, which ends fairly early: in mass ascent w_s decreases with increase of w_m, other conditions being equal [4, 8], while in the ascent of consecutive single bubbles w_s increases [6], but the rate of its increase lags considerably behind w_m.

Transition from the regime evidently occurs at a definite finite value of w_1 before $\frac{w_m}{w_s} = 1$, when it reaches infinity.

At the moment of transition, w_1 attains its highest value in the given conditions; the liquid occupies the minimum and the gas the maximum cross section of the vessel.

By combining Equations (4) and (3), referred to this moment, we have

$$(w_m)_{cr} = \frac{(F_g)_{max}}{F} \cdot w_s. \tag{5}$$

The relationship $H = \left(1 + \frac{w_m}{w_s}\right) h$ [6] and Equation (5) gives

$$H_{cr} = \left[1 + \frac{(F_g)_{max}}{F}\right] h, \tag{6}$$

where H is the height of the gas–liquid mixture and h is the height of the liquid.

As, in all cases, $\frac{F_g}{F} < 1$, it is always true that

$$\left[1 + \frac{(F_g)_{max}}{F}\right] < 2 \text{ and } \frac{H_{cr}}{2} < 2, \tag{7}$$

from which it follows that in the free ascent of bubbles the content of gas in the layer of mixture is always less than half the layer.

According to Equation (5) the physical meaning of the moment of transition is that the gas volume in the layer of mixture reaches a limiting value when its upward displacement is possible only in the form of a continuous stream which occupies the maximum fraction, in these conditions, of the vessel cross section. Further continuance of the free ascent of individual bubbles, therefore, becomes impossible. Equation (4) shows that only two transition routes are possible.

1) In absence of special conditions which ensure the stability of the ascending bubbles as separate phase units, they coalesce into a continuous stream of gas, and as a result, the rate of emersion of the gas rises sharply; w_s is replaced by the speed of the stream (w_j), which is very much greater. Therefore, the condition $\frac{w_m}{w_j} < 1$ is always obeyed in the process, and the sign of w_1 (Equation 4) remains unchanged, so that the direction of the descending liquid stream is unaltered. This transition route is usual, and with high layers of liquid, it is the only route (apart from surface foaming). After the transition, only the descending liquid stream survives of the former streams; the other two disappear and two new streams appear: the continuous stream of gas and an ascending liquid stream. This last originates as the result of liquid friction between gas and liquid, and is therefore found in the immediate vicinity of the interphase. In wide vessels, the situation may be complicated by the formation of spray and mist in the gas stream. This regime, which can be described as the continuous stream regime in a narrow vessel (tube) was studied by Semenov [9]. We will consider it separately. At the start of the transition, the continuous stream regime will not be stable because to maintain it, the feed rate of the gas must be considerably above the critical speed $(w_m)_{cr}$. At the moment of transition, as soon as coalescence of the bubbles is complete, the gas breaks through the layer at the speed of the stream, with a consequent sharp decrease in the gas content of the mixture, and the free ascent of bubbles is restored; the whole cycle is then repeated again. This alternation of the regimes covers a wide range of gas speeds, from $(w_m)_{cr}$ up to quantitative equalization of the gas entering the layer with the gas leaving the layer as a continuous stream, i.e., up to

$$(w_g)_{cr} = \frac{(F_g)\max}{F} \cdot w_j, \tag{8}$$

where w_g is the virtual gas speed $= w_m$. The alternation of the regimes is accompanied by large fluctuations of the level of the mixture (pulsation), the level falling in continuous stream conditions and rising in conditions of free bubble ascent. This transition has been experimentally observed by Kuzminykh et al. [4].

2) When the process obeys the condition $\frac{w_m}{w_s} > 1$, w_1 (Equation 4) becomes negative, so that the descending liquid stream now ascends. As the direction of this stream coincides with the direction of the mixture, the two combine; instead of the previous three streams, there are now two: ascending liquid and emerging gas. The number of streams may decrease to one if the rates of displacement of the gas and liquid become equal. In this transition, the gas should retain the order of magnitude of its former rate of ascent, which is possible only if the nature of the liquid and the hydrodynamic conditions of the process confer such stability to the bubbles that they can withstand the condensing action of the layer of mixture at the moment of transition. It has been shown [9] that at such speeds of gas ascent, the forces of viscous friction are far from sufficient for the formation of a descending liquid stream. Evidently this role is played by forces which confer stability on the bubbles. Because of these forces, the liquid film around the bubbles becomes either stationary or renewable and stable in character [2]. Thus, this transition route involves foam formation.

Foam formation depends on the nature and stability of the foam films. If the latter are renewable, two ascending streams operate in the foam regime. There is then very intensive mass and heat exchange between the phases [1, 3, 6]. If the foam films are stationary, only one stream of the mixture (foam) operates.

As has been shown (Equation 7), the transition occurs at a gas content of less than half the mixture, and therefore, at the start of the transition, the foam layer is able to hold only a small part of the liquid, retained by the gas in the form of foam films. The main bulk of the liquid remains under the foam layer, where another regime is established, most commonly of a mixed character. Therefore, the transition will be accompanied by a sharp fall in the level of the mixture and the formation of a minimum on the curve.

The end of this mixed regime and the start of the foam regime can be defined by the condition

$$(w_g^f)_{cr} = k_f w_f \tag{9}$$

where $(w_g^f)_{cr}$ is the critical gas speed, k_f is the gas–liquid volume ratio in the foam layer, w_f is the renewal rate of the foam films.

Such are the hydrodynamic regimes in the ascent of a gas through a liquid layer. A further, more detailed study of the process from the aspects touched upon, would give a clearer hydrodynamic picture of these regimes.

EXPERIMENTAL

The apparatus described in the previous paper [6] was used to carry out two series of experiments : 1) the heights of the layer of mixture were measured for various initial heights of the distilled water layer and for different air feed rates, supplied into the layer in the form of columns of successive bubbles; 2) similar measurements were performed with mass foaming of small bubbles (average diameter about 3 mm at the start of ascent). In this series of experiments, the air was supplied into the layer by means of a glass bubbler plate with 20 holes instead of a nozzle. The average hole size was 1.3 mm. At low air feed rates, some of the holes remained inactive.

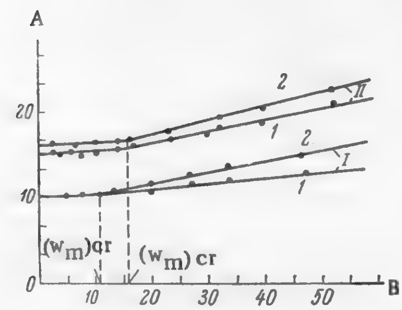

Fig. 1. Variation of the average speed of ascent with gas speed.
First tube d = 14 mm (I), second tube d = 20 mm (II).
A) Average ascent speed $(w_s)_{av}$ (in cm/sec.), B) gas speed w_m (in cm/sec). Initial height of liquid layer $\underline{h}$ (in cm): 1) 30, 2) 50.

The experiments showed that the initial height of the liquid layer has a decisive influence both on the ascent speed of the gas, and on the nature of the hydrodynamic regime which prevails. The ascent speed of consecutive bubble columns slowly increases with layer thickness; the same effects occur, but to a greater extent, in mass bubble ascent. Because of this, transition does not occur simultaneously at different heights in the layer; different regimes are established at different heights of the layer and the transition effect is smoothed out appreciably in high layers of mixture.

Fig. 1 shows the course of the variation of the average rate of ascent of successive bubbles in columns, with the gas speed. The transition is clearly shown by breaks in the lines for both tubes. The experimental points refer to initial heights of 30 and 50 cm for the liquid layers; the transition is less pronounced with thicker layers.

The transition points on the graphs show that the ratio $\frac{(F_g)max}{F}$ is close to unity.

After the transition, the level of the mixture begins to fluctuate increasingly with increasing gas flow rate. This makes exact determination of the layer height difficult. At high gas speeds (above 0.7 m/second) measurement becomes almost impossible. The points in Fig. 1 represent the results of numerous experiments, the maximum level being taken.

Fig. 2 gives curves for the variation of the average speed of ascent with gas speed for mass bubble ascent. Curve 1 shows that when the initial layer height is 50 cm, the transition is less pronounced. In this case, the decrease in the height of the layer with increasing gas speed is partly compensated by the accelerating influence of the initial height of the layer, and at low gas speeds it is even possible to observe visually, the growth of the bubble during its ascent.

For an initial layer height of 30 cm (Curve 2) the transition is clearly and sharply defined. It is accompanied by the formation of columns of gas in the mass of the mixture. The gas columns arise in the center of the tube and then spread rapidly and approach the periphery. The moment of their appearance is clearly indicated by deepening of the color the the mixture at these points.

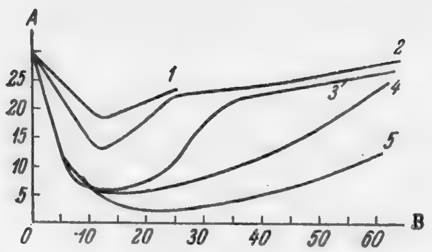

Fig. 2. Variation of the average speed of ascent with gas speed.
A) Average ascent speed $(w_s)_{av}$ (in cm/sec.), B) gas speed w_m (in cm/sec.). Initial height of liquid layer h (in cm): 1) 50, 2) 30, 3) 20, 4) 10, 5) 2.5 (from the data of Kuzminykh et al. [4]).

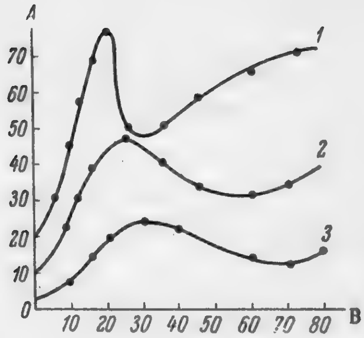

Fig. 3. Variation of the height of the layer of mixture with gas speed.
A) Height of layer h_m (in cm), B) gas speed w_m (in cm/sec.)
Initial height of liquid layer h (in cm): 1) 20, 2) 10, 3) 2.5

With initial layer heights of 20 and 10 cm (Curves 3 and 4) the process is accompanied by foam formation. This begins at low gas speeds in our conditions at 0.03 m/second. The foam layer appears on the surface of the mixture, and then deepens with increasing gas speed. The presence of the foam layer distorts the true picture of the variation of the average ascent speed, and therefore the transition point on the curves is displaced and spread out; this is more pronounced with smaller initial layer heights. This is clearly seen in Curve 5, based on the data of Kuzminykh et al. [4]. The transition point in foam formation is more clearly seen on curves for the variation of layer height with gas speed, shown in Fig. 3.

As was to be expected, the level of the mixture falls sharply at the transition point, and then begins to rise. This is less pronounced with very thin initial layers of liquid (Curve 3).

The curves in Fig. 2 show that the tendency to foam formation increases with decrease of the initial liquid layer thickness. The explanation is that the bubbles do not have time to coalesce in ascending through a thin liquid layer, and are therefore, more capable of foam formation.

SUMMARY

1. The ascent of a gas through a liquid layer may occur in regimes which differ in nature and fundamental hydrodynamic characteristics, and which may be distinguished by appropriate criteria.

2. At low gas speeds, the regime (a), consisting of the free ascent of bubbles through the liquid medium, is established; this is usually termed the bubbling process. Three streams operate in these conditions: the stream of the ascending bubbles, the stream of descending liquid, and the stream of ascending gas–liquid mixture. The speeds of these streams are interrelated by the equation $w_l = \frac{w_m}{1 - \frac{w_m}{w_s}}$.

3. When the speed of the mixture reaches a value of $(w_m)_{cr}$, regime (a) passes into the mixed regime (b). This consists of an alternation of regime (a) with the continuous streaming regime (c). It is a transitional regime: as the gas speed increases, the fraction occupied by (a) diminishes and disappears at a gas speed equal to $(w_g)_{cr}$.

4. In the region $w_g \geq (w_g)_{cr}$ the stable continuous streaming regime (c) is established. Here, three continuous streams operate: streams of ascending and descending liquid, situated around the gas stream.

5. In a high liquid layer, the transition occurs at different times at different heights in the layer, so that different hydrodynamic regimes prevail at different levels in the layer.

6. Under special conditions, regime (a) can pass into the foam regime. Depending on the nature of the foam films, one or two streams operate in this regime. At the start of the transition, the foam originates on the surface of the mixture; with increase of gas speed, the foam layer deepens and embraces the whole layer at a gas speed defined by $(w_g^f)_{cr} = k_f w_f$.

LITERATURE CITED

[1] M. E. Pozin, I. P. Mukhlenov, E. S. Turmakina, and E. Ya. Tarat, J. Appl. Chem. 27, 12 (1954) (T.p.9).*

[2] M. E. Pozin, E. S. Turmakina, J. Appl. Chem. 27, 1170 (1954) (T. p. 1109).*

[3] I. P. Mukhlenov and E. S. Turmakina, J. Appl. Chem. 28, 135, 345 (1955) (T.p. 125, 323).*

[4] I. N. Kuzminykh, L. S. Akselrod, Zh. A. Koval, and A. I. Rodionov, J. Chem. Ind. 2, 86 (1954).

[5] L. S. Akselrod and V. V. Dilman, J. Chem. Ind. 1, 28 (1954)

[6] R. A. Melikyan, J. Appl. Chem. 29, No. 12 (1956).

[7] K. N. Shabalin, Friction Between Gas and Liquid in the Technology of Absorption Processes (Metallurgy Press, 1943).

[8] I. N. Kuzminykh and Zh. A. Koval, J. Appl. Chem. 28 (1955).

[9] P. A. Semenov, J. Tech. Phys. 14, Nos. 7-8 (1944).

Received July 2, 1955

* T. p. = C. B. Translation pagination.

NATURE OF THE GAS–LIQUID DISPERSE SYSTEM*

M. E. Pozin, I. P. Mukhlenov, and E. Ya. Tarat

The Lensoviet Technological Institute, Leningrad

Processes which occur in the ascent of single gas bubbles through liquid layers have long been studied. The Soviet literature contains more than twenty publications on the subject; many investigations have also been reported in foreign publications. This problem is also dealt with in Melikyan's paper [1]; the author studied the ascent of bubbles in liquid layers in long and relatively narrow tubes, and investigated the hydrodynamics of the gas and liquid streams which arise in the process. His work will help to elucidate the operation of narrow gas lifts in which the ratios of the diameters of the tube and gas bubbles are similar to those investigated by him.

However, in our opinion Melikyan's proposed quantitative expression of the speeds of the streams of ascending bubbles, descending liquid, and ascending gas–liquid mixture is not accurate, even when applied to narrow gas lifts. The speed of the descending liquid stream is incorrectly referred to the whole cross section occupied by the liquid [1] (Formula 2), as part of the cross section should be referred to the ascending liquid stream, entrained by the gas bubbles as the result of friction. Melikyan's assumption of the existence of three coexistent streams, in general valid with reference to narrow gas lifts, is inappropriately used by him to explain the hydrodynamics in bubbling and foam equipment. The hydrodynamics of sieve and cap equipment used in industry differs in principle from the hydrodynamics of gas lifts, primarily by the absence of a stream of ascending gas–liquid mixture. The statistical average speed of the liquid is such that the projection of its vector on the vertical axis is zero, i.e., all the vertical pulsations of the liquid mutually cancel each other. Therefore the concepts of "average speed of the descending liquid stream" and "average speed of ascent of the gas–liquid mixture" used by Melikyan, and considered by him to be "determining criteria," are not applicable to sieve and cap apparatus. Although the author refers to our publications (see pages 39 and 40 of this issue) in asserting that if the foam films "are renewable, two ascending streams operate in the foam regime" and that "if the foam films are stationary, only one stream of mixture (foam) operates" these assertions are by no means in agreement with our experiments and do not follow from them.

It must be pointed out that Melikyan, like many other workers, identifies the height of the overflow baffle with the height of the original liquid layer, which is quite wrong. During operation the baffle supports not a layer of liquid, but a gas–liquid layer, which may contain 2-4 times less liquid than the original layer. Above the overflow baffle there is a considerable gas–liquid layer, the height of which depends not only on the composition of the gas, but on the liquid flow rate per unit width of baffle ($m^3/m \cdot$ hour). Therefore Melikyan's comparison of his experiments, performed in a non-flow model, with the experiments of Kuzminykh, in which water flowed along the grid of the apparatus, is not valid. In Kuzminykh's experiments the height of the original liquid layer was not 25 mm, as is considered by Melikyan, but 10-15 mm.

What, then, is the nature of the hydrodynamic regime of a liquid–layer in a sieve apparatus, and what determines it?

The determinable parameters of the regime are usually considered to be [2-9] the height of the gas–liquid layer H (or its density γ, inversely proportional to H) and the hydraulic resistance Δ P. The determining parameters are the gas speed w_g, the liquid flow speed w_l, or the liquid flow rate $\underline{i}$, the height of the overflow baffle h_b, the area of the overflow opening S_0 or its height $\underline{a}$ in equipment with external overflow, the viscosity of the liquid μ_1, the density of the liquid γ_1, and the surface tension σ at the liquid–gas interface. The

* With reference to R. A. Melikyan's paper in this issue, p. 37.

interaction is also influenced by the physical properties of the gas, but this effect is not determining. Thus, two relationships must be determined to define the hydrodynamics of the gas–liquid layer:

$$H = f_1 (w_g; i; h_b; S_0; \mu_l; \gamma_l; \sigma), \quad (1)$$

$$\Delta P = f_2 (w_g; i; h_b; S_0; \mu_l; \gamma_l; \sigma). \quad (2)$$

The quantitative relationships between the determinable and individual determining parameters for certain bubbling regime conditions have been established in a number of publications by Soviet and foreign workers [4-16 and others].

The dependence of H and ΔP on individual parameters in Equations (1) and (2) in relation to the foam regime has been determined in our investigations [2, 3, 8, 17, 18] and also in part by Kuzminykh and his coworkers [5-7].

It has been proved [2-9, 14, 15] that the principal parameter which determines the hydrodynamic regime in the gas–liquid layer is the gas speed w_g referred to the total cross section of the apparatus. The publications cited give curves for the variation of the height of the gas–liquid layer with w_g. Let us consider the variation of the character of a gas–liquid disperse system on the tray of a sieve apparatus, with increasing gas speed. At low gas speeds, not exceeding the free ascent speed w_a of bubbles of this gas in the given liquid, we have a typical bubble layer, in which the gas bubbles under the action of Archimedes forces ascend freely in the liquid at speeds of 0.1-0.4 m/second [19-22]. Only in the thin layer of liquid adjacent to the grid does the rate of motion of the gas approach to its speed in the openings, so that the bubble speed decreases from several meters per second after it has become detached from the opening to some tenths of a meter per second in the bubble layer. However, it is characteristic even of typical bubbling that above the bubble zone, in which the main mass of the liquid is contained, there is usually a foam zone, and above this a spray zone (Fig. 1), the last two zones containing only a small fraction of the whole liquid.

The reason for the formation of a foam zone at low gas speeds is that the kinetic energy of the emerging gas bubbles may be insufficient to overcome the mechanical strength of the surface film, and especially of the adsorption layer of surface-active substances. Therefore, a zone of rather immobile cellular structurized foam, often resembling a honeycomb, is formed over a typical bubble layer. The height of this foam layer for a given gas speed is determined by the time necessary for destruction of its cells, i.e., by the strength of the surface layers.

A spray zone of one concentration or another is always present above the gas–liquid layer in which the liquid constitutes a continuous phase. According to our observations and to literature data [11, 23, 24], when gas bubbles emerge from the layer of liquid (foam) and the surface film is broken spray is always formed, which is raised to various heights, depending on its degree of dispersion and the gas speed, above the liquid or foam layer. As the gas speed increases, the foam zone increases at the expense of the bubble zone.

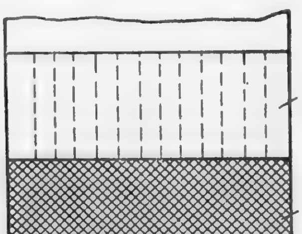

Fig. 1. Zones of the reaction space above a sieve plate. a) Bubble zone, b) foam zone, c) spray zone.

When a gas speed w_g = 0.5-0.7 m/second is reached in the full cross section of the apparatus, the disperse system usually becomes mainly foam, and a typical bubble layer several millimeters thick only remains close to the grid, and a spray zone containing an insignificant mass of liquid is also retained.

Free ascent of bubbles without accumulation of gas in the liquid is possible only in the condition that the gas speed related to the full cross section of the apparatus $w_g < w_f \varphi_g$, where φ_g is the fraction of the cross section occupied by bubbles. If the forced stream of gas introduced through the grid results in $w_g > w_f \varphi_g$, then free ascent of bubbles will not remove all the gas entering the gas–liquid layer. Therefore, when $w_g > w_f \varphi_g$, simultaneously with formation of cellular foam, the layer of which grows from the liquid surface into its depth, gas bubbles begin to accumulate in the liquid layer itself, leading to the formation of mobile foam. Further

increase of the gas speed alters the height of the layer and the nature of the foam. Simultaneously with formation of mobile foam within the liquid layer, destruction of the immobile foam cells occurs. Thus, an increase of the gas speed produces a gradual transition from the bubbling regime to a mobile foam regime. In the transitional regime the total foam height decreases after reaching a maximum in many cases, especially in liquids capable of forming stable colloidal foams. Predominance of the layer of cellular structurized foam, corresponding to the intermediate regime between bubbling and a suspended layer of mobile foam, is usually found over a fairly wide range of gas speeds: from $w_g = 0.5$ to $w_g = 1.0$ m/second. In this range the foam becomes increasingly mobile with increase of w_g and at $w_g = 1.0$-1.3 m/second it is converted into a strongly turbulent layer of mobile foam. Mobile foam differs in structure from stable foam, and consists of vortex streams of bubbles, gas streams, and liquid films. The transition from cellular foam to a suspended layer of turbulent mobile foam has been observed by all who have studied this effect. Having obtained a suspended liquid layer in conditions somewhat different from ours [2, 3], Kuzminykh and his associates [6, 7] described the conditions for its formation as "an entirely different hydrodynamic regime," in contrast to the conditions in which a layer of cellular foam of low mobility is formed. From our point of view, this regime is more correctly described as the foam regime, as foam is the accepted term for a disperse system consisting of a gas and a liquid, irrespective of its structure.

The gas speed w_g which corresponds to complete conversion of cellular into mobile foam depends on the height of the original liquid layer from which the foam is formed, the free section of the grid, the surface tension at the gas–liquid interface, and other conditions.

The speed of the translational motion only of the gas in the mobile foam layer (without consideration of pulsating and vortex motion) is several times (on the average, 10 times) as high as the speed of bubble ascent. Mass collisions therefore occur between the bubbles and the gas stream, accompanied by coalescence or fragmentation of the bubbles, transitions from bubbles to vortex streams, and re-formation of bubbles. The liquid may become drawn out into extremely thin films, then again form drops or layers, again thin out into films, etc. Thus, an enormous increase of interphase surface, rapidly renewed, occurs in the mobile foam layer, with especially vigorous agitation of the gas phase, which has lower inertia and viscosity than the liquid phase. These are the factors which cause the sharp increase of mass and heat transfer in the mobile film layer in comparison with the bubbling layer at equal liquid flow rates.

While cellular foam is formed when gas bubbles leave the liquid layer at low speeds mainly because of the presence of adsorption layers, which provide a certain mechanical strength and a corresponding durability of the cells, mobile foam is formed within the liquid by collisions between bubbles and gas streams moving at high speeds. Bubble collisions and filling of the liquid with gas are determined by the kinetic energy of the gas, and therefore the whole liquid may be converted into mobile foam on interaction of an inert gas even with a pure liquid, irrespective of the presence of adsorption layers at the gas–liquid interface.

Mobile foam is the dominant type of two-phase disperse system over a considerable range of gas speeds, usually from $w_g = 0.7$-1.3 m/second to $w_g = 3.0$-4.0 m/second, according to other conditions. However, as the gas speed increases in this range, the nature of the mobile foam and the volume fraction of gas in it change considerably. In the transition from cellular structural form to mobile foam the gas bubbles decrease in size, and on further increase of w_g the foam acquires a streaming vortex character.

The volume fraction φ_g of the gas may be expressed in terms of the height of the original liquid layer h_0 and the foam height H

$$\varphi_g = \frac{H - h_0}{H} = 1 - \frac{h_0}{H} \tag{3}$$

or in terms of the densities of the liquid γ_l, gas γ_g, and foam γ_f

$$\varphi_g = \frac{\gamma_l - \gamma_f}{\gamma_l - \gamma_g}. \tag{4}$$

If the density of the gas γ_g is regarded as negligible in comparison with γ_1, then

$$\varphi_g = 1 - \frac{\gamma_f}{\gamma_1} \tag{5}$$

For a bubbling layer, $\varphi_g < 0.5$, is typical, and for a foam layer, $\varphi_g > 0.5$. At high values of h_0, φ_g increases continuously with gas speed from the appearance of the foam layer to its destruction. At low values of h_0 the transition from cellular to mobile foam is accompanied by decrease of φ_g owing to decrease of the bubble size, while a subsequent increase of gas speed again produces an increase in the fraction of the gas in the foam layer to $\varphi_g \simeq 0.9$.

The volume fraction φ_1 of liquid in the foam can also be expressed as the ratio of the initial layer height h_0 and the foam layer H:

$$\varphi_1 = \frac{h_0}{H} . \tag{6}$$

It is obvious that as the gas speed increases, φ_1 varies inversely with φ_g.

The specific area of contact F between the gas and liquid in foam layer conditions cannot yet be determined analytically or experimentally, but it can be taken into account under given boundary conditions as a function of the specific volume of the foam or of the specific height of the foam. We note that for a given grid area the specific volume of the foam is equal to its specific height:

$$\frac{V_f}{V_1} = \frac{H}{h_0} = H_{sp} \tag{7}$$

For a given average equivalent radius of curvature of the gas bubbles (more correctly, liquid films)

$$F = B \cdot H_{sp} \tag{8}$$

where B is a proportionality factor.

In accordance with Equations (4) and (6), the specific height of the foam can be expressed in terms of the volume fractions of the gas and liquid in the foam:

$$H_{sp} = \frac{H}{h_0} = \frac{\varphi_g + \varphi_1}{\varphi_1} = \frac{1}{\varphi_1} = \frac{1}{1 - \varphi_g} . \tag{9}$$

From Equations (3), (4), (6), neglecting γ_g because of its small value relative to γ_1, we have

$$\varphi_1 = \frac{h_0}{H} = \gamma_f^0 , \tag{10}$$

where γ_f^0 is the density of the foam relative to the density of the liquid taken as unity.

The true density of the foam will be

$$\gamma_f = \gamma_1 \cdot \frac{h_0}{H} . \tag{11}$$

Hence the specific height of the foam can be expressed in terms of densities

$$H_{sp} = \frac{1}{\gamma_f^0} = \frac{\gamma_1}{\gamma_f} . \tag{12}$$

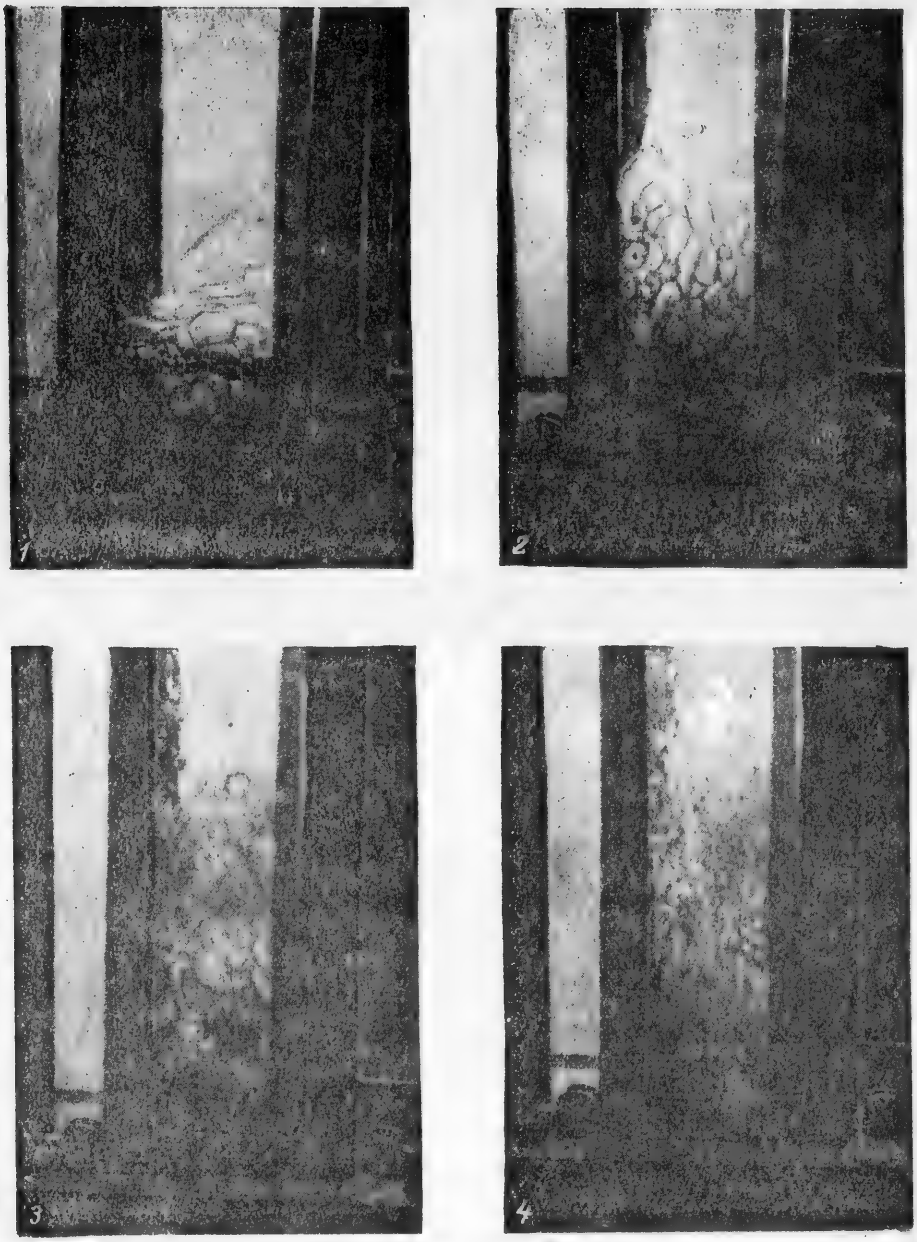

Fig. 2. Variation of the nature of the gas–liquid layer with increasing gas speed. Air– water system. Apparatus without liquid overflow. Gas speeds w_g (in m/sec.): 1) 0.3, 2) 1.0, 3) 2.0, 4) 3.0.

The amount of spray usually decreases somewhat in the transition from the bubble to the foam layer. If the gas speeds are still not high, most of the spray separates out and returns to the foam layer. On further increase of the gas speed, spray formation progressively increases and carry-over of the spray increases to a yet greater extent.

At gas speeds w_g = 3.0-4.0 m/second, depending on conditions, the spray zone becomes dominant, and a considerable part of the liquid becomes completely suspended in the gas and carried out by it.

Thus, with the remaining conditions maintained, quantitative changes of the gas speed twice result in a transition into a new qualitative state of the two-phase system: from a bubble layer to a foam layer at one range of speeds, and from a foam layer to a stream of suspended spray at other, considerably higher, gas speeds.

Variations of the height and nature of the gas–liquid system with increasing gas speed are clearly shown in the photographs in Fig. 2. Fig. 2,1 shows a typical bubbling regime with a bubble zone below and a small layer of cellular foam ($w_g \approx 0.3$ m/second). Fig. 2,2 gives an idea of the cellular foam regime in the transition to mobile foam ($w_g \approx 1$ m/sec.). Fig. 2,3 shows a photograph of mobile foam at $w_g \approx 2$ m/second, and Fig. 2,4 at $w_g \approx 3$ m/second.

The gas speed range corresponding to a given type of disperse system can be greatly varied by alteration of the conditions.

SUMMARY

1. The determining criteria proposed by Melikyan for evaluation of the hydrodynamic regime of the ascent of gas bubbles in a liquid layer are not suitable for characterization of the conditions in industrial sieve apparatus.

2. The hydrodynamic regime in sieve apparatus is mainly determined by the speed of the gas stream, which influences the nature of the gas–liquid system on the sieve plate: the bubbling regime which is established at low gas speeds is replaced by foam regime at higher speeds. The foam structure also changes with increasing gas speed.

3. Heat and mass transfer processes are most rapid in a layer of dynamic mobile foam, which constitutes a suspended layer consisting of films and streams of liquid intimately mixed with bubbles and streams of gas.

LITERATURE CITED

[1] R. A. Melikyan, J. Appl. Chem. 30, No. 1, 38 (1957).

[2] M. E. Pozin, I. P. Mukhlenov, E. S. Tumarkina, and E. Ya. Tarat, The Foam Method for Gas and Liquid Treatment (State Chem. Press, 1955).

[3] M. E. Pozin, I. P. Mukhlenov, E. S. Tumarkina and E. Ya. Tarat, J. Appl. Chem. 27, No. 1, 13 (1954).

[4] I. P. Usyukin and L. S. Akselrod, Oxygen 1, Nos. 1 and 2, 5 (1949).

[5] Zh. A. Koval, Candidate's Dissertation (Moscow Chem. Tech. Inst., 1954).

[6] I. N. Kuzminykh, L. S. Akselrod, Zh. A. Koval, and A. I. Rodionov, J. Chem. Ind. 2, 86 (1954).

[7] I. N. Kuzminykh and A. I. Rodionov, Trans. Moscow Chem. Tech. Inst. 18, 109 (1954).

[8] M. E. Pozin, I. P. Mukhlenov, Proc. Acad. Sci. USSR, New Series 92, No. 2, 393 (1953).

[9] L. S. Akselrod and V. V. Dilman, J. Chem. Ind. 1, 28 (1954).

[10] V. N. Stabnikov, Chem. Mach. 6, 2, 14 (1937); 7, 1, 6 (1938); 9, 2, 9 (1940).

[11] V. N. Stabnikov and S. E. Kharin, Theoretical Bases of Alcohol Distillation and Rectification (Food Ind. Press, 1951).

[12] N. M. Zhavoronkov and I. E. Furmer, Oxygen 5, 9 (1947).

[13] E. Kirschbaum, Destiller- und Rektifiziertechnik (Berlin, 1940).

[14] J. A. Gerster, A. P. Colburn, W. E. Bonnet and T. W. Carmodi, Chem. Eng. Progr. 45, 12, 716 (1949).

[15] J. A. Gerster, W. E. Bonnet and J. Hess, Chem. Eng. Progr. 47, 10, 523; 12, 621 (1951).*

[16] F. D. Mayfield, W. L. Church, A. C. Creen and D. C. Lei, Ind. Eng. Chem. 44, 9, 2238 (1952).

[17] M. E. Pozin and E. S. Tumarkina, J. Appl. Chem. 27, No. 11, 1170 and 1180 (1954).

* As in original–Publisher's note.

[18] M. E. Pozin, I. P. Mukhlenov, and E. Ya. Tarat, Foam Method for Removal of Dust, Smoke, and Fog From Gases (State Chem. Press, 1953).

[19] K. N. Shabalin, S. F. Kyrlov, and V. I. Oborin, J. Chem. Ind. 1, 10 (1939).

[20] N. I. Smirnov and V. L. Ruban, J. Appl. Chem. 22, No. 10, 1068 (1949); 26, No. 1, 110 (1953).

[21] V. G. Levich, Physicochemical Hydrodynamics (Acad. Sci. USSR Press, 1952).

[22] D. W. Van Krewelen and P. J. Hoftijzer, Chem. Eng. Progr. 46, 1, 29 (1950).

[23] V. G. Gleim, Drop Carry-Over and its Laws, Proc. Novocherkassk Conference on Boiler Chemistry (1952).

[24] S. S. Kutateladze, Heat Transfer in Condensation and Boiling (Machinery State Press, 1952).

Received October 24, 1955.

pH OF THE START OF PRECIPITATION OF GALLIUM HYDROXIDE AND DETERMINATION OF ITS SOLUBILITY PRODUCT

P. N. Kovalenko

The V. M. Molotov State University, Rostov on Don

Gallium, one of the rarest elements, is nevertheless widely distributed in nature and is usually found in very small quantities, mainly in conjunction with aluminum, iron, indium, zinc, etc., in many zinc blendes (up to 0.002%), iron ores, bauxite, and kaolin [1]. Commercial aluminum often contains traces of gallium.

Gallium is a member of the same group as aluminum and has many properties in common with it. Like aluminum salts, gallium salts have a great tendency to hydrolysis; gallium and aluminum salts are precipitated as the hydroxides at approximately the same solution pH.

It seems likely that their solubility products also have approximately the same numerical value [2]. Therefore, when aluminum is precipitated by ammonia, gallium is precipitated with it and is usually taken as aluminum if its presence has not been previously detected and taken into account in calculation of the results.

The pH of the start of precipitation of gallium hydroxide and its solubility product have not previously been studied, and their determination is of great interest to chemical technologists and analysts.

More detailed information on the chemical properties of gallium is to be found in the papers by Moser and Brukl [3].

The object of the present investigation was to determine the pH range of gallium hydroxide precipitation by a polarographic method, and to calculate its solubility product.

EXPERIMENTAL

The pH of the start of precipitation of metal hydroxides is related to their solubility products. The solubility products of the hydroxides are calculated by determination of the hydrogen ion concentrations at which the precipitates are formed, and of the concentrations of the precipitated ions.

The existing methods for determining the pH of the start of precipitation of metal hydroxides and for determining their solubility products are tedious, insufficiently accurate, and have poor reproducibility [4, 5]; in some cases the techniques required are complex [6, 7].

The results obtained by different methods [7-11] vary considerably.

To determine the pH of the start of precipitation of gallium hydroxide and to find its solubility product, we used a polarographic method, whereby it is possible to determine the constant value of the solubility product by extrapolation of the straight line (plotted in $\log K_s - C^n_{Me}$ coordinates) to its intersection with the ordinate axis.

This constant value, which corresponds to the solubility product at infinitely low concentration of the metal ions, when the activity coefficient is unity, we shall term the activity product (K_a) [7, 12].

Solutions of chemically pure gallium chloride, previously purified by twofold hydrolytic precipitation, were used for the work. The purified gallium salt was dissolved in distilled water slightly acidified with

hydrochloric acid, and tested for impurities: for aluminum by means of aluminon, for zinc by means of dithizone, and also for iron and other metals.

The solution concentrations were determined gravimetrically by precipitation of the gallium by dilute ammonia solution in presence of methyl red [13]. The original solutions used for polarography contained $0.79 \cdot 10^{-3}$, $1.19 \cdot 10^{-3}$ and $1.59 \cdot 10^{-3}$ g-ion/liter.

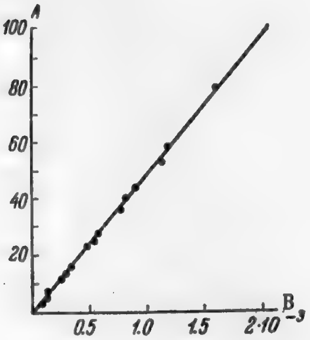

Fig. 1. Calibration graph for polarography of gallium with 0.02 N hydrochloric acid solution as the background electrolyte. (Soln. temp. 20°, S = 1 : 25). A) Height of the diffusion current wave h (in mm), B) concentration of the original analyzed solution (mole/liter).

The background solution for polarography of the gallium solutions of the original concentrations was 0.02-0.03 N hydrochloric acid. The temperature of the solutions was 20°.

The polarography was carried out at pH values from 2.8 to 4.2. Ammonia solution was used to give the required pH values. The solutions were held at a definite pH for half an hour and then polarographed. It was found that this time is quite sufficient to establish a state of equilibrium in the gallium hydroxide solutions. For suppression of the polarographic maximum, one drop of 0.1% methyl red was added to 10.0 ml of the solution.

The M-7-200 visual polarograph (made in 1946), constructed at the Scientific Research Institute for Chemistry (in Gorky) was used. A mirror galvanometer of absolute sensitivity: $3.2 \cdot 10^{-3}$ A/mm·m; $R_{ext} = 200\Omega$, $R_{cr} = 400\Omega$, was used. The distance between the center of the galvanometer mirror and the scale was 0.25 m. The capillary constant was

$$m^{\frac{2}{3}}t^{\frac{1}{6}} = 1.355\,\text{mg}^{\frac{2}{3}}\,\text{sec}^{-\frac{1}{2}}.$$

The hydrogen ion concentration was determined potentiometrically by means of the quinhydrone electrode. Calculation of the diffusion current strength i_d in microamperes from the polarographic wave height h in millimeters was carried out by means of the formula

$$i_d = \frac{ab \cdot h \cdot 10^6}{l},$$

where a is the absolute sensitivity of the galvanometer, b is the shunt ratio for lowering the absolute sensitivity of the galvanometer, l is the distance from the center of the galvanometer mirror to the scale in m, and 10^6 is the factor for conversion of amperes to microamperes.

For polarographic determinations of gallium ion concentration, the addition method, and the method involving the use of a calibration graph passing through the coordinate origin (Fig. 1) were used. Each determination was made at least 3-4 times. The table gives the average determination results.

The variation of the height of the diffusion wave for gallium chloride with solution pH is shown in Fig. 2. The diffusion waves for gallium found in determinations in solutions of pH below 3.0 were accompanied by maxima difficult to suppress by surface-active substances. However, these maxima did not hinder the determination of the diffusion wave heights.

At a definite hydrogen ion concentration, formation of solid hydroxide phase began, and the height of the diffusion wave decreased sharply owing to the decrease of the gallium ion concentration. Fig. 3 shows the course of the curves plotted in gallium ion concentration – solution pH coordinates, which indicate the dependence of the pH of solid gallium hydroxide formation on the gallium salt concentration.

It is important to note that, irrespective of the concentrations of the original gallium chloride solutions,

Variation of the Height of the Diffusion Wave and Gallium Ion Concentration with Variations of the Solution pH

Diffusion wave height (mm)	Diffusion current strength (in μ A)	Solution pH	Gallium concentration (g-ion/liter)
82.5	26.50	2.80	$1.60 \cdot 10^{-3}$
81.5	26.20	3.02	$1.60 \cdot 10^{-3}$
80.0	25.60	3.04	$1.59 \cdot 10^{-3}$
58.0	18.60	3.10	$1.17 \cdot 10^{-3}$
44.0	14.10	3.19	$0.88 \cdot 10^{-3}$
40.0	12.80	3.23	$0.80 \cdot 10^{-3}$
28.0	8.90	3.30	$0.556 \cdot 10^{-3}$
24.0	7.70	3.40	$0.48 \cdot 10^{-3}$
17.0	5.45	3.57	$0.34 \cdot 10^{-3}$
15.0	4.80	3.66	$0.30 \cdot 10^{-3}$
8.0	2.56	3.73	$0.16 \cdot 10^{-3}$
4.0	1.28	3.88	$0.08 \cdot 10^{-3}$
0.0	0.0	4.20	0.0
54.0	17.3	3.02	$1.12 \cdot 10^{-3}$
52.0	16.5	3.06	$1.03 \cdot 10^{-3}$
45.0	14.5	3.23	$0.9 \cdot 10^{-3}$
26.0	8.32	3.38	$0.52 \cdot 10^{-3}$
16.5	5.28	3.61	$0.33 \cdot 10^{-3}$
12.0	3.84	3.68	$0.24 \cdot 10^{-3}$
7.0	2.24	3.75	$0.14 \cdot 10^{-3}$
6.0	1.92	3.97	$0.12 \cdot 10^{-3}$
0.0	0.0	4.22	0.0
37.0	11.80	3.02	$0.79 \cdot 10^{-3}$
36.5	11.70	3.04	$0.76 \cdot 10^{-3}$
30.0	9.60	3.16	$0.605 \cdot 10^{-3}$
27.0	8.65	3.29	$0.545 \cdot 10^{-3}$
24.0	7.70	3.36	$0.485 \cdot 10^{-3}$
16.0	5.12	3.50	$0.322 \cdot 10^{-3}$
12.0	3.84	3.57	$0.242 \cdot 10^{-3}$
8.0	2.56	3.81	$0.161 \cdot 10^{-3}$
0.0	0.0	4.30	0.0

the precipitation of the gallium hydroxide is completed at the same pH value. The precipitation curves, corresponding to the initial concentrations of the gallium solutions, all meet at the same point on the abscissa axis, at pH = 4.2 (Fig. 3).

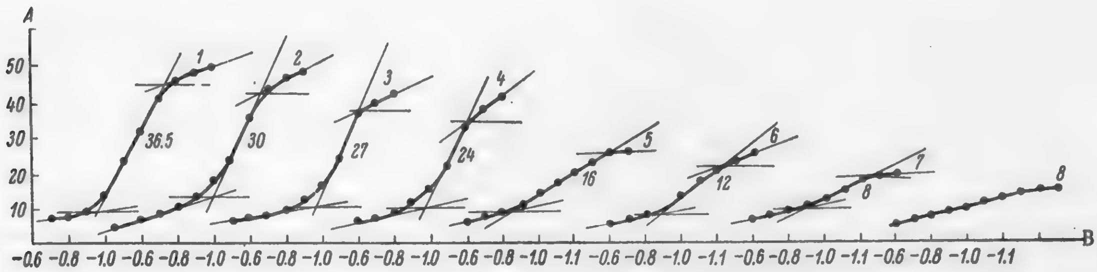

Fig. 2. Dependence of the magnitude of the gallium chloride diffusion current on the solution pH. Initial concentration of gallium chloride $0.79 \cdot 10^{-3}$ g-ion/liter, S = 1:25.
A) Height of diffusion current wave h (mm), B) potential (v). Solution pH: 1) 3.02, 2) 3.16, 3) 3.29, 4) 3.36, 5) 3.52, 6) 3.57, 7) 3.81, 8) 4.09.

As these curves show, an increase of the pH of gallium chloride solutions from 2.8 to 3.04-3.08 practically does not alter the diffusion current strength during polarography. The slight decrease of i_d in this pH range was probably caused by changes in the mobility of gallium ions with increase in the pH of the polarographic solutions; this effect had been observed by us earlier [12].

A decrease of i_d is found from a pH of 3.04 to 3.08, depending on the concentration of the original gallium solution used. The solubility products of metal hydroxides can be calculated from the diffusion current strength and the hydrogen ion concentration [2].

In the present instance, the proportionality factor K = 16.0 in the equation used, and therefore,

$$K_{s_{Ga^{\cdots}}} = i_d \cdot C^3_{OH'} \cdot 6.25 \cdot 10^{-5},$$

where $i_d \cdot 6.25 \cdot 10^{-5}$ is the expression used for calculation of the gallium concentration in the course of formation of the solid phase (see table). It was assumed in calculation of K_s that the activity coefficient of the ion in question was unity, owing to the high dilution of the solutions.

The variation of K_s with gallium concentration in the original solution and in the course of precipitation as the hydroxide is explained by changes of the ionic strength of the solution. Fig. 4 shows the variation of log K_s with the gallium ion concentration in the solution.

A constant value for K_s is obtained when the active concentration product (K_a) is used instead of the formal concentrations of the gallium ions [2, 12]. This product K_a is found by determination of the functional relationship between $-\log K_s$ and the concentration of the ions. Fig. 4 shows that $-\log K_s$ and the gallium ion concentration, which diminishes with decrease of hydrogen ion concentration owing to increased hydrolysis, are linearly related by the expression

$$-\log K_s = a + b \cdot C_{Ga^{\cdots}}, \tag{1}$$

where a is the negative logarithm of the solubility product when the ion activity is unity. Extrapolation of the straight lines in Fig. 4 to their intersection with the ordinate axis gives the value of $-\log K_s$ at infinitely low concentration of gallium ions in solution; their activity coefficient is unity. Then a = $-\log K_s$ is the logarithm of the activity product; b is the slope, the tangent of the angle α, which is

$$\tan \alpha = b = \frac{-\log K_s + \log K_a}{C_{Ga^{\cdots}}}, \tag{2}$$

where $C_{Ga^{\cdots}}$ is the gallium ion concentration, which changes with increasing solution pH.

All the straight lines, irrespective of the initial gallium ion concentration, cut off an equal intercept along the ordinate, $-\log K_a$ = const = -34.0.

Therefore the solubility product of gallium hydroxide $K_a = 1 \cdot 10^{-34}$. This constant does not depend on the initial concentration of the gallium solution.

The lines in Fig. 4 have different slopes according to the initial concentrations of gallium ions in the solutions undergoing hydrolysis. The lower the concentration of the original gallium solution, the greater the slope. However, the product of the slope constant (b) and the concentration of the initial gallium solution C_{init} is found to be constant:

$$b \cdot C_{Ga^{\cdots}init} = \text{const} \cong 2.08,$$

i.e., these two quantities are in strict inverse proportion (Fig. 5).

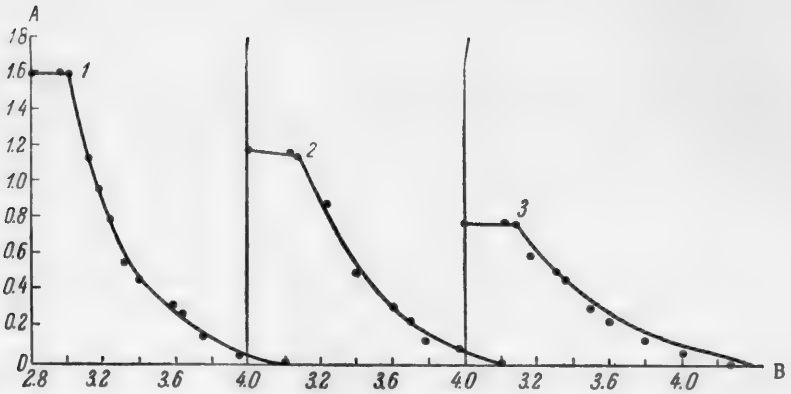

Fig. 3. Variation of the pH of the start of precipitation of gallium chloride with its concentration in the original solution.
Solution temperature 20°.
A) Gallium concentration (in mg-ion/liter), B) solution pH. Gallium concentration (in g-ion/liter): 1) $1.60 \cdot 10^{-3}$, 2) $1.19 \cdot 10^{-3}$, 3) $0.79 \cdot 10^{-3}$.

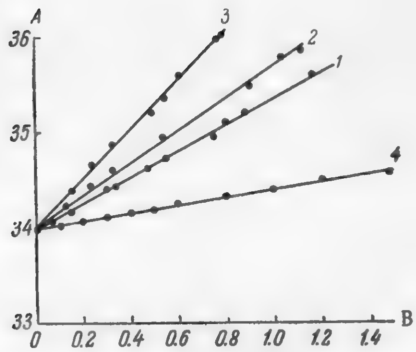

Fig. 4. Variation of $-\log K_s$ with gallium ion concentration, which changes with the solution pH.
A) $-\log K_s$, B) gallium concentration (in mg-ion/liter). Initial concentrations of gallium ions and slope constants, respectively: 1) $1.59 \cdot 10^{-3}$ and 1.31 2) $1.19 \cdot 10^{-3}$ and 1.71, 3) $0.79 \cdot 10^{-3}$ and 2.63, 4) $5 \cdot 10^{-3}$ and 0.416.
$K = b \cdot C_{Ga^{\cdots}\ init} = 2.08$.

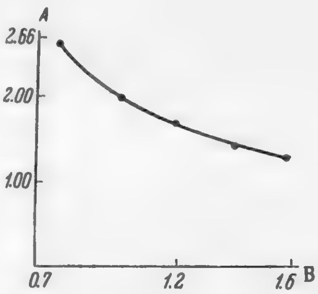

Fig. 5. Variation of the slope constant b with initial gallium concentration. $b \cdot C_{init} = \text{const} = 2.08$.
A) Slope constant b, B) gallium concentration (in mg-ion/liter).

Then

$$-\log K_s = -\log K_a + \frac{k}{C_{init}} \cdot C_{Ga^{\cdots}}. \tag{3}$$

When k has been found, the slope constant b can be calculated for any initial gallium concentration, and hence K_s for any gallium salt concentration, which depends on the solution pH (above 3.0). For example, for a gallium concentration of $5 \cdot 10^{-3}$ g-ion/liter b is 0.416. The solubility products calculated from Formula (3), based on $K_a = 1 \cdot 10^{-34}$ and b = 0.416, agree satisfactorily with the experimentally determined values.

SUMMARY

1. It is shown that the diffusion current strength is directly proportional to gallium chloride concentration.

2. The course of hydrolysis of gallium chloride as a function of the pH and initial solution concentration has been studied. It was found that the pH of the start of formation of solid gallium hydroxide depends on the gallium salt concentration. The precipitation of a $1.60 \cdot 10^{-3}$ molar solution of gallium begins at pH = 3.04; $1.19 \cdot 10^{-3}$ molar, at pH = 3.0, and $0.79 \cdot 10^{-3}$ at pH = 3.08. However, the precipitation of gallium, with any initial concentration, ends at the same solution pH.

3. Variations of K_s with gallium concentration in the original solutions are explained by changes in the ionic strength of the solutions. Independently of the initial gallium concentration, the straight lines representing $-\log K_s$ as a function of the gallium concentration, which diminishes with increasing pH, all meet at the same point in the ordinate axis, representing an infinitely dilute gallium solution.

This K_s value corresponds to complete dissociation of gallium hydroxide, and is a constant quantity, the activity product (K_a), which is independent of the initial gallium salt concentration; its value for gallium hydroxide is $1 \cdot 10^{-34}$.

4. The following formula is given for calculation of the activity product:

$$K_a = 1.10^{\log Ks + \frac{k}{C\ \mathrm{init}} C_{Ga^{\cdots}}},$$

where C_{init} is the initial gallium concentration, $C_{Ga^{\cdots}}$ is the gallium concentration decreasing during hydrolysis with increase of solution pH, and $\underline{k}$ is a constant, obtained by multiplication of C_{init} by the slope constant (b) equal to $\frac{\log K_s + \log K_a}{C_{Ga^{\cdots}}}$.

LITERATURE CITED

[1] W. N. Hartley and H. R. Ramoge, Trans. Chem. Soc. 71, 533 (1897).

[2] P. N. Kovalenko and V. N. Nestorovich, Ukrain. Chem. J. 18, 6, 635 (1952).

[3] L. Moser and A. Brukl, Monatsh. Chem. 50, 657 (1928); 51, 73 (1929).

[4] H. T. Britton, Hydrogen Ions, (United Sci. -Tech. Press, Chem. Theoret. Press, 1936), 284.

[5] B. N. Ivanov-Emin and G. A. Ostroumov, J. Gen. Chem. 14, 772, 778 (1944).

[6] A. F. Kupustinsky, Proc. Acad. Sci. USSR 28, 40 (1940).

[7] N. V. Akselrud and Ya. A. Fialkov, Ukrain. Chem. J. 16, 283, 296 (1950); Ya. A. Fialkov and N. V. Akselrud, ibid. 16, 75 (1950).

[8] N. A. Kertman, Qualitative Chemical Semimicroanalysis (State Chem. Press, 1949), 236.

[9] N. A. Tananaev, Analytical Chemistry (united Sci. -Tech. Press, 1934), 302.

[10] H. Remy and A. Kuhlmann, Z. Anal. Chem. 65, 16 (1924).

[11] H. Busch, Z. allgem. anorg. Chem. 161 (1927).

[12] P. N. Kovalenko, J. Appl. Chem. 26, 8, 814 (1953) (T. p. 741).*

[13] W. F. Hillebrand and G. E. Lundell, Applied Inorganic Analysis (United Sci. -Tech. Press, 1935), 427.

[14] O. N. Morozova, Chemistry of the Rare Elements, (1951), 53.

Received July 16, 1955.

* T. p. = C. B. Translation pagination.

THE RATE OF OXIDATION OF COPPER IN NITRIC ACID

N. N. Milyutin and A. I. Shultin

Reactions between metals and aqueous solutions are both of theoretical and practical interest. They are theoretically interesting from the viewpoint of the kinetics of heterogeneous processes which involve a potential difference at the metal-solution interphase. Their applied interest is in relation to studies of the mechanism and rates of metal corrosion and of electrolysis.

In the modern theoretical view of the mechanism of such reactions, they are regarded as complex heterogeneous processes consisting of several conjugate steps. These steps, which are not elementary, are as follows: transfer of metal ions from the crystal lattice into solution, reduction of the ions at the metal surface; reduction of the oxidizing agent, its oxidation, and also the transfer of the reacting particles [1-4].

The general rate of the process is determined by the step of the greatest "kinetic weight" [5], i.e., by the step which has the maximum influence on the rate of the process.

In conditions of anodic polarization of the external emf, the rate of the metal oxidation reaction (transfer of its ions into solution) is determined by the nature of the polarization curve for the metal; i.e., in absence of complicating factors it obeys the equation

$$i_a = Ke^{\frac{\beta_1(\varphi - \psi_1)n_m F}{RT}}, \tag{1}$$

where i_a is the rate of metal oxidation in electrical units (current density), K is a constant, β_1 is the coefficient for the influence of the potential difference in the dense part of the double layer on the activation energy of ionization of the metal, φ is the potential difference in the double layer, ψ_1 is the potential difference in the diffuse part of the double layer, n_m is the valence of the metal ions in the form in which they enter the solution, F and R are constants, T is the absolute temperature.

After some transformations, Equation (1) may be written in logarithmic form as follows:

$$\varphi = a + b \log i_a + \psi_1. \tag{2}$$

Hence it follows that the logarithm of the oxidation rate of the metal is a linear function of the stationary potential. It is evident that the conditions for the spontaneous solution of a metal differ from the conditions for its solution in anodic polarization only in the source of polarization. In anodic solution, the source of polarization of the metal is the external emf. In spontaneous oxidation (solution in an oxidizing agent) the source of polarization is the oxidation–reduction potential of the solution itself. Hence the oxidation of a metal in solution may be represented by Equation (1), i.e., the oxidation rate of a metal is determined by the course of its anodic polarization curve.

The validity of these generalizations would be confirmed if the relationship between the logarithm of the solution rate of the metal and its stationary potential was found to be linear, with a slope factor b in agreement with the theoretical value. As is known, the value of this factor for a bivalent metal at 25° is 0.059. The investigations of several workers [6-8], carried out with metals oxidized by hydrogen ions, confirm this

interpretation of the solution of metals. In a number of cases good agreement was found between the experimental results and the theory.

The solution of active metals in strong solutions of acids is a kind of ideal case, as the cathode process is a relatively simple reaction (reduction of hydrogen ions). It is evident that for further development of the theory it is necessary to test the applicability of Equation (1) to a wider range of metals, and to oxidation not by hydrogen ions only, but by other, more powerful and more complex oxidizing agents. Great interest attaches in this connection to the work of Bagotskaya [9] on the oxidation rate of mercury by oxygen. It was found that the oxidation rate of an inactive metal – mercury – also depends on an electrochemical mechanism and is described by Equation (1). Investigations of this kind have not been made with metals with positive standard equilibrium potentials and without such a perfect surface as liquid mercury.

To test the applicability of Equation (1) to the oxidation of copper, we studied the dependence of the reaction rate on the stationary potential in solutions of nitric acid of various concentrations.

EXPERIMENTAL

A cell made of glass was used for the experiments. The material used was electrolytic copper. The specimens were approximately 10 mm long and 1 mm across. The electrodes were fixed in the holder by means of polystyrene warmed in an electric oven. The experimental temperatures (25 and 35°) were obtained automatically in a water thermostat to an accuracy of ± 0.05°.

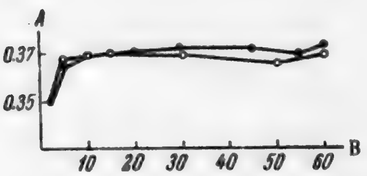

Fig. 1. Variation of the potential of copper undergoing oxidation in nitric acid, with time. A) Potential φ (in v), B) time (in min).

The nitric acid solutions were made from redistilled chemically pure acid and redistilled water. They were kept in Jena glass bottles with ground stoppers. The volume of acid solution used for each experiment was 250 ml.

The specimen was immersed in the corresponding acid solution in a cell and its potential was measured by the usual compensation method with the aid of a PV-2 potentiometer. At the start of the experiment the measurements were made at short time intervals (5-10 minutes), and after a constant potential became established, at longer intervals. The value of the stationary potential was found from a potential – time graph. Such a graph is shown in Fig. 1, for the variation of the potential of copper while being dissolved in 5.35 molar nitric acid solution. The fluctuations of potential in steady state conditions did not, as a rule, exceed 2-3 mv. The potentials were represented on the hydrogen scale. The oxidation rate of copper was determined from the loss in weight of the specimen during the experiment, and was expressed in $g/m^2 \cdot$ hour. The duration of the experiment was so chosen that the induction period (the time required to reach a constant potential) did not exceed 10-15% of the total time of the experiment. The main experiments were performed at 25° with acid of 3.28, 4.70, 6.34, 7.65, 9.72, 11.65 molar concentrations. The reproducibility was satisfactory: individual determinations of the rate did not differ from each other by more than 20%. The results of these experiments are given in Table 1, the data in which were used to plot the logarithm of the solution rate against the potential (Fig. 2, line 1).

The graph shows that a linear relationship exists between the logarithm of the solution rate and the stationary potential. The slope factor of the straight line is 0.056, which differs from the theoretical value by 0.003. The entirely satisfactory agreement between the experimental and theoretically calculated values of the slope factor shows that Equation (2) is applicable to the spontaneous solution of copper. The value of the constant a in Equation (2) can also be found from experimental data. It is 0.195. Therefore the following equation represents the relationship between the logarithm of the copper oxidation rate and the stationary potential:

$$\varphi = 0.195 + 0.056 \log v.$$

To find the step which determines the total rate of the process, the influence of temperature on the oxidation rate and the potential of copper was investigated. The oxidation rate and the potential of copper at 35° were determined for this purpose. The results of these experiments are givon in Table 2, and were used to plot

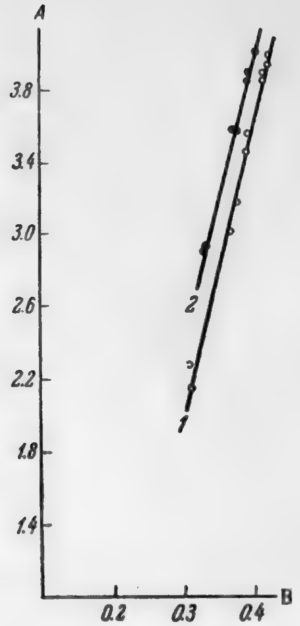

Fig. 2. Dependence of the logarithm of the oxidation rate of copper in nitric acid on the stationary potential. A) log v, B) stationary potential φ (volts).
Temperature of experiment (in °C): 1) 25, 2) 35.

TABLE 1

Oxidation of Copper in Nitric Acid at 25°.

HNO_3 concentration (molar)	Specimen No.	Duration of experiment (hours)	Solution rate ($g/m^2 \cdot hour$)	Stationary potential (V)
3.28	1	8.5	3.7	0.265
	2	9.5	3.1	0.245
4.70	1	4.0	149.5	0.316
	2	3.0	185.0	0.310
6.34	1	1.0	1250.0	0.369
	2	1.0	1550.0	0.372
7.65	1	1.0	2920.0	0.387
	2	1.0	3630.0	0.390
9.72	1	0.5	7270.0	0.409
	2	0.7	8020.0	0.412
11.65	1	0.33	9060.0	0.417
	2	0.33	8700.0	0.420

the logarithm of the solution rate against the potential (Fig. 2, line 2).

This graph shows that at 35° the relationship between the logarithm of the oxidation rate and the potential is again linear. The slope factor in this instance coincides with the theoretical value of 0.061. An increase of temperature by 10° results in a considerable increase of the solution rate of copper. For a 3.28 molar solution of nitric acid the temperature coefficient is ~5. In more highly concentrated acid the temperature coefficient is lower (~2), while for oxidation in 11.65 molar acid solution it is 1.3. A temperature coefficient of two or more indicates that the oxidation of copper in these conditions is limited by the rate of the electrochemical reaction at the copper surface.

TABLE 2

Oxidation of Copper in Nitric Acid at 35°.

HNO_3 concentration (molar)	Specimen No.	Duration of experiment (hours)	Solution rate ($g/m^2 \cdot hour$)	Stationary potential (V)
4.70	1	3.0	852	0.336
	2	4.0	808	0.338
6.36	1	1.0	3710	0.375
	2	1.0	3690	0.380
7.65	1	0.5	7700	0.393
	2	0.5	7000	0.393
11.65	1	0.25	12230	0.405
	2	0.25	10740	0.404

An interesting fact is the decrease of the temperature coefficient with increasing acid concentration. This may be explained as follows. At moderate concentrations the rate of the whole process is determined by the reaction rate, as the temperature coefficient is two or more. At higher acid concentrations, a change takes place in the kinetic weights of the diffusion of the oxidizing agent and of the surface reaction, with a relative increase of the former. This situation occurs if the polarization of the metal by the solution, having reached a considerable value, causes the electrochemical reactions – oxidation of the metal and reduction of the oxidizing agent – to proceed so rapidly that the layer adjacent to the electrode becomes greatly impoverished in the oxidizing agent. In such conditions its supply by diffusion into the electrode layer is not adequate, and therefore the rate of the whole process begins to be determined by the diffusion rate of the oxidant to the metal surface. The temperature coefficient is then 1.3.

The experimental data (Table 2 and Fig. 2) show that in this case the change from one determining factor to the other

does not affect the linear nature of the relationship between the logarithm of the copper oxidation rate and the potential. This is quite natural as the process became limited by diffusion in the cathode reaction, which cannot influence the anode polarization curves of the dissolving metal, which represent the kinetics of its oxidation process.

Comparison of the anode polarization curves for copper, obtained in studies of spontaneous diffusion at different temperatures (25 and 35°) shows that the plot of the logarithm of the oxidation rate against the potential at 35° is shifted in the direction of lower potentials relative to the plot representing the oxidation rate at 25° (Fig. 2). This means that the value of a in Equation (2) increases with increasing temperature, which is also entirely in agreement with theory.

The value of a in Equation (2) in expanded form is

$$a = -\frac{RT}{\beta_1 n_m F} \ln K,$$

from which it follows that the absolute value of a increases with increasing temperature owing to increase of T and especially of K, resulting in a shift of the plot. Consequently, at higher temperatures the same shift of potential from the equilibrium value results in a higher oxidation rate of copper than at lower temperatures.

SUMMARY

1. It has been shown in a study of the oxidation rate of copper in nitric acid solutions of different concentrations that the oxidation rate of copper is determined by an electrochemical mechanism, and can be represented by the following equation

$$\varphi = 0.195 + 0.056 \log v.$$

2. It is shown that increase of temperature greatly increases the oxidation rate of copper without affecting the linear relationship between the logarithm of the oxidation rate and the potential.

3. It is shown that the step which determines the oxidation rate of copper is the electrochemical reaction at the copper surface at moderate nitric acid concentrations, and probably the diffusion of oxidant to the copper surface at nitric acid concentrations above 11 molar.

LITERATURE CITED

[1] V. V. Skorcheletti and A. I. Shultin, Chemical Destruction of Metals (State United Sci. -Tech. Press, 1934), 17.

[2] Ya. V. Durdin, Annals Leningrad State Univ. 40, 4 (1939).

[3] A. I. Shultin, J. Phys. Chem. 15, 370 (1941).

[4] Ya. M. Kolotyrkin, J. Phys. Chem. 25, 1248 (1951).

[5] Ya. V. Durdin, J. Phys. Chem. 16, 1375 (1946).

[6] C. Wagner and W. Traud, Z. Electrochem. 44, 391 (1938).

[7] Ya. M. Kolotyrkin and A. N. Frumkin, J. Phys. Chem. 15, 346 (1941).

[8] Ya. M. Kolotyrkin, J. Phys. Chem. 27, 1344 (1935).

[9] A. I. Bagotskaya, J. Phys. Chem. 25, 459 (1951).

Received November 14, 1955.

BRIGHT NICKEL PLATING

A. M. Ozerov

Stalingrad Institute of Municipal Engineers

The production of bright coatings by direct electrolysis, acceleration of electroplating processes, replacement of complex by simpler electrolyte compositions, the use of alternating current in cathodic deposition of metals – these are the main directions in the development of technical electroplating.

Numerous researches and patent specifications have dealt with nickel plating; the subject has been described by Lainer, Kudryavtsev [1], and Kadaner [2].

Kudryavtsev, jointly with Korolkov and Fedurkin [3], has made a detailed study of the production of bright nickel coatings and developed the appropriate formulations and electrolysis conditions. As the result of this work, bright nickel plating under the usual current conditions has been industrially adopted.

At the present time the production of high-quality cathode deposits of metals with definite physicochemical properties is based mainly on the selection of suitable electrolysis conditions by variations of the electrolyte composition and concentration, additions of salts of other metals and organic substances, variations of temperature and current density, etc. However, variation of the physicochemical conditions of electrolysis is not the only or the ideal solution of the problem of obtaining metal coatings of high quality. On the contrary, it has defects which are inconvenient in production.

From the viewpoint of production requirements, the most convenient and simplest technological process would be one in which an electrolyte of simple composition is used for electrolysis, and the structure and quality of the metal coatings are regulated, say, by variations of the conditions for supplying electricity to the bath.

Interesting investigations of the cathodic deposition of metals by pulsating current have been carried out by Krivtsov [4]; Belyaev, Korolenko, and Filimonova [5]* studied processes of nickel plating with the use of alternating current. Bakhvalov [6], and Vene and Nikolaeva [7]* studied the effects of periodic changes in the direction of the current on the electrodeposition of metals. The work of Bakhvalov has assisted in the adoption of alternating currents for electroplating with copper and zinc. Sysoev and Chernenko [8] studied the electrodeposition. of copper by currents of different degrees of rectification, using a selenium rectifier for this purpose. They reported that if a current containing "an anodic component" is used, the deposits formed are dark, rough, and coarsely crystalline.

The present paper gives new data on the electrodeposition of nickel in electrical conditions differing from any described in the literature. By the use, not of a direct current, but of a "variable" current (changing periodically in magnitude and partially in direction) for electrolysis, it has proved possible to influence the structure and properties of cathode coatings by purely electrical means.

EXPERIMENTAL

The current converters used were based on one half period (a) and two half period (b) selenium rectifier circuits shown in Fig. 1.** By variations of the ratio of the sections $\underline{m}$ and $(n - m)$ of the secondary winding of

* A brief description of the present state of the problem of the use of alternating current for electrolytic processes is also given here.

** The current converter circuits were designed by A. V. Shilnikov.

the transformer and choice of suitable resistances, it was possible to obtain different electric current characteristics: a) current pulsating at a frequency of 50 cycles/second and periodically varying in magnitude (Curve 3 in Fig. 2 and the oscillogram in Fig. 3, a); b) alternating current at a frequency of 50 cycles/second with a small controllable anodic current (with 1:6 and 1:4 ratios of the maximum amplitudes b and a of the anodic and cathodic currents, respectively (Curve 4 in Fig. 2 and the oscillogram in Fig. 3, b). The current curve was determined by means of the EO-7 electronic oscillograph. These current transformers are simple to use and can be successfully used in factory conditions.

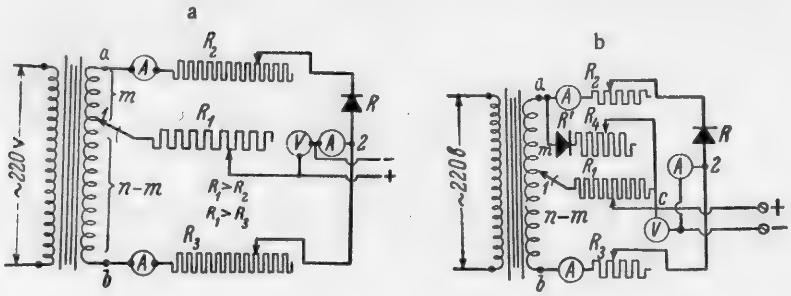

Fig. 1. Current converter circuits.

To determine the predominant effects of electrical conditions on the properties of cathode deposits, electrolysis was also carried out with the use of a direct current (Curve 1, Fig. 2) and a direct pulsating current (Curve 2, Fig. 2) obtained by means of a mechanical current breaker of the collector type.

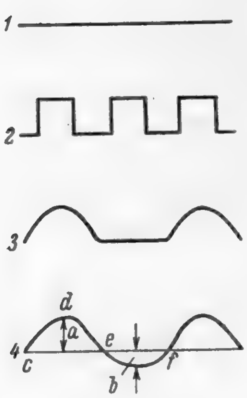

Fig. 2. Electric current characteristics.
Curves: 1) Direct current from a storage battery, 2) direct pulsating current (10 breaks per second), 3) pulsating current of 50 cycles per second, periodically varying in magnitude, 4) alternating current of 50 cycles/second frequency with a small anodic current (1:4 ratio of anodic current b to cathodic current a).

The electrolysis was performed in a glass vessel 1 liter in capacity, with nickel anodes, with vigorous mechanical stirring of the circulating electrolyte (six-fold change in 1 hour) fed from below and removed from the top of the cell. The cell was placed in a thermostat, and the experiments were performed at 30, 50 and 70° (to an accuracy of ± 0.5°). The cathodes were copper foil plates previously treated with nitric acid and electropolished for 0.5 minute in an electrolyte containing H_3PO_4 (1.6) 1200 g/liter, CrO_3 120 g/liter, d = 1.6 g/cc, at D_A = 40 A/dm^2. The double working surface of each cathode was 5 cm^2.

The polarization curves were obtained by the usual compensation method with the aid of the P-4 potentiometer. The reference electrode was a mercurous half-cell (2N H_2SO_4 solution). The electrolyte tube was drawn out to a fine tip and was led to the cathode surface from below at an angle of 50-60°; below the cathode the tube was bent through 90° in a horizontal plane. This prevented the entry of bubbles into the tip of the tube and masking of the cathode surface. Before the polarization curves were determined, the cathode was in each case coated for 10 minutes with a dense, finely crystalline nickel deposit from the electrolyte under investigation at a current density of 2 A/dm^2. In view of the instability of the equilibrium potential of the nickel electrolyte, the correct sequence of all the operations was carefully maintained.

A diagram of the apparatus is shown in Fig. 4

Chemically pure reagents were used. The $NiSO_4 \cdot 7H_2O$ was recrystallized. In some cases Kudryavstev's brightening additive,

consisting of sodium 2, 6- (or 2, 7)-disulfonaphthalate, prepared by the method described by Kadaner [2], was added to the electrolyte.

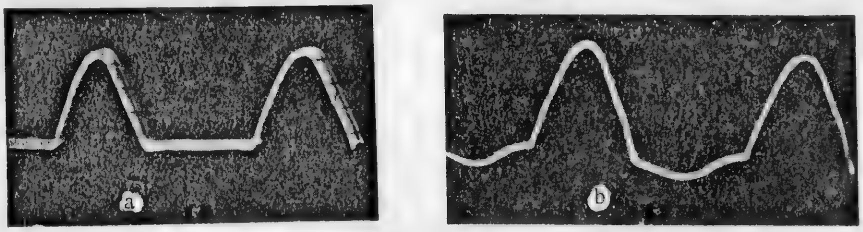

Fig. 3. Electric current oscillograms. a) Pulsating current of 50 cycles/second, periodically varying in magnitude, b) alternating current of 50 cycles/second frequency with a small cathodic current.

The nickel coatings were tested for porosity (All-Union State Standard 3247-46), for thickness by the drop method (All-Union State Standard 3003-50) and for reflecting power (visually). Microphotographs were taken of some specimens under a magnification of 313 with the aid of the MIM-6 microscope.

It is known that one condition for acceleration of metal electrocoating processes is the use of more highly concentrated circulating electrolytes at high temperatures with vigorous stirring, so that higher current densities can be used.

The nickel plating process at high current densities has been studied in detail for many years by Mashovets, Pasechnik, and Popova [9], and also by Kudryavtsev [1].

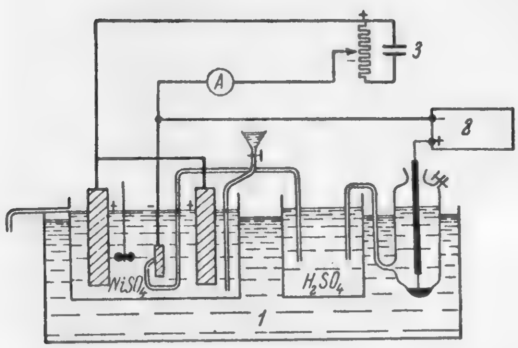

Fig. 4. Diagram of the equipment. 1) Thermostat, 2) potentiometer, 3) generator.

The data of the earlier investigations were used in our study of the electrodeposition of nickel from solutions of the following compositions (in g/liter): A) 250 $NiSO_4 \cdot 7H_2O$, 25 $NiCl_2$, 40 H_3BO_3; B) 140 $NiSO_4 \cdot 7H_2O$, 100 $Na_2SO_4 \cdot 10H_2O$, 30 H_3BO_3, 6 NaCl, pH = 5.6-5.8 (composition used at the Stalingrad Copper Equipment Factory); C) 350 $NiSO_4 \cdot 7H_2O$, 10 H_2SO_4, 30 H_3BO_3; D) 350 $NiSO_4 \cdot 7H_2O$, 10 H_2SO_4; E) 350 $NiSO_4 \cdot 7H_2O$, 10 H_2SO_4, 3 $C_{10}H_6(SO_3Na)_2$.

Under factory conditions, the current density in electrolyte B) did not exceed 1 A/dm^2, but with continuous filtration and vigorous agitation by means of air it was increased to 2 A/dm^2. However, the nickel coatings formed were dull, and generally porous and pitted.

Preliminary investigations of the electrodeposition of nickel in circulating, vigorously agitated electrolyte B) showed that when the cathode was polarized by type 3 current (Fig. 2) the nickel coatings obtained were dense, semilustrous almost free from pores, while with polarization by type 4 current (Fig. 2) dense semilustrous nonporous nickel coatings may be obtained at a current density of 4 A/dm^2.

---

* The tests of the nickel coatings for porosity and thickness were made and the microphotographs taken by the head of the laboratory of the Stalingrad Copper Equipment Factory, A. M. Sapozhnikov, in factory conditions.

Addition of 4.5 g of $C_{10}H_6(SO_3Na)_2$ per liter to the electrolyte improves the quality of the coatings, which are, as a rule, bright. If the cathode is polarized by type 3 current, slight peeling of the nickel coatings occurs at a current density of 5 A/dm^2, while with type 4 current dense bright coatings are obtained at 6 A/dm^2.

In experiments with electrolyte A, with a higher nickel content, dense, semilustrous nickel coatings could be obtained at a current density of 6 A/dm^2.

More detailed studies of the electrodeposition of nickel were carried out with electrolytes C, D, and E with high $NiSO_4$ contents.

A comparison of the cathodic nickel deposits obtained by electrolysis of electrolyte C by means of currents of different characteristics, shows that with polarization of the electrode by direct current of type 1 the nickel deposits are dense, dull, and porous (4 pores/cm^2) and more coarsely crystalline (Fig. 5, a) while with current type 4, the surfaces of the deposits (under the same conditions) become smoother, semilustrous, and more finely crystalline,* free from pores (Fig. 5, b). If the electrode is polarized by current of types 2 and 3 under the same conditions, the deposit surface becomes smoother (than with the use of direct current), but the deposits formed are still porous (average 3 pores/cm^2).

A decrease of the porosity of nickel coatings resulting from superposition of an alternating on a direct current has been previously reported by Vagramyan and Sutyagina [10].

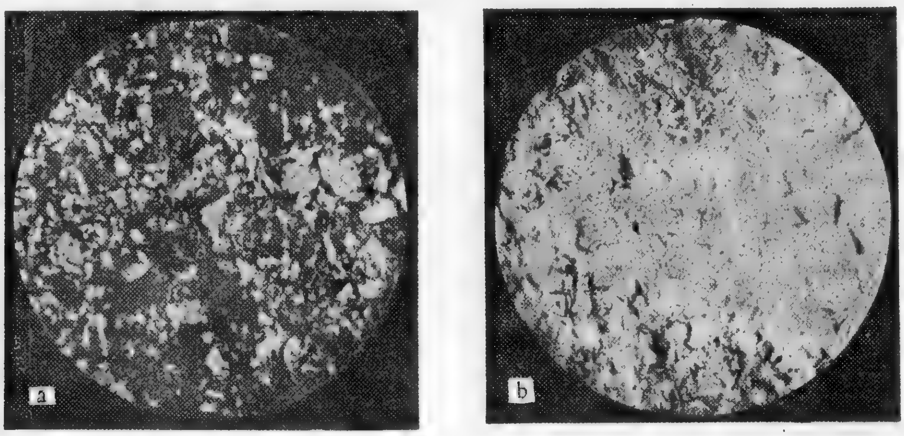

Fig. 5. Surface of a nickel deposit obtained from electrolyte C at 30° and a current density of 4 A/dm^2. a) Direct current type 1, 4 pores/cm^2, b) current type 4, no pores.

It is known that addition of boric acid to the electrolyte assists stabilization of the pH value, and prevents the electrolyte near the cathode becoming excessively alkaline as the result of rapid discharge and evolution of hydrogen at high current densities.

Experiments showed that in the cathodic deposition of nickel from electrolyte C (with addition of H_3BO_3) at 30° (even at D_k = 20 A/dm^2) no visible film of $Ni(OH)_2$ or basic nickel salts was formed, while with the use of electrolyte D (without H_3BO_3) at 30° a visible greenish film was already formed at D_k = 15 A/dm^2.

In investigations of the influence of temperature on the structure of nickel deposits it was found that at 30°, as a rule, smooth semilustrous nickel deposits are obtained from electrolyte D at current densities up to 8 A/dm^2 (with polarization of the electrode by current types 3 and 4), at 50° under the same conditions the deposits formed are less lustrous, while at 70° only smooth dull deposits are formed. The layer of solution near the electrode also becomes less alkaline at higher temperatures; for example, while at 30° and D_k = 15 A/dm^2 a visible greenish film of $Ni(OH)_2$ is formed at the cathode (mainly below and at the edges), at 50° it is formed

* The terms "coarsely crystalline" and "finely crystalline" are not used to indicate the crystal size, but merely to characterize the surface of the deposits.

at $D_k = 20\ A/dm^2$, while at 70°, even at $D_k = 24\ A/dm^2$, a visible film is not formed.

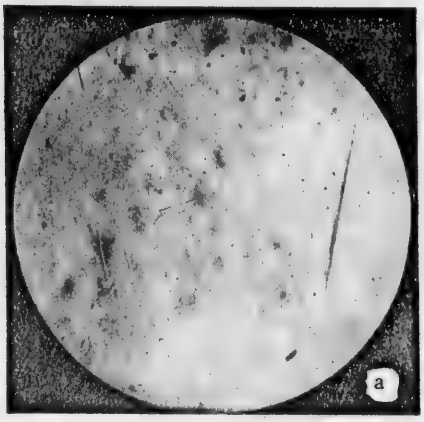

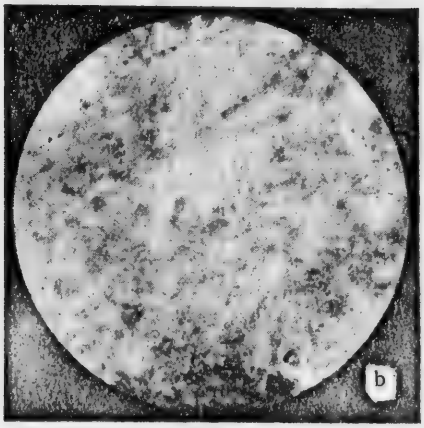

Fig. 6. Surface of a nickel deposit obtained from electrolyte E at 30° and $D_k = 4\ A/dm^2$. A) Current type 3, 1 pore/cm^2; b) current type 4, no pores.

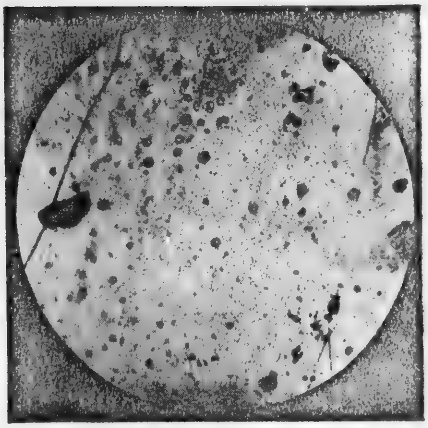

Fig. 7. Surface of a nickel deposit obtained from electrolyte C with addition of 0.5 g gelatin per liter at 30° and $D_k = 3\ A/dm^2$. Current type 3, 3 pores/cm^2.

As the temperature increases, the current density range for satisfactory coatings widens considerably; for example, while at 30° and with polarization of the electrode by current type 4 some peeling of the nickel at the lower end of the anode already occurs at $D_k = 10\ A/dm^2$, at 70° smooth dull coatings are still obtained at $D_k = 20\ A/dm^2$.

Electrolyte E (with addition of 3 g of $C_{10}H_6(SO_3Na)_2$ per liter) as a rule gives bright nickel coatings. It is interesting to note that while at 30° and with polarization of the electrode by current type 3 smooth bright deposits are obtained (Fig. 6, a), when current type 4 is used smooth bright deposits are only obtained at $D_k = 1\text{-}3\ A/dm^2$, while with further increase of current density the deposits become less bright and a white film is formed at the lower end of the cathode (Fig. 6, b). With increasing temperature and current density the amount of white film on the cathode decreases and the deposits obtained are brighter; for example, at $t = 70°$ smooth semilustrous deposits were obtained at $D_k = 18\ A/dm^2$ (current type 4).

Separate experiments were performed to study the effect of additions of gelatin (to electrolyte C) on the structure of nickel coatings. The deposits formed are again bright, with numerous small surface lumps (Fig. 7). Some peeling of the deposits was observed; this does not occur in cathodic deposition of nickel from the same electrolyte under the same conditions, but without addition of gelatin.

DISCUSSION OF RESULTS

It is known that under the ordinary electrical conditions all the factors which increase cathode polarization favor the formation of a finely crystalline structure. Metals of the iron group differ considerably from other metals in their electrochemical properties. For their deposition from solutions of simple salts, it is necessary to polarize the cathode considerably in the negative direction from the equilibrium potential, and the

deposits formed are,as a rule, dense, homogeneous, and finely crystalline. The causes of the high polarization and the formation of finely crystalline deposits, have formed the subject of numerous investigations, which have been reviewed by Vagramyan [11].

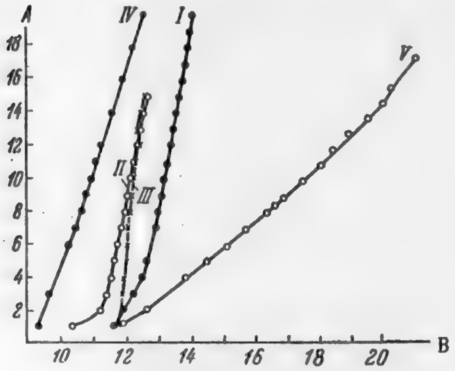

Fig. 8. Variation of potential with current density in the cathodic deposition of nickel from an electrolyte containing (in g/liter); 350 $NiSO_4 \cdot 7H_2O$ + $10H_2SO_4$ + $30H_3BO_3$ (with agitation, temperature 30°) with different electric current characteristics. A) Current density D_k (in A/dm²), B) potential E (in v). Electric current types: I) 1, II) 2, III) 3, IV) 4, V) 3 + 3 g/liter of $C_{10}H_6(SO_3Na)_2$.

Detailed investigations of the mechanism of the electrodeposition of nickel have been made by Vozdvizhensky [12], Polukarov [13], Kuznetsov [14], and Esin and Loshkarev [15], and recently by Gorbunova et al. [16] and by Vagramyan et al. [10, 11].

The question of the cause of the high polarization and of the mechanism of the formation of bright deposits has not yet been finally settled.

The data in the table and in Fig. 8 show that with polarization of the cathode by current of types 2 and 3 the potentials of the nickel electrodes coincide at the higher current densities, and their values are more positive than with polarization by direct current type 1, while with polarization of the electrode by current type 4 the potentials are still more electropositive.

A similar relationship was previously discovered by Gorbunova and Sutyagina [17] who studied the electrodeposition of copper with an alternating current applied to the cell.

Addition of 3 g/liter of $C_{10}H_6(SO_3Na)_2$ to the electrolyte results in a sharp shift of potential in the electronegative direction (Fig. 8, Curve 5), indicating a considerable retardation of the electrode process.

Fig. 9 shows that an approximately linear relationship holds between the potential and the logarithm of the current density in electrodeposition. (On addition of 3 g/liter of $C_{10}H_6(SO_3Na)_2$ to the electrolyte this relationship becomes more complex). This indicates considerable predominance of chemical polarization, which may be caused by a number of factors, such as retarded ionic discharge and retarded formation and growth of two-dimensional nuclei. A considerable proportion of the observed overvoltage (particularly after introduction of the additive) is probably due to passivation of the nickel electrode. Passivation is caused by adsorption of foreign particles at the electrode surface and the formation of oxide films of either amorphous or crystalline structure. In consequence, the metal surface may become coated by insulating or conducting layers of various degrees of continuity.

Gorbunova et al. [16] showed that a bright surface is formed during solution (electropolishing) or deposition of a metal under a film of the hydroxide or basic salts of nickel, which they detected in the form of rings in the electron diffraction diagrams obtained from bright nickel deposits.

The influence of surface-active substances and the mechanism of activated penetration of ions through the adsorbed film in the formation of finely crystalline deposits has been studied by Loshkarev and Kryukova [18].

On the basis of the results obtained by these authors and of the experimental data given in the present paper, the following hypothesis is advanced concerning the cause of formation of bright nickel deposits on polarization of the electrode by currents type 3 and 4. In polarization by type 3 current, the electrode becomes increasingly passivated during the brief intervals without current as the result of oxidation and adsorption of foreign particles on its surface. The high value of the work of formation of nuclei at the passivated surface and the subsequent brief interval during which the current passes lead to the formation, in presence of considerable overvoltage, of localized packets of nuclei, the spread of which over the already passivated surface of the previous layer is difficult. At the same time, because of the sharp fall in concentration around the nucleus, the region

Relationship Between the Potential E (V) and Current Density D (A/dm^2) in the Cathodic Deposition of Nickel with Different Current

	$-E$ (in v)																
	Electrolyte C, temperature 30°, stirring					Electrolyte D, circulated, stirring						Electrolyte E, circulated, stirring					
D (A/dm^2)	current 1	current 2	current 3	current 4	current 3 *	30° curr. 3	30° curr. 4	50° curr. 3	50° curr. 4	70° curr. 3	70° curr. 4	30° curr. 3	30° curr. 4	50° curr. 3	50° curr. 4	70° curr. 3	70° curr. 4
0	0.422	0.434	0.551	0.597	1.011	0.532	0.523	0.537	0.527	0.565	0.553	0.690	0.463	0.740	0.545	0.678	0.587
1	1.162	1.033	1.169	0.930	1.189	1.135	0.971	1.114	0.976	1.057	0.948	1.088	0.926	1.058	0.923	1.059	0.949
2	1.189	1.118	1.176	—	1.258	1.151	1.002	1.130	0.998	1.073	0.959	1.110	0.949	1.083	0.980	1.078	0.964
3	1.218	1.138	1.186	0.960	1.321	1.163	1.018	1.140	1.012	1.081	0.968	1.131	0.983	1.107	1.007	1.086	0.975
4	1.245	1.150	1.192	—	1.378	1.170	1.030	1.147	1.026	1.088	0.975	1.145	1.033	1.113	1.021	1.096	0.935
5	1.259	1.161	1.201	0.988	1.443	1.180	1.040	1.155	1.037	1.092	0.981	1.175	1.081	1.138	1.033	1.110	0.998
6	1.269	1.712	1.201	1.022	1.506	1.914	1.053	1.161	1.049	1.098	0.988	1.214	1.129	1.158	1.049	1.118	1.007
7	1.281	1.182	1.202	1.046	1.565	1.201	1.071	1.167	1.059	1.102	0.993	1.266	1.210	1.170	1.059	1.125	1.012
8	1.291	1.194	1.208	1.062	1.627	1.211	1.096	1.172	1.072	1.106	0.997	1.335	1.291	1.183	1.071	1.131	1.019
9	1.301	1.201	1.214	1.077	1.686	1.202	1.130	—	—	—	—	1.376	1.360	1.192	1.089	1.137	1.025
10	1.310	1.210	1.217	1.090	1.744	1.214	1.162	1.181	1.095	1.113	1.008	1.453	1.458	1.198	1.109	1.147	1.028
11	1.318	1.218	1.222	1.103	1.805	—	—	—	—	—	—	—	—	—	—	—	—
12	1.333	1.229	1.232	1.118	1.839	1.245	1.210	1.191	1.124	1.122	1.019	1.813	1.974	1.221	1.150	1.159	1.041
13	1.338	1.239	1.239	—	1.886	—	—	—	—	—	—	—	—	—	—	—	—
14	1.347	1.249	1.240	1.153	1.950	1.294	1.318	1.205	1.155	1.128	1.029	1.860	1.978	1.245	1.198	1.172	1.054
15	1.355	—	—	—	1.998	1.338	—	—	—	—	—	—	—	—	—	—	—
16	1.364	1.263	1.258	1.180	2.023	—	1.356	1.222	1.204	1.135	1.040	1.228	2.083	1.272	1.249	1.180	1.063
17	1.371	—	—	—	2.033	—	—	—	—	—	—	—	—	—	—	—	—
18	1.379	—	1.274	1.215	2.093	—	1.678	1.241	1.240	1.142	1.051	—	—	1.306	1.318	1.192	1.080
19	1.388	—	—	—	—	—	—	—	—	—	—	—	—	—	—	—	—
20	1.394	1.314	—	1.245	—	—	1.818**	1.291**	1.305**	1.148	1.061	—	—	1.343	1.383	1.200	1.095
21	—	—	—	—	—	—	—	—	—	—	—	—	—	—	—	—	—
22	—	—	—	—	—	—	—	—	—	—	—	—	—	—	—	—	—
23	—	—	—	—	—	—	—	—	—	—	—	—	—	—	—	—	—
24	—	—	—	—	—	—	—	—	—	—	1.079	—	—	—	1.478***	1.228	1.126

* +3 g/liter $C_{10}H_6(SO_3Na)_2$.

** Ni $(OH)_2$ formed on cathode.

*** Black film and Ni $(OH)_2$ formed on cathode.

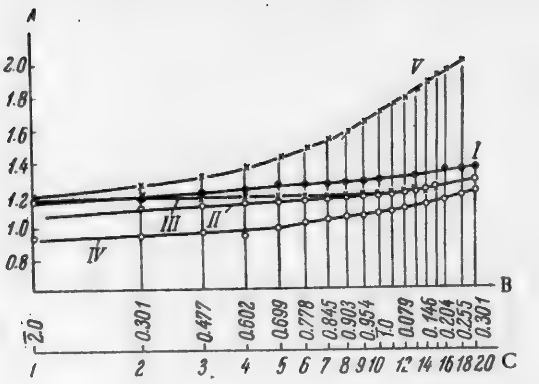

Fig. 9. Variation of cathode potential with logarithm of the current density in electrolysis of a solution containing (in g/liter): 350 $NiSO_4 \cdot 7H_2O$ + 10H_2SO_4 + 30H_3BO_3 (with agitation, temperature 30°) with different current characteristics.
A) Potential E (in v), B) log D_k, C) current density D_k (in A/dm^2).
Electric current types: I) 1, II) 2, III) 3, IV) 4, V) 3 + + 3 g/liter of $C_{10}H_6(SO_3Na)_2$.

of its growth diminishes to a very small size. This results in the formation of finely crystalline deposits. Moreover, polarization of the electrode by pulsating current type 3, with periodic variations of magnitude, results in periodic variations of the potential, which in turn leads to a redistribution of the localized sites of nucleus formation over the already passivated surface. The final result is the formation of smoother finely crystalline deposits than those formed in polarization by direct current.

Addition of $C_{10}H_6(SO_3Na)_2$ to the electrolyte established a constant definite pH value in the layer nearest the electrode, stabilizes the film of adsorbed foreign particles on the electrode surface, hinders still further the spread of the packets of nuclei over the more highly passivated electrode surface, and leads to the formation of brighter deposits.

The cessation of growth of adjacently growing crystals as the result of their passivation is one reason for the formation of pores between them.

Polarization of the electrode by alternating current type 4 with an anodic component leads to a smoother bright surface of the nickel deposits. The explanation is that while the cathode is under the brief influence of the anodic component all the charged regions of the surface are eliminated and the surface is filled with homogeneous crystalline planes.

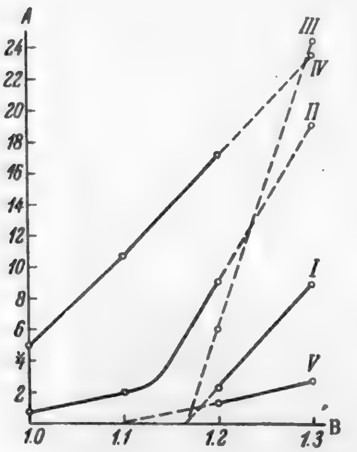

Fig. 10. Rates of electrodeposition of nickel at equal values of the cathode potential (E = 1, 1.1, 1.2, 1.3 v) with different current characteristics. Electrolyte composition (in g/liter): 350 $NiSO_4$ + 7H_2O + 10H_2SO_4 + 30H_3BO_3 (with agitation, temperature 30°).
A) Electrodeposition rate D (in A/dm^2), B) potential E (in v). Electric current types: I) 1, II) 2, III) 3, IV) 4, V) 3+3 g/liter of $C_{10}H_6(SO_3Na)_2$.

The decrease of porosity in polarization of the electrode by type 4 current is explained by decreased adsorption of the passivating substances which hinder the growth and coalescence of the crystals. This decrease of passivator activity leads to formation of denser deposits.

The decreased overvoltage in the electrodeposition of nickel in polarization of the electrode by type 4 current is caused by changes in the composition of the layer of solution nearest the electrode and the weakened action of the passivators. The reason is that during the brief anodic polarization of the cathode, equalization of the solution concentration in the layer nearest the electrode occurs, and the nickel hydroxide particles, being positively charged, not only cannot be deposited at the cathode but even move away from it. On the other hand, as a result of the brief anodic polarization of the cathode, hydroxyl ions will be discharged on it, and this will lead to acidification of the layer nearest the electrode and partial destruction of the previously formed particles of nickel hydroxide or basic salts. In consequence, the rate of the electrode process should increase.

In fact, it follows from Fig. 10 that if the rate of electrodeposition of nickel by type 3 current (at E = -1.2 v) is taken as unity, with polarization of the electrode by type 4 current the rate becomes approximately 3.

Increase of the electrolyte temperature weakens the effect of the additive, diminishes the passivation of the electrode surface, intensifies diffusion processes (and therefore equalization of the electrolyte concentrations), causes the catholyte layer to become

less alkaline, and so leads to formation of more coarsely crystalline, less smooth, and dull nickel deposits.

SUMMARY

1. In a study of the electrodeposition of nickel by different types of electric current, it was shown that the use of "alternating" current in nickel plating is advantageous.

2. A hypothesis is advanced to explain the formation of smooth, bright nickel coatings of low porosity by the use of a pulsating current periodically varying in magnitude, and of an alternating current with an "anodic component."

LITERATURE CITED

[1] V. I. Lainer and N. T. Kudryavtsev, Fundamentals of Electroplating, 1 (Metallurgy Press, 1953).

[2] L. I. Kadaner, Latest Advances in Electroplating (Kharkov State Univ. Press, 1951).

[3] N. T. Kudryavtsev, O. M. Korolkov and V. V. Fedurkin, J. Appl. Chem. 22, 586 (1949).

[4] A. K. Krivtsov, Deposition of Metals with Pulsating Current, Author's Summary of Candidate's Dissertation (Ivanovo, 1952).

[5] P. P. Belyaev, N. K. Korolenko and G. V. Filimonova, Metallic Coatings in Chemical Equipment Construction (Machinery State Press, 1954), 15, 150.

[6] G. T. Bakhvalov, Trans. 2nd All-Union Conf. on Theoretical and Applied Electrochemistry (Acad. Sci. Ukrainian SSR Press, Kiev, 1949), 202(Doctorate Dissertation).

[7] Yu. A. Vene and S. A. Nikolaeva, J. Phys. Chem. 5, 811 (1955).

[8] A. N. Sysoev and V. G. Chernenko, Trans. Kharkov Polytech. Inst. 1, 88 (1952).

[9] V. P. Mashovets, S. Ya. Pasechnik and M. G. Popova, Bull. Mendeleev All-Union Chem. Soc. 2 (1938); S. Ya. Pasechnik and M. G. Popova, Trans. 2nd All-Union Conf. Theoret. Appl. Electrochem. (Acad. Sci. Ukrainian SSR Press, Kiev, 1949), 386-391.

[10] A. T. Vagramyan and A. A. Sutyagina, Bull. Acad. Sci. USSR, Div. Chem. Sci. 3, 410 (1952).

[11] A. T. Vagramyan, Electrodeposition of Metals (Acad. Sci. USSR Press, 1950).

[12] G. S. Vozdvizhensky, Trans. Kirov Chem. Tech. Inst. Kazan 10, 18-24 (1947), J. Appl. Chem. 21, 11, 1095 (1948); 22, 9, 318 (1947); 22, 11, 1171 (1947); 22, 12, 1255 (1947).

[13] M. N. Polukarov, J. Gen. Chem. 19, 1583 (1949).

[14] V. V. Kuznetsov, J. Phys. Chem. 24, 574 (1950).

[15] O. A. Esin and M. A. Loshkarev, J. Phys. Chem. 13, 186 (1939).

[16] K. M. Gorbunova, T. V. Ivanovskaya, and N. A. Shishakov, J. Phys. Chem. 25, 981 (1951); K. M. Gorbunova, T. V. Ivanovskaya, and O. S. Popova, Trans. Electrochem. Conf(Acad. Sci. USSR Press, 1953), 396.

[17] K. M. Gorbunova and A. A. Sutyagina, J. Phys. Chem. 3, 542 (1955).

[18] M. A. Loshkarev and A. A. Kryukova, Proc. Acad. Sci. USSR 62, 97 (1948); M. A. Loshkarev, Doctorate Dissertation, Inst. Phys. Chem. (Acad. Sci. USSR, Moscow, 1948).

Received June 7, 1955.

INFLUENCE OF (SURFACE) MICRORELIEF ON THE CURRENT DISTRIBUTION ON ELECTRODES

L. I. Kadaner

In most investigations of the distribution of current and metal over electrode surfaces the influence of electrochemical or macrogeometrical factors is considered; the influence of the nature of the cathode surface is generally not taken into account. Nevertheless, the state of the electrode surfaces may have a considerable influence on the current distribution.

In a study of current distribution over electrode surfaces we observed that the current densities on somewhat rougher cathode plates were higher than on smooth plates closer to the anodes.

The following experiment was performed to determine the influence of the state of the surface on the current distribution. Five cathode plates of equal size, cut from the same copper sheet, were fixed in a holder and placed at equal distances from the anode in a rectangular electrolytic cell filled with electrolyte of the composition: $CuSO_4 \cdot 5H_2O$ 200 g/liter, H_2SO_4 50 g/liter (Fig. 1).

Each plate was clamped in the holder by means of a contacting screw. The rear sides of the cathode plates were insulated by means of a chemically resistant lacquer.

Current was supplied separately to each plate from the commutator K. The current strength at each plate was measured in turn by means of the group of commutator switches or a group switch and the ammeter A_2. The total current strength at all the electrodes, measured by the ammeter A_1, was kept constant by means of the rheostat R_1. In order to eliminate the influence of the potential drop in the ammeter A_2 and thereby to ensure an equal potential at all the electrodes, a compensating rheostat R_2 was included in the circuit. The galvanometer g was used to detect the instant of compensation.

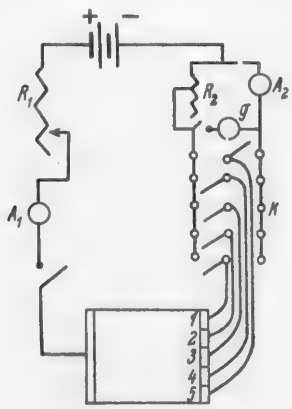

Fig. 1. Circuit diagram of apparatus for measurement of current densities at different regions of the electrode.

This apparatus was used to measure the current strength at each electrode (plate). Two of the plates (1 and 3) were then coated with spongy copper, and the current strength was then again measured at each electrode under the same conditions, first with the same total current strength, and then at a higher total strength. The results are given in Table 1.

These results demonstrate the significant influence of microrelief on current density distribution, determined by polarization differences at the smooth and spongy surfaces. It should be noted that with increasing current density the influence of differences in the microrelief becomes less appreciable, which is to be attributed to a lag of the increase of potential behind the increase of the ohmic component.

The influence of microrelief on the distribution of current over the cathode surface can be elucidated by consideration of a model consisting of a rectangular electrolytic cell with one anode and two cathode plates parallel to each other (Fig. 2). One of the cathode plates has a smooth surface while the other is covered with a layer of spongy copper.

TABLE 1

Influence of Microrelief on Current Density Distribution

Electrode characteristics	Av. current density (A/dm²)	Current density as % of average density	Current distribution at electrodes				
			1	2	3	4	5
Surfaces of all electrodes smooth	0.124	Current density (in A/dm²)	0.125	0.124	0.124	0.123	0.123
Surfaces of electrodes 2, 4, 5 smooth Electrodes 1 and 3 covered with spongy copper	0.116	Current density (in A/dm²)	0.164	0.062	0.186	0.071	0.098
		Percentage of average current density	142	54	162	62	85
	0.85	Current density (in A/dm²)	1.16	0.62	1.29	0.67	0.80
		Percentage of average current density	130	70	145	75	90
	1.75	Current density (in A/dm²)	1.96	1.39	2.20	1.44	1.56
		Percentage of average current density	115	81	138	84	92

Let us consider the current distribution at each cathode plate. Since the dimensions of the cathode plates are much less than their distance from the anode, it may be assumed that the field set up by the cathode plates does not influence the distribution of current at the anode. In this case the field superposition principle may be applied. In the model under consideration the uniform field of the plane anode is superposed on the field of the two plates K_1 and K_2, meeting at an angle of 180° [1]. Accordingly, the current density at any region of the cathode is determined by the current densities due to two superposed fields (we assume that the lines of force enter and leave the electrodes at right angles).

The current density component due to the uniform anode field will be the same at any region of the cathode.

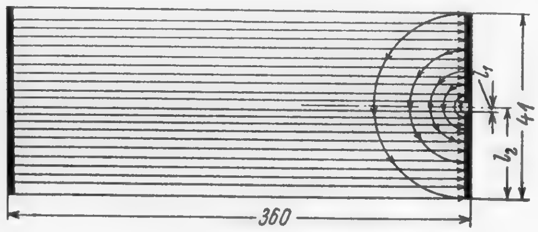

Fig. 2. Diagram of the field in a three-electrode system in a rectangular electrolytic cell

The field between the two cathode plates is set up as the result of the difference of cathodic polarization at the smooth and spongy surfaces, and consequently, of the potential difference.

The current strength at the cathode region dl, caused by the field of the cathodes is

$$di = Dhdl = \frac{\Delta e}{\rho \frac{\pi l}{hdl}} = \frac{f(D_0 - D) - f_1(D_0 + D)}{\rho \frac{\pi l}{hdl}}, \tag{1}$$

where Δe is the potential difference between the regions dl of the two cathodes, ρ is the specific resistance of the electrolyte, πl is the length of the tube of force, dl is the width of the tube of force; h is the height of the working part of the electrode; D_0 is the current density component due to the anode field; D is the current density component due to the field of the electrodes K_1 and K_2, which has a positive value at the region dl of the spongy cathode, and a negative value at the corresponding region of the smooth cathode.

The current density at the region dl of the spongy cathode will be $D_0 + D$ and the potential $f_1(D_0 + D)$.* The current density at the region dl of the smooth cathode will correspondingly be $D_0 - D$ and the potential $f(D_0 - D)$.

If it is assumed as a first approximation that electrode polarization in the copper sulfate electrolyte is proportional to the current density, i.e., that $e = b + aD$ (where a and b are constants), and that the potential at the spongy electrode remains practically unchanged on variation of the current strength because of the extensively developed surface, and its value is b, then the expression (1) becomes

$$di = \frac{b + a(D_0 - D) - b}{\rho \frac{\pi l}{hdl}} = Dhdl; \quad D = \frac{aD_0}{\pi\rho l + a}. \tag{2}$$

The current strength at the cathodes K_1 and K_2, due to their field, will be

$$i_c = \int_{l_1}^{l_2} Dhdl = \int_{l_1}^{l_2} \frac{aD_0 h}{\pi\rho l + a}\, dl = \frac{ahD_0}{\pi\rho} \ln \frac{a + \pi\rho l_2}{a + \pi\rho l_1}. \tag{3}$$

The current strength i_a at the cathodes, due to the uniform anode field, will be

$$i_a = D_0 (l_2 - l_1) h. \tag{4}$$

The actual current strength at each cathode will be

$$i_1 = i_a + i_c = D_0 h (l_2 - l_1) + \frac{ahD_0}{\pi\rho} \ln \frac{a + \pi\rho l_2}{a + \pi\rho l_1}, \tag{5}$$

$$i_2 = i_a - i_c = D_0 h (l_2 - l_1) - \frac{ahD_0}{\pi\rho} \ln \frac{a + \pi\rho l_2}{a + \pi\rho l_1}. \tag{6}$$

Correspondingly, the average current density at each cathode will be

$$D_1 = D_0 + \frac{aD_0}{\pi\rho (l_2 - l_1)} \ln \frac{a + \pi\rho l_2}{a + \pi\rho l_1}, \tag{7}$$

$$D_2 = D_0 - \frac{aD_0}{\pi\rho (l_2 - l_1)} \ln \frac{a + \pi\rho l_2}{a + \pi\rho l_1}. \tag{8}$$

* Calculation based on the apparent current density.

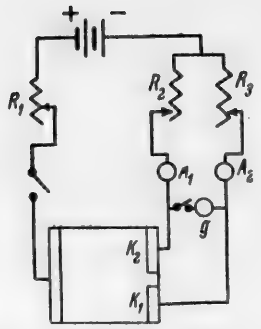

Fig. 3. Circuit for current measurement in a system with two cathodes.

Experimental verification of formula (3) showed fairly good agreement (considering the simplifying assumptions made) between the calculated and experimental results, at least adequate for qualitative conclusions.

The experimental verification was performed with the use of a cell of the dimensions shown in Fig. 2, and also in a cell 21 mm wide. The current strength at each electrode was recorded by means of the ammeters A_1 and A_2 (Fig. 3). Equality of potentials was regulated by means of the rheostats R_2 and R_1 and recorded by the zero position of the galvanometer needles. One of the electrodes had a smooth and the other a spongy surface. The rear sides of the electrodes were insulated. The gap between the electrodes was 0.5 mm. The dimensions of the working parts of the cathodes were 20×40 mm (Variant I) and 10×40 mm (Variant II).

In calculations of the current strength by Formula (3) a was taken as 0.086 v/A dm^2 [2] and $\rho = 5.5$ Ω· cm [3].

The value of i_c was calculated from the experimental data by the formula $i_c = \frac{i_1 - i_2}{2}$.

The results of the determinations and the calculated and experimental values of i_c are given in Table 2.

As formulas (7) and (8) show, the difference between the current densities at the cathode regions with different surfaces will be greater with smaller dimensions of these cathode regions, with higher conductance, and with greater cathode polarization. This is confirmed by the experimental data.

Thus, in an acid copper electrolyte, with an average current density of 1.65 A/dm^2 and cathodes 20×40 mm (Variant I), the current density at the spongy electrode is 2.8 times the value at the smooth electrode; with 10×40 mm cathodes (Variant (II) under the same conditions the current density is 4.8 times as great at the spongy electrode.

In a nickel electrolyte, where the the electrolyte resistance is higher and the polarizability of the electrodes is less than in the acid copper electrolyte, the differences of current density between the spongy and smooth cathodes are considerably less.

The results obtained with the acid tin plating electrolyte are interesting. It is known that the cathode potential in this electrolyte increases relatively little in the low current density range. Accordingly, at an average current density of 0.275 A/dm^2, the current density at the spongy electrode was 2.7 times as high as at the smooth electrode. At higher current densities the potential rises sharply and, as the table shows, at an average current density of 1.02 A/dm^2 the current density on the spongy electrode becomes 4.8 times as high as on the smooth. On further increase of current density the increase of potential again slows down. This is accompanied by evolution of hydrogen at the smooth cathode. Accordingly, at an average current density of 2.37 A/dm^2 the current density at the spongy electrode is only 1.5 times that at the smooth electrode.

The considerable influence of microrelief on current distribution at the electrodes provides an explanation for the rapid formation of spongy deposits around the electrode edges at high current densities. Initially a roughness appears at the edges, leading to a local decrease of cathodic polarization and to a redistribution of current densities. As a result, the roughness increases still further and spongy material is formed, leading to further redistribution of current densities with a considerable current density increase at the electrode edges.

The influence of spongy deposit formation at the edges of the electrode on current density redistribution can be clearly demonstrated by experiments with a special model. The apparatus described above (Fig. 1) was used to measure the current densities at three electrodes (Fig. 4) in acid copper and zincate electrolytes. The electrodes 1 and 2 served as models of the edges of a laminar rectangular electrode.

The current strength was first measured when all the electrodes had a smooth surface. Then electrodes 1 and 2 were coated with spongy copper (for measurements in acid copper electrolyte) or spongy zinc (for measurements in zincate electrolyte) and the current strength was again measured. The results are given in Tables 3 and 4.

TABLE 2

Current Density Relationships at Smooth and Spongy Electrodes

Electrolyte characteristics	Current strength at electrodes (in A)		Average current density D_0 (in A/dm^2)	Current strength due to electrode potential difference	
	smooth surface	spongy surface		calcu-lated	experimental
Composition of acid tin plating electrolyte (in g/liter): $SnSO_4$ 30, H_2SO_4 90, cresol 6, glue 1 (Variant I)	0.012	0.032*	0.275	—	0.010
	0.018	0.062	0.500	—	0.022
	0.028	0.136	1.02	—	0.054
	0.124**	0.200	2.02	—	0.038
	0.152**	0.228	2.37	—	0.038
Composition of acid copper electrolyte (in g/liter): $CuSO_4 \cdot 5H_2O$ 200, H_2SO_4 50 (Variant I)	0.005***	0.035	0.32	0.010	0.015
	0.020	0.090	0.68	0.021	0.035
	0.070	0.195	1.65	0.051	0.0625
	0.082	0.220	1.89	0.058	0.069
Acid copper electrolyte (Variant II)	0.015***	0.100	1.37	0.028	0.0425
	0.023	0.110	1.65	0.034	0.045
Composition of nickel electrolyte (in g/liter): $NiSO_4 \cdot 7H_2O$ 180, $Na_2SO_4 \cdot 10H_2O$ 40, $MgSO_4 \cdot 7H_2O$ 45, H_3BO_3 20, NaCl 7 (Variant I)	0.023***	0.042	0.41	—	0.0095
	0.030	0.060	0.56	—	0.015
	0.065	0.130	1.22	—	0.0325
Composition of zincate electrolyte (in g/liter): ZnO 11, NaOH 80, $SnCl_2$ 0.2, H_2O_2 1 1 ml/liter; t = 40°	0.018	0.036	0.34	—	—
	0.028	0.058	0.54	—	—

* Cathode was covered with slightly spongy copper.

** Hydrogen was evolved at the smooth electrode.

*** The cathode was covered with spongy copper in an electrolyte of the composition: $CuSO_4 \cdot 5H_2O$ 25 g/liter, H_2SO_4 50 g/liter at $D_C = 5$ A/dm^2 for 5 minutes.

TABLE 3

Results of Current Strength and Density Measurements
Electrolyte composition (in g/liter): $CuSO_4 \cdot 5H_2O$ 200, H_2SO_4 50; temperature 19°

Electrode characteristics	Current at all 3 electrodes (A)	Current at electrodes 1 and 2 (A)	Av. current density (in A/dm^2)	Curr. density at	Curr. density at electro. 3 (in A/dm^2)
Surface of all three electrodes smooth	0.21	0.055	0.82	1.74	0.69
Surface of electrode 3 smooth, Elec. 1 & 2 spongy	0.21	0.125	0.82	3.97	0.38
Surface of electrode 3 smooth, Elec. 1 & 2 spongy	0.21	0.175	0.82	5.55	0.15

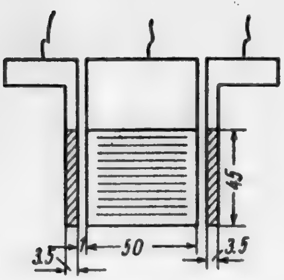

Fig. 4. Model of the edge of a laminar rectangular electrode.

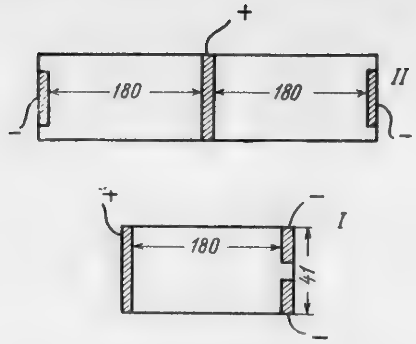

Fig. 5. Electrode arrangement in the Haring and Blum installation.

TABLE 4

Results of Current Strength and Density Measurements

Electrolyte composition (in g/liter): ZnO 11, NaOH 80, $SnCl_2$ 0.2; H_2O_2 1 ml/liter; temperature 40°

Electrode characteristics	Current at all 3 electrodes (A)	Current at electrodes 1 and 2 (A)	Av. Current density (in A/dm²)	Curr. density at electro. 1 and 2 (in A/dm²)	Curr. density at electro. 3 (in A/dm²)
Surface of all three electrodes smooth	0.31	0.047	1.21	1.49	1.17
Surface of electrode 3 smooth. Elec. 1 & 2 spongy	0.31	0.150	1.21	4.76	0.71

The results indicate a considerable redistribution of current on sponge formation at the electrodes, leading to a sharp increase in the the rate of sponge formation. On the other hand, the decrease of current density at the smooth part of the surface is an important factor. Thus, at an average current density of 0.82 A/dm^2, when the surface of all three electrodes was smooth, the current density at electrode 3 was 0.69 A/dm^2. When electrodes 1 and 2 were covered with spongy copper, the current density at the smooth electrode 3 fell sharply and was 5.5 times smaller than the average current density.

It should be noted in this connection that cases are known in electroplating practice when the growth of spongy zinc or nickel dendrites on the floor or other parts of bell-type cells results in a considerable decrease of productivity for a given current strength. This can be explained by the decrease of polarization at the spongy growths or dendrites, leading to a sharp decrease of the fraction of the current used for deposition of the metal on the plated articles.

This leads to the practical conclusion that spongy deposits or dendrites are inadmissible on suspension and contact devices in bell-type cells, on projecting edges of articles, on metal screens, etc. To prevent the possibility of sponge or dendrite formation, the geometrical forms and dimensions of the screens, suspension devices, etc., must be suitably chosen. If the formation of spongy and dendritic deposits cannot be prevented, they must be systematically removed and not allowed to grow.

The influence of different types of electrode treatment on the distribution of current at the electrodes is of practical interest. For this purpose we measured current density distributions in the apparatus shown in Fig. 2, between polished plates, plates which had been sandblasted, and plates treated with a file. The results are given in Tables 5 and 6.

TABLE 5

Current Density Relationships at Electrodes in Acid Tin Plating Electrolyte
Electrolyte composition (in g/liter): $SnSO_4$ 30, H_2SO_4 90, cresol 6, glue 1

Electrode (cathode) characteristics	Current strength (in A)		Ratio of current densities at electrodes I and II
	at electrode I	at electrode II	
Electrode I, smooth (after rolling) Electrode II, polished	0.116 0.058	0.072 0.036	1.61 1.62
Electrode I, smooth (after rolling) Electrode II, polished	0.090 0.045	0.078 0.038	1.15 1.17
Electrode I, sandblasted Electrode II, polished	0.032 0.076 0.116 0.160	0.018 0.040 0.078 0.144	1.78 1.90 1.49 1.11
Electrode I, covered with bright electrolytic tin deposit Electrode II, covered with rough gray tin deposit	0.032 0.044 0.080	0.052 0.065 0.112	0.62 0.68 0.72

TABLE 6

Current Density Relationships at Electrodes in Acid Copper Electrolyte

Electrode Characteristics	Current strength (in A)		Ratio of current densities at electrodes I, II.
	at electrode I	at electrode II	
Electrode I, filed	0.106	0.084	1.26
Electrode II, polished	0.140	0.104	1.34

The results show that the current densities at surfaces subjected to different mechanical treatments differ so much that this must be taken into account in electroplating practice. Therefore, articles with differently prepared surfaces should not be placed in a cell simultaneously.

It should be pointed out that the influence of microrelief on the distribution of current at electrodes depends on the configuration of the field. For example, in the Haring and Blum installation the influence of microrelief is considerably less than for electrodes arranged side by side, and sometimes it may even be neglected for practical purposes. This can be seen from the results of measurements made with the electrodes arranged as shown in Fig. 5 (Table 7).

It should be noted also that many workers have reported changes of current distribution at the electrodes in the course of electrolysis. This is easily explained in the light of the present results. During electrolysis the quality of the electrode surface changes continuously, and the variation depends on the current density in a particular region, which leads to a redistribution of current densities.

TABLE 7

Current Density Relationships at Spongy and Smooth Electrodes in Relation to the Nature of the Field (Fig. 5)

Electrode characteristics	Average current density (in A/dm²)	Ratio of current densities at electrodes I and II		Electrolyte composition (in g/liter)
		field I	field II	
Electrode I, smooth; Electrode II, covered with spongy copper layer	0.3	6.25	1.17	$CuSO_4 \cdot 5H_2O$ 200, H_2SO_4 50
	0.8	4.86	1.08	
Electrode I, smooth; Electrode II, covered with slightly spongy copper	0.4	3.74	1.6	$SnSO_4$ 30, H_2SO_4 90, cresol 6, glue 1
	0.7	3.45	1.21	

Finally, the important influence of microrelief which we have discovered also makes it possible to augment Kudryavtsev's views [4] on the causes of formation of spongy deposits at the cathode surface at low current densities in zincate electrolytes. According to Kudryatsev, metal sols are transferred to the cathode and initiate disordered crystal growth on it. The subsequent rapid spongy growth is not explained. In the light of the present results the rapid spongy growth may be explained by local decreases of polarization, the small dimensions of the spongy regions (see formulas (7) and (8) and the consequent sharp local increases of current density.

SUMMARY

1. The significant influence of microrelief on the current distribution at electrode surfaces has been demonstrated.

2. The influence of microrelief is greater at higher electrode polarization and electrolyte conductivity, and with smaller dimensions of the cathode regions differing in their microrelief characteristics. The influence of microrelief depends on the field configuration.

3. The influence of microrelief on current distribution explains the rapid growth of spongy deposits, and can be used to augment the views of N. T. Kudryavtsev on the causes of sponge formation at low current densitites in zincate electrolytes.

4. The results show that it is necessary to exclude the possibility of sponge and dendrite formation,not only on projecting edges of articles but also on contact devices and screens, and that articles with surfaces of a different character should not be placed in the plating bath simultaneously.

LITERATURE CITED

[1] R. L. Neiman and P. L. Kalantarov, Theoretical Principles of Electrotechnology, III (State Power Press, Moscow–Leningrad, 1948).

[2] S. V. Gorbachev and R. M. Vasenin, J. Phys. Chem. 27, 231 (1953).

[3] V. I. Lainer and N. T. Kudryavtsev, Fundamentals of Electroplating (Metallurgy Press, Moscow, 1953).

[4] N. T. Kudryavtsev, Proc. Acad. Sci. USSR 72, 93 (1950).

Received April 5, 1955

DIFFUSION COPPER PLATING

N. S. Gorbunov and A. G. Latukhova

Institute of Physical Chemistry, Academy of Sciences USSR

Copper is one of the relatively(chemically) inactive metals. It has a high coefficient of electrical and heat conductivity and is easily alloyed with metals such as tin, zinc, and nickel, forming bronze, brass and cupronickel alloys which are widely used in industry.

The solubility of iron in copper is very low. The solubility of iron in the solid state at 1100° is 4%, and this decreases sharply with decrease of temperature.

Copper coatings applied to iron by various methods are widely used in industry. The commonest methods are the electroplating method [1] the mechanothermal (hot rolling) chemical contact method used for the production of thin copper coatings, and the diffusion method.

Thickness and structure of diffusion copper coatings. A mixture of copper powder and aluminum oxide was used for the production of diffusion copper coatings. The specimens to be coated were placed in small metal cases and covered with the powdered mixture.

TABLE 1

Thickness of Diffusion Copper Layer as a Function of the Temperature and Treatment Time

Time (hours)	Layer thickness (in μ) at temperature (°C)		
	1150°	1200°	1250°
1	68	70	74
2	77	87	93
3	95	108	115
4	110	118	124

The diffusion copper plating was carried out in a reducing hydrogen atmosphere in a continuous stream of hydrogen. The specimens were also cooled in a stream of hydrogen [2,3].

The thickness of the copper layers formed was determined metallographically. To prevent the layer from chipping off and the edges from bending over, the specimens were pressed into polymethyl methacrylate (Plexiglas) by Tsitrin's method [4] before the grinding and polishing. The sections were etched by 5% solution of nitric acid in ethyl alcohol.

Table 1 gives data on the thickness of the diffusion copper coatings obtained at different temperatures and in different treatment times.

The results in Table 1 show that the thickness of the diffusion coating increases continously with increasing temperature and time of the diffusion process.

The figure shows microphotographs of the structure of the diffusion copper layer formed on the iron specimen surface under different diffusion conditions. The microphotographs show that the diffusion copper layer can be distinguished fairly clearly from the base metal. A thin layer of pure copper can be seen in some regions. Deposition of pure copper can also be seen at the grain boundaries, as pure copper is liberated from solid solutions of copper in iron on cooling of the specimens. The diffusion copper layers shown in the microphotographs were applied in 3 hours at 1150 and 1250°.

The thicknesses of the diffusion copper layers were calculated from the formula

$$L = 2\sqrt{At}\,.\,e^{-B/2T}.$$

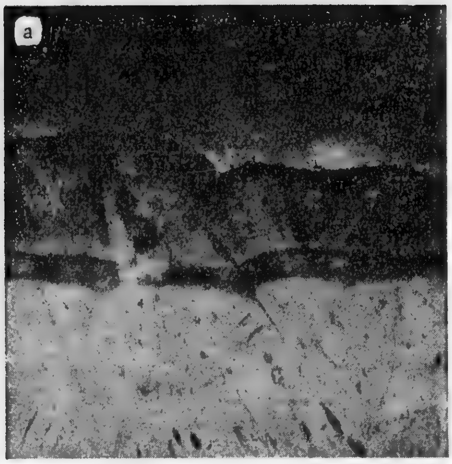

Microphotographs of the structure of diffusion copper layers on the surfaces of iron specimens (× 340). Coating conditions: a) temperature 1150° time 3 hours; b) temperature 1250°, time 3 hours.

where L is the layer thickness (in cm), t is the time (in seconds), T is the temperature, and A and B are constants.

The constants A and B were determined from two equations based on the experimental data. Their values were: $A = 2.7 \cdot 10^{-6}$ and $B = 10{,}230$.

Table 2 gives the thicknesses of the diffusion copper layers found experimentally for different temperatures and treatment times, and calculated from the above equation.

The results in Table 2 show fairly good agreement between the experimental and calculated values for the thickness of the diffusion copper layers.

TABLE 2

Experimental and Calculated Values for the Thickness of Diffusion Copper Layers

Absolute temperature (°K)	Time (hours)	Thickness of diffusion copper layer (in μ)	
		experimental	calculated
1423	1	68	54
	2	(77)	(77)
	3	95	94
	4	110	109
1473	1	70	62
	2	(87)	(87)
	3	108	106
	4	118	123
1523	1	74	70
	2	93	97
	3	115	120
	4	124	138

Changes in the weight and dimensions of specimens after diffusion copper plating. The diffusion copper plating process is accompanied by changes in the weight and dimensions of the specimens. Table 3 gives data on weight changes, and Table 4, on dimensional changes, of specimens in relation to the conditions of treatment.

The results in Tables 3 and 4 show that higher temperatures and longer diffusion treatment times result in greater increases in the weight and diameter of the specimens. Dimensional increases after copper plating must be taken into consideration if the dimensions of the articles must be strictly controlled.

Properties of diffusion copper layers. The corrosion resistance of diffusion copper layers was tested in aqueous solutions of hydrochloric acid, sodium chloride, and sodium sulfate, at 10, 3, and 5% concentrations respectively. The test objects were iron specimens after diffusion copper plating at 1200° for 3 or 4 hours. The test specimens were completely immersed in the solutions by means of glass hooks.

The corrosion tests were carried out at room temperature by the usual method for determining corrosion resistance from the change in weight.

Table 5 gives the results of tests on control iron specimens and iron specimens after diffusion copper coating, in salt solutions and in aqueous hydrochloric acid.

TABLE 3

Changes in Weight of Specimens for Different Conditions of Diffusion Copper Plating

Time (hours)	Increase of weight (in mg/cm²) at temperature (°C)		
	1150°	1200°	1250°
1	—	7.05	9.92
2	4.66	8.75	14.25
3	5.32	10.00	16.64
4	7.07	11.75	19.75

TABLE 4

Increase of Diameter of Specimens for Different Conditions of Diffusion Copper Plating

Time (hours)	Increase of diameter of specimens (in μ) at temperature (°C)		
	1150°	1200°	1250°
1	—	10	40
2	30	40	—
3	40	50	60
4	45	60	70

TABLE 5

Corrosion of Original and Copper-Plated Armco Iron in Various Corrosive Media

Time (days)	Weight losses (in mg/cm²) in solutions of					
	10%-hydrochloric acid		3%-sodium chloride		5% sodium sulfate	
	coated	original	coated	original	coated	original
1	0.3	4.95	0.27	0.27	0.17	0.17
2	0.62	9.77	0.57	0.62	0.45	0.45
3	0.87	13.50	0.77	0.80	0.47	0.70
4	1.12	16.95	0.97	1.25	0.60	0.82
5	1.62	21.27	1.12	1.20	0.80	1.00
10	3.47	59.25	2.05	2.35	1.50	1.87

The corrosion test results in Table 5 show that specimens covered with a diffusion copper layer are more resistant to corrosion by 10% aqueous hydrochloric acid than the original iron. However, the diffusion copper coatings have practically no protective effect against corrosion of the metal in salt solutions.

The high corrosion resistance of iron specimens coated with copper in atmospheric conditions should be noted. Even prolonged exposure to air (5-6 months) produces no appreciable weight increase or change in the external appearance of the specimens.

Diffusion copper plating can therefore be recommended for corrosion protection of iron articles in atmospheric conditions; this can be used for the protection of electrotechnical equipment parts, especially if high electrical conductance in the surface layer must be preserved.

LITERATURE CITED

[1] V.I. Lainer and N.T. Kudryavtsev, Fundamentals of Electroplating, Metallurgy Press (1953).

[2] N. A. Izgaryshev and E. S. Sarkisov, J. Gen. Chem. 22, 321 (1939).

[3] N. S. Gorbunov and F. S. Baryshanskaya, Proc. Acad. Sci. USSR, 9, 37 (1942).

[4] F. N. Tsitrin, Bull. Automobile Ind. 9 (1944).

Received May 17, 1955

DIMENSIONAL CHANGES OF ALUMINUM ALLOY ARTICLES IN ANODIC OXIDATION

A. V. Shreider

Anodic oxidation (anodizing) is a widely used method for producing coatings on the surface of articles made from aluminum and its alloys. In addition to increasing the corrosion resistance [1-13], anodizing is now used as a method for conferring to the surface metal layer the required color [14-25], hardness [26-29] abrasion resistance [7, 15, 19, 27, 29-33], erosion resistance [29, 32, 34-36], electrical resistance [7,8, 29, 31, 37-39] and heat insulating properties [29]. Anodizing can also be used to control the quality of the material in aluminum alloy articles [40-45], to form relief and plane images [46-47], to protect aluminum reflectors against dulling [48-49], and to ensure firm adhesion of electroplated coatings to the surface of aluminum alloy articles [50-53].

In modern practice of precision machine and instrument construction by mass production, parts are produced with a high degree of dimensional precision. The thickness of electroplated coatings can be taken into account relatively simply, as this can be easily regulated to an accuracy of $\pm 1\mu$ by control of the plating conditions.

Quite a different situation exists in the widely used processes of anodic oxidation of parts made from aluminum alloys to a high degree of precision.

In anodic oxidation, conversion of the metal to the oxide is accompanied by dissolution of the metal, partial dissolution of the newly formed oxide, and hydration of the anodic oxide film. The film grows by gradual conversion of progressively deeper metal layers into oxide.

Growth of the oxide "into the depth of the metal" is associated with its porous structure and with filling of the pore canals of the film with electrolyte [2].

Since the specific volume of the oxide is greater than the specific volume of the original metal [54-56], the main process of conversion of the metal into oxide is accompanied by a dimensional increase. Some swelling of the porous oxide during hydration also results in a slight dimensional increase [26]. On the other hand, the dissolution of the metal and oxide accompanying the oxide formation decreases the dimensions of the article.

Statements in the literature [7, 8] that in the usual anodizing conditions the increase of the oxide level above the metal level is from $^1/_3$ to $^1/_2$ of the thickness of the oxide film, are inaccurate. These results were obtained by estimations of dimensional changes in a few sets of anodizing conditions, and were unjustifiably extended to all the numerous variations of anodizing conditions, without consideration of variations of anodizing conditions which influence film formation and solution and have a significant influence on the dimensions [57].

Moreover, these estimations did not take into account the effects of the chemical composition and structure of the aluminum alloys, whereas the nature of the alloy has a very strong influence on the dimensional changes. For example, under the same anodizing conditions (25% H_2SO_4, 20-22°, 100 minutes, 1.5 A/dm^2), specimens of an aluminum-magnesium-silicon alloy without copper showed a surface thickness increase of the order of 35μ, while in specimens of an aluminum alloy with a high copper content the dimensional increase does not exceed 1-3 μ [58].

In the formation of a thick oxide layer, by Tomashov's method [27], the increase of the oxide level above the metal level rises from 0.47 - 0.61 of the oxide thickness as the current density increases from 2 to 6 A/dm^2. These results are well reproducible [36], but they represent the dimensional changes in only one, although practically important, specific anodizing process. This process differs from the usual anodic oxidation

processes by the specially intensive cooling, which has a very strong retarding effect on the dissolution of the metal and oxide.

The greatest variations of dimensional changes in precision parts of machines, equipment, and instruments are met in anodizing practice. Depending on the conditions of the anodic oxidation process, the nature of the metal, and even the configuration, anodizing may result in various increases and decreases of the wall thickness.

Absence of any dimensional change after anodizing is the consequence of mutual compensation of processes which decrease and processes which increase the wall thickness, and this result may be possible under definite anodizing conditions. For this, the technological process must either not include preparation of the surface for anodizing by treatment in alkaline solutions, or must be so designed that the growth of the oxide level above the metal level in anodizing should balance the loss in the alkaline solution. The latter method, however, is not used in practice because of the relatively high metal loss and the serious deterioration of the surface finish after preparation in alkaline solution.

Determination of dimensional changes by direct measurement would not give reproducible results, as aluminum alloy specimens cannot be made to an accuracy greater than that of the first class, while for measurements by means of optical instruments (accuracy of $\pm\ 0.2\ \mu$) the specimens must be made to an accuracy of $\pm\ 0.5\ \mu$; with less accurately made specimens the measurement results will be unreliable becauses of differences in the dimensions of the specimens at neighboring points.

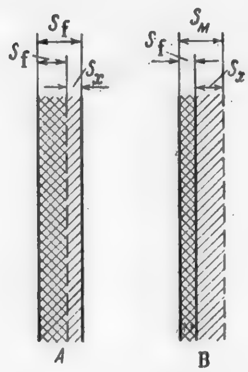

Figure 1. Dimensional changes in anodic oxidation. A) Increase, B) decrease of the wall thickness of the article. The broken line represents the level of the metal surface before anodizing.

For approximate determinations, a gravimetric method [55] has been developed, based on threefold weighing of the specimens (to an accuracy of 0.0001 g): before anodizing (P_1), after anodizing (P_2), and after removal of the anodic oxide film (P_3). The difference ($P_2 - P_3$) gives the weight of the film and the difference ($P_1 - P_3$) gives the weight of the metal oxidized during the anodizing.

The "lateral" dimensional change of the specimen (S_x) is found from the difference between the thickness of the oxide film formed (S_f) and the thickness of the metal oxidized during anodizing (S_M) (Fig. 1), and is calculated from the formula

$$S_x = S_f - S_M = \frac{P_2 - P_3}{\gamma_f \cdot F} - \frac{P_1 - P_3}{\gamma_M \cdot F}, \qquad (1)$$

where F is the surface area of the anodized specimen γ_M is the density of the metal, and γ_f is the density of the oxide film.

In calculations by Formula (1), the sign of S_x shows whether the anodizing has produced an increase (+) or a decrease (—) of dimensions.

The bulk density of the films formed by anodizing with internal cooling to temperatures close to 0° is assumed to be 2.74 [26]. For films made under the usual anodizing conditions γ_f may be taken as 2.44 without serious error [38]. This value should not differ seriously for films obtained by means of sulfuric and chromic acid treatment, while in films formed in sulfuric acid the pores are larger; this is balanced by the considerably greater density of the pores in films formed by anodizing in chromic acid solutions.

In determinations of dimensional changes as the result of anodizing with upward temperature deviations of the electrolyte it is necessary to take into account the fact that the bulk density of the film must decrease below 2.44 owing to increased porosity of the oxide.

However, the error caused by the use of values in the range 2.2-2.4 for calculation in such cases is not large, as in anodizing in baths at increased electrolyte temperatures metal dissolution processes predominate over film formation processes ($S_f \ll S_M$). *

Sufficiently accurate results can only be obtained if the films are dissolved in a reagent which has practically no effect on the base metal. Good results are obtained by removal of the films in a solution of 20 g CrO_3 and 35 ml H_3PO_4 (density 1.6) per liter at 89-91° for 20 minutes. The average thickness (S_a) of metal removed during solution of the film then does not exceed 0.05μ for AK-6 and AMg alloys, and 0.5μ for aged Duralumin D-1. The value of S_a may be ignored in determinations of dimensional changes, as this value is a component both of the minuend and of the subtrahend in the calculation:

$$S'_x = S'_f - S'_M = \frac{P_2 - (P_3 + P_a)}{F \cdot \gamma_f} - \frac{P_1 - (P_3 + P_a)}{F \cdot \gamma_M}. \qquad (2)$$

This is confirmed by the following estimate of the error f which arises in calculation of S_x with S_a ignored:

$$f = S'_x - S_x = \frac{P_a}{F \cdot \gamma_f} - \frac{P_a}{\gamma_M \cdot F} = \frac{\gamma_M \cdot P_a - \gamma_a \cdot P_a}{F \cdot \gamma_M \cdot \gamma_f} =$$

$$= \frac{P_a}{F \cdot \gamma_M}\left[\frac{\gamma_M - \gamma_a}{\gamma_f}\right] = \frac{\gamma_M - \gamma}{\gamma_f} \cdot S_a. \qquad (3)$$

For D-1 ($\gamma_m = 2.80$, $\gamma_f = 2.44$, $S_a = 0.5\ \mu$) this error is

$$f = \frac{2.80 - 2.44}{2.44} \cdot S_a = 0.15 \cdot S_a = 0.15 \cdot 0.5 = 0.075\mu.$$

A subsidiary result obtained in gravimetric determinations is measurement of a practically important quantity— the thickness of the anodic oxide films: the thickness is a measure of the anticorrosion protection provided by the film. In calculations of film thickness

$$S'_f = \frac{P_2 - P_3 - P_a}{F \cdot \gamma_f} = S_f - S_a \qquad (4)$$

for Duralumin D-1 the value $S_a = 0.5\,\mu$ is taken into account. For AMg and AK-5 the value $S_a = 0.05\,\mu$ may be neglected in the calculations.

The proposed method may give erronous results if the actual surface area differs greatly from the specified value. This was verified by determinations of the surface microgeometry by evaluation of $H_{m.s.}$ ** by means of the Abbott profilograph, and construction of profilograms with the aid of the Brush profilometer; the results were used to plot the surface microprofile.

* During preparation of the present paper for publication, a report has appeared stating that the bulk density of films formed at electrolyte temperatures of the order of 50° may fall to 1.8 [59].

** $H_{m.s.}$ is the root mean square deviation of the depressions and projections of the surface microprofile from the median line.

TABLE 1

Influence of Type of Surface Treatment of AMg Alloy on the Actual Surface Area

Type of treatment after polishing	Surface smoothness $H_{m.s.}$ (in μ)	Ratio of actual to specified surface area (in %)
	0.25-0.30	100.02
Anodizing in 3% CrO_3 solution at 40 v, 36° and 60 minutes exposure	0.25-0.35	100.27
Anodizing under the same conditions and removal of films in solution of CrO_3 + H_3PO_4	1.00-1.25	102.41
Etching for 2 minutes in a solution of 10 g NaOH, 50 g Na_3PO_4, and 20 g water glass per liter at 65°	1.25-1.50	104.85
Anodizing 50 minutes in 20% H_2SO_4 solution at 45° and 1 A/dm^2	3.75-4.25	110.34
Blasting by quartz sand sifted through No.100 sieve, under excess pressure of 1.5 atm.	6.00-6.25	117.06

TABLE 2

Specimen Materials

Aluminum alloy type	Chemical composition (%)						Heat treatment		
	Cu	Mg	Mn	Fe	Ni	Si	heating temp. before water quencing(°C)	aging: temperature (°C)	aging: time (hours)
D-1	4.20	0.45	0.58	0.49	—	0.38	500 ± 5	Natural	
AMg	—	2.02	0.22	0.06	—	0.13	Not performed (as delivered)		
AK-6	2.10	0.51	0.55	0.22	—	0.94	510 ± 5	160 ± 5	15
AK-4	2.34	1.44	0.12	1.33	1.19	0.80	530 ± 5	185 ± 5	10

In calculations of the actual surface area, only contour lines of the microprofile with $H_{m.s.}$ not less than 0.25 μ were taken into account; smaller projections and depressions of the surface microrelief cannot affect the accuracy of calculation of practically important changes in dimensions of the articles and film thickness. The results of these determinations are given in Table 1.

As the actual surface area does not exceed the specified value by more than 10%, even after the relatively strong etching during sulfuric acid anodizing at 45° with 50 minutes exposure, the deviations of the results of the approximate estimations from the actual values will always lie within the accuracy limits of this method for determination of dimensional changes (+ 20%).

The main experiments were performed with smoothly polished cylindrical specimens of 40 cm^2 surface area; the anodizing was carried out in a porcelain vessel 5 liters in capacity, with lead cathodes. To eliminate the influence of changes in the electrolyte composition, the solution was replaced by fresh solution after the anodizing of every 5 specimens. The specimens were degreased by means of B-70 gasoline before anodizing. Data on the specimen materials are contained in Table 2.

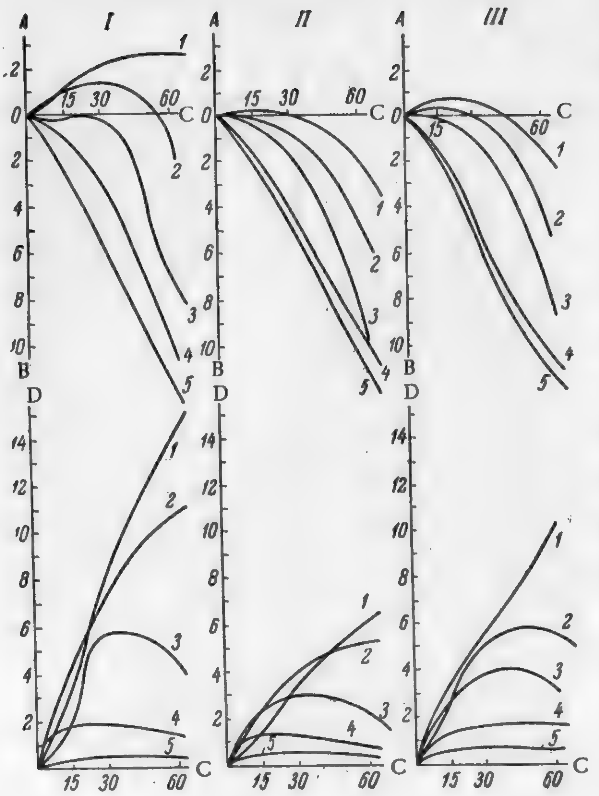

Fig. 2. Variation of dimensional (lateral) changes of articles with anodizing time in 20% H_2SO_4 solution at a current density of 1 A/dm^2.
A) Increase of oxide level above the metal surface level before anodizing (in μ), B) decrease of the level relative to the level of the metal before anodizing (in μ), C) exposure time during anodic polarization (minutes), D) thickness of oxide film (in μ); Electrolyte temperature (in °C): 1) 20, 2) 25, 3) 30, 4) 40, 5) 50.
Alloys: I) AMg, II) D-1 III) AK-6.

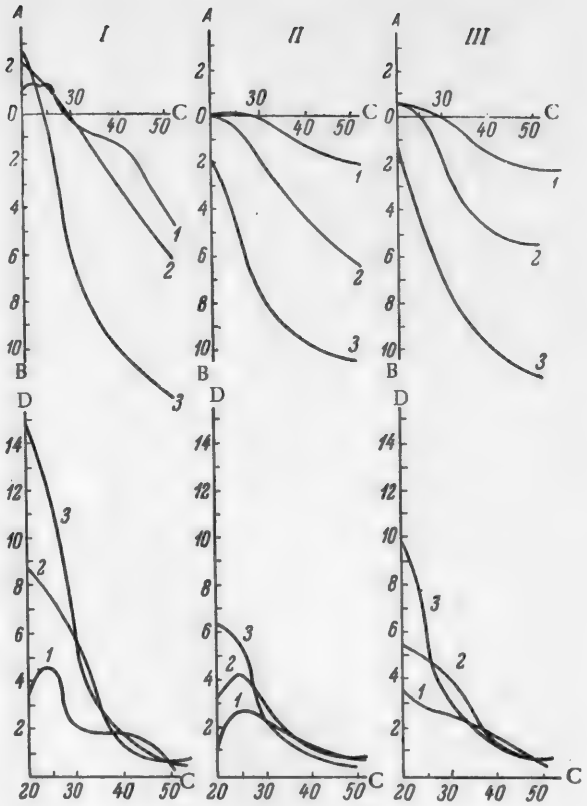

Fig.3. Variation of dimensional (lateral) change of articles with electrolyte temperature in anodizing in 20 % H_2SO_4 solution at a current density of 1 A/dm^2.
A) Increase of oxide level above the metal surface level before anodizing (in μ), B) decrease of the level relative to the level of the metal before anodizing (in μ), C) electrolyte temperature (°C), D) thickness of oxide film (in μ).
Anodizing exposure times (minutes): 1) 15, 2) 30, 3) 60.
Alloys: I) AMg, II) D-1, III) AK-6.

The method described above was used to study the influence of temperature and treatment time on dimensional changes and thickness of anodic oxide films for three of the commonest anodizing processes: 1) in 20% H_2SO_4 at current density 1 A/dm^2 (Figs. 2 and 3); 2) in 3% CrO_3 solution with the voltage rising from zero to 40 v during the first 15 minutes and then held at that level (Figs. 4 and 5); 3) in 10% CrO_3 solution with the voltage rising to 40 v in 5 minutes and then held at 40 v (Figs. 6 and 7).

Analysis of the resultant diagrams shows that increase of the electrolyte working temperature has a very great influence on the decrease of the wall thickness of the anodized parts. Solution processes begin to predominate with increasing exposure to the anodizing bath. The transition from increase to decrease of wall thickness occurs increasingly early with increase of the electrolyte temperature. The tendency to a decrease in the wall thickness increases in the transition from the homogeneous AMg alloy to multiphase alloys. The chemical activity of the working solution has a strong effect on the dimensional changes.

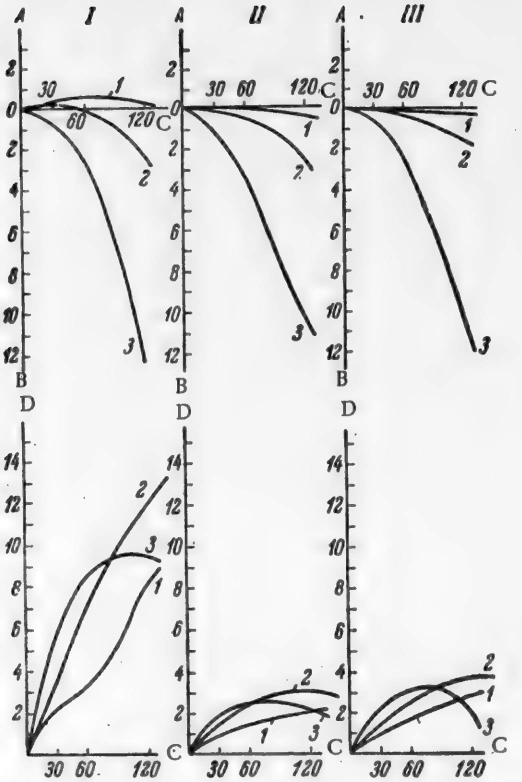

Fig. 4. Variation of dimensional (lateral) changes of articles with anodizing time in 3% CrO_3 solution at 40 v.
A) Increase of oxide level above the metal surface level before anodizing (in μ), B) decrease of the level relative to the level of the metal before anodizing (in μ), C) exposure time during anodic polarization (minutes), D) thickness of oxide film (in μ).
Electrolyte temperature (°C): 1) 30, 2) 40, 3) 50.
Alloys: I) AMg, II), D-1, III) AK-6.

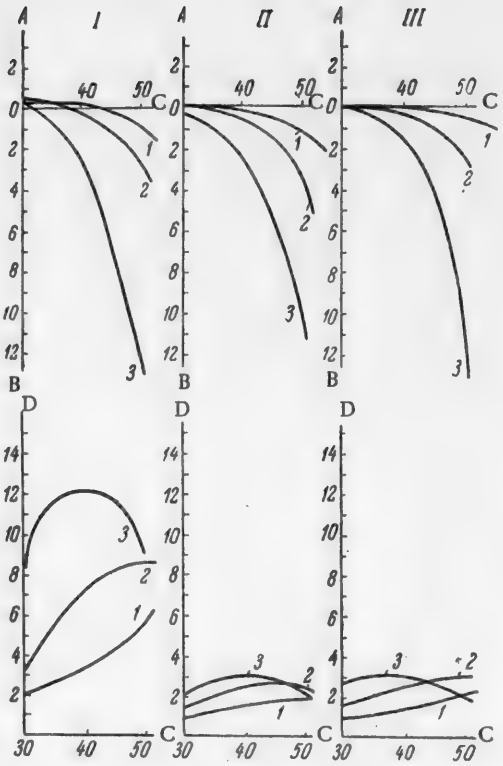

Fig. 5. Variation of dimensional (lateral) changes of articles with electrolyte temperature in anodizing in 3 % CrO_3 solution at 40 v.
A) Increase of oxide level above the metal surface level before anodizing (in μ), B) decrease of the level relative to the level of the metal before anodizing (in μ), C) electrolyte temperature (°C), D) thickness of oxide film (in μ).
Anodizing exposure times (minutes): 1) 30, 2) 60, 3) 120.
Alloys : I) AMg, II) D-1, III) AK-6.

Therefore treatment in the less active 3% CrO_3 solution results in smaller dimensional changes than anodizing in 20% H_2SO_4. With increasing concentration (and therefore with decreasing pH and increasing activity) of the chromic acid electrolyte the decrease of wall thickness during anodizing becomes much greater; therefore treatment in 10% CrO_3 solution is accompanied by a considerably greater decrease of wall thickness than treatment in 3% CrO_3 solution.

Precision parts should be anodized in 3% CrO_3 solution also because the temperature fluctuations from the specified value which may occur in production conditions result in smaller dimensional variations than those which occur during treatment in 20% H_2SO_4 and 10% CrO_3 solution.

The observed relationships governing the dimensional changes of anodized articles are to be explained by the influence of the process conditions on the electrolyte temperature in the pore canals, i.e., by the influence of the conditions on the actual temperature in the film formation zone. With increasing bath temperature the rate of heat removal is diminished and the dissolution of the oxide and metal increases. An increase of current density without alteration of the other process parameters results in an increase of the

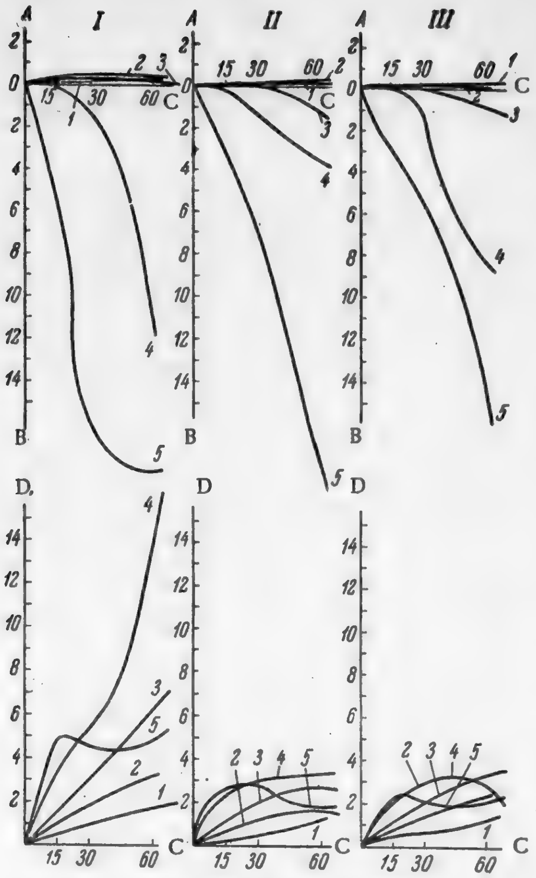

Fig. 6. Variation of dimensional (lateral) changes of articles with anodizing time in 10% CrO_3 solution at 40 v.
A) Increase of oxide level above the metal surface level before anodizing (in μ), B) decrease of the level relative to the level of the metal before anodizing (in μ), C) exposure time during anodic polarization (minutes), D) thickness of oxide film (in μ).
Electrolyte temperature (°C) : 1)20, 2) 30, 3) 40, 4) 50, 5) 60.
Alloys: I) AMg, II) D-1, III) AK-6.

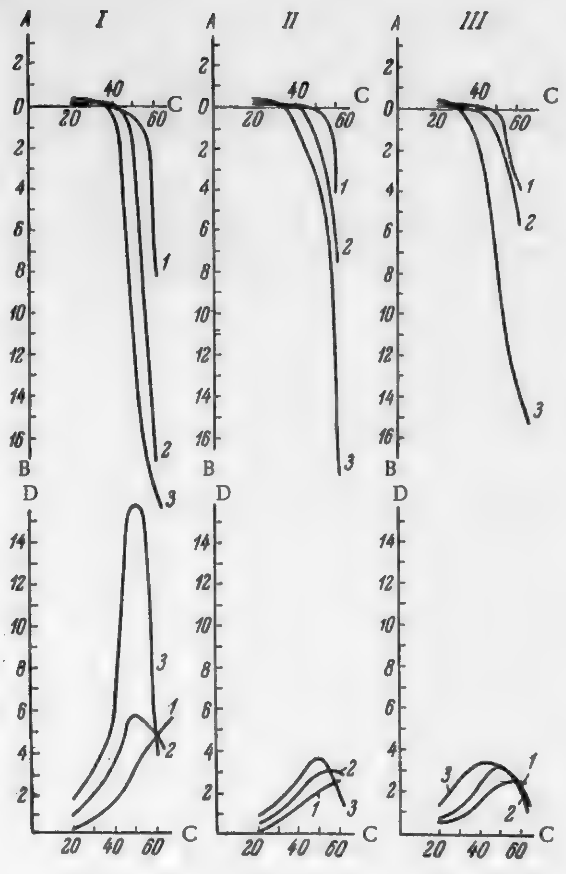

Fig. 7. Variation of dimensional (lateral) changes of articles with electrolyte temperature in anodizing in 10% CrO_3 solution at 40 v.
A) Increase of oxide level above the metal surface level before anodizing (in μ), B) decrease of the level relative to the level of the metal before anodizing (in μ), C) electrolyte temperature (°C) , D) thickness of oxide film (in μ).
Anodizing exposure times (minutes): 1) 15, 2) 30, 3) 60.
Alloys: I) AMg, II) D-1, III) AK-6.

electrolyte temperature in the pores. This not only intensifies the solution processes, but may retard the anodic oxidation of aluminum; this retardation is caused by formation of bubbles in the pore canals [60] , which increase the resistance of the electrolyte in the pores, so that the current which forms the films is diminished.

Increase of the anodizing time increases the length of the pore canals in the oxide, and therefore also the resistance of the electrolyte in them. Without special devices for cooling the metal (the so-called "internal cooling" of the articles), heat removal does not compensate for the Joule heat evolved and the heat of the exothermic oxidation reaction:

$$2Al + \frac{3}{2} O_2 \longrightarrow Al_2O_3 + 378{,}000 \text{ cal/mole} \quad [61]$$

Therefore an increase of anodizing time results in increases of the temperature and the solvent power of the electrolyte in the pores; the higher is the electrolyte temperature in the pores, the shorter is the time before compensation occurs between processes which cause increase and decrease of the wall thickness during anodizing.

The relationship between film thickness and variations of wall thickness of anodized articles depends in a complex manner on the conditions of film formation and the nature of the metal. The limiting film thickness is reached increasingly rapidly at higher electrolyte temperatures.

The absolute value of the limiting film thickness in the sulfuric acid anodizing process increases with decreasing electrolyte temperature. This is the basis for the possibility of forming very thick oxide layers by anodizing in sulfuric acid at low temperatures. "Internal cooling" removes heat from the film formation zone and allows higher current densities to be used. This is associated with the fairly high activity of the sulfuric acid electrolyte. The less active chromic acid electrolytes yield the maximum limiting film thickness at a certain optimum temperature. At this temperature the electrolyte activity is such that the balance between film formation and dissolution of the oxide creates the conditions for the formation of the thickest films. More vigorous dissolution processes occur in the anodizing of multiphase alloys than in the anodizing of homogeneous alloys; therefore the thickness of the oxide films is considerably greater on AMg alloy than on AK-6 and D-1.

In practical applications of the data shown graphically in Figs. 3-8 is necessary to take into account the method of surface preparation and also the configuration characteristics of the anodized articles.

Preparation in alkaline solutions is accompanied by a decrease in wall thickness (this decrease was not considered in the main investigation, when the specimen surfaces were prepared not in alkaline solutions but in gasoline). For parts with exact dimensions, the surface preparation before anodizing can only be carried out by organic solvents (gasoline, acetone, RDV, etc.)

The view held in electroplating practice that the throwing power of electrolytes is the cause of differences in the quality and thickness of coatings on different surfaces of articles of complex configuration is not valid for the anodizing process. The reason is that coatings of considerable electrical resistance are formed in anodizing. In anodic oxidation the coatings on different regions of the surface will be increasingly uniform with increasing resistance of the oxide film formed and with increasing electrolyte conductance. From this viewpoint, in such electrolytes as 20 % H_2SO_4 solution and 3 and 10% CrO_3 solutions, which are characterized by fairly high anode potential differences in film formation and fairly high conductances, the properties of the films should vary very little between surfaces close to the cathode and those at considerable distances from it. The differences which are nevertheless observed in the course of film formation between the cavities and external surface regions of articles of complex configuration may be attributed to local differences of electrolyte temperature. In view of the exothermic nature of the anodizing process, the actual electrolyte temperature is higher in the cavities of the articles than in the main bulk of the solution. Therefore, as the result of anodizing, the wall thickness is diminished more in the cavities than externally. In order to bring the dimensional changes in the cavities and on the outside closer together, the removal of heat from the cavities must be improved. This is effected by vigorous air agitation of the electrolyte and by suspension of the anodized articles in such a way that the electrolyte circulation in the cavities is improved by convection, air agitation, and electrode gas evolution.

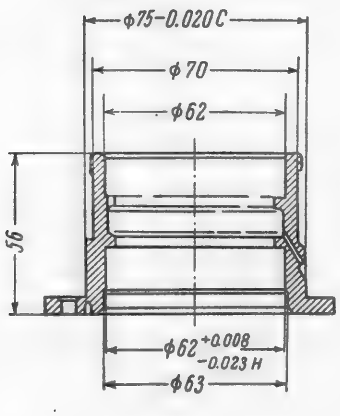

Fig. 8. Hollow article made of AK-4, used for determination of the effect of configuration on dimensional changes in anodizing.

The above is confirmed by results, given in Table 3, of a test, performed under works conditions, of the accuracy of the gravimetric method for determination of dimensional changes of articles during anodizing.

This part of the work was carried out with parts with exact external and internal fitting diameters, made of AK-4 (Fig.8); The fitting diameters were measured before and after anodizing, internally by means of a passimeter, and externally by a mechanical lever instrument, to an accuracy of 1 μ. The measurement points were approximately fixed by means of identification marks on the edge faces of the parts. Nevertheless, such great variability of the results was found that the final conclusions were based on the results of parallel tests of 60 similar parts.

The dimensional changes were also determined by the gravimetric method in cylindrical specimens of the same material. (The results of parallel gravimetric determinations agreed within 10 %.)

TABLE 3

Effects of Configuration of the Parts and Method of Surface Preparation on Dimensional Changes in Alloy AK-4 During Anodizing (Comparison of results of gravimetric determinations and driect measurements.)

Method of surface preparation before anodizing	Anodizing electrolyte	Anodizing conditions	Changes of lateral diameter (in μ) *		
			in cylindrical specimens **	in machine parts ***	
			external	external	internal
Etching 2 minutes in a solution of 10g NaOH, 50 g Na_3PO_4, and 20 g water glass per liter at 65 °	20% H_2SO_4 solution	20°, 1 A/dm², 30 min.	−5.1	−4.5	−7.5
Cleaning with B-70 gasoline	20% H_2SO_4 solution	20°, 1 A/dm², 30 min.	+0.4	+0.5	−1.5
	3% CrO_3 solution	40°, 40 V, 60 min.	−0.6	−0.5	−1.0

* The (+) sign indicates an increase of oxide level above the metal level, and the (−) sign shows a decrease of oxide level relative to the metal level before anodizing.
** Gravimetric method, mean of 5 determinations.
*** Direct measurement, mean of 60 determinations.

SUMMARY

1. In anodizing of precision articles from aluminum alloys, rejects are produced owing to changes in the exact dimensions.

2. The nature of the dimensional changes is determined by the anodizing conditions and also by the chemical composition and structure of the metal.

3. The graphs, obtained by a gravimetric method which has been developed, representing the influence of anodizing conditions on dimensional changes of the homogeneous AMg alloy and the multiphase high strength AK-6 and D-1 alloys, demonstrate the important influence of electrolyte temperature on the dimensional changes.

4. The relationships which have been established for the film dimensions and thicknesses are explained on the basis of a hypothesis that film formation and solution processes proceed in parallel during anodizing, and that these processes are influenced by the electrolyte temperature in the film formation region (i.e., at the lower ends of the pore canals penetrating the oxide).

5. The dimensional changes are also strongly influenced by the method of preparing the surface before anodizing and by the configuration of the anodized articles.

6. For minimum dimensional changes in anodizing for corrosion protection of precision parts, the surface should be prepared by the use of organic solvents (and not alkaline solutions), and the anodic oxidation should be carried out in 3% CrO_3 solution at 34-42°, at 40 v for 45-60 minutes.

LITERATURE CITED

[1] V. O. Krenig, R. S. Ambartsumyan, Corrosion of Metals in Aviation, State Defense Press (1941).

[2] V. G. Akimov, N. D. Tomashov, M. N. Tyukina, Symposium, Accelerated Method of Corrosion protection, Acad. Sci. USSR Press, 7-82 (1946).

[3] A. N. Tumanov, N. A. Makarov, Symposium, Corrosion and Protection of Aluminum Alloys, State Defense Press, 75-88 (1949).

[4] S. E. Pavlov, Corrosion of Duralumin, State Defense Press (1949).

[5] A. V. Shreider, Symposium, Atmospheric Corrosion of Metals, Metallurgy Press, 170-183 (1951).

[6] A. Jenny, The Anodic Oxidation of Aluminum and its Alloys, New York (1940).

[7] F. Elszner, Aluminiumoberflachenschutz durch electrolytische Oxydation, Leipzig (1943)

[8] M. Schenk, Werstoffe Aluminium und seine anodische Oxydation, Bern (1948).

[9] E. G. Savage, Protection and Electrodeposition of metals, 3, Reports 14, 15, London, 155-170 (1951).

[10] S. Wernick, Sheet Metal Industries, 29,307, 1027-1040 (1952).

[11] P. P. Belyaev, TEKSO Chart, 592/50 (1947).

[12] O. E. Kirchner, Corrosion, 7, 5, 161-177 (1951).

[13] N. E. Promisel, G. S. Mustin, Corrosion, 7, 10, 339-352 (1951).

[14] G. M. Badalyan, Protection of Metals by Phosphate and Oxide Films, State Shipbuilding Ind.Press (1952).

[15] M. N. Rozov, Proc. Tech. Conf. on Metallic Coatings, State Local Ind. Press (1948).

[16] M. L. Shulman, V. I. Zhukova, LDTM Information Sheet, 40, (104) (1949).

[17] B. C. Lewsey, Electroplating, 5, 8, 250-253 (1952).

[18] A. P. Penn, Metal Finishing, 81, 19, 367-369 (1952).

[19] W. W. Hübner, Aluminium, 30, 7, 283-284 (1954).

[20] M. Buckeley-Lisegang, A. Buckeley, Metalloberfläche 6, 3, A38-A41 (1952).

[21] L. S. Lukashova, TEKSO Chart, 1209/19 (1950).

[22] A. V. Shreider, TEKSO Chart, 112/26 (1947).

[23] H. von Uslar, Metalloberfläche, 4, 12, B183-B186 (1950).

[24] N. N. Komarov, TEKSO Chart, 1374/35 (1949).

[25] A.I. Volfson, Coloration of Aluminum and Aluminum Alloy Instrument Parts, Inst. Tech. Econ. Inf., Acad. Sci. USSR (1955).

[26] N. D. TomashovM. N. Tyukina, A.V. Byalobzhesky, Investigations of Metal Corrosion, Inst. Phys. Chem. Acad. Sci. USSR, 110-145 (1951).

[27] N. D. Tomashov, Bull. Engineers and Technicians,2, 59-63 (1946).

[28] H. Johnson, Product Engineering 25, 9, 136-139 (1954).

[29] A. W. Brace, Electroplating & Metal Finishing 7, 10, 376-379 (1954).

[30] Materials and Methods, 32, 2, 62-64 (1950).

[31] Light Metals, 15,167, 46-48 (1952).

[32] A.V. Shreider. Factory Labs., 19, 1, 28-32 (1953).

[33] Machinery (L) 84, 2160, 735-739 (1954).

[34] A. Arlt, ASTM, 40, 968 (1940).

[35] R. C. Spooner, Canad. J. Technology, 29, II,479-491 (1951).

[36] N. D. Tomashov, A. V. Shreider, A. V. Byalobzhesky, J. Appl. Chem., 26, 12, 1252-1257 (1953).*

[37] E. I. W. Wervey, Chem. Abstr, 48, 7, 3818 (1954).

[38] E. M. Zaretsky, V. N. Uspenskaya, E. B. Kats, Factory Labs., 18,2, 188-192 (1952).

[39] W. Ruff, Aluminio, 20, 6, 540-552 (1951).

[40] A. V. Shreider, Factory Labs., 16, 12, 1436-1439 (1950).

[41] A. V. Shreider, TEKSO Chart, 280/3 (1951).

[42] S. Wernick, Sheet Metal Industries, 28, 288, 373-383 (1951).

[43] J. Hrenguel, P. Lelong, Comptes Rendus 232, 24, 2218-2220 (1951).

[44] L. J. Darker, Trans. Amer. Soc. for Metals, 42,347-356 (1950).

[45] P. W. Mott, M. B. Waldron, Report 13, Protection and Electrodeposition of Metals, 3 London,149-154 (1951).

[46] G. O. Taylor, Metallurgia, 44, 265, 243-244 (1951).

[47] E. Hermann, Metalloberfläche 6, 12, B177-B182 (1954).

[48] R. Lattey, Metalloberfläche, 6 A41-A48 (1952).

[49] V. I. Lainer, Electropolishing and Etching of Metals, State Machinery Press (1948).

[50] B. E. Bunce, Electroplating, 6, 9, 317-323 (1953).

[51] R. H. Keller, Metal Finishing, 48, 12, 56-64 (1950).

[52] J. H. James, H. Page, Product Engineering, 25, 12, 167-170 (1954).

[53] R. C. Spooner, D. P. Seraphim, Galvano, 23, 211, 9-12 (1954).

[54] F. Elszner, Aluminium, 25, 9, 310-315 (1943).

[55] A. V. Shreider, Factory Labs., 21, 6 (1955).

[56] A. V. Shreider, J. Phys. Chem., 24, 4, 455-458 (1950).

[57] J. Hrenguel, Lelong, Revue de Metallurgie, 51, 7, 411-418 (1954).

[58] Eloxalmitteilungen L. P. W. Schering, S. E. H., V. A. W.

[59] R. C. Spooner, J. Electroch. Soc. 102, 4 (1955).

[60] M. S. Hunter, P. Fowle, J. Electroch. Soc., 101, 10, 514-519 (1954).

[61] I. V. Krotov, J. Phys. Chem., 28, 9, 1550-1554 (1954).

Received May 11, 1955

* Original Russian pagination. See C. B. Translation.

ELECTROCHEMICAL TINNING OF SHEET IRON FROM HALIDE SOLUTIONS

V. P. Kochergin, T. A. Nimvitskaya, and M. Ya. Vyunova

The Urals Scientific Research Institute for Ferrous Metals

It was shown in an earlier paper [1] that the electrodeposition of tin on cold rolled sheet iron from hydrochloric acid solutions containing simple salts (sodium and stannous chlorides) and surface-active organic additions results in formation of tin coatings which gather into drops when fused by the contact method. This drop formation did not occur only on surface fusion of tin coatings deposited from the above acid solutions on cold rolled sheet previously treated in an alkaline stannate solution for 1-2 seconds at a current density of 1-2 A/dm^2. The tin plate so produced had a mirrorlike appearance and the coating had low porosity. However, the introduction of a preliminary stannate treatment of the metal into the continuous tinning line does not fully satisfy the basic requirements of the rapid electrochemical method for tin plate production [2]. It was therefore necessary to find halide solutions from which it is possible to obtain tin deposits which fuse without drop formation on cold rolled sheet without the above preliminary treatment.

The present paper contains the results of an investigation of the electrochemical method for tinning strip iron from chloride–fluoride solutions. Despite the use of such solutions in high speed tin plating [3], the literature contains only a few brief reports on the subject [2, 4, 5]. This information is inadequate for modern development of the high speed electrochemical tinning process, as the reports describe either the arrangement of the continuous plating line without any indication of the composition of the solutions and electrolysis conditions [3], or give the results of kinetic studies of the electrode processes and the conditions for the production of dense, finely granular deposits without consideration of the quality of surface fusion of these deposits [6].

EXPERIMENTAL

It is known that only finely crystalline dense tin deposits melt without droplet formation [7]. The production of such deposits is possible in most cases with the use of high cathode polarization. An increase of the cathode polarization in electrodeposition of tin from solutions of simple tin salts can be effected not only by addition of surface active agents (phenol, α and β-naphtols, etc.), but also by addition of complex-forming inorganic compounds [6, 8]. The fluorides of ammonium and sodium act as such complex-formers in halide solutions. Fluoride ions (in contrast to chloride ions [1]) in presence of stannous ions, are capable of forming electrostatic (ionic) complexes [9] of the composition $Na_2[SnCl_2F_2]$ or $[NH_4]_2[SnCl_2F_2]$ [10].

To confirm the complex-forming activity of fluoride ions in the electrodeposition of tin from halide solutions, the variation of cathode polarization with the concentrations of ammonium and sodium fluorides (Figure 1), hydrochloric acid (Figure 2), and stannous chloride (Figure 3) was studied by the direct compensation method [6] with the aid of the Urals Chemical Scientific Research Institute electronic voltmeter. These investigations were carried out at 20° with "analytical grade" chemical reagents. Figures 1, 2 and 3 show that in the probable conditions of ionic complex formation by Sn^{2+} (with increase of the NaF or NH_4F concentration and decrease of HCl and $SnCl_2$ content) the cathod polarization increases. An increase of polarization is also observed on addition of colloidal and surface-active substances* to the solution, such as glue and gelatin (Figure 4), phenol and α-naphtol (Fig. 5). It follows from Figure 4 that gelatin (1 g/liter has a greater effect on the cathode polarization than glue (1 g/liter). This effect increases with increasing gelatin concentration up to 5 g/liter. However, an increase of the gelatin content in the solution above 1 g/liter is undesirable because of the decreased stability of such solutions. Figure 5 shows the influence of the concentration of surface -

* The following additions were also tested: salicylic, sulfosalicylic, and disulfonaphthalic acids, sulfophenol, o-cresol, sulfocresol, and anisidine.

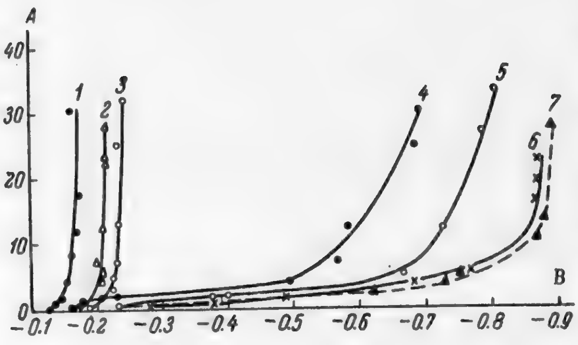

Fig. 1. Influence of NaF and NH_4F concentrations in solution on cathode polarization in the electrodeposition of tin.
Solution composition: $SnCl_2$ 0.25 mole/liter, HCl 3-4 g/liter, gelatin 1 g/liter. A) Cathode current density (in A/dm^2), B) cathode potential (v).
NH_4F content (in mole/liter): 1) 0.4, 4) 0.6, 5) 0.9, 7) 0.4.
NaF content (in mole/liter): 2) 0.4, 3) 0.6, 6) 0.9, 7) 0.4.

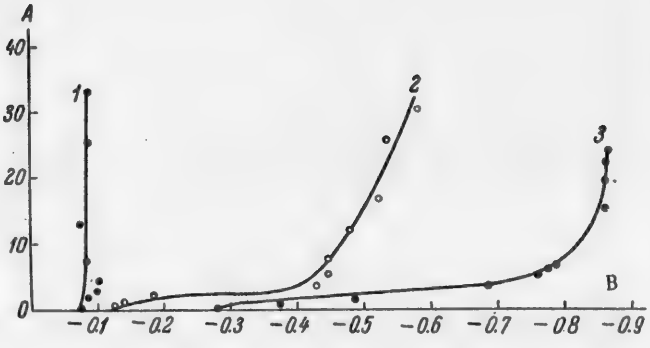

Fig. 2. Influence of free hydrochloric acid concentration on the cathode polarization in the electrodeposition of tin.
Solution composition: $SnCl_2$ 0.25 mole/liter, NaF 0.9 mole/liter, gelatin 1 g/liter. A) Cathode current density (in A/dm^2), B) cathode potential (v).
HCl content (in g/liter): 1) 18, 2) 12, 3) 4.

active additions of phenol and α-naphthol on cathode polarization in the electrodeposition of tin from chloride [1] and chloride-fluoride solutions. It is seen that the appreciable increase of cathode polarization is caused not by the surface-active additions, but by the complex-forming sodium fluoride. An interesting feature is that the polarization is changed little by the surface-active substances, despite the fourfold increase of, for example, the phenol concentration in the solution. Some decrease of the cathode polarization was observed when the temperature of the halide solutions was raised from 20 to 50°.

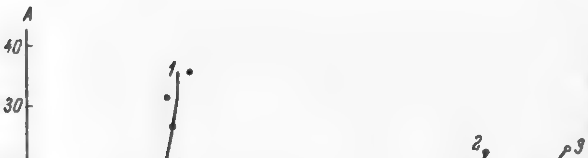

Fig. 3. Influence of the concentration of stannous tin on cathode polarization in the electrodeposition of tin.
Solution composition: NaF 0.9 mole/liter, HCl 3-4 g/liter, gelatin 1 g/liter. $SnCl_2$ content (mole/liter): 1) 0.4, 2) 0.25, 3) 0.15.
A) Cathode current density (in A/dm^2), B) cathode potential (v).

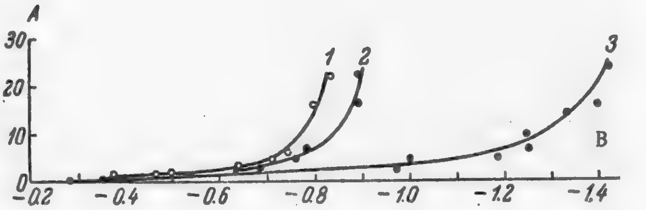

Fig. 4. Influence of glue and gelatin concentrations on cathode polarization in the electrodeposition of tin.
Solution composition: $SnCl_2$ 0.25 mole/liter, NaF 0.9 mole/liter, HCl 3-4 g/liter.
A) Cathode current density (in A/dm^2), B) cathode potential (v).
1) Glue 1 g/liter, 2 and 3) gelatin 1 and 5 g/liter.

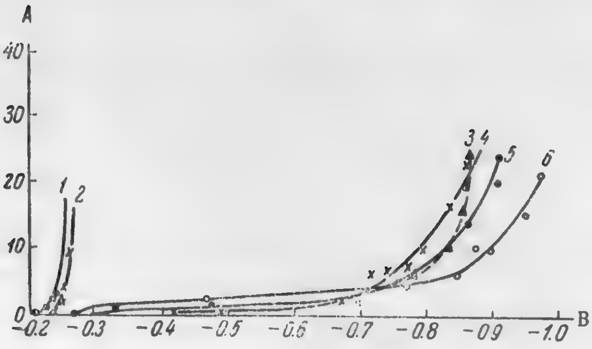

Fig. 5. Influence of phenol and α-naphthol concentrations on cathode polarization in the electrodeposition of tin.
A) Cathode current density (in A/dm^2), B) cathode potential (v).
Additions: 1) phenol 0.20 mole/liter;* 2) α-naphthol 0.2 g/liter [1];* 3) without additions; 4) α-naphthol 0.1 g/liter;** 5) phenol 0.05 mole/liter;** 6) phenol 0.2 mole/liter.**

Thus, from studies of variations of cathode polarization under the influence of various factors it has been possible to determine the conditions in which dense, finely granular tin deposits, which do not from drops during surface fusion by the contact method, [7] may be deposited.

The method described previously [1] was used for the electrodeposition of tin from the above halide solutions and for the surface fusion of the cathodic tin deposits (not more than 1-1.5 μ thick). The new feature of the present experiments was that in most cases the tin was deposited not on flat but on cylindrical cathodes, made from cold rolled sheet iron and rotating at 100-200 r.p.m.

Studies of the quality of cathode tin deposits obtained from a solution containing $SnCl_2$ (0.25 mole /liter), HCl (3-4 g/liter), and gelatin (1 g/liter), in relation to the concentrations of ammonium or sodium fluoride, surface-active additions, and electrolysis conditions, showed that the quality of the deposits is improved with increasing fluoride concentration, cathode current density (from 15 to 35 A/dm^2) and temperature (from 20 to 50°). Thus, if the solution contains 0.25-0.4 mole/liter of ammonium or sodium fluoride at 20°, then the deposits formed at 15-25 A/dm^2 contain loose dendrites or spongy tin. However, if the solution temperature is raised to 50°, and the NaF concentration to 0.9 mole/liter (or the NH_4F concentration to 1.2 moles/liter, dense finely crystalline tin deposits are formed at 15, 25, and 35 A/dm^2. These deposits (in contrast to the former) in most cases fused without drop formation, but with a wavy surface.

The above characteristics of the electrodeposition of tin from halide solutions containing complex ions have a certain resemblance to the deposition of tin from alkaline stannate solutions, in which tin ions are also present in complex anions [7].

As cathode polarization increases in presence of organic additions, an improvement in the quality of the deposits is to be expected in the electrodeposition of tin. The effects of such additions on the quality of the tin deposits was studied with the use of a solution containing $SnCl_2$ 0.25 mole/liter, HCl 3-4 g/liter, gelatin 1 g/liter, and NaF or NH_4F 0.6, 0.9, and 1.2 mole/liter. Numerous experiments showed that the quality of the deposits obtained from this solution with different phenol contents (0.05, 0.1, and 0.2 mole/liter) is improved not only by the presence of fluorides, but also of phenol if its concentration does not exceed 0.1 mole/liter in presence of NaF and 0.2 mole/liter in presence of NH_4F, and if the cathode current density is 25-35 A/dm^2.

The specimens obtained by this method had a bright external appearance after surface fusion. Similar results were obtained when o-cresol or sulfocresol (0.1-0.2 mole/liter) were added to the solutions. However, additions of sulfophenol, disulfonaphthalic, salicylic, or sulfosalicylic acids or anisidine did not improve the quality of the deposits. It should be noted that no increase of the cathode polarization was observed in most cases in presence of these additions.

* To a solution with the composition: (in g/liter): $SnCl_2$ 25, NaCl 5, HCl 10, glue 1.

** To a solution with the composition: $SnCl_2$ 0.25 mole/liter, NaF 0.9 mole/liter, HCl 3-4 g/liter, gelatin 1 g/liter.

TABLE 1

Variation of the Cathode Current Efficiency with the Concentrations of NaF, NH_4F, Phenol, and Sulfocresol, Solution Temperature, and Cathode Current Density

Solution composition: $SnCl_2$ 0.25 mole/liter, HCl 3-4 g/liter, gelatin 1 g/liter, NaF, or NH_4F, phenol, sulfocresol

Solution No.	Concentration (in mole/liter):				Temperature (°C)	Cathode current efficiency (%) at cathode current densities		
	NaF	NH_4F	phenol	sulfocresol		15	25	35
1	0.60	—	—	—	50	—	99.7	82.5
2	0.90	—	—	—	50	99.9	94.5	80.9
3	—	0.60	—	—	50	98.5	88.4	76.6
4	—	0.90	—	—	50	—	88.4	72.5
5	—	1.20	—	—	50	100	92.2	88.1
6	—	1.20	—	—	65	100	98.9	95.1
7	—	0.60	0.20	—	45	100	92.5	85.7
8	—	0.90	0.20	—	65	100	97.0	86.1
9	0.90	—	0.05	—	50	99.3	91.8	83.3
10	0.90	—	0.10	—	50	97.7	97.2	87.3
11	0.90	—	0.20	—	50	97.9	90.6	83.0
12	—	0.60	—	0.06	20	90.5	81.2	75.1
13	—	0.60	—	0.06	50	99.7	93.0	89.9
14	—	0.60	—	0.12	50	100	97.7	90.4

The results of determinations of cathode current efficiency [11] are given in Table 1. From Table 1 it follows that the cathode current efficiency diminishes somewhat with increase of current density from 15 to 35 A/dm^2, and of fluoride concentration, and with decrease of the temperature from 65 to 20°; the organic additions - phenol and sulfocresol-favored its increase. A similar decrease of current efficiency as a function of current density, temperature, and alkali concentration is found in alkaline stannate solutions [7].

Thus, the above investigations provided factual data on the dependence of cathode polarization and quality of cathode tin deposits on solution composition and electrolysis conditions, necessary for carrying out electrochemical tinning in industrial installations, and in particular in the semiworks scale laboratoy installation,* which is not described here for reasons of space.

The preparation of the metal band (100 mm wide, manufactured by the "Zaporozhstal" factory) for electrodeposition of tin in the experimental installation was the same as before [1]. The solutions used for the tinning had the compositions shown in Table 2. The solution temperature was 50-65°, the cathode current density D_C was 15.25 and 35 A/dm^2, and the tin coatings were about 0.5, 1.0, 1.5, and 2 μ thick.

TABLE 2

Compositions of Solutions Tested for Electrochemical Tinning of Band Iron in the Experimental Semiworks Scale Installation

Solution No.	$SnCl_2$ (mole/liter)	NaF (mole/liter)	NH_4F (mole/liter)	HCl (g/liter)	Gelatin (g/liter)	Phenol (mole/liter)	Sulfocresol (mole/liter)
1	0.25	0.6	—	3—4	1	—	—
2	0.25	0.9	—	3—4	1	—	—
3	0.25	—	0.6	3—4	1	—	—
4	0.25	—	0.9	3—4	1	—	—
5	0.25	—	1.2	5	1	—	—
6	0.25	0.9	—	3—4	1	0.05	—
7	0.25	0.9	—	3—4	1	0.1	—
8	0.25	—	0.6	3—4	1	—	0.025
9	0.25	—	0.6	3—4	1	—	0.1
10	0.25	—	0.9	3—4	1	0.05	—

* A. N. Kruglov took part in this work.

The tests showed that the cathode tin deposits obtained from solutions No. 1 and 3 (Table 2) at D_c = 15 A/dm² and with NaF and NH_4F concentrations not over 0.6 mole/liter were generally covered with a gray film, which formed into spreading drops during contact fusion. Denser deposits which fused well were obtained from solutions No. 2 and 4 at D_c = 25 and especially 35 A/dm². The quality of the deposits was improved considerably on addition of phenol (0.05 mole /liter) to solutions No. 6 and 10, and on increase of D_c to 35 A/dm². With a phenol concentration of 0.1 mole/liter the deposits were coated with a gray film. Sulfocresol had a favorable effect on the quality of the tin deposits in a concentration of 0.1 mole/liter (solution No. 9); when its content was lower (solution No. 8), spongy tin was deposited and formed drops during surface fusion.

The fused tin deposits were cooled in hot water (70-90°). By this it was possible to eliminate the formation of a surface pattern on the tin plate surface, which occurred when the fused tin plate was cooled in cold running water and which gave the tin plate a dull (unsatisfactory) appearance.

The tin plate obtained (after the surface fusion) had a coating 1-1.5 μ thick with about 2-4 pores per 1 cm². After passivation, oiling, or lacquering, the porosity of the coating should be further diminished [2].

It follows from the above investigation that rapid electrochemical tinning of sheet iron can be effected from a solution, stable to hydrolysis and oxidation, containing $SnCl_2$ 0.25 mole/liter, NaF 0.9 mole/liter, phenol (organic additive) 0.05 mole/liter, gelatin 1 g/liter, and HCl 3-4 g/liter (at current density D_c = =25-35 A/dm², solution temperature 50-65°, and current efficiency η_c = 91.8% at D_c = 25 A/dm² and η_c = 83% at D_c = 35 A/dm²).

The principal technological index of the above solution is the product $\eta_c D_c C$ (where C is the electrochemical equivalent in g/A • hour), with the value 35 • 83 • 2.2 = 6391. This is 2.5, 3.8, and 25 times as large as the analogous index for sulfuric acid [2], chloride [1] and alkaline stannate [2] solutions, respectively. It follows that halide solutions will gradually displace all the other types of solutions used in modern rapid electrochemical tin-plating practice.

SUMMARY

1. In a study of the kinetics of the electrode processes in electrodeposition of tin from halide solutions it was shown that cathode polarization increases with increasing concentrations of sodium and ammonium fluorides and of organic additions (gelatin or phenol), with decreasing contents of hydrochloric acid and stannous chloride, and with a decrease of the solution temperature from 50 to 20°.

2. Increase of the ammonium and sodium fluoride contents in the halide solutions, additions of up to 0.05 mole/liter phenol and up to 0.1 g/liter sulfocresol, increase of the solution temperature to 50-65°, and of the cathode current density to 35 A/dm², all favor the formation of dense finely granular deposits of tin which fuse without forming drops.

3. A halide solution has been developed for the electrochemical production of tin plate at cathode current densities of 25-35 A/dm² with a current efficiency of 83-90%.

LITERATURE CITED

[1] V. P. Kochergin, T. A. Nimvitskaya, M. Ya . Vyunova, J. Appl. Chem., 28, 59 (1956).*

[2] A. I. Vitkin, Tin Plate, Metallurgy Press (1951).

[3] W. E. Hoare, Sheet & Metal Indust. 28, 288 (1952).

[4] A. M. Yampolsky, Electroplating Technology, State Machinery Press (1952).

[5] A. I. Vitkin, Bull. Central Inst. Information, Ministry of Ferrous Metals, 17 (1954).

[6] O. A. Esin, M. A. Loshkarev, V. I. Sotnikova, J. Gen. Chem., 9, 1412 (1939); M. A. Loshkarev, A.A. Kryukova, J.Phys. Chem., 22, 7 (1948); M. A. Loshkarev, V. I. Sotnikova, J. Appl. Chem., 24, 4(1951) ; I. E. Gurevich, J. Appl. Chem., 28, 285 (1955).

* Original Russian pagination. See C. B. Translation.

[7] V. I. Lainer and N. T. Kudryavtsev, Fundamentals of Electroplating, 1 (1953).

[8] N. A. Izgaryshev and S. V. Gorbachev, Course of Theoretical Electrochemistry, 340-342 (1951).

[9] K. B. Yatsimirsky, Thermochemistry of Complex Compounds, Acad. Sci. USSR Press, 112-117 (1951); A. A. Grinberg and K. B. Yatsimirsky, Bull. Acad. Sci. USSR, Div. Chem. Sci., 2 (1952).*

[10] D. Cuthbertson J, Electroch. Soc., 100, 3, 107-109 (1953).

[11] D. S. Abramson and S. Orlova, Control of Electrolytes and of the Quality of Galvanic Coatings (1950).

Received May 10, 1955

* Original Russian pagination. See C. B. Translation.

SYNTHESIS OF ARTIFICIAL TANNING AGENTS OF THE SULFONATED NOVOLAK TYPE *

D. Tishchenko and I. Uvarov

Leningrad Wood Technology Academy

All the countries of the temperate belt are deficient in vegetable tanning materials and have to import them from tropical countries (quebracho, mimosa, mangrove, etc.). The first synthetic tanning agents of any value were patented by Stiasny [1], who developed two methods for the production of "syntans": 1) phenol or a mixture of phenols is condensed with formaldehyde to a Novolak, which is sulfonated to give Novolak-sulfonic acids, which are syntans; 2) phenol or a mixture of phenols is converted into phenolsulfonic acids, which are condensed with formaldehyde to give a mixture of syntans. The technological leather tanning properties of such syntans ("Neradols") are not very good, especially of those made by the second method, and they are used only as auxiliary tanning agents which facilitate the solution of vegetable tanning extracts and accelerate tanning by the latter.

From 1913 up to the present time, numerous patents have appeared [2] describing various modifications of Stiasny's methods, but the quality of these syntans is still not high, and they are not suitable for independent tanning of hides. In the 1930's German firms put several brands of high-quality synthetic tanning agents on the market, which were apparently suitable for independent tanning of hides [3] ("Tanigans"). No information on their chemical structure and production methods is contained in the available literature, and only their applications and technological properties are described.

Syntans made by Stiasny's first method (sulfonated Novolaks) are somewhat better than those made by the second method (condensation products of phenolsulfonic acids with formaldehyde). In syntans made by the first method not every phenol ring contains a sulfo group, while in those made by the second method every ring should contain a sulfo group. In both cases the synthesis of the polycondensate cannot be regulated, and yields a variegated mixture of products of different molecular weight and different physicochemical and technological tanning properties. The phenolsulfonic acids and the sulfonic acids derived from diphenylmethane derivatives present in these mixtures have no tanning properties, which leads to a decreased quality of these syntans, waste of reagents, and increased amounts of harmful effluents. The tanning action of the more highly molecular parts of these syntans can only be judged indirectly as they cannot be isolated pure from the mixtures.

Controversy still continues in the technical literature [4] concerning the necessary number of phenol rings in the Novolak chain of a sulfonated syntan for the best tanning properties, and the best ratio of phenol rings to sulfo groups. These arguments are largely speculative, and not adequately based on direct experimental evidence. They can only be settled if a method can be found for synthesizing Novolaks of predetermined molecular weight (number of phenol rings) and for introducing into a molecule of such a Novolak, one acid group to give a chemically individual "model" syntan. Studies of the physicochemical and technological tanning properties of "model" syntans would make it possible to establish the main theoretical principles of the chemistry, technology, and applications of sulfonated syntans or synthetic tanning agents of allied structure.

---

* Further information and the experimental part of the investigation had to be omitted for reasons of space. This work forms part of I. P. Uvarov's dissertation for the degree of Candidate of Technical Sciences (Leningrad, Wood Technology Academy, 1954).

However, this theoretical solution of the problem is itself not sufficient for the industrial production of high quality synthetic tanning agents. There is no doubt that the best tanning agents should be synthesized, totally or at least partially, from polyhydric phenols, which are at present not available technically, and therefore it is also necessary to find a sufficiently powerful supply of polyhydric phenols. The present investigation deals with these problems.

The following routes for the production of "model" syntans were considered.

1) Condensation of 1 mole of some phenolsufonic acid having two free ortho or para positions relative to the phenol hydroxyl, with 2 moles of formaldehyde and 2 moles of a phenol with at least one free ortho or para position:

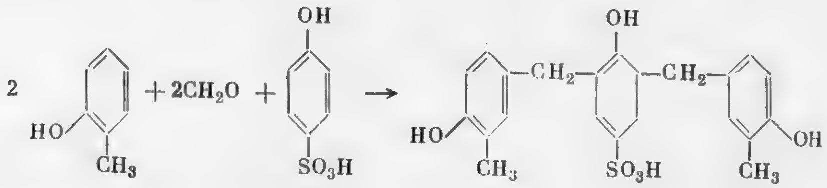

Despite wide variations of the experimental conditions (time, temperature, pH of the medium, concentration of the reagents), condensation of this type could not be effected. The phenolsulfonic acid did not react, while the phenol reacted with formaldehyde to give an insoluble nonsulfonated Novolak.

2) Condensation of dimethylolphenolsufonic acids with phenols:

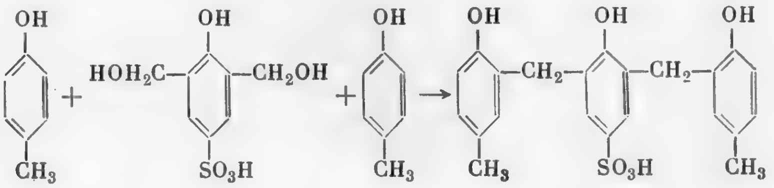

This condensation also could not be effected, nor the condensation of methylolphenols with phenolsulfonic acids nor a number of other intended condensations in which one of the components was some phenol or Novolak of definite structure (see below), another was some phenolsulfonic acid or Novolak-sulfonic acid, and the third was formaldehyde. It was necessary to accept the fact that the sulfo group prevents condensation in all cases, or that the rate of condensation of phenols and Novolaks with formaldehyde is considerably higher than the rate of their condensation with formaldehyde and sulfonic acids and of sulfonic acids with formaldehyde.

3) Synthesis of Novolaks of definite structure and molecular weight (individual Novolaks) with subsequent introduction of acid groups into them. It is known that phenols in an alkaline medium add on formaldehyde in the ortho and para positions to form phenol alcohols (methylol phenols), and the latter condense with phenols in an acid medium to form Novolaks. Koebner [5] used these properties of phenol alcohols to synthesize individual Novolaks containing 3, 4, 5, 6, and 7 p-cresol residues in the chain, from p-cresol and dimethylol-p-cresol. His method requires the use of organic solvents and a large excess of p-cresol which is later removed from the reaction product, and is fairly complicated. The preparation of individual Novolaks from other phenols has not been described.

We have confirmed that any phenol in an alkaline medium, slowly in the cold and rapidly on heating, adds on a number of formaldehyde molecules equal to the number of free ortho and para positions relative to its hydroxyl (or hydroxyls). In the preparation of methylol derivatives from mixtures of phenols it is necessary to determine (for example, by bromination) the number of free ortho and para positions per average molecular weight of the mixture, and to use mixtures with not less than two such positions for the production of syntans.

. If a mixture contains a considerable proportion of phenols with one free position (for example, methylguaiacol or 2, 4-dimethylphenol), the latter will form monomethylol derivatives with formaldehyde, and these, on subsequent condensation with any phenol and introduction of an acid group, will yield diphenylmethane derivatives which do not have tanning properties. Koebner produced a three-ring Novolak by mixing dimethylol-p-cresol with a large excess of p-cresol, and then adding an acid catalyst. The reaction was vigorous, and it was necessary to remove a large quantity of heat from the reaction mixture in a short time, and then to distill off excess p-cresol under vacuum. We have found that the following method for the preparation of three-ring Novolaks is considerably more advantageous. To an aqueous suspension of 2 moles of any phenol or mixture of phenols with not less than two free ortho and para positions an acid catalyst is added and then an aqueous solution or aqueous suspension of any dimethylolphenol or of a mixture of dimethylol phenols is added (with cooling and stirring); the reaction mixture always contains excess phenols, which ensures a quantitative yield of the three-ring Novolak; the rate of supply of the dimethylol phenols determines the quantity of heat liberated per unit time, which simplifies the course of the synthesis and the necessary apparatus.

This method was used to synthesize three-ring Novolaks from dimethylol-p-cresol and the following phenols: phenol, o-cresol (No 1), guaiacol (No 2) and pyrocatechol (No 3), of the general formula

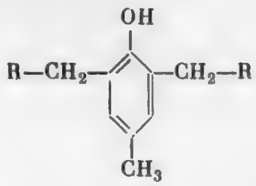

where R is the residue of one of the above phenols.

A four-ring Novolak was prepared by condensation of (dimethyloldihydroxydimethyl) diphenylmethane [6] with o-cresol in an acid medium:

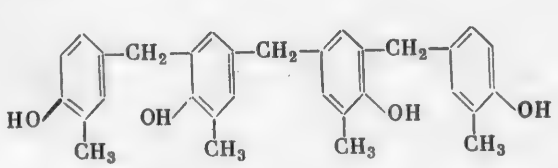

(4)

A five-ring Novolak was prepared by the following method: vanillyl alcohol was condensed with o-cresol to give methyldihydroxydiphenylmethane, and 2 moles of the latter was condensed with 1 mole of dimethylol-p-cresol

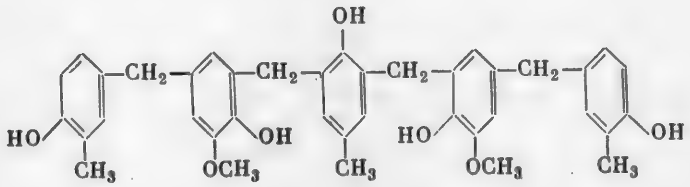

(5)

A seven-ring Novolak was obtained by condensation of 2 moles of the three-ring Novolak No.1 with 1 mole of dimethylol-p-cresol

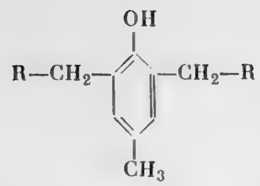

(6)

where R is theNo. 1 Novolak residue.

Elementary analyses of these Novolaks and determinations of their molecular weights were in agreement with the above structural formulas.

According to our observations, condensation of dimethylol phenols with phenols commences spontaneously and proceeds with evolution of heat (for three-ring Novolaks). Condensation of dimethyloldiphenylmethanes with phenols (for four-ring Novolaks) requires heating to 50-60°, and that of hydroxydiphenylmethanes with dimethylol phenols (five-ring Novolaks) requires heating to 80-100°. Formation of the seven-ring Novolak by condensation of the three - ring product with a dimethylol phenol occurs at 110-115°. Condensation of linear polynuclear Novolaks with dimethylol phenols to give a three-dimensional structure commences at 125-130° . For example, in the preparation of a three-ring Novolak by condensation of a dimethylol phenol with a phenol, the formation of a seven-ring Novolak is also possible. However, as three-ring Novolaks are formed at normal temperatures and seven-ring at 110-115°, the latter will not be formed if the temperature of the reaction mixture does not exceed 80-100°; this was confirmed by our experiments.

For the preparation of "model" syntan it was necessary to find a method for introducing one acid group into each of these Novolaks. This problem was solved as follows: to a cooled solution of the Novolak in acetic acid, strong sulfuric acid was added with stirring until a small sample of the reaction mixture was completely soluble in a large volume of water; an equal volume of water was then added to the mixture, and water and acetic acid were removed under vacuum produced by a water-jet pump; the residue was diluted with an equal volume of water, when the syntan was precipitated, being insoluble in a relatively strong aqueous solution of sulfuric acid. For analysis, the syntan samples were dissolved in water to remove sulfuric acid, precipitated by strong hydrochloric acid, and dried by suction and under vacuum over solid caustic alkali. Analyses showed that one sulfo group was introduced into these Novolaks by this method. The "model" syntans so obtained were designated by the same numbers as the corresponding Novolaks (Nos 1-7) . The above sulfonation method is, of course, not suitable technically and was only used by us for preparation of "model" syntans.

It has long been known that water-insoluble phenols can be converted into water-soluble derivatives by heating with solutions containing sodium sulfite and formaldehyde [7]. Such compounds are usually assigned the structure of substituted methanesulfonic acids $R{-}CH_2{\cdot}SO_2OH$ (I). This method has also been used for conversion of Novolaks into synthetic tanning agents [8]. It is known that such tanning agents yield a leather with a higher shrinkage temperature than those obtained by sulfonation of Novolaks, and that in equimolecular solutions the former have a higher pH than the latter. Consequently the former are weaker acids than the latter. If, as is assumed, both are sulfonic acids, this difference in their properties is inexplicable. It has been shown fairly long ago [8] that formaldehyde bisulfite is a salt of the ester of methanediol and sulfurous acid: $HO{-}CH_2{-}O{-}SO{-}ONa$. In that case the reaction products of Novolaks with formaldehyde bisulfite should be esters of methylol Novolaks and sulfurous acid: $R{-}O{-}SO{-}OH$ (II), where R is the methylol Novolak residue, and should be saponified by aqueous alkali to form a methylol Novolak insoluble in water, and the neutral metal sulfite. If, however, these products are derivatives of methanesulfonic acids, their composition should remain unchanged by boiling with aqueous alkali. We found that when these products are boiled with alkali a water-insoluble Novolak and a sulfite are formed, which decides the question of their structure in favor of Formula (II). (sulfurous acid esters) and explains their lower acidity in comparison with sulfonated Novolaks. The reaction of Novolaks with formaldehyde bisulfite we shall, for brevity, term formalsulfiting. This reaction is more suitable than sulfonation of Novolaks with strong sulfuric acid, for technical, equipment, economical, and many other considerations. It was necessary to determine the conditions for its use.

The reaction of formaldehyde with sulfite in aqueous solution is an equilibrium reaction:

$$CH_2O + HOH + Na_2SO_3 \rightleftharpoons NaOH + HO{-}CH_2{-}O{-}SO{-}ONa.$$

When such a solution interacts with a Novolak, either the formaldehyde or the formaldehyde bisulfite may react at the greater rate. In the first case, a Novolak of more than doubled molecular weight will mainly be formed, and in the second, the required syntan. Our investigations (with the use of the Novolaks of known structure described above) showed that Novolaks of doubled molecular weight are formed almost entirely if methoxyphenol residues, for example, of guaiacol, are present at each end of the original Novolak molecule (No. 2), and a syntan is not formed. If monohydric phenol residues are present at the ends, a mixture of syntans is formed: one with the same number of phenol rings as in the original Novolak, and the other with double that number (for example, from Novolak No. 1)

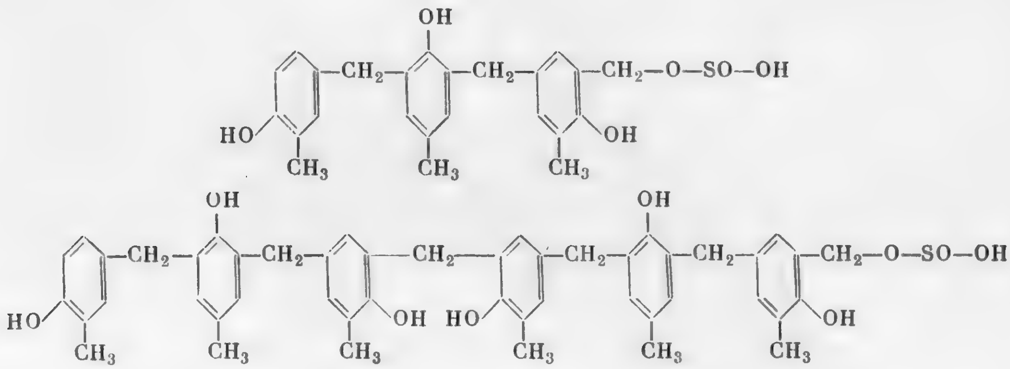

This syntan is listed below as No 7.

If polyhydric phenol residues are present at the ends (for example, Novolak No. 3), then the desired formalsulfite reaction becomes complete, with formation of a syntan.

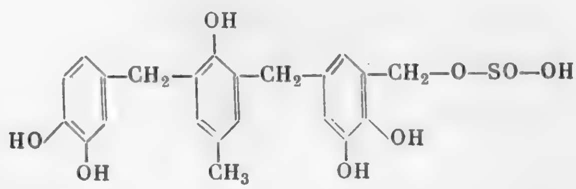

Consequently, Novolaks of the first group can be converted into syntans only by sulfonation, and Novolaks of the second group by sulfonation and by formalsulfiting.

Novolaks Nos. 1-6 were sulfonated by the above method in acetic acid solution and converted into "model" sulfosyntans, listed below under the corresponding numbers.

It was stated above that high-quality syntans should be synthesized completely or partially from polyhydric phenols, but that the solution of this problem is at present impossible because these are not technically available.

By thermolysis of wood (by gasification or dry distillation) it is possible to obtain at least 3-4% of a phenol mixture on the weight of the wood, which is tens of times the yield obtained by the coking of coal. Even now sufficient phenols can be obtained from wood to produce considerable amounts of syntans, while in the near future the output of such phenols should increase considerably. These phenols contain incompletely etherified methyl ethers of pyrocatechol, pyrogallol, and their homologs, in amounts which increase with the boiling temperature of the phenol fraction. These mixtures contain considerable amounts of phenols with one free reactive position

(X) relative to the phenolic hydroxyl (for example, methyl- and propylguaiacols)

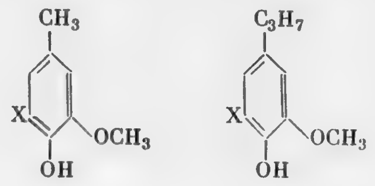

Such phenols condense with dimethylol phenols to give Novolaks without free reactive positions, and therefore unsuitable for the production of syntans, such as

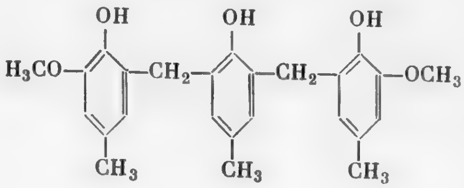

If these methoxy phenols are converted into the corresponding polyhydric phenols by saponification of the methoxy groups, the resultant phenols will have new free reactive positions relative to the phenolic hydroxyls formed, for example

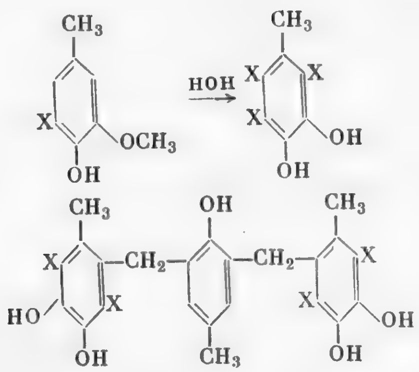

Therefore any fraction of phenols from wood, after saponification of the methoxyl groups, becomes suitable both for production of dimethylol phenols and for condensation with methylol phenols to give three-ring multinuclear Novolaks.

We have discovered a technically and economically suitable method for saponification of methoxy phenols, whereby it is possible to obtain polyhydric phenols in any desired quantitites from tars obtained by thermolysis of wood; this solves the problem of the industrial production of high quality artificial tanning agents.

Phenols obtained by thermolysis of wood, boiling at 180 -212°, contain phenol, o-,m- and p-cresols, o-ethylphenol, and not less than 40% guaiacol. These phenols have not less than two free ortho and para positions and are suitable for the preparation of dimethylol phenols. The higher boiling fractions after saponification of the methoxyl groups are also suitable for this and for condensation with dimethylol phenols to give Novolaks. Syntans Nos. 8 and 9 were prepared in this way.

Syntan No 8: the phenol fraction from the thermolysis of wood boiling at 240-290° was saponified, and 1 mole of the phenols, consisting mainly of pyrocatechol, pyrogallol, and their homologs, was condensed in an alkaline medium with 2 moles of formaldehyde; 1 mole of the mixture of the dimethylol phenols so formed

was condensed in an acid medium with 2 moles of the saponified phenols to give three-ring Novolaks; these were heated with a solution of formaldehyde (1 mole) and sulfite (1 mole) to give the syntan.

Syntan No. 9 was made similarly, but the mixture of dimethylol phenols was obtained from the unsaponified phenol fraction obtained by thermolysis of wood, with b.p. 180-212°.

In this method of syntan production all the reagents used can be utilized almost completely.

The above method yields a mixture of dimethylol phenols in an alkaline solution; dimethylol phenols are precipitated almost quantitatively from the solution by sulfurous acid, while the solution contains half the sulfite required for formalsufiting of the Novolak, for example,

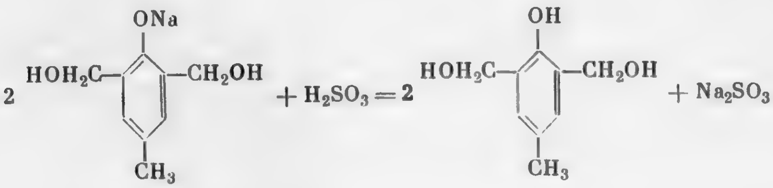

1 mole of the resultant dimethylol phenols is dispersed in water containing 0.05-0.1% of hydrochloric or any strong acid, and 2 moles of saponified phenols (see above) is added to the mixture with stirring and cooling; the yield of water-insoluble three-ring Novolak is quantitative, for example,

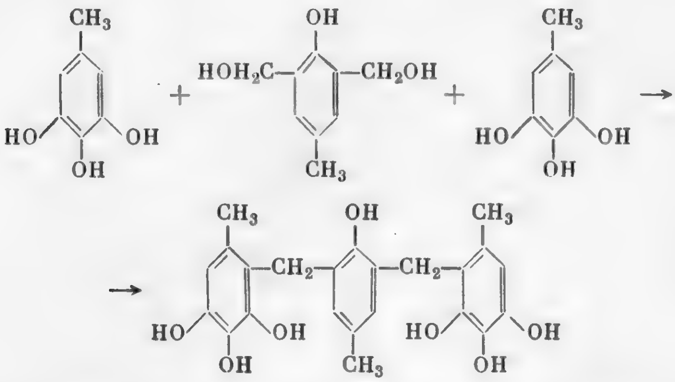

A mixture of aqueous solutions of 1 mole of formaldehyde and 1.5 mole of sulfite is heated to boiling with 1 mole of the Novolak, a syntan being formed, for example,

$$CH_2O + HOH + Na_2SO_3 \rightleftarrows HO{-}CH_2{-}O{-}SO{-}ONa + NaOH$$

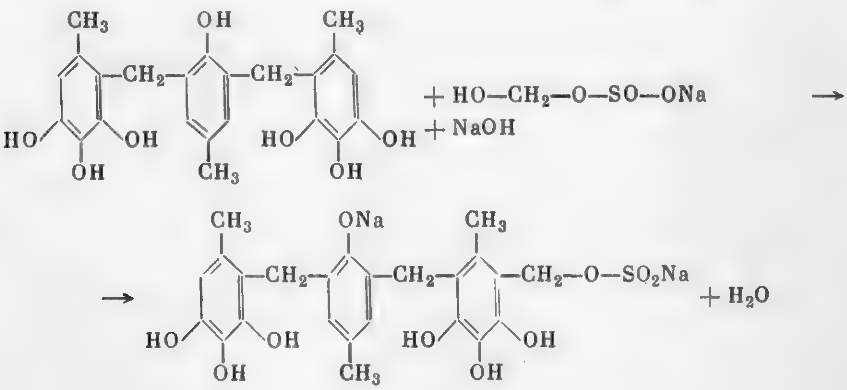

A solution of sodium phenolate of the methylol Novolak sulfite ester is acidified with sulfurous acid; not less than 95% of the methylol Novolak sulfite ester sodium salt (the final product, the syntan) is precipitated, while sodium sulfite remains in solution:

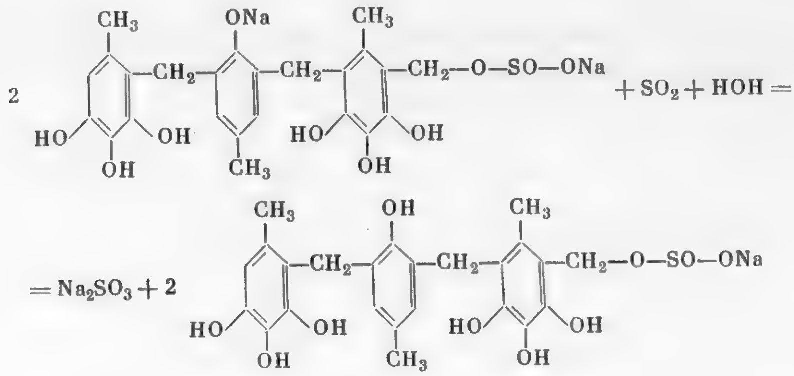

Properties of Syntans of Definite Chemical Structure and Known Molecular Weight

1. All the syntans obtained, with from 3 to 7 phenolic residues and 1 acid group in the molecule, are soluble in water; this disproves the assumption that there must be a definite ratio between the number of phenol rings and the number of acid groups in the syntan molecule.

2. The pH of the solutions of the sulfonated syntans obtained, in the concentrations used for hide tanning, varies between 2.2. and 2.8, increasing with increasing molecular weight of the syntan, i.e., with decrease of the sulfo group concentration in the solution. The pH of similar solutions of formalsulfited syntans varies between 4.5 and 5.5, i.e., it corresponds to the pH of vegetable tanning solutions; therefore, to avoid loss of strength in the leather, solutions of sulfonated syntans should be buffered (to pH ≈ 4.5) for tanning of hides. Partial neutralization of the sulfonated syntan solutions to pH = 4.5 is not admissible, as salts of sulfonated syntans have no tanning action. Hide tanning by solutions of formalsufited syntans does not require the use of buffer mixtures. The above pH data refer to solutions of syntan samples precipitated from aqueous solutions by strong hydrochloric acid and dried in a vacuum under alkali to remove water and hydrogen chloride.

3. In determinations of the purity (content of tanning substance in a dry weighed sample) of our syntans by the All-Union unified method, we used syntan samples precipitated from the production solutions by strong hydrochloric acid and not completely free from hydrochloric acid, and therefore the pH of their solutions was below the values stated above (≈ 2.0); this was raised to 4.0 during analysis by addition of caustic soda. In these conditions the purity of syntans Nos. 1-8 was between 59 and 75% (detanning time 120 minutes) as at pH = 4 the sulfonated syntans are partially neutralized, and their salts have no tanning action; these purity values must be considered too low. At pH =4.0 the formalsulfited syntans are not neutralized, while the hydrochloric acid is not completely neutralized and partly binds the acid capacity of the collagen, which should again give low purity values. As our "model " syntans are individual chemical substances, it is impossible for some of their molecules and not others to be tanning agents. To confirm this, we determined the purity of syntans Nos. 1 and 6 in acetate buffer solution (pH ≈ 4.5), and obtained the values 92 and 96 %; the same values were obtained in a study of the effect of pH of an analytical solution (4g syntan per liter) on the takeup of syntans by leather powder: for sulfonated syntans Nos. 1-6 the purity fell from 68-81% at pH = 3.0 to 40-63% at pH = 5.0, while for the formalsufited syntans Nos. 7 and 8 the variations were much less. A study of the effect of time on the detanning of analytical solutions of our syntans showed (for times of 10, 30, and 120 minutes) that: a) under equal conditions the detanning rate decreases with increasing molecular weight of the syntan; b) with similar molecular weights the detanning rate increases with increase of the number of polar (methoxyl and hydroxyl) lyophilic groups in the syntan; c) the detanning rate, under similar conditions, is independent of the nature of the acid group (sulfo group or sulfite ester residue). Determinations of the purity of "model" syntans Nos. 1-7 in relation to the analytical solution concentration showed that an increase of concentration from 3 to 6 g/liter (pH = 4.0,

time 2 hours) did not affect the purity of the three-ring syntans Nos 1-3 and decreased the purity of the syntans Nos 4-7, of higher-molecular weight, in proportion to the molecular weight increase (from 4 to 17%), which is probably caused by tanning of the leather-powder surface by high-molecular syntans (see data on tanning, below) ; for the "technological "syntans Nos. 8 and 9, based on multinuclear phenols, increase of the analytical solution concentration does not influence the purity, as they are three-ring syntans.

4. The salting-out value of our "model" syntans, by Labzin's method, with 11% common salt solution, varies between 60 and 80%.

5. None of our syntans gives a precipitate on mixing in various proportions with willow extract. On mixing in equal amounts with the mixture: oak 60%, spruce 20% anthracine syntan 20% (" auxiliary tanning agent "), slight precipitates were formed only by Syntans Nos.6 and 7; the hide tanning time by these mixtures was the same as for vegetable tanning agents, whereas this time is much greater for certain "model" syntans. It follows that "slow model " syntans can be converted into "rapid"by addition of auxiliary tanning agents. An experiment with syntan No. 9 showed that complete penetration of belting leather hide is three times as rapid on addition of sulfite cellulose extract to a solution of this syntan.

Tanning of specimens of chromed belting hide, to determine the characteristics of our syntans, was carried out by four methods: 1) two-bath at high pH values (≈ 4.0), 2) two-bath at low pH values (≈ 2.5), 3) by weak liquors with a gradually rising concentration of the tanning agents at low pH values, 4) combined (syntan + oak extract 50:50) at high pH values; the control was oak extract.

The results are presented in the table below:

Syntan No.	Tanning method	Extractable matter (%)	Ash content (%)	Tanning number	Gravimetric yield number	Volume yield number	Density of rolled leather	Leather shrinkage temperature (°C)	pH of KCl extract
2	2	5.2	1.0	66.6	246	330	0.745	52	3.6
2	3	3.2	1.5	78.6	252	280	0.900	62	3.3
2	1	8.2	3.0	48.8	227	316	0.719	78	6.6
3	2	2.8	1.0	91.7	259	388	0.667	65	2.9
3	3	3.5	2.9	87.1	275	336	0.819	—	3.0
5	1	4.8	2.6	30.4	194	240	0.808	70	5.2
6	1	1.0	2.1	20.8	173	226	0.765	81	4.8
7	3	3.1	1.8	61.8	241	347	0.694	68	3.6
7	2	4.4	2.0	62.8	266	300	0.886	68	3.9
7	4	8.5	2.0	53.1	243	342	0.710	83	5.3
8	4	8.0	2.1	53.0	227	321	0.708	87	5.5
8	2	3.8	1.8	45.4	224	312	0.717	76	3.5
8	1	5.6	2.8	45.7	227	342	0.633	90	4.0
8	3	4.3	1.6	53.0	235	307	0.765	79	3.8
1	1	3.7	5.6	46.0	222	296	0.750	72	6.2
7	1	5.9	2.7	35.2	222	320	0.693	83	6.1
Control	1	9.5	2.9	41.5	213	311	0.685	88	4.6

As the table shows, all the "model" syntans and "technological " syntan No.8 give a leather with a low shrinkage temperature at low pH values, which is undoubtedly due to hydrolysis of the hide collagen. At high pH values "model" syntans yield a leather with a shrinkage temperature near or equal to the shrinkage temperature of leather tanned with oak extract, while the "technological " syntan No.8 made from polyhydric phenols from wood is superior to oak extract in this respect. The extractable matter in leather tanned by all our syntans is lower than in vegetable-tanned leather, which indicates that these syntans are firmly bound by the hide collagen. With two exceptions,the ash content of these leathers is also lower than that of vegetable-tanned leathers. The tanning time (not shown in the table) for complete penetration of the hide by the "model" syntans is considerably greater than for oak extract, but in mixtures with the latter it is not greater than for the control, and the quality of the leather is higher than that of vegetable-tanned leather in all respects. The gravimetric yield of leather obtained with the use of our syntans (with two exceptions—syntans Nos.5 and 6 at low pH values) is higher than with oak extract. The same is true of the tanning numbers and volume yields. The pH of potassium chloride extracts of leathers tanned with our syntans at higher pH values does not greatly vary in either direction from the corresponding value for vegetable-tanned leathers, which ensures their keeping qualities.

These results show that nearly all the "model " syntans (with their physicochemical properties taken into account) are independent tanning agents which yield leather of fairly high quality, while the "technological" syntan No. 8 made from phenols obtained from wood is superior to oak extract in all respects. The slowness of tanning by "model" syntans is avoided if they are mixed with vegetable tanning agents, whereby their range of application may be extended. It can therefore be claimed that we have developed the theory and technology of production of high quality artificial tanning agents (syntans) from individual phenols and mixtures of phenols of any origin, and have discovered a source of raw materials (saponified methoxy phenols and polyhydric phenols from wood) for the production of the best syntans.

LITERATURE CITED

[1] E. Stiasny, German Patents 262558 and 291457.

[2] Soviet Patents 11157 and 12219.

[3] Stather, Herfeld, Collegium 510 (1937).

[4] Kuntzel, Schwank, Collegium. 847 (1940).

[5] Koebner, Ztschr. Angew. Chemie, 46, 118, 251 (1933).

[6] Granger, Ind. Eng. Chem.,444 (1932).

[7] German Patents 87335, 265855, 285772, and British Patents 154162, 471968, and others.

[8] Glimm. Inaugural – Dissertation. Freiburg (1902).

Received January 3, 1956.

EMULSION COPOLYMERIZATION OF VINYLIDENE CHLORIDE WITH VINYL CHLORIDE

I. P. Losev and G.Ya. Gordon

Copolymers of vinylidene chloride with vinyl chloride are of great interest and have become of definite practical importance. Polymers for many fields of application can be obtained mainly by variation of the proportions of the initial monomers [1-3]. These are primarily materials with better processing characteristics than vinyl chloride polymers. Copolymers with good solubility in esters, chlorinated hydrocarbons, etc., should also be mentioned. They are used as film formers which yield strong, elastic, nonflammable and chemically resistant coatings. Finally, with a high vinylidene chloride content (80% and over), difficultly soluble products with relatively high softening temperatures are obtained. They may be used for production of strong threads, tubes, films, chemically resistant materials, seat materials, etc., by extrusion. Aqueous dispersions of these copolymers have an independent field of application. They are mainly used for fabric finishing, as adhesives, and for application of continuous elastic coatings.

By the theory of copolymerization [4-6], the copolymer composition may vary considerably with different yields of the reaction products. This is important with regard to determination of the degree of homogeneity of copolymers in relation to their practical utilization.

Data on the copolymerization of these monomers have been obtained by Medvedev, Abkin, Khomikovsky, and Zabolotskaya [6], for emulsion copolymerization in presence of benzoyl peroxide. The use of water-soluble initiators, in particular persulfates, is preferable in a number of cases.

It was necessary to determine the extent to which the general laws of copolymerization are valid in such conditions. In the present investigation the composition of copolymers obtained at different degrees of conversion in presence of ammonium persulfate as initiator and aliphatic sodium sulfonates as emulsifiers (latex method) was determined.

EXPERIMENTAL

The polymerization was carried out at 40° in a lead-lined autoclave 4 liters in capacity, fitted with a blade stirrer (120 r.p.m.), a thermometer socket, and a needle valve for supplying the vinyl chloride from a weighed cylinder. The apparatus was placed in a water bath fitted with an insulated Nichrome electric heater. A constant temperature (± 0.5°), measured by means of a resistance thermometer connected to an automatic recording current ratio meter, was maintained by means of a contact thermometer and an electromagnetic relay.

The autoclave was blown through and then charged with 1250 ml of an aqueous solution containing 0.2% ammonium persulfate and 1% "sulfonate" emulsifier, consisting of a mixture of sodium salts of alkyl sulfonic acids. The total monomer charge was about 500g. The vinylidene chloride was freshly distilled (30-32°) in presence of 1% ethyl alcohol. The latter is a mild inhibitor for vinylidene chloride, preventing formation of peroxide compounds and retarding spontaneous polymerization. The required amount of vinylidene chloride was placed in the autoclave, and vinyl chloride was then added from a weighed cylinder. The reaction was effected with continuous stirring for different times. The contents of the autoclave were then cooled to room temperature, the pressure was equalized, and the residual unreacted monomers were removed by heating to 60°. The latex obtained was coagulated by a saturated sodium chloride solution at room temperature. The coagulated polymer was filtered off, washed thoroughly with distilled water, and dried.

Determination of the chlorine content of the copolymers. The method of Schenk and Puell [7], somewhat modified by us, was used; this method is based on combustion of the substance in presence of calcium oxide. The absolute values of differences between parallel determinations did not exceed 0.3-0.4%. 0.1-0.15 g of the polymer was weighed out into a small quartz crucible and calcium oxide was added. The crucible was then covered by a large quartz crucible, the crucibles were inverted, and the space between them filled with calcium oxide. The combustion was effected by careful heating by means of a burner; this was followed by ignition for 30 minutes in a muffle furnace at 720-750°. The contents of the crucibles were dissolved in 4 N nitric acid. After filtration, 0.1 N silver nitrate solution was added for precipitation. This was followed by heating at 60° for 2-3 hours; the precipitate was filtered off on a weighed glass crucible with a porous plate No. 4. The silver chloride was washed with 1% aqueous nitric acid, then with water and acetone. It was dried for 1 hour at 60°.

The composition of the copolymer was calculated from the results of chlorine determinations in the separate polymerization products of both monomers. The vinyl chloride polymer prepared under similar conditions contained 56.35% chlorine; the vinylidene chloride polymer contained 71.3%. Three series of copolymerization experiments were carried out, with different contents of the original monomers (about 20, 39, and 59% of vinylidene chloride). The experimentally determined compositions were compared with the values calculated by means of the "simplified equation" proposed by Medvedev, Abkin, and Gindin [4]. By the theory of copolymerization (for the monomer pair studied), this Equation (I) gives a fairly exact value at considerable degrees of conversion.

$$\frac{[A]}{[A_0]}=\left[\frac{[B]}{[B_0]}\right]^K \qquad \text{(I)}$$

[A] and [B] are the molar quantities of unreacted vinyl chloride and vinylidene chloride at some instant during the polymerization; $[A_0]$ and $[B_0]$ are the analogous values for the original monomer mixture.

$$K=\frac{\alpha\frac{[A_0]}{[\ \ ]}+1}{\beta+\frac{[A_0]}{[B_0]}}.$$

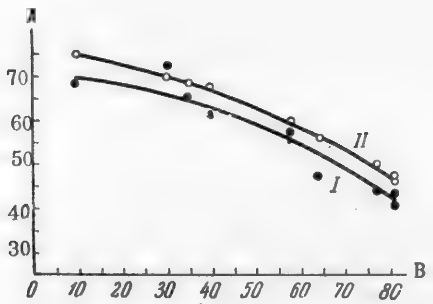

Fig. 1. Variation of copolymer composition for various degrees of conversion. A) Content of bound vinylidene chloride (in %); B) polymer yield (in %), I) experimental data, II) calculated data.

Here α represents the ratio of the rate constant for the reaction of a polymer radical terminating in a vinyl chloride unit with its own monomer, to the rate constant for the reaction of the same radical with vinylidene chloride; β is the corresponding ratio for the other monomer. In the present instance $\alpha = 0.20$, $\beta = 4.50$ [6].

The total molar content of combined vinylidene chloride in the copolymer at a given instant will be:

$$b=\frac{[B_0]-[B]}{[B_0]-[B]+[A_0]-[A]}. \qquad \text{(II)}$$

Equation (I) can be represented by an A=f(B) curve. To find the values of [A] and [B] at a given degree of conversion a for one mole of the original monomer mixture, we have

$$[A]+[B]=1-a. \qquad \text{(III)}$$

The coordinates of the point of intersection of the straight line representing Equation (III) with the curve

for A=f (B) give the required values of [A] and [B]. Equation (II) is then used to calculate first the molar and then the percentage composition (by weight) of the monomer. Table 1 gives the experimental data and the calculated results.

Fig. 1 gives curves for the variation of the copolymer composition for various degrees of conversion, at an initial monomer ratio corresponding to a vinylidene chloride content of about 39% (Nos. 1-9 in Table 1). The experimental data and the values calculated from Equation (I) are shown. A characteristic feature is the lower content of vinylidene chloride in the copolymer. This cannot be attributed to the accuracy of the values of the constants α and β determined for copolymerization under different conditions. They give the closest approximation to the experimental results by comparison with other values found from the results of other experiments.

TABLE 1

Comparison of Experimental and Calculated Copolymer Compositions for Different Yields

No.	Vinlyidene chloride content in the original monomer mixture (%)	Amounts of 100% monomers taken (in g)		Polymer yield			Content of combined vinylidene chloride in copolymer (%)	
		vinylidene chloride	vinyl chloride	in g	as % of the monomers	in mole fractions	from experimental data	calculated
1	39.4	196	302	48	9.6	0.087	68.7	74.8
2	39.2	196	295	147	30.0	0.259	72.5	70.2
3	39.4	196	301	173	34.8	0.310	65.3	68.5
4	38.9	196	299	197	39.8	0.359	62.0	67.7
5	38.4	196	302	287	57.8	0.533	57.5	60.0
6	39.5	196	301	318	64.0	0.618	47.4	56.4
7	39.0	196	298	380	77.0	0.754	44.6	50.3
8	39.4	196	302	402	80.7	0.802	40.9	47.6
9	39.4	196	302	403	81.0	0.831	43.7	46.2
10	19.7	98	401	125	25.1	0.222	47.1	46.9
11	20.2	98	385	190	38.9	0.364	39.8	40.9
12	20.0	98	393	377	76.7	0.762	21.6	25.5
13	58.5	294	208	122	24.3	0.215	82.2	84.9
14	59.2	294	203	167	33.6	0.297	82.6	84.0
15	59.0	294	205	214	42.9	0.384	81.2	82.3
16	58.0	294	213	353	69.7	0.672	65.5	74.7

It is seen that the distance between the curves in Fig. 1 is almost constant, corresponding to approximately 5 % of the absolute content of vinylidene chloride. Table 2 gives the calculated amounts of combined vinylidene chloride relative to the original monomer mixture for different degrees of conversion. These are based on smoothed curves from Fig. 1., when the vinylidene chloride content before polymerization was about 39%.

A comparison of the calculated results with the data found from the experimental graph (Fig. 1) shows that the amount of combined vinylidene chloride ceases to increase after 78% yield. Therefore the degree of utilization of this monomer at that point is about 88%. This gives reason to believe that in the copolymerization conditions studied-vinylidene chloride is consumed not only in formation of high-polymeric products, but evidently also in simultaneous reactions accompanied by formation of low-molecular compounds. This may be related to the oxidizing action of persulfate. Moreover, there are reports in the literature [8] that persulfate residues combine with vinyl compounds to form products which have an emulsifying action. Rutovsky *et al.*, who used ammonium and potassium persulfates as initiators, achieved "emulsifier-free" emulsion polymerization [7].

The general form of the curves shown in Fig. 1 is reminiscent of graphs of functions of the type $y=A-Be^{Cx}$ where A, B, and C are constants. It was therefore found possible to represent the copolymer composition by means of the empirical formula

$$\gamma = 77.2 - 6.166\, e^{0.0213\pi}. \tag{IV}$$

TABLE 2

Utilization of Vinlidene Chloride for Various Degrees of Conversion in Copolymerization
(From the graphs in Fig. 1)

Polymer yield (in %)	Amount of combined vinylidene chloride relative to orig. monomer mixture (%)		Polymer yield (in %)	Amount of combined vinlyidene chloride relative to	
	experimental curve	calculated		experimental curve	calculated
10	6.25	7.48	50	29.65	32.0
15	10.35	11.02	55	31.40	34.10
20	13.60	14.50	60	32.70	35.8
25	16.72	17.80	65	33.80	37.0
30	19.71	21.0	70	34.51	38.1
35	22.60	24.1	75	34.60	39.0
40	25.12	27.0	80	34.56	39.4
45	27.60	29.7			

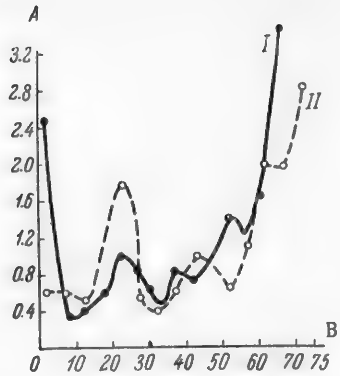

Fig. 2. Fractional composition of the copolymer (differential curves). A) Relative amounts of the fractions, B) contents of combined vinylidene chloride in the fractions (in %). I) Experimental data, II) calculated data.

Here π is the yield of polymer (in %), and γ is the content of combined vinylidene chloride in the copolymer. The composition of the product at various stages of conversion can be easily found by means of this formula, but the constants A,B, and C must obviously be determined each time for the actual polymerization conditions (initiator concentration, emulsifier concentration, presence of impurities, reaction temperature, etc.) Table 3 gives the results found from the graph for the experimental composition (Fig. 1), compared with those calculated from Formula (IV).

Data on variations of the content of combined vinylidene chloride in the copolymer at various degrees of conversion characterize the fractional composition of the product. For this, it is necessary to compare the increase in the amount of one of the polymerized monomers with the increase of the total yield of polymerization products. Fig. 2 gives differential curves for composition

TABLE 3

Use of the Empirical Formula $\gamma = 77.2 - 6.166\, e^{0.0213 \pi}$ to Find the Copolymer Composition

Polymer yield (%)	Content of combined vinylidene chloride in the polymer (%)		Polymer yield (%)	Content of combined vinylidene chloride in the polymer (%)	
	from composition diag. (Fig. 1)	from formula (IV)		from composition diag. (Fig. 1)	from formula (IV)
10	69.5	69.5	50	59.3	59.3
20	68.0	67.8	60	54.5	55.0
30	65.7	65.5	70	49.3	49.8
40	62.8	62.7	80	43.2	43.3

distribution, based on the graphs in Fig. 1, i. e., at a vinylidene chloride content of about 39% in the original monomer mixture.

The distribution curves show the presence of two principal maxima, corresponding to fractions rich in vinyl chloride and fractions rich in vinylidene chloride. Nevertheless, these characteristics, which are indicative of the complex nature of the copolymer formed, do not prevent, for example, good solubility for the production of lacquers. The products of individual polymerization, in particular vinylidene chloride polymer, are considerably less soluble.

SUMMARY

1. The variation of the composition of vinylidene chloride – vinyl chloride copolymers, made by the aqueous emulsion method in presence of persulfate at various degrees of conversion, approximately conforms to the known simplified copolymerization equation. The observed decrease of the actual amount of combined vinylidene chloride must be primarily attributed to side reactions in which this monomer is consumed to form low-molecular substances.

2. The composition of the copolymerization products can be represented by the empirical formula $y = A - Be^{Cx}$, where x is the polymer yield (in %) and y is the vinylidene chloride content (in %). The constants A, B, and C were determined experimentally for the copolymerization conditions used.

3. The copolymers obtained, in agreement with theory, are characterized by two principal maxima, corresponding to fractions rich in vinylidene chloride at the beginning of the process, and in vinyl chloride near the end.

LITERATURE CITED

[1] R. C. Reinhardt, Ind. Eng. Chem.,35, 422 (1943).

[2] H. Hopf, C. Rautenschtrauch, Makromol. Chem., 6,39 (1951),

[3] P. Kranzlein, Kunststoffe, 41, 421 (1951).

[4] A.D. Abkin, S.S. Medvedev, L. Gindin, Trans. 3rd All-Union Conf. on High Molecular Compounds (1945); J. Phys. Chem., 21, 1269 (1947).

[5] F. R. Mayo, F.M. Lewis, J. Am. Chem. Soc., 66, 2050 (1944).

[6] A. D. Abkin, S.S. Medvedev, P.M. Khomikovsky, E.V. Zabolotskaya, J.Phys. Chem., 27,1516 (1953).

[7] B.N. Rutovsky, A.V. Davankov, J. Chem. Ind., 2-3,36 (1944).

[8] J. M. Willis, Ind. Eng. Chem., 41, 2272 (1949).

Received June 21, 1955.

STUDIES OF THE CONVERSION OF SATURATED CARBON CHAIN POLYMERS

COMMUNICATION 4. SPECTROSCOPIC INVESTIGATIONS, IN THE INFRARED REGION, OF POLYMETHYLENE AND THE PRODUCTS OF ITS CONVERSION INTO A THREE-DIMENSIONAL POLYMER

A.Ya. Drinberg, N.S. Demchenko, O.N. Setkina, and N.M. Gopshtein

The Lensoviet Technological Institute, Leningrad

Polymethylene,* which is soluble in organic solvents at 60°, is oxidized when heated in air above 150° and is converted into an infusible and insoluble product [1, 2].

Polymethylene is a linear saturated polymer. The change in its properties can probably be attributed to the fact that atomic groups formed as the result of oxidation join the individual polymethylene chains into a three- dimensional structure.

In the present investigation an attempt was made to elucidate the structure of the oxidation product of polymethylene by studies of its infrared spectrum.

EXPERIMENTAL

Method of measurement. The measurements were made with the aid of a Hilger D-88 spectrometer with a rock-salt prism. The light source was a Nichrome band heated by an alternating current. The infrared radiation receiver was a schwarz thermopile with a type M-21 galvanometer made by No.531 Works, with the following characteristics: current sensitivity $C_I \approx 0.75-2.3 \cdot 10^{-9}$ A/mm·m; voltage sensitivity $C_V \approx 7.8-2.6 \cdot 10^{-9}$ V/mm·m; critical resistance $R_{ext.cr} \approx 10000-780$ ohms; vibration period $T_0 \approx 4.0$ sec.

The spectral range emitted by the monochromator at about 10 μ is approximately 10 cm^{-1}.

The deflections of the galvanometer mirror were used to plot curves for the transmission of infrared radiation (in%) as a function of the wavelength.

Preparation of the specimens. The starting material used was polymethylene with the following characteristics: molecular weight 25000-26000, melting point 115°, decomposition temperature 300°, solubility in xylene at 60° 100%, tensile strength of film 50μ thick 76 kg/cm^{-2}, elongation 7%, swelling in water in 10 days 0.09%.

Free polymethylene films were made from 8% solution of polymethylene in xylene of prepared glass surfaces at the following temperatures: original linear polymer at 120° for 3 hours, and three-dimensional insoluble polymer at 170-180° for 3 hours in the air.

Results of the Determinations.

Figure 1 shows the spectrum of the original polymethylene.

Figure 1 shows that the spectrum contains two strong bands at 1450 cm^{-1} and 720 cm^{-1} and a number of weak bands. The 720 cm^{-1} band is characteristic of long hydrocarbon chains [3]. The 1450 cm^{-1} band is due to the presence of CH_2 or CH_3 groups.

The 1370 cm^{-1} band is also characteristic of CH_3 groups. This band is very weak in the spectrum of polymethylene. This indicates that the number of CH_3 groups is not large and that the 1450 cm^{-1} band is due largely to CH_2 groups of the hydrocarbon chain. Thus, the infrared spectrum of polymethylene indicates that it consists of long hydrocarbon chains with very little branching.

* The authors use the terms "Polymethylene" and "Polyethylene" interchangeably—Publisher's note.

The polymethylene spectra reported by Thompson [4] contain a band at 1379 cm^{-1}. From its intensity it was calculated that there is one CH_3 group for 50 CH_2 groups.

Our specimens contained considerably less CH_3 groups and therefore the molecules contained relatively few branchings.

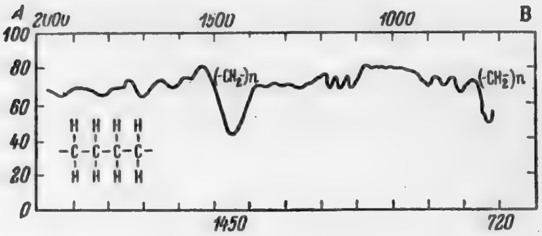

Fig. 1. Absorption spectrum of polymethylene in the infrared region. A) Infrared transmission (%), B) frequency (in cm^{-1}).

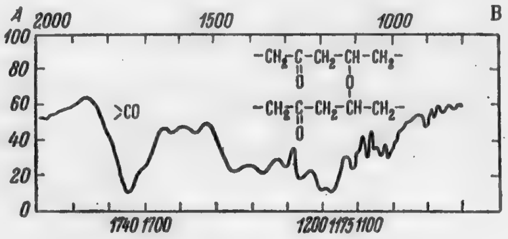

Fig. 2. Absorption spectrum of polymethylene of a three-dimensional structure in the infrared region. A) Infrared transmission (%), B) frequency (in cm^{-1}).

In addition, the weak bands at 1600-1750 cm^{-1} and 1100-1200 cm^{-1} observed in the spectrum are caused by small amounts of oxidation products.

The absorption spectrum of polymethylene converted into the three-dimensional polymer (Fig. 2) differs from the spectrum of the original material by a strong band at 1700 cm^{-1} and 1740 cm^{-1}, associated with the carbonyl group, and several bands in the region 1000-1400 cm^{-1}.

Among the bands in the frequency region 1000-1400 cm^{-1}, as Fig. 2 shows, strong bands at 1175-1200 cm^{-1} are particularly prominent. This region of the spectrum from 8.0 μ (1250 cm^{-1}) to 8.8 μ (1150 cm^{-1}) is attributed by Thompson [4] to vibration of the $-C-O-C-$ skeleton, modified in some cases by the presence of the carbonyl group, $O=C-O-C-$.

Thus, these bands are characteristic of compounds of the type $R-CO-O-R$ and $R-O-R$.

As already stated, the purpose of the present investigation was to determine the nature of the atomic groups linking the individual polymethylene chains into a three-dimensional polymer. These groups arise as the result of oxidation and it is to be expected that they contain oxygen.

It is unlikely that the individual polymethylene chains are linked by ester groups as shown below:

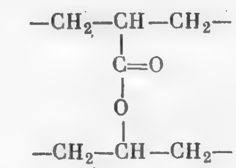

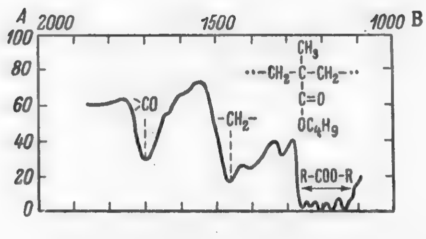

Fig. 3. Absorption spectrum of polybutyl methacrylate in the infrared region. A) Infrared transmission (%); B) frequency (in cm^{-1}).

Such groups can only arise as the result of oxidation in a side branch of the chain. The spectrum of linear polymethylene, however, indicates weak chain branching.

The spectrum of polybutyl methacrylate (Fig. 3) shows that the form of the bands in an ester differs appreciably from the form of the bands in polymethylene converted into a three-dimensional polymer. Esters have 4-5 strong bands in the 1100—1250 cm^{-1} region; the three-dimensional polymethylene has only two strong bands at 1175—1200 cm^{-1}.

The more likely hypothesis is that the individual polymethylene chains are linked by ether groupings:

$$\begin{array}{c} -CH_2-\underset{|}{CH}-CH_2- \\ O \\ -CH_2-\overset{|}{CH}-CH_2- \end{array} \qquad (2)$$

The infrared spectrum of diisopropyl ether has, like polymethylene converted into a three-dimensional polymer, two strong bands at 1100—1170 cm^{-1} [5], characteristic of an ether group linked to secondary carbon atoms. The frequencies of the bands for a primary ether group $-CH_2-CH_2-O-CH_2-CH_2-$. . .are lower. Ethers of this structure have one band at 1100 cm^{-1}.

To confirm this hypothesis on the structure of three-dimensional polymethylene, the position of the oxygen bridge was investigated to determine whether it is present in the linear chain or whether it serves as a link between the chains to form the three-dimensional insoluble polymer.

If the oxygen is present in the linear chain, the formation of the three-dimensional polymer may be effected by carbon-carbon bonds:

$$\begin{array}{l} -CH_2-O-CH_2-\underset{|}{CH}-\underset{\underset{O}{\|}}{C}-CH_2- \\ -CH_2-O-CH_2-\overset{|}{CH}-\underset{\underset{O}{\|}}{C}-CH_2- \end{array} \qquad (3)$$

As an example of a compound containing an ether linkage in the linear chain, ethylene oxide polymer was prepared (molecular weight 1140, m.p. 48-50°). The structure of this polymer can be represented as $-CH_2-CH_2-O-CH_2-CH_2-O-$.

The infrared absorption spectrum of this polymer was investigated, and is shown in Fig. 4.

The ethylene oxide polymer spectrum has two bands at 1100—1142 cm^{-1}. Their frequencies are lower than in secondary ethers.

The foregoing leads to the conclusion that the conversion product of polymethylene has the structure represented by Scheme (2).

The strong bands at 1700—1740 cm^{-1} are due to ketone groups which are probably side products of oxidation and do not play any significant role in the formation of the three-dimensional polymer.

The hypothesis that the structure of oxidized polymethylene involves cross linking by oxygen bridges may be verified by a chemical method—by destruction of the ether bonds. If the three-dimensional insoluble polymethylene polymer is in fact formed with the aid of ether linkages, the polymer should again become soluble after destruction of these linkages. The three-dimensional insoluble polymethylene polymer was therefore treated with a mixture of hydriodic acid and red phosphorus at 150° for 48 hours, as it is known that any existing ether linkages are destroyed under such conditions [6]. Study of the product formed as the result of this treatment showed that it has m.p. of about 112°, is completely soluble in xylene on heating, and is white (the three-dimensional polymers are slightly colored). Thus, the product again acquires the properties of the original polymer.

The infrared absorption spectrum of the product obtained after hydriodic acid treatment was also investigated (Fig.5). It was found that the strong ether linkage bands at 1175-1200 cm^{-1} disappeared.

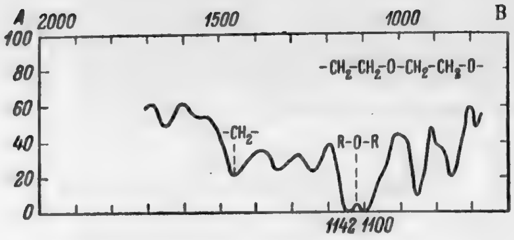

Fig. 4. Absorption spectrum of ethylene oxide polymer in the infrared region. A) Infrared transmission, (%) B) frequency (in cm^{-1}).

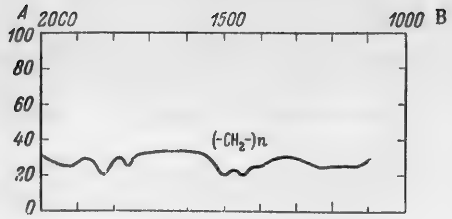

Fig. 5. Absorption spectrum of three-dimensional polymethylene polymer in the infrared region after treatment by hydriodic acid. A) Infrared absorption*(%), B) frequency (in cm^{-1}).

SUMMARY

1. A study of the infrared absorption spectra of linear and three-dimensional polymethylene polymers showed that the spectrum of the latter differs from that of the former by the appearance of new bands in the 1700 cm^{-1} and 1200-1100 cm^{-1} regions, due to formation of oxygen compounds during conversion of the polymethylene at high temperatures in the air.

2. A comparison of the characteristic features of the absorption spectra of the three-dimensional polymer and of typical oxygen compounds showed that the formation of oxygen bridges of the ether type is of primary significance in the oxidation and formation of the three-dimensional polymer.

3. The following structure can be ascribed to three-dimensional polymethylene on the basis of a comparison of the absorption spectra of ethers and esters with that of the three-dimensional polymer:

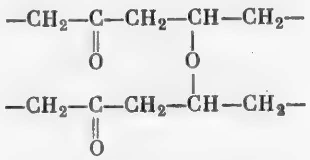

(4)

The ketone group bands observed in the spectra of the linear and three-dimensional polymers are due to side products formed by oxidation.

4. The formation of three-dimensional polymethylene polymer by means of oxygen bridges was confirmed chemically, as after treatment with hydriodic acid, which destroys ether groups, the properties of the polymer become similar to the properties of the original linear polymethylene.

LITERATURE CITED

[1] Hunter, Oakes, Brit. Plast.,17, 190, 94 (1945).

[2] A. Ya. Drinberg and N.S. Demchenko, J. Appl. Chem., 25, 1, 57 (1952).**

[3] V. M. Chulanovsky, Introduction to Molecular Spectrum Analysis, Tech. Press (1951).

[4] H. W. Thompson, A.P. Torkington, Trans. Far. Soc., 41, 4-5, 248 (1945).

[5] R. B. Barnes, U. Liddel, N.Z. Williams, Infrared Spectroscopy (1944).

[6] Staudinger, Schwalbach, Liebigs Annalen der Chemie, 488, 11 (1931).

Received June 26, 1956.

* As in original Publisher's note.

** Original Russian pagination. See C. B. Translation.

THE TECHNOLOGY OF NITRON (NITRILON) POLYACRYLONITRILE FIBER

E. S. Roskin

The S. M. Kirov Textile Institute, Leningrad

By the decision of the XXth Congress of the C.P.S.U., industrial production of "nitron" polyacrylonitrile fiber is being organized in our country during the current Five-Year Plan [1].

Work on a Soviet polyacrylonitrile fiber, nitron ("nitrilon") was first started in 1950 in the S. M. Kirov Textile Institute, Leningrad [2, 3], and parallel work has been done at the All-Union Scientific Research Institute for Artificial Fibers [4].

The present paper contains the results of certain investigations, carried out at the Kirov Textile Institute, on wet spinning conditions and on selection of spinning baths which would give a polyacrylonitrile fiber with properties for technical purposes and consumer goods.

EXPERIMENTAL

The fibers were extruded in a laboratory-type spinning machine and in a specially designed experimental staple fiber spinning machine with five spinning positions with 3200-hole spinnerets.

In all cases acrylonitrile polymer of molecular weight 25,000-50,000, was used, synthesized by the static polymerization method [3, 5], the industrial development of which was carried out jointly with an undertaking of the Ministry of Chemical Industry (engineers E. A. Kulev and A. I. Konkhin). Spinning solutions of 16-18% concentration were made by dissolving the polymer in dimethylformamide for 2-3 hours with stirring and heating to 40-50°. The solutions were kept at 40° for 3-5 hours for de-aeration and better homogenization.

The filtered spinning solution was fed into a gear pump at 20-25° by means of air or nitrogen at 2-3 atmospheres pressure. From the gear pump the solution entered a filter candle, and then the spinneret. Streams of the solution from the spinneret were directed into a precipitating liquid (spinning bath) for coagulation, where the actual thread formation took place.

The threads coagulated in the spinning bath were collected on a receiving roller and then directed to a plasticizing bath, where they were stretched. The spinning was in all cases carried out at a negative tension at the spinneret. The fibers were then washed and dried in the unstretched state.

The substances tested for the spinning bath liquors were polyethylene glycol phenyl ethers with the general formula alkyl—$\langle\quad\rangle$ $O(CH_2CH_2O)_nH$, where the alkyl radical contains 8-12 carbon atoms (known as Products OP-7 and OP-10), castor oil, carbon tetrachloride, butyl alcohol, water, and others. The spinning bath liquors were in most cases used for the plasticizing baths.

The spinning baths used and the properties of the fibers contained are discussed below.*

* Engineers V. V. Darvin, V. V. Averyanova, and S. I. Dmitrieva took part in the work.

Polyethylene Glycol Alkyl Phenyl Ethers (Products OP-7 and OP-10)

These substances are now synthesized on a large industrial scale by condensation of fatty and aromatic alcohols with ethylene oxide. They are oily viscous liquids with a weak specific musty odor; they are readily soluble in water and have good wetting and emulsifying powers, being nonionic surface- active compounds. The coagulation was effected at 35-90° and the coagulated threads were drawn off at speeds from 6 to 12 m/ minute.

The spinning bath liquor was electrically heated to the required temperature. The length of the thread path in the coagulating bath was 200-400 mm at an immersion depth of 50-60 mm.The plasticizing bath used was OP-10, glycerol, or castor oil.

The plasticization process was carried out at 90-110° at an immersion depth of 20-30 mm, with a total immersion path of 50-20 mm [6].

After the plasticization bath the threads were collected on a second collecting roller rotating at a speed which gave 800-5000% stretch to the fibers.

TABLE 1

Physical and Mechanical Properties of Fibers Obtained With the Use of OP-10 for the Spinning Bath

Average tensile strength for 100 single filaments (in g)	Average extension from 100 tensile tests (in %)	Average (metric) number of filament from 1600-filament tow	Breaking length (in km)	Average fiber cross section (in μ)	Stretch (in %)	Coefficient of variation σ	Probable error (in %)
10.71	24.14	4629	49.58	190	1310	2.54	2.00
12.40	25.76	3997	49.56	220	1140	2.60	2.96
11.66	23.10	3908	45.57	224	1110	3.45	3.96
10.44	24.47	3997	41.70	220	1140	2.52	3.36
10.78	23.80	3725	40.15	235	1060	1.87	2.36
9.26	24.68	3573	33.09	245	1020	2.40	3.64
22.11	41.50	1164	25.74	430	580	—	—
16.10	53.70	325	5.23	2500	0	—	—

After washing in water and drying, the fibers were used for processing into textiles.

The dimethylformamide content in the spinning and plasticizing baths was allowed to rise to 25-30%. The fineness of the fibers was regulated mainly by variations of the negative tension at the spinneret and of the collection rate at the second roller.

The fibers did not need any subsequent additional finishing operations. After drying,the fibers acquired a stable crimp, so that special crimping processes were not needed.

Nitron produced by the above method has high softness, elasticity, strength, and crimp, and very closely resembles high quality wool fibers or natural silk, depending on the spinning temperature and the degree of stretch. Articles and yarn made from the fibers are almost indistinguishable from pure wool yarn and corresponding woolen articles not only visually and organoleptically, but in heat insulation properties.

The recovery of dimethylformamide and OP-10 was effected by 3-4 fold dilution of the spent spinning bath followed by heating to 80-90° [7]. The bath then separated into two layers; the first consisted of OP-10 with a small amount of dimenthylformamide, and the second of water rich in dimethylformamide.

The dimethylformamide was then recovered by distillation of the aqueous solutions.

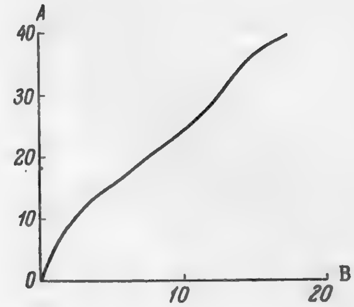

Fig. 1. Load–extension curve for the fiber. A) Load (in g/denier), B) extension (in %).

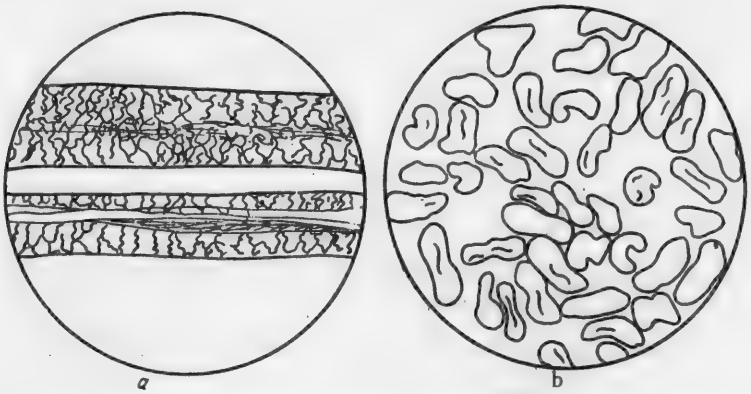

Fig. 2. Fiber microphotographs in the longitudinal (a) and transverse (b) directions.

Dimethylformamide can also be recovered by distillation of the spent spinning bath under vacuum.

In this case copious frothing took place, which greatly interfered with the distillation. To prevent frothing, 0.1-0.2% of mineral oil must be added to the liquid for distillation.

Castor Oil

Medical and technical castor oil were tested as the spinning bath liquor. The results were the same in both cases.

The spinning bath temperature was maintained at 50-100°. The plasticization process was effected by means of glycerol, OP-10, or castor oil at 100-140°. All the other spinning conditions were the same as for OP-10 spinning bath.

Table 2 presents data on the physical and mechanical properties of the fibers.

TABLE 2

Physical and Mechanical Properties of Fibers Obtained With the Use of Castor Oil for the Spinning Bath

Average tensile strength for 100 single filaments (in g)	Average extension from 100 tensile tests (in %)	Average (metric) number of filament from 1600-filament tow	Breaking length (in km)	Average fiber cross section (in μ)	Stretch (in %)	Coefficient of variation σ	Probable error (in %)
9.71	21.19	4380	42.49	200	1250	2.35	3.42
9.14	26.40	4212	38.48	208	1200	2.20	3.40
9.37	25.63	3821	35.70	230	1090	2.60	3.10
9.08	19.80	3643	33.08	241	1040	3.00	4.55
8.41	40.10	3085	25.09	280	890	2.60	4.35
18.13	43.80	1154	20.92	480	521	—	—

Some individual fiber specimens had a breaking length of up to 55-60 km with 20-22% extension at break. In external appearance and organoleptic properties the fibers were considerably superior to all other fibers obtained in our experiments, having a soft luster, high elasticity, resilience, and softness.

Washing of the fibers presented some difficulties owing to the insolubility of castor oil.

The use of OP-10 as plasticizing bath considerably facilitated washing, as it acted as a surface-active and emulsifying substance.

The treatment of the fibers with certain organic solvents (ligroine, carbon tetrachloride, etc.) instead of water washing was studied, and is very promising. This process can be carried out in ordinary automatic continuous extraction equipment, in which washing of the fiber and recovery of the solvent can be effected simultaneously. The recovery of dimethylformamide from spent spinning baths can also be effected by previous dilution of the baths with water followed by separation of the castor oil layer from the lower aqueous layer containing dissolved dimethylformamide [7].

The small amount of dimethylformamide which remains in the castor oil is useful in the subsequent use of the recovered oil as spinning bath.

The aqueous dimethylformamide solution was separated by the usual methods.

Prolonged use of castor oil as spinning bath liquor without recovery gradually led to its contamination with certain oxidation and decomposition products, which became noticeable by the darkening of the liquid. It was found that darkening of the liquid could be prevented by addition of up to 5% glycerol, which formed a separate layer below.

Carbon Tetrachloride

One of the distinctive characteristics of the use of carbon tetrachloride as spinning bath is the possibility of carrying out the process at room temperatures. This gives, even before drawing, an elastic fiber with a high luster and a breaking length of up to 7-8 kilometers.

The unoriented fiber, on leaving the spinning bath, is sent directly to the stretching devices, special plasticization processes being omitted. The carbon tetrachloride which remains in the fibers and gradually evaporates acts as plasticizer. Fibers with up to 400% stretch, with a breaking length of up to 25-26 kilometers and 25-30% extension at break were made in this way.

Considerably stronger fibers were obtained by additional stretching over surfaces heated to 110-115° or in a plasticizing bath heated to the same temperature and containing the usual liquid used for plasticization (OP-10, glycerol, glycol, etc.).

Water heated to the boil can be used as a plasticizing bath.

The fibers were stretched 1500-2000% during the drawing process, and were then wound on collecting devices, not requiring any additional finishing operations.

When heated surfaces were used for the stretching, special drying of the fibers was not required.

Table 3 gives some of the fiber characteristics.

Dimethylformamide was recovered from the spinning baths by simple distillation, which was easily achieved owing to the large difference in the boiling points of the components of the mixture.

The main defect of the process is the relatively high toxicity of carbon tetrachloride. It was found that addition of a small amount of water to the spinning bath ensured safe working conditions from the health aspect, as the water formed a thin layer on top which prevented evaporation of the volatile carbon tetrachloride. All the other spinning conditions were the same as before.

Butyl Alcohol

As in the case of carbon tetrachloride, the spinning bath was used at room temperature. The plasticization and stretching were performed at 110-120° with the use of the liquids discussed above (OP-10, castor oil, etc).

TABLE 3

Physical and Mechanical Properties of Fibers Obtained With the Use of Carbon Tetrachloride at 20° for the Spinning Bath

Plasticization	Plasticization stretch temperature (in °C)	Stretch (in %)	Average metric number of a single filament	Breaking length (in km)	Extension (in %)
Without plasticization	—	400	980	25.1	60
Water–steam	100	500	1172	25.9	51
Water–steam	100	700	1667	33.6	22
Water–steam	100	700	1507	26.0	38
OP-10	108	1050	1800	37.0	19
Castor oil	110	1150	1900	39.0	19
Metal surface	110	1050	1800	36.0	17

Much better results were obtained after addition of 0.5-1.0% by weight of surface-active substances such as OP-10 to the butyl alcohol.

Such additions produced an average increase of 10-15% in the fiber strength and extension at break. With the use of added OP-10, fibers stretched 1200-1500% were obtained, with a breaking length of 40-45 kilometers and 20-22% extension at break.

All the other spinning conditions were as before.

Water and Aqueous Dimethylformamide Solutions

It is known from patent data and foreign experience that water, or, more accurately, dilute aqueous dimethylformamide solutions can be used as spinning bath liquor. However, this method is mainly applicable to the production of staple fiber, the spinning of which is simpler than continuous filament spinning. Fibers produced in aqueous spinning baths are usually more harsh and brittle than the fibers made with the use of organic spinning baths.

The quality of the fibers obtained from aqueous baths may be improved considerably by addition to the baths of 0.5-1.0% of surface-active substances, such as OP-10. It is then also possible to obtain the fibers in the form of continuous filaments of up to 40-45 kilometers breaking length with 20-22% extension at break.

The following are typical conditions for the spinning and production of such fibers. Spinning bath composition (in %) : water 86.4-84.4, dimethylformamide 13 -15, OP-10 0.5, glycerol 0.1. Spinning bath temperature 25°.

The fibers were stretched on heated surfaces (120-130°) or in plasticizing baths consisting of glycerol, OP-10, glycol, etc., at 130-140°.

The fibers were dried before reaching the heated surfaces or plasticizing bath. Good results were obtained by plasticization and stretching of the fibers in steam at 120-125°. Preliminary drying was not required in this case.

Comparative experiments showed that fibers made by the above method have, on the average, 12-15% better properties than fibers made with the use of aqueous dimethylformamide baths only, both with regard to tensile strength and to extension at break.

All the other spinning conditions were as before.

SUMMARY

In tests of polyethylene glycol phenyl ethers (OP-7 and OP-10), castor oil, carbon tetrachloride, butyl alcohol containing OP-10, and aqueous dimethylformamide containing OP-10 as spinning baths for polyacrylonitrile fibers it was shown that nitron polyacrylonitrile fiber with good physical and technical properties can be produced.

LITERATURE CITED

[1] Directives of the XXth Assembly of the C.P.S.U. on the Sixth Five-Year Plan for the Development of the National Economy of the USSR in 1956-1960, State Political Press (1950).

[2] E.S. Roskin, Scientific-Technical Conference of the Kirov Textile Institute, Leningrad, Summaries of Papers, 39-45 (1954).

[3] E. S. Roskin, Trans. Kirov Text. Inst. Leningrad, 6, 77-90 (1955).

[4] V. E. Kotina and V. S. Klimenkov, Trans All-Union Sci. Res. Inst. Artificial Fibers, 2, 109-114 (1955).

[5] A. Hunjar, H. Reichert, Faserforsch u. Textiltechn., 5, 1-8 (1954).

[6] E. S. Roskin, " Method for Formation of Polyacrylonitrile Fiber", Author's Certif. 101311 (April 9, 1954).

[7] E. S. Roskin, " Method of Spinning Bath Recovery," Author's Certif. 99887 (May 25, 1953).

Received June 5, 1955.

COMMUNICATION VI. CATALYTIC CONVERSION OF PRIMARY ALCOHOLS OF ISO-STRUCTURE INTO KETONES

B.A. Bolotov, K.P. Katkova, and S.B. Izraileva

It was reported in previous publications on studies of catalytic conversion of primary alcohols of normal structure that the principal products of such conversion over activated copper catalysts at 250-275° are esters (yield about 60%) and at 325-350°, symmetrical ketones (yield 45-55%) [1,2]. It was noted that the yields of esters and ketones increase with increasing molecular weight of the alcohol. The resultant gases were found to contain considerable amounts of carbon monoxide, which suggested the possibility of conversion of alcohols into ketones according to the following scheme:

$$RCH_2OH \xrightarrow{-H_2} RCHO \rightarrow RCHOHRCHO \xrightarrow[-H_2]{-CO} RCOR.$$

An investigation of conversion reactions of alcohols and aldehydes of iso structure over Cr_2O_3 catalyst, performed earlier by Komarewsky and Smith [3] led these authors to conclude that ketones are formed if the carbon atom in the α position contains no substituents. Otherwise, only aldehydes are formed in good yield. In fact, α substituted alcohols (isobutyl alcohol, 2-methylpentanol, etc.) did not yield ketones and these alcohols only underwent dehydrogenation to the corresponding aldehydes. Under the same conditions isoamyl alcohol and isovaleraldehyde formed diisobutyl ketone in 17.6 and 29.9% yields. The explanation offered for these results was that α substituted aldehydes cannot undergo aldol condensation which precedes the ketone formation reaction.

The present paper deals with a study of the conditions of ketone formation from primary alcohols of iso structure over the copper catalysts used previously in work on ethyl alcohol [4,5]. It was found in these studies that isobutyl and isoamyl alcohols are converted into ketones of iso structure at temperatures of 425-450° and space velocities of 150-200. At 250-300° the main reaction products are esters: isobutyl isobutyrate and isoamyl isovalerate, the yield of which reaches 40%. As the temperature is increased to 360° the ester yield decreases and the aldehyde yield begins to increase until a new reaction of ketone formation commences at the catalyst; at 425° this becomes the principal reaction.

EXPERIMENTAL

These reactions were studied over a copper catalyst activated with ThO_2 [6] and reduced in a current of hydrogen at 275-300°. The experiments were performed in a laboratory apparatus described earlier [4]; the temperature range was 250 to 450°, with hydrogen and the origin alcohol in 1:1 molar ratio. The liquid condensates obtained in the experiments, the yield of which reached 60-98% according to the experimental conditions, were subjected to fractional distillation. The fractions were analyzed for aldehyde, ester, acid, and ketone contents. The distillation and analysis data were used to calculate the yields of the reaction products relative to the original alcohol.

The calculated results are given in Tables 1-4.

Catalytic conversion of isobutyl alcohol. The starting material for the experiments was freshly distilled primary isobutyl alcohol with b.p. 107—108°, d_4^{20} 0.8027, n_D^{20} 1.3954 (literature data [7]: b.p. 108.1°, d_4^{20} 0.8020, n_D^{15} 1.3976).

In order to determine the maximum yields of diisopropyl ketone and the variations in the composition of the reaction products with temperature and space velocity, the experiments were performed over a temperature range of 275-475° at a space velocity (s.v.) of 150, and at temperatures of 400 and 425° at various space velocities.

TABLE 1

Catalytic Conversion of Isobutyl Alcohol as a Function of the Temperature

Temperature (°C)	Amount of condensate (%)	Gas composition (vol.%)				Yields (in weight % of the orig. alcohol)			
		CO_2	C_nH_{2n}	CO	H_2	Isobutyraldehyde	Isobutyl alcohol	Diisopropyl ketone	Isobutyl isobutyrate
275	97.7	0.2	0.9	0.0	98.9	10.0	57.5	0.0	28.8
325	62.5	3.6	3.0	1.9	92.5	13.2	21.0	5.7	21.4
350	78.0	3.3	2.0	1.6	92.9	23.4	16.0	17.5	19.3
375	86.8	3.2	2.0	2.8	94.0	17.8	34.3	20.0	11.4
400	80.0	2.4	1.7	5.4	90.5	13.2	21.0	27.2	6.5
425	80.2	2.1	0.4	5.8	91.5	3.5	20.0	56.0	3.2
450	60.4	3.1	2.1	5.0	89.6	0.5	5.7	50.5	1.0
475	58.5	4.8	4.2	4.1	86.6	2.3	6.6	46.0	1.7

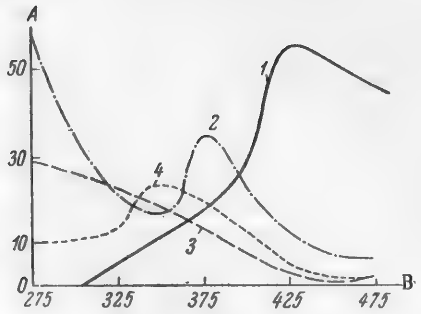

Fig. 1. Effect of temperature on the yields of ketone, aldehyde, and ester from isobutyl alcohol at s.v. 150. A) Yields (in weight % of the original alcohol), B) temperature (°C). 1) Diisopropyl ketone, 2) isobutyl alcohol, 3) isobutyl isobutyrate, 4) isobutyraldehyde.

The results of the investigations are given in Table 1 and Figure 1. At 275-325° the principal reaction is dehydrogenation of the alcohol, leading to aldehyde formation, with subsequent condensation of the latter to the ester isobutyl isobutyrate. At 350-400° the ester yield decreases, with a simultaneous increase of the amounts of aldehyde and ketone in the condensate. This indicates a change of catalyst function. While at the lower temperatures (250-300°) condensation of aldehyde to ester took place, at temperatures above 375° aldol condensation begins, with subsequent conversion of aldol to ketone. Considerable amounts of ketone are formed only at temperatures above 400°, when the contents of aldehyde and the original alcohol in the condensate greatly decrease. Thus the temperature required for the formation of ketone from isobutyl alcohol over a copper catalyst is 100° higher than for alcohols of normal structure. The yield of diisopropyl ketone at 425-450° is 50-56%.

Figure 1 shows three curves, which clearly demonstrate the variation of the composition of the reaction products with the temperature. Each curve has a clearly defined maximum; the 1st corresponds to the ester (temperature 275°), the 2nd to the aldehyde (temperature 350-375°), and the 3rd to the ketone (temperature 425-450°). The aldehyde curve also shows that the highest yield of aldehyde precedes the start of ketone formation. It is evident that the aldehyde is the main intermediate product in ketone formation. Moreover, in the conditions of ketone formation, the resultant gas has the highest carbon monoxide content, which also confirms the theory advanced earlier [2] concerning the aldol mechanism of ketone formation from primary alcohols.

To determine the influence of space velocity (s.v.) on the ketone yield, and also on the formation of intermediate reaction products (aldehyde and ester), experiments were performed at temperatures of 400 and 425° with various contact times (3600/s.v. • second). The results of the experiments are shown in Table 2 and Fig. 2. It is seen from these results that the ketone yields increase with contact time. To obtain the maximum ketone yield at 400° the contact time must be increased 3 to 4-fold in comparison with 425°. At the same temperature, but with a smaller contact time, the ester and aldehyde yields increase very little and most of the alcohol remains unchanged (≃50%). The carbon monoxide content of the gases increases considerably with contact time. These results also confirm the hypothesis that ketones are formed from aldehydes by way of the aldol condensation reaction, without an intermediate stage of ester formation.

TABLE 2

Variation of the Composition of the Reaction Products in the Conversion of Isobutyl Alcohol with Contact Time

Temperature (°C)	Contact time (seconds)	Condensate yield (%)	Gas composition (vol. %)				Yield (in wt. % of the original alcohol)			
			CO_2	C_nH_{2n}	CO	H_2	Isobutyraldehyde	Isobutyl alcohol	diisopropyl ketone	Isobutyl isobutyrate
400	10.3	92.0	1.5	0.7	3.7	94.0	9.2	58.0	10.3	11.1
	14.4	90.2	1.6	0.8	5.5	92.2	10.7	45.4	14.4	14.1
	24.0	81.0	2.1	0.8	7.8	89.1	8.8	22.3	33.8	6.1
	65.5	62.3	2.8	3.6	14.1	64.0	2.8	4.2	52.5	0.0
425	10.3	80.0	2.7	1.5	7.7	88.0	9.2	33.6	30.8	6.0
	14.4	87.0	3.0	1.1	10.8	85.0	10.2	12.7	50.0	5.0
	24.0	72.0	3.1	1.0	11.0	82.8	5.5	8.0	51.5	2.3
	48.0	70.2	2.0	1.3	12.0	84.3	1.8	9.0	55.5	2.7
	102.7	64.5	1.8	1.4	14.9	81.7	0.3	4.0	52.5	3.3

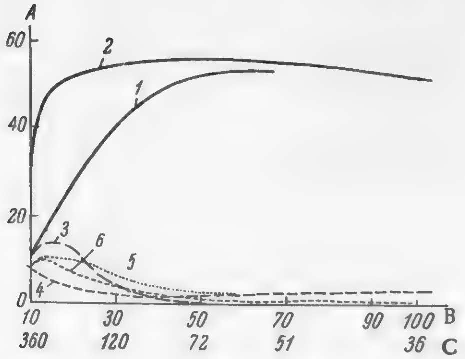

Fig. 2. Effect of contact time on the yields of ketone, ester, and aldehyde from isobutyl alcohol at temperatures of 400° (1, 3, 5) and 425° (2, 4; 6). A) Yield (in weight % of the original alcohol), B) contact time (seconds), C) space velocity. 1,2) Diisopropyl ketone, 3,4) isobutyl isobutyrate, 5,6) isobutyraldehyde.

Catalytic conversion of isoamyl alcohol. The catalytic conversion of primary isoamyl alcohol was studied in the conditions described above for isobutyl alcohol. The alcohol used was distilled fermentation isoamyl alcohol with b.p. 130-132°, d_4^{18} 0.815 and n_D^{20} 1.4074 (literature data [7]: b.p. 132.0°, d_4^{20} 0.8091, n_D^{20} 1.4085).

Table 3 and Figure 3 show the results of experiments carried out over the temperature range 250-450° and s.v. 150. An examination of the results reveals the same relationships for the variation of the composition of the reaction products as in the experiments with isobutyl alcohol. At 250-300° the main reaction product is an ester, isoamyl isovalerate. At 350° the maximum yield of isovaleraldehyde is obtained, the ester yield decreases, and small amounts of diisobutyl ketone appear in the condensate. In these conditions the condensate also contains considerable amounts of unreacted alcohol and unreacted aldehyde. At 400-450° conversion of the aldehyde to diisobutyl ketone occurs, and the yield of the latter at 425-450° is 37%.

Variations of the contact time (temperature 425°) influence the composition of the condensate formed. Increase of the reaction time from 10 to 50 seconds raises the diisobutyl ketone yield from 12 to 40% and lowers the contents of alcohol, ester, and aldehyde in the condensate. The data of Table 4 show that the optimum conditions for the production of the ketone from the alcohol are a temperature of 425° and a contact time of 24-50 seconds (s.v. 70-150). Increase of the contact time to 90 seconds leads to a decrease of the ketone yield owing to intensification of high-molecular condensation products.

As in the experiments with isobutyl alcohol, the carbon monoxide content of the gas increases considerably with increasing ketone yield, which once again indicates that the ketone is formed through the intermediate stages of aldehyde and aldol formation. The presence of small amounts of CC_2 and unsaturated hydrocarbons in the gas indicates the possibility of a reaction of ester decomposition, which also leads to ketone formation.

All the compounds obtained by catalytic conversion of alcohols with an iso structure were isolated pure and characterized by determination of their physicochemical constants and also by formation of derivatives. The results are given in Table 5.

TABLE 3

Catalytic Conversion of Isoamyl Alcohol as a Function of the Temperature

Temperature (°C)	Condensate yield (weight %)	Yields (in wt. % of the original alcohol)			
		Isovaleraldehyde	Alcohol	Diisobutyl ketone	Ester
250	98.0	10.0	44.0	0.0	45.5
275	85.0	12.0	25.0	3.0	46.0
300	80.0	17.0	20.0	3.6	36.5
330	81.0	24.0	12.5	7.3	33.0
355	87.5	34.0	13.0	16.0	19.0
375	87.5	13.5	26.0	30.5	8.5
405	83.0	8.7	26.0	33.7	7.0
425	66.5	7.1	12.0	37.0	3.5
450	58.5	2.1	7.0	35.5	7.0

TABLE 4

Variation of the Composition of the Reaction Products in the Conversion of Isoamyl Alcohol with Contact Time at 425°

Experimental Conditions		Condensate yield (%)	Gas composition (volume %)				Yields (in wt. % of the orig. alcohol)			
s.v.	Contact time (sec.)		CO_2	C_nH_{2n}	CO	H_2	Aldehyde	Alcohol	Diisobutyl ketone	Ester
350	10	81.5	3.9	4.0	3.5	88.5	8.0	50.0	12.3	9.7
240	15	76.0	5.0	4.3	4.4	86.0	7.9	36.0	17.0	7.3
154	23	79.5	5.0	2.6	7.0	85.2	6.1	25.0	38.0	6.8
72	50	65.0	5.3	7.8	6.0	80.5	1.8	12.6	39.5	4.9
38	97	59.0	3.9	5.7	10.4	78.5	1.8	13.0	34.0	3.8

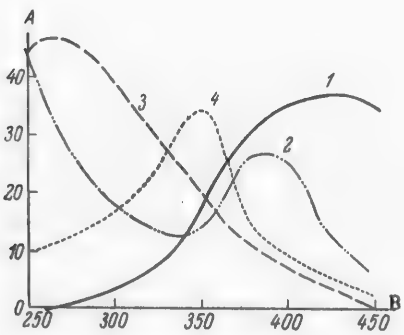

Fig. 3. Effect of temperature on the yields of ketone, aldehyde, and ester at s.v. = 150. A) Yields (in weight % of the original alcohol), B) temperature (°C). 1) Diisobutyl ketone, 2) isoamyl alcohol, 3) isoamyl isovalerate, 4) isovaleraldehyde.

TABLE 5

Physicochemical Constants of the Compounds Isolated

Compound	Boiling point (°C)		Density d_4^{20}		Refractive index n_D^{20}		Melting points of derivatives (°C)					
							Semicarbazone		2,4-dinitrophenylhydrazone		Dimethone	
	Found	Literature data	Found	Literature data	Found	Literature data	Found	Literature data	Found	Literature data	Found	Literature data
Isobutyraldehyde [7]	61—61.5	64.0	0.8007	0.7938	1.3769	1.3730	125	125—126	182.0	182.0	153.0	154
Isovaleraldehyde [7]	92—93	92.5	0.7820	0.7845	1.4058	1.39225	131.5	132.0	—	—	154.0	154—155
Isobutyl isobutyrate [7]	147.0	148.7	0.8551	$0.8752^{0°}$	1.3990	1.3999	—	—	—	—	—	—
Isoamyl isovalerate [7]	189—190	190.4	0.8570	$0.8583^{18.7°}$	1.4140	$1.4130^{18.7°}$	—	—	—	—	—	—
Diisopropyl ketone [7]	124—124.3	124.0	0.8038	0.8108	1.3996	1.4001	157	149; 160	89.0	88.0	—	—
Diisobutyl ketone [8]	165.5	165—166	0.8122	$0.8051^{21°}$	1.4120	$1.4120^{21°}$	121—122 [7]	122	92.0	92.0	—	—

SUMMARY

1. Primary isobutyl and isoamyl alcohols are converted over activated copper catalyst into esters at 250-300°, and into aldehydes at 330-350°, in yields of 45 and 25-30% respectively, calculated on the original alcohol.

2. The formation of ketones from alcohols of iso structure occurs at temperatures 100° higher than from alcohols of normal structure. The yield of diisobutylketone from isoamyl alcohol at 425-450° is 40-55%.

3. Isobutyl alcohol, with a substituted carbon atom in the α-position, can be converted into diisopropyl ketone at 425-450° with yields of 50-56%.

4. The course of the conversion of alcohols of isostructure through the aldehydes to give esters or ketones, according to the temperature conditions, confirms the earlier hypothesis of an aldol mechanism of ketone formation.

LITERATURE CITED

[1] B. A. Bolotov, P. M. Adrov, and L. K. Prokhorova, J. Appl. Chem. 28, 511 (1955). *

[2] B. A. Bolotov, B. N. Dolgov, and K. P. Katkova, J. Appl. Chem. 28, 414 (1955). *

[3] V. I. Komarewsky, and I. G. Smith, J. Am. Chem. Soc. 66, 1117 (1944).

[4] B. N. Dolgov, B. A. Bolotov, and L. A. Komissarova, J. Appl. Chem. 28, 71 (1955).

[5] B. A. Bolotov, B. N. Dolgov, and P. M. Adrov, J. Appl. Chem. 28, 299 (1955).

[6] B. A. Bolotov, and B. N. Dolgov, Authors' Claim No. 92622 (1950).

[7] E. Huntress and S. Mulliken, Identification of Pure Organic Compounds (1946).

[8] Dictionary of Organic Compounds, 1, 873 (1949).

Received July 2, 1955

* Original Russian Pagination, See C.B. Translation

STUDY OF THE CHEMICAL STABILITY AND STRUCTURE FORMATION OF CONCENTRATED VISCOSE SOLUTIONS AT ELEVATED TEMPERATURES

N. V. Mikhailov and N. N. Zavyalova

Studies of the structuro-mechanical properties of concentrated polymer solutions are of great theoretical and practical importance.

Determination of the fundamental laws determining the relationship between chemical stability, viscosity, and the ability of viscose solutions to form threads is a necessary condition for the successful conversion of cellulose in the production of artificial fibers.

A specific characteristic of cellulose xanthate solutions is the existence of a complex relationship between the properties of the concentrated solutions and the chemical processes associated with hydrolysis of the cellulose ester, which occur in them over prolonged periods.

For this reason, the task of increasing considerably the concentrations of viscose solutions, which has become of increasing practical importance in recent years in relation to increased plant productivity and to the production of super-strong hydrate cellulose fibers for technical purposes [1], cannot be successfully accomplished without elucidation of the relationship between the structuro-mechanical properties and chemical stability of concentrated solutions at various temperatures.

It is known from the literature that the stability of viscose solutions is influenced by concentrations of alkali and cellulose, the presence of side products, temperature, and other factors. Many authors [2-6] had established earlier that the highest stability of 8% viscose solutions is found at 7-9% caustic soda concentrations. In a later study [7] similar experiments were performed with 5% viscoses. It was found that with NaOH solutions from 1.5 to 7.3% concentrations the rate at which thiocarbonate groups are split off from cellulose xanthate diminishes, while above 7.3% it increases.

The rate at which thiocarbonate groups are split off also diminishes with increasing cellulose concentration in the viscose [7-9]. An increase of 10° in the temperature of viscose solutions produces a nearly 3-fold increase in the rate at which thiocarbonate groups are split off [10].

It must be pointed out, however, that all these data refer to viscose solutions containing 5-8% cellulose.

There is almost no information in the literature on studies of the stability of viscose solutions of higher concentrations, while interest in such solutions is continuously increasing. It is known that new methods have now been developed for the spinning of fibers from concentrated solutions [1], which yield hydrate cellulose fibers of exceptional fineness, 2-3 μ in diameter, and with a strength of up to 100 kg/mm^2, which is greater than the strength of any other known natural or synthetic fibers.

Earlier we performed investigations [11] to determine the possibility of decreasing the viscosity of concentrated viscose solutions. It was found that the viscosity of such solutions mostly depends on the NaOH: cellulose ratio and the degree of esterification of the cellulose. The present communication contains the results of further investigations of the influence of temperature on the viscosity and chemical stability of concentrated viscose solutions containing from 8 to 14% cellulose.

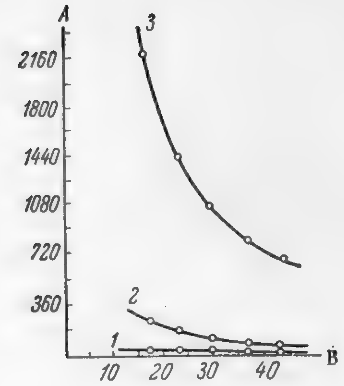

Fig. 1. Variation of viscosity of viscose solutions with different cellulose concentrations as a function of the temperature. A) Viscosity η (in poises), B) temperature (°C). Cellulose concentrations (%): 1) 8.5; 2) 10.94; 3) 13.36.

EXPERIMENTAL

Influence of temperature on viscosity of viscose solutions. Viscose solutions were prepared with different cellulose concentrations from 8 to 14%, from alkali cellulose aged for somewhat different times (16 and 19 hours). The NaOH:cellulose ratio was about 0.9. The viscosity was determined by the falling ball method with a 3 mm ball.

The variations of viscose viscosity with temperature for different cellulose concentrations are shown in Fig.1. These results were used to calculate the temperature coefficients of the viscosity of the viscose solutions, given in Table 1.

In the next series of experiments the same method was used to determine the temperature coefficients of the viscosity of viscose solutions differing in chemical stability, determined by the NH_4Cl ripeness figure. 11% viscose solutions were used for the viscosity determinations.

The results are given in Table 2.

TABLE 1

Calculated Temperature Coefficients of Viscosity of Viscose Solutions

Cellulose concentration (%)	Temperature coefficients of viscosity in temperature ranges					
	15–25°		25–35°		35–45°	
	Alkali cellulose aging times (hours)					
	16	19	16	19	16	19
13.36	—	2.00	—	1.53	—	1.38
11.19	2.0	—	1.66	—	1.38	—
10.94	—	1.85	—	1.60	—	1.38
9.40	1.75	—	1.50	—	1.43	—
8.50	—	1.73	—	1.58	—	1.42
7.30	1.52	—	1.48	—	1.40	—

TABLE 2

Calculated Temperature Coefficients of Viscosity of Chemically Stable Viscose Solutions

Viscose No.	NH_4Cl ripeness	Temperature coefficients of viscosity in temperature ranges	
		20–30°	30–40°
1	17.0	1.65	1.51
	12.5	1.52	1.23
	9.0	1.32	—
	6.0	1.42	—
2	14.5	1.58	—
	9.5	1.40	—
	6.9	1.52	—

Variation of the viscosity of viscose solutions in relation to ripeness at different ripening times. Viscose solutions containing 11% cellulose, with NaOH: cellulose ratio $\approx$ 1.0 were used.

The solutions were kept in a thermostat at 20 and 30°. Samples were taken at definite time intervals and their viscosities determined. The viscosity was determined at 20° in both cases.

The results are shown in Fig. 2.

Variation of the stability of viscose in relation to various factors. Effect of alkali concentration. Viscose solutions containing $\approx$12% cellulose and different alkali contents: 12.5, 9.7, and 7.5%, were prepared. The solutions were made simultaneously from the same cellulose xanthate.

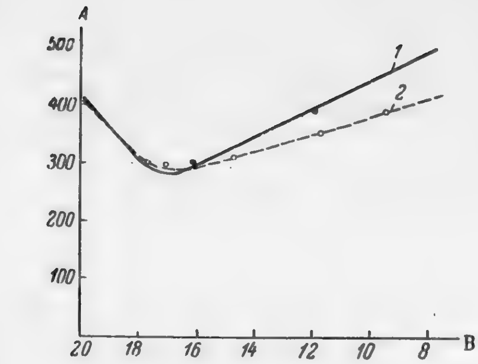

Fig. 2. Variation of the viscosity of viscose solutions with time at different temperatures.
A) Viscosity η (in sec), B) NH_4Cl ripeness.
Temperature (°C): 1) 30, 2) 20.

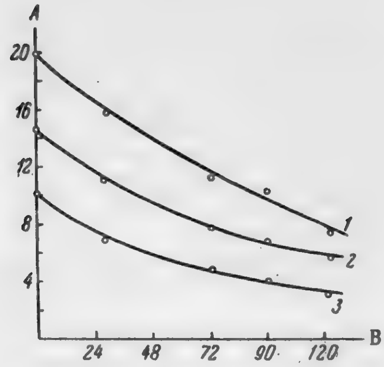

Fig. 3. Variation of the ripeness of viscose solutions (cellulose concentration 12%) with time.
A) NH_4Cl ripeness, B) time (hours).
NaOH concentration and NaOH: cellulose ratio respectively: 1) 12.6, 1.05, 2) 9.7, 0.8, 3) 7.6, 0.63.

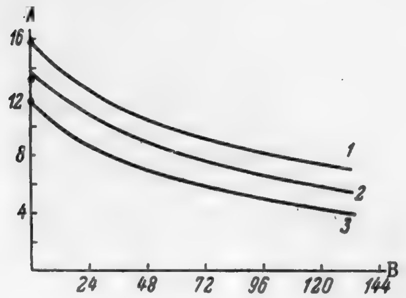

Fig. 4. Variation of the ripeness of viscose solutions (alkali concentration 8.2%) with time.
A) NH_4Cl ripeness, B) time (hours). Cellulose concentration (%) and NaOH:cellulose ratio respectively: 1) 8, 1; 2) 10, 0.8; 3) 12, 0.68.

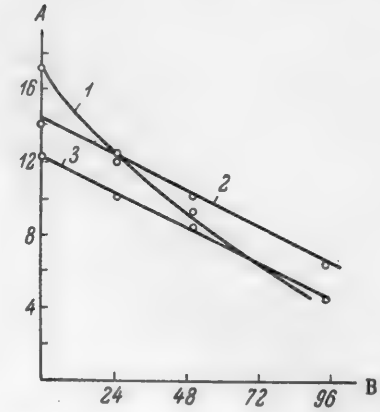

Fig. 5. Variation of the ripeness of viscose solutions (NaOH:cellulose ratio ≈ 0.6) with time. A) NH_4Cl ripeness, B) time (hours). Cellulose concentration (%): 1) 14, 2) 10, 3) 8.

The viscose solutions were kept in a thermostat for several days at 20°. Their NH_4Cl ripeness was determined every 2-4 hours.

The results are shown in Fig. 3.

<u>Influence of the NaOH:cellulose ratio.</u> Viscose solutions were prepared with equal contents of caustic soda, ≈ 8.2%, and different cellulose concentrations: 8, 10, and 12%. The viscose solutions were kept under the same conditions for several days. The results are shown in Fig. 4.

<u>Influence of cellulose concentration.</u> For these experiments viscose solutions were prepared with the same NaOH: cellulose ratio, ≈ 0.6, and with different cellulose concentrations: 8, 10, and 14, and 8, 10, and 12 % . The second series of experiments differed from the first only in that a different batch of cellulose xanthate was used. The viscose solutions were again kept for several days under the same conditions at about 20°.

The results of ripeness determinations for these viscose solutions at various times are shown in Figs. 5 and 6 respectively.

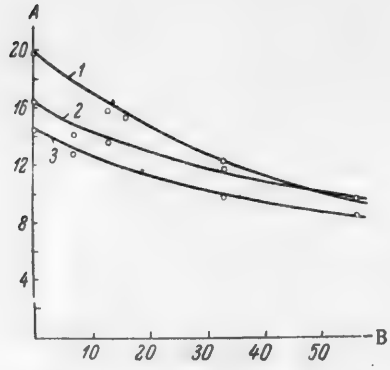

Fig. 6. Variation of the ripeness of viscose solutions (NaOH:cellulose ratio ≈ 0.6) with time. A) NH_4Cl ripeness, B) time (hours) Cellulose concentration (%). 1) 12; 2) 10; 3) 8.

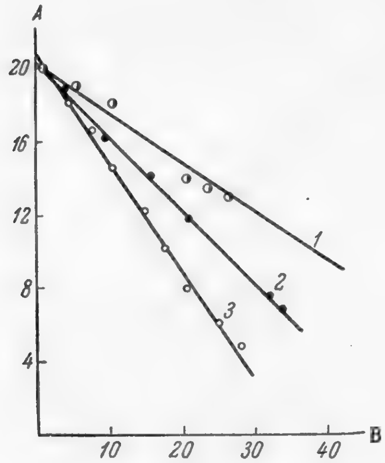

Fig. 7. Variation of the ripeness of 12% viscose with time for different temperatures. A) NH_4Cl ripeness, B) time (hours). Temperature (°C): 1) 25, 2) 30, 3) 35.

Influence of temperature on the ripeness of viscose solutions. Viscose solutions with NaOH: cellulose ratio ≈ 0.8 and cellulose concentration ≈ 12% were kept at temperatures of 25,30, and 35°. Other viscose solutions with different cellulose concentrations were kept at 30°. Their NH_4Cl ripeness was determined at intervals of several hours.

The results are shown in Figs. 7 and 8.

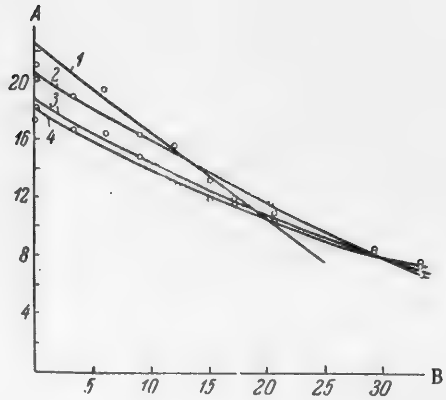

Fig. 8. Variation of the ripeness of viscoses with different cellulose concentrations at 30°, with time. A) NH_4Cl ripeness, B) time (hours). Cellulose concentration (%) : 1) 14, 2) 12, 3) 10, 4) 8.

DISCUSSION OF RESULTS

An examination of the experimental data on the variation of the viscosity of viscose solutions with temperature, and of the corresponding temperature coefficients of viscosity, shown in Fig. 1 and Table 1, indicates that an increase of temperature considerably lowers the viscosity of viscose solutions. As was to be expected, the influence of temperature on the viscosity of concentrated viscose solutions increases with the cellulose content in the solution, which provides additional confirmation of the predominant role of structure formation in the variations of the total viscosity of concentrated solutions.

This is clearly demonstrated by the curves for the variation of viscosity with temperature in Fig. 1, which show that in solutions with a cellulose content over 13% the viscosity decreases approximately from 2000 to 500 poises, and in 11% solutions only from 250 to 100 poises. However, as the temperature increases, the fall of viscosity diminishes, as shown by changes of the temperature coefficients. Their values are higher at lower temperatures and higher cellulose concentrations.

The data in Table 2 show that the temperature coefficients of viscosity also depend on the viscose ripeness. Their values as a function of the ripeness pass through a minimum.

It is seen from Table 2 that this minimum, which corresponds to the least variation of viscosity with the temperature, occurs at the region of moderate ripeness, of about 9 by the NH_4Cl index. The minimum viscosity (Fig. 2) corresponds to an NH_4Cl figure of about 17. There is thus some divergence between the region of minimum viscosity and the minimum of the temperature coefficient of viscosity in the ripeness range of viscose solutions. The existence of these minima indicates the influence of 2 opposing factors. The view had been advanced earlier [10,11] that viscose viscosity in the ripening process is influenced by xanthate solubility and structurization with the formation of a spatial network of intermolecular bonds.

The continuous solution of the xanthate results in a viscosity decrease. The increase of viscosity along the second branch of the curve is explained by the commencing aggregation.

For 8% viscoses the viscosity minimum corresponds to an NH_4Cl ripeness of 9-10. In more concentrated solutions the structurization factor predominates, and the viscosity minimum is shifted in the direction of lower ripeness (≈ 17).

On the basis of the above, the fact that the ripeness range corresponding to the viscosity minimum does not agree with the range for the temperature coefficient, may be attributed to different effects of temperature on these two factors: solubility and structure formation. The cause of the different rates of increase of the viscosity of viscose solutions during ripening is not quite clear (Fig. 2). This investigation does not provide sufficient data to explain this effect.

The results of experiments on the stability of concentrated viscose solutions, shown in Fig.3, indicate that, with equal cellulose concentrations, solutions with higher alkali concentrations are more stable. At the same time, a comparison of the curves in Fig. 3 shows that, with an equal content of caustic soda, viscoses with lower cellulose contents are more stable. These results are not quite clear at first sight. However, everything is explained if the results are examined in relation to the NaOH:cellulose ratio. Viscoses with a lower NaOH: cellulose ratio are less stable (Fig. 4). At the same time, it is known from earlier work that the amount of alkali bound with the free hydroxyl groups of the xanthate increases in proportion to the NaOH:cellulose ratio. No such relationship was found for the free alkali concentration in viscose.

Consequently, to determine the influence of cellulose concentration on the stability of spinning solutions, viscose solutions with the same NaOH:cellulose ratio were taken.

The results, shown in Figs. 5 and 6, indicate that in both cases the ripeness figure remains higher for 10% than for 8% viscoses over the whole ripening time.

Viscoses with 12 and 14% cellulose have a high ripeness figure only at a low degree of ripeness. After some time (1-2 days) the ripeness figure of these viscose solutions becomes lower than that of 8% solutions. It follows that in the spinning of viscoses with a NH_4Cl ripeness figure above 10 a longer time is required for this ripeness to be reached in viscoses with cellulose concentrations of 10-12% (with an NaOH: cellulose ratio ≈ 0.8—1). For the spinning of viscoses of greater ripeness (≈ 5—7) the optimum concentrations are 10-11%. It must be pointed out that these results refer to viscose solutions kept in a thermostat at 20°. Figure 7 shows the variations of the ripeness of viscoses with the same cellulose concentrations at 30°.

These curves show that in this case also viscose solutions with cellulose concentrations of 10-12% have higher ripeness figures over a wide ripeness range.

From the results in Fig. 8 it is seen that the same value of NH_4Cl ripeness is reached after about 17 hours at 35°, after twenty four hours at 30°, and after ~40 hours at 25°.

SUMMARY

1. The relationship between the stability of viscose solutions of high concentrations up to 14% and the viscose composition and temperature has been determined.

2. Studies of viscose solutions with high cellulose contents showed that at elevated temperatures (25-30°) a considerable decrease of structural viscosity occurs, with practically acceptable rates of change of the chemical stability of these solutions. The results indicate the possibility of using highly concentrated viscose solutions for the spinning of viscose fibers.

LITERATURE CITED

[1] N. Drish and L. Soep, Text. Research J., 23, 8, 513—521 (1953); French Patent 1023194 (19 March, '53); Bull. Inst. Text. France, 42, 128 (1953).

[2] Z. A. Rogovin, Artificial Fibers, 11, 4 (1931).

[3] A. S. Shpitalnyi and A.I. Meos, Artificial Fibers, 5-6, 5 (1932).

[4] E. Heuser and M. Schuster, Cellulosechemie, 7, 10, 137 (1926).

[5] T. Lieser, Ann., 464, 43 (1928).

[6] D ' Ans and Jager, Kunstseide, 8, 17 (1926).

[7] A, Matthes, Faserforschung and Textiltechnik, 4, 127 (1952).

[8] S. M. Lipatov, Koll.-Z., 49, 441 (1929).

[9] V. I. Sharkov, Chemistry of Viscose, United Sci. Tech. Press, 147 (1935).

[10] N. N. Zavyalova, Candidate's Dissertation, Leningrad Text. Inst. (1952).

[11] N. V. Mikhailov, N. N. Zavyalova, Artificial Fibers, 6, 89 (1954) ; J. Appl. Chem., 29, 1,97 (1956).*

Received May 17, 1955.

---

* Original Russian pagination. See C. B. Translation.

INFLUENCE OF METAL IONS ON THE PROPERTIES OF ETHYLCELLULOSE

COMMUNICATION V. THE QUANTITY OF CARBOXYL GROUPS IN ETHYLCELLULOSE AND THEIR INFLUENCE ON THE MECHANICAL PROPERTIES

O. G. Efremova, I. K. Kosyreva, A.F. Kondrashova, and S.A.Glikman

The changes in the elastico-viscous characteristics of ethylcellulose gels, and in some other properties, which occur when small amounts of metal oxides or salts of weak acids are introduced into the composition of ethyl cellulose, were tentatively attributed in our previous publications to interaction of these compounds with the carboxyl groups of ethylcellulose [1]. This hypothesis was in agreement with the reports found in the literature concerning the existing relationships between the carboxyl group contents of cellulose derivatives, the increase of viscosity of ethylcellulose [2] and acetylcellulose [3], and the rate of gelation of nitrocellulose lacquers [4] on addition of oxides and salts of metals.

However, this explanation of the mechanism of the action of metal ions introduced into ethylcellulose required direct confirmation. This could be provided by comparative data for ethylcelluloses differing only in their carboxyl group contents, with the same degree of polymerization and the same ethoxyl number.

Production samples of ethylcellulose often differ fairly appreciably in their degree of oxidation, but, as our investigations showed, the increase in the number of carboxyl groups during oxidation is accompanied by partial decomposition of the molecules, leading to a decrease of the average degree of polymerization. We did not succeed in obtaining ethylcellulose preparations suitable for comparative studies by additional chemical treatment of prepared samples. For example, by oxidation of ethylcellulose in acetone solution by potassium permanganate in presence of sulfuric acid, we obtained a product with a somewhat increased carboxyl group content, but the intrinsic viscosity fell considerably: from 1.68 to 0.96.

Better results were obtained by carboxymethylation of ethylcellulose. The reaction of carboxymethylated cellulose formation has been studied in detail by Danilov and Krestinskaya [5]. We carried out the carboxymethylation of ethylcellulose by the method developed by Evans and Spurlin [2], which consists of the interaction of ethylcellulose dissolved in a mixture of benzene and methanol with monochloroacetic acid. The reaction is carried out in an alkaline medium produced by addition of a solution of metallic sodium in methyl alcohol to the reaction mixture. As the result of carboxymethylation the molecular weight of the ethylcellulose remained almost unchanged, but the number of carboxyl groups greatly increased. By introduction of equal amounts of $Ca(OH)_2$ into the original and carboxymethylated ethylcelluloses we were able to determine the changes in the elastico-plastic properties of both preparations.

The methods used for the preliminary treatment of the ethylcellulose, ash removal, introduction of calcium hydroxide (0.2% on the weight of ethylcellulose), preparation of solutions and gels, and determination of solution viscosities and elastico-viscous properties of the gels did not differ from those described in our previous communications [1].

Two methods were used for carboxyl group determination in the ethylcellulose, which gave concordant results (within 5-10%) : a) titration of acetone solutions by 0.05 N aqueous NaOH solution with thymolphthalein indicator, b) reaction with barium o-nitrophenate. In both cases the samples for analysis were very carefully de-ashed by threefold precipitation from aqueous acetone solutions containing 0.2% HCl, with subsequent washing to remove Cl^- ions and check determinations of the latter by a mercurimetric method [6].

The reaction with barium o-nitrophenate was used by Malm and his associates [3] for determination of carboxyl groups in acetylcellulose. As ethylcellulose does not swell in aqueous barium o-nitrophenate, we were obliged to modify this method somewhat, using aqueous acetone solutions of ethyl cellulose. In view of the fact that the fractions of lowest molecular weight were dissolved in the process, ultrafiltration was used.

TABLE 1

Carboxyl Group Contents of Ethylcellulose Samples

Sample	Intrinsic viscosity (η)	Carboxyl group content (in microequivalents per 1 g ethylcellulose)	Number of monomer units per 1 carboxyl group
I	2.00	40	111
II	1.66	50	87
III	0.96	85	55
IV	0.88	100	43

Table 1 gives data on the carboxyl group contents of several ethylcellulose samples.

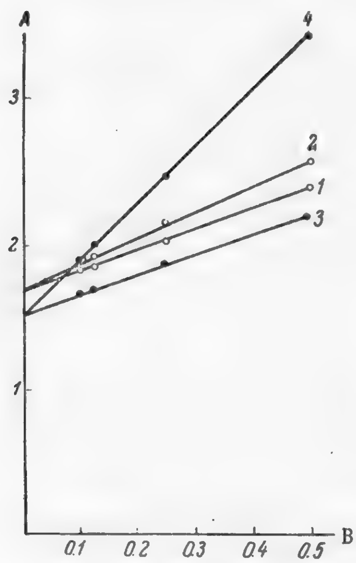

Fig. 1. Variation of the viscosity of ethylcellulose solutions in alcohol–benzene mixture (1:4) with the concentration. A) Reduced viscosity η_{sp}/c, B) concentration c(in g/ 100 ml). 1) Sample II, 2) sample II treated with calcium hydroxide, 3) sample II, carboxymethylated, 4) sample II, carboxymethylated and treated with calcium hydroxide.

The preparation of sample III differed from that of I and II by a longer period of alkali cellulose aging; sample IV was prepared with the use of hot mercerization. Thus, an increase of the aging time and mercerization temperature not only yields a low-viscosity ethylcellulose, but the product contains a higher number of carboxyl groups than usual.

Sample II, the characteristics of which are given in Table 1, was carboxymethylated as described above. The average number of carboxyl groups in its molecules was thereby increased to one carboxyl group per 30 anhydroglucose units (as against 1:87 in the original substance). Both samples, the original (II) and the carboxymethylated (II^{cm}), were treated with calcium hydroxide under the same conditions, to give samples II_{Ca} and II^{cm}_{Ca}.

Figure 1 shows the variation of the reduced viscosity of solutions of all four samples in alcohol—benzene mixture (1:4) with the concentration.

It is seen that carboxymethylation resulted in a slight decrease of the intrinsic viscosity (to give $[\eta] = 1.52$ as compared with $[\eta] = 1.66$ for the original sample) but did not affect the slope of the $\eta_{sp}/c = f(c)$ lines. Treatment with calcium hydroxide, on the other hand, increased the slope of the viscosity—concentration plot without affecting the intrinsic viscosity. These results characterize the nature of the processes a) of the partial decomposition of ethylcellulose molecules during carboxymethylation, accompanied by oxidation , and b) of increased intermolecular interaction after replacement of hydrogen in the carboxyl groups by calcium. The role of this factor is more prominent for sample II^{cm}_{Ca}, with a higher carboxyl group content. This is characterized quantitatively by increase of the $k' = \frac{\eta_{sp}/c - [\eta]}{[\eta]^2 c}$ from 0.55 to 0.67 for the original sample, and from 0.61 to 1.75 for the carboxymethylated sample (Table 2). This is also supported by the elastico-viscous characteristics of 12% ethylcellulose gels with dibutyl phthalate.

The data in Table 2 show that introduction of Ca^{++} ions into ethylcellulose results in a considerable increase of all the elastico-viscous characteristics. However, in the case of carboxymethylated ethylcellulose containing more carboxyl groups, Ca^{++} ions have a greater effect. For example, the elastic modulus is increased 2.5-fold, while for the original sample the increase is only 1.5-fold, the relaxation viscosity is increased 40-fold (as against an 8-fold increase for the original sample), and the elastic limit is increased 7-fold (as against 2.5-fold for the original sample).

TABLE 2

Elastico-Viscous Characterists of Ehylcellulose Samples

Sample	Number of anhy-droglucose units per 1 carboxyl group	Intrinsic viscosity [η]	k'	$E_1 \cdot 10^{-3}$ (dynes/cm^2)	$E_2 \cdot 10^{-3}$ (dynes/cm^2)	$\eta \cdot 10^{-5}$ (poises)	$\eta_2 \cdot 10^{-6}$ (poises)	P_c (dynes/cm^2)
II	87	1.66	0.55	11.9	0.8	0.3	0.5	70
II_{Ca}	87	1.66	0.67	17.9	2.3	2.3	1.4	166
II^{cm}	30	1.52	0.61	14.3	1.2	1.2	0.3	110
II^{cm}_{Ca}	30	1.52	1.75	35.8	6.4	50.0	1.2	800

These quantitative relationships can hardly be explained other than by the interaction of carboxyl groups of ethylcellulose with calcium hydroxide: the gel structure becomes stronger and the solution viscosity higher with increase in the number of calcium ions bound by the carboxyl groups.

It is seen that the elasticity characteristics and the relaxation viscosity of carboxymethylated ethylcellulose gels (without calcium) are higher than those of the original sample, while the intrinsic viscosity of the carboxymethylated sample is lower than that of the original. This can also be attributed to differences in the carboxyl group content. Hydrogen bonds between the carboxyl groups of polymer molecules strengthen gel structure. However, this structure is strengthened still more after introduction of calcium ions into the carboxyl groups, as the energy of R—COO—Ca—OOC—R ionic bonds is higher than the energy of hydrogen bonds.

As is known, the usual mineral impurities in ethylcellulose are present not only as metal oxides, but also as salts, including chlorides.

It is reported in the literature [7] that calcium salts with different anions have different effects on the properties of acetylcellulose solutions. Addition of $Ca(CH_3COO)_2$ results in gelation of the solution, while $CaCl_2$ and $Ca(NO_3)_2$ produce only slight viscosity increases. However, we found no such reports in the literature with reference to ethylcellulose.

In order to clarify this problem we de-ashed a production sample of ethylcellulose (ethoxyl number 48.5% [η] = 1.50, carboxyl group content 50 microequivalents per 1 g ethylcellulose) and converted it into samples containing various metal oxides and salts. The metallic compounds were introduced in quantities corresponding to 0.007 g-equiv. of metal per 100 g ethylcellulose, or approximately 1.5 g-equiv. of metal per 1 g-equiv. carboxyl groups. The methods of de-ashing and introduction of metal compounds were the same as previously used [1].

It was found that the viscosity of alcohol—benzene solutions (1:4) and the intrinsic viscosity of the samples so obtained did not differ from the values for the de-ashed sample. The probable explanation is that total solvation of hydroxyl and carboxyl groups by the polar solvent takes place in the mixture of a polar and nonpolar solvent, preventing formation of ionic bonds and increase of viscosity.

For investigation of the elastico-plastic properties of ethylcellulose gels with dibutyl phthalate we used the Rebinder and Veiler method [8], observing a number of special conditions described in the previous communications [1]. However, the elastic limit of gels made from ethylcellulose containing chlorides,

and also from ashless ethylcellulose, was close to the shearing stress set up by the plate (70 dynes/ cm^2). Therefore, in such cases a somewhat different procedure was used for determinations of the elastico-plastic constants. The cell with the gel was placed on the raising table of the instrument 12-16 hours before the experiment, and the plate was attached to the dynamometer spring and balanced by an appropriate extension of the spring. The deformation of these gels was determined at three different shearing stresses, with progressive increases to the stress but without interruption of the experiment. As a result, stepwise curves were obtained which represented the kinetics of gel deformation at different shearing stresses.

Fig. 2. Deformation kinetics of 12% gel of a de-ashed ethylcellulose sample at different shearing stresses. A) Deformation E (in cm), B) time τ (in min.). Shearing stresses (in dynes/cm^2): 1) 107, 2) 160, 3) 214.

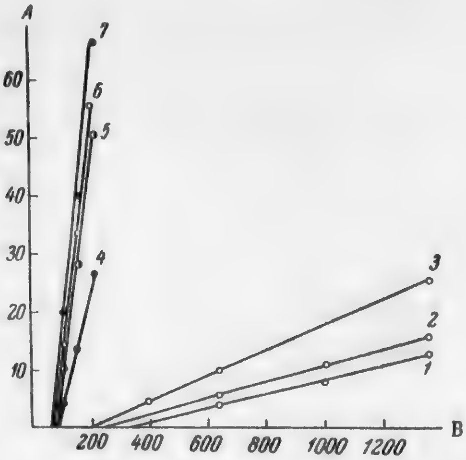

Fig. 3. Dependence of steady flow rate on shearing stress for 12% ethylcellulose gels in dibutylphthalate. A) Steady flow rate $\frac{\Delta\epsilon}{\Delta\tau} \cdot 10^4$ (cm/sec.) B) shearing stress P (dynes/cm^2). Metal compounds added: 1) $Ca(OH)_2$, 2) $NiC_2H_3O_2$, 3) NaOH, 4) $CaCl_2$, 5) NaCl, 6) no addition, 7) $NiCl_2$.

In illustration, Figure 2 shows the deformation kinetics of a 12 % gel of a de-ashed ethylcellulose sample at different shearing stresses. The elastic limit was determined, as usual, by extrapolation to the abscissa axis of straight lines drawn through points corresponding to the steady flow rates at various shearing stresses (Figure 3).

The data on the deformation kinetics and elastic limits were used to calculate the elastico-viscous characteristics of the gels, which are given in Table 3.

TABLE 3

Elastico-Viscous Characteristics of 12% Ethylcellulose Gels with Dibutyl Phthalate (Temperature 22°)

Metal compounds added to ethylcellulose	$E_1 \cdot 10^{-3}$ (dynes/cm^2)	$E_2 \cdot 10^{-3}$ (dynes/cm^2)	η_1 10^{-5} (poises)	$\eta_2 \cdot 10^{-5}$ (poises)	P_c (dynes/cm^2)
	12.0	1.0	0.25	0.17	73
NaCl	12.0	1.3	0.27	0.17	80
$CaCl_2$	12.0	1.2	0.53	0.17	85
$NiCl_2$	9.0	0.7	0.22	0.19	64
NaOH	18.0	0.9	4.5	0.9	200
$Ca(OH)_2$	43.0	6.0	7.4	3.3	375
$Ni(CH_3COO)_2$	35.9	2.3	6.8	1.8	250

It follows from the results in Table 3 that the nature of the influence of the electrolytes added to ethylcellulose depends not only on the cation but also on the anion. Salts of a strong acid ($NaCl$, $CaCl_2$, and $NiCl_2$) have almost no effect on the elastico-viscous properties of gels. However, addition of a salt of a weak acid – $Ni(CH_3COO)_2$, or bases, $NaOH$ and $Ca(OH)_2$, results in fairly considerable increases in all the elastico-viscous constants. Thus, the elastic limit is increased 3 to 5-fold, the relaxation viscosity 15 to 30-fold, and the elasticity modulus 1.5 to 3-fold.

These differences in the action of electrolytes can be explained as follows. It seems that interaction of $Ca(OH)_2$ and $Ni(CH_3COO)_2$ with carboxyl groups of ethylcellulose results in the formation of cross bonds which strengthen the gel structure. Sodium hydroxide, as was reported earlier [1] also, although to a lesser extent, increases the elastico-viscous constants of the gels. However, on addition of chlorides of these metals, the "weak cellulosic acid" (a term proposed by Heymann and Rabinov [9]) does not displace the strong hydrochloric acid from its salts, and therefore they do not have any appreciable effect on the elastico-plastic properties of the gels.

It should be noted that metal oxides effect not only the elastico-viscous characteristics of ethylcellulose gels, but also the properties of ethylcellulose films prepared by the usual method from 8% solutions in alcohol–benzene mixture. For example, the addition of 0.1% of $Ca(OH)_2$ or $Fe(OH)_3$ on the weight of the polymer to ethylcellulose raised the average tensile strength values from 627 kg/cm^2 (for the ashless sample) to 745 and 723 kg/cm^2 (for samples containing calcium and iron). However, the brittleness of the films was also increased: the number of flexures to failure fell from 3100 to 1230 and 1450 respectively.

SUMMARY

1. Two methods, giving concordant results, have been used for carboxyl group determinations in ethylcellulose samples. It was found that different ethylcellulose samples may have different carboxyl group contents according to the preparation conditions; for example, from one group per 43 monomer units in the ethylcellulose molecular chain to one group per 111 units.

2. It was shown that carboxymethylation of ethylcellulose results in an increase of the carboxyl group content, a slight increase of intrinsic viscosity, and an increase of the elastico-viscous constants of the gels.

3. Addition of small amounts of calcium hydroxide to carboxymethylated ethylcellulose results in considerably greater increases in the elastico-viscous characteristics of the gels than are produced by analogous treatment of the original ethylcellulose.

4. It was found that, in contrast to the action of metal oxides and salts of weak acids, chlorides have no appreciable influence on the elastico-plastic properties of ethylcellulose gels.

5. Addition of metal hydroxides to ethylcellulose influences the properties of ethylcellulose films, increasing their tensile strength and decreasing the number of bends to failure.

6. The characteristics of the variations in the mechanical properties of ethylcellulose and carboxymethylated ethylcellulose are in agreement with the data obtained on the contents of carboxyl groups and various metal compounds in the samples studied.

LITERATURE CITED

[1] O. G. Efremova and S. A. Glikman, Proc. Acad. Sci. USSR, 81, 1089 (1951); J. Gen. Chem., 24, 1427 (1954).*

[2] E. Evans and H. Spurlin, J. Am. Chem. Soc., 72, 4750 (1950).

[3] G. Malm, L. Tanghe, G. Smith, Ind. Eng. Chem., 42, 730 (1950).

[4] H. Campbell and P. Johnson, J. Polym. Sci. 3, 735 (1948).

[5] S. Danilov and N. Krestinskaya, Plastics, 4, 6 (1933).

[6] L. N. Lapin and R. Kh. Zamanov, Hygiene and Sanitation, 10 (1954).

* Original Russian pagination. See C. B. Translation.

[7] S. Danilov, Yu. Goldfarb, E. Zaitseva, J. Appl. Chem., 12, 85 (1939).

[8] S. Veiler and P. Rebinder, Proc. Acad. Sci. USSR, 49, 354 (1945).

[9] E. Heymann and G. Rabinov, J. Phys. Chem., 45, 1152 (1941).

Received July 11, 1955

NONIONIC SURFACE-ACTIVE AGENTS FROM THE PRODUCTS OF CHEMICAL PROCESSING OF PETROLEUMS AND TARS DERIVED FROM COAL AND SHALE

N. D. Gadaskina, D. M. Rudkovsky, and E.Ya. Yarzhemskaya

Because of their wetting, emulsifying, and detergent properties, surface-active agents are used in the most diverse branches of industry. Thus, they are widely used in the textile industry in the processing and dyeing of wool, cotton, and artificial fibers. The efficient application of various economic poisons in agriculture is made possible by the use of surface-active agents. Surface-active agents are used in the petroleum industry in drilling and petroleum production; for improving the specific properties of oils, greases, anticorrosion additives; for emulsion breaking, froth prevention, and many other purposes. Processes of ore and coal flotation are based on the use of surface-active substances.

This far from complete list shows that it is necessary to adopt existing syntheses of surface-active substances widely in industry, and also to intensify in every way the further development of new syntheses.

Moreover, in our view, it is necessary to popularize surface-active agents extensively and to carry out special laboratory investigations relating to the suitability of different samples or groups of surface-active substances for various branches of industry.

As is known, surface-active substances may be ionic or nonionic.

Nonionic surface-active substances are mainly made by condensation of organic compounds containing active hydrogen atoms, with ethylene oxide. The hydrophobic part of the molecule consists of an alcohol, phenol, acid, amide, etc. residue, and the hydrophilic part, of a polyethylene oxide chain of any length. These wide possibilities for varying the composition make it possible to synthesize a variety of nonionic surface-active substances with different physicochemical properties.

Intermediates for the main processes for the production of surface-active agents can be obtained by the chemical conversion of petroleum and tars derived from coal and shale. For example, synthetic phenol is obtained together with ketones by oxidation of alkyl benzenes. In addition to synthetic phenol, cresols and xylenols obtained from coal and shale tars may be used. For alkylation of phenol and its homologs any sources of unsaturated hydrocarbons may be used, namely: polymers of propylene and butylenes, petroleum cracking fractions, shale oil and synthol process fractions, and light fractions from contact coking.

The production of primary alcohols of various molecular weights from unsaturated hydrocarbons, carbon monoxide, and hydrogen (the Oxo process) can also be based on appropriate fractions of any products rich in unsaturated hydrocarbons. The incomplete oxidation of paraffinic hydrocarbons may serve as a source of alcohols.

Fatty acids of different molecular weights are obtained by extensive oxidation of paraffinic hydrocarbons and by oxidation of aldehydes from the Oxo process. In addition to fatty acids, natural naphthenic acids ("asidols") may be used as starting materials for the synthesis of nonionic surface-active agents.

The present investigation was carried out in collaboration with the Institute of Petroleum of the Academy of Sciences USSR, for the purpose of selecting surface-active agents which improve the oil-removing properties of the water pumped into the stratum.

Other aims and directions developed as the work progressed. As a result, a considerable number of syntheses and tests of surface-active agents were performed. The starting materials were both technical products widely used in industry, and products new in our industry, the adoption of which is now only beginning.

The properties of the surface-active agents were evaluated by determinations of the surface tension of aqueous solutions of these substances at the solution–air interface and at the interface with vaseline oil, contact angles at a paraffin wax surface, tendency to foam formation, and foam stability.

The condensation products of ethylene oxide and fractions of technical phenols (previously alkylated and nonalkylated), alcohols, and acids were synthesized and tested. The methods of phenol alkylation and condensation with ethylene oxide (oxyethylation) and the results of the tests are described below.

In our opinion the results are of interest both to the various possible users of surface-active substances and to those who deal with sources of raw materials which might be used for the syntheses.

EXPERIMENTAL

Alkylation of technical phenols. The alkylation of phenol by unsaturated hydrocarbons is a well known reaction, frequently described in the literature and used in industry. This reaction proceeds in presence of acid catalysts, metal chlorides, and boron fluoride.

The process is somewhat more complicated in the alkylation of technical phenol fractions containing cresols and xylenols. Because of the orienting influence of the hydroxyl group, which directs substituents mainly into the para position, and possibly "steric hindrance" also, not all the components of cresol—xylenol fractions can be alkylated. As a result, the yields of alkylated products are somewhat lower than in the alkylation of phenol.

A flask fitted with a thermometer, stirrer, and separating funnel was used for the laboratory syntheses. When sulfuric acid was used as catalyst, the phenol fraction and the fraction containing unsaturated hydrocarbons were charged into the flask. The acid (94% concentration) was added gradually, the temperature not being allowed to rise above 30°. After the acid had been added, the reaction mixture was stirred for 3 hours at 20°. The amount of acid was 0.3-0.4 mole per 1 mole of phenol. The molar ratio of phenols to unsaturated hydrocarbons was 1:1. When benzenesulfonic acid was used as catalyst, the phenol fraction and the catalyst in 1:0.15 molar ratio were charged into the flask. The hydrocarbons were slowly added from the separating funnel at 80-85°. At the end of the addition the temperature was raised to 110° and the mixture was stirred for 4-5 hours. The molar ratio of phenols to unsaturated hydrocarbons was 1:1.5. In both cases the mixture was washed with water at the end of the reaction until the acid reaction disappeared, and the saturated and unreacted unsaturated hydrocarbons were distilled off under vacuum.

Condensation with ethylene oxide. The molecule of a nonionic surface-active agent is hydrated on contact with water and becomes soluble as the result of hydrogen bond interaction between water molecules and the ether oxygen atoms of the polyethylene glycol chain. An optimum ratio between the hydrophobic and hydrophilic part of the molecule exists for every such compound. If the amount of ethylene oxide is insufficient, the condensation products have poor solubility in water; with excess ethylene oxide the condensation products usually have somewhat decreased surface-active properties.

The condensation with ethylene oxide was carried out in a flask fitted with a bubbling device for ethylene oxide, a thermometer, condenser, and stirrer. The starting compound and the catalyst (2-3% of NaOH in the form of 50% solution) were charged into the flask and heated to 180-200° in a stream of nitrogen with stirring until water was completely removed. Gaseous ethylene oxide was then fed into the reaction mixture at at definite rate from a steel cylinder. The unreacted ethylene oxide was condensed in a spiral trap immersed in ice and salt, and then entered a wash bottle where it was combined with sodium bisulfite solution.

After the required amount of ethylene oxide had been added, the reaction mixture was cooled in a stream of nitrogen. The amount of ethylene oxide which reacted was estimated from the increase in weight of the starting compound.

Condensation products of alkyl-phenols with ethylene oxide. Phenol fractions isolated from Baltic shale and Cheremkhovo coal tars were condensed with ethylene oxide in order to obtain analogs of OP-7. * It was shown that light fractions of technical phenols yield less effective surface-active agents than those obtained from heavy fractions (Table 1). This was to be expected, as the number of side chains, and to some extent also their length, is less in the light than in the heavy technical phenols.

TABLE 1

Properties of Aqueous Solutions of Oxyethylated Fractions of Technical Phenols

Designation of synthesis product	Boiling range of phenol fraction (° C)	Surface tension (in dynes/cm) of solutions of 0.01% (I) and 0.1% (II) concentration at boundary with				Contact angle of 0.10% solution	Foam numbers of 0.10% solution (in ml) **
		Air		Vaseline oil			
		I	II	I	II		
Comm'l OP-7 sample	—	63.3	36.7	16.7	4.4	55	485
$CP_{124}E_{11}$ *	50—95 (6)***	62.6	51.4	32.6	14.7	—	50
$CP_{127}E_{8}$	95—130 (6)	63.1	45.5	38.9	15.7	—	20
$CP_{156}E_{10}$	130—175 (8)	60.4	42.2	26.7	9.4	—	150
$SP_{130}E_{9}$	34—91 (1)	69.0	55.9	—	—	80	0
$SP_{143}E_{9}$	91—104 (1)	67.9	55.4	—	—	—	0
$SP_{154}E_{8}$	104—140 (1)	66.3	45.2	—	—	77	48
$SP_{170}E_{8}$	140—155 (1)	64.9	40.4	22.5	8.4	66	330

* CP—coal tar phenols; SP—shale phenols; subscripts to P—molecular weights of the phenols; E—ethylene oxide; subscripts to E—moles of ethylene oxide per 1 mole of phenol.

** Foam unstable.

*** Figures in parentheses represent residual pressures in mm Hg.

In view of the fact that the presence of long side chains in phenols increases the surface activity of oxyethylation products, the light technical phenols from coal tar, consisting mainly of cresols and xylenols, were alkylated by unsaturated hydrocarbons of synthol process fractions, propylene trimers, and cracking process fractions. The alkylated products were condensed with ethylene oxide.

Comparative tests of aqueous solutions of the synthesized products and OP-7 (Table 2) show that light technical phenol fractions after alkylation with unsaturated hydrocarbons of various origins, containing 8-12 carbon atoms, yield entirely satisfactory starting materials for the synthesis of nonionic surface-active agents. These products are chracterized by low surface tension of their aqueous solutions at the interface with vaseline oil.

Heavier phenol fractions may be used for direct oxyethylation. Although the surface-active agents so obtained are less effective than those obtained as the result of alkylation, their production is much simpler because the alkylation stage is eliminated. A characteristic property of oxyethylated heavy phenol solutions is their ability to give stable emulsions.

* OP-7 is a nonionic surface-active agent synthesized on a phenol basis. It is widely used in the textile industry. It was used in the present investigation as a standard of comparison with the analogous substances synthesized from technical products.

TABLE 2

Properties of Aqueous Solutions of Condensation Products of Alkylated Technical Pehnols with Ethylene Oxide

Designation of synthesis product	Alkylation catalyst	Surface tension (in dynes/cm) of solutions of 0.1% (I) and 0.1% (II) concentration at boundary with				Contact angle of 0.10% solution	Foam numbers of 0.10% solution (in ml)	
		Air		Vaseline Oil			Immediately	After 8 min.
		I	II	I	II			
Comm'l OP-7 sample	—	63.3	36.7	16.7	4.4	55	485	485
C $ACPE_{10}$ **	H_2SO_4	61.1	36.6	14.6	4.9	58	530	520
C $ACPE_8$	*	57.8	37.8	17.4	5.0	60	355	20
C $ACPE_8$	H_2SO_4	56.6	37.8	13.9	6.8	59	270	0
T $ACPE_8$	H_2SO_4	58.3	34.4	12.1	2.5	60	505	500
C $ACPE_9$	H_2SO_4	56.1	38.8	10.2	2.6	57	435	30
S $ACPE_9$	H_2SO_4	58.9	36.7	13.6	3.6	52	540	0
S $ACPE_8$	*	51.1	38.9	18.3	6.7	62	475	0

*Benzenesulfonic acid

**The first letter in the designation is the initial of the alkylating component: C—cracking process fraction, T—trimer of propylene, S—shale oil benzine. ACP and ASP are alkylated coal and shale phenols. E is ethylene oxide; subscripts to E —moles of ethylene oxide per 1 mole of alkylated phenols.

TABLE 3

Properties of Aqueous Solutions of Condensation Products of Oxo Synthesis Alcohols with Ethylene Oxide

Designation of synthesis product A_nE_m*	Starting material for alcohol synthesis	Surface tension (in dynes/cm) of solutions of 0.01(I) and 0.1%(II) concentration at boundary with				Contact angle of 0.10% solution	Foam numbers of 0.10% solution (in ml)	
		Air		Vaseline oil			Immediately	After 3 min.
		I	II	I	II			
A_7E_8	Synthol	63.1	51.3	32.1	20.0	—	0	0
A_9E_8	Synthol	60.4	38.5	25.1	10.3	—	560	0
$A_{10}E_8$	Synthol	51.0	30.0	21.1	9.8	44	500	250
$A_{10}E_8$	Shale tar	51.0	30.0	25.1	9.1	44	500	50
$A_{10}E_8$	Cracking products	52.8	31.1	21.9	10.1	52	500	40
$A_{11}E_8$	Synthol	51.1	30.0	—	—	43	525	375
$A_{11}E_9$	Shale tar	51.6	30.5	—	—	45	525	360
$A_{12}E_{10}$	Cracking products	55.5	32.2	20.1	8.0	55	485	200
$A_{13}E_{12}$	Cracking products	50.5	32.2	14.4	5.9	50	520	520
$A_{14}E_9$	Cracking products	50.5	32.8	13.8	5.6	50	540	540
$A_{15}E_{16}$	Cracking products	64.4	42.2	—	—	—	520	520
$A_{16}E_{16}$	Cracking products	58.9	37.2	—	—	—	510	510

* An represents an alcohol containing an average of a carbon atoms in the chain; E_m represents m molecules of ethylene oxide per 1 mole alcohol.

Condensation products of Oxo synthesis alcohols with ethylene oxide. Primary alcohols obtained by the Oxo process (by addition of carbon monoxide and hydrogen to a molecule of an unsaturated hydrocarbon) yield effective surface-active agents on condensation with ethylene oxide (Table 3). As the alcohol molecule increases from $C_7H_{15}OH$ to $C_{18}H_{37}OH$, the amount of ethylene oxide per 1 mole of alcohol required to give water-soluble products must be increased. The substances obtained from alcohols containing from 10 to 14 carbon atoms are the most effective.

The origin of the alcohol has no appreciable influence on the quality of the oxyethylation products, although there is some decrease in the effectiveness with increased branching of the carbon chain (compare the products of cracking with those from synthol or shale).

Table 4 contains data on the influence of the amount of ethylene oxide in the molecule on the properties of the surface-active agents.

TABLE 4

Properties of Aqueous Solutions of Condensation Products of Decyl Alcohols with Various Amounts of Ethylene Oxide

Designation of synthesis products A_nE_m *	Surface tension (in dynes/cm) of solutions of 0.01% (I) and 0.1% (II) concentration at boundary with				Contact angle of 0.1% solution	Foam numbers of 0.10% solution (in ml)	
	Air		Vaseline oil			Immediately	After 3 min.
	I	II	I	II			
$A_{10}E_5$ **	46.9	27.0	21.8	7.8	86	500	490
$A_{10}E_8$	51.4	28.4	23.2	7.8	88	500	200
$A_{10}E_{24}$	57.8	43.6	—	—	77	200	20

* Designations as in Table 3.

** 1% aqueous solution of $A_{10}O_5$ is strongly opalescent.

TABLE 5

Properties of Aqueous Solutions of Condensation Products of Acids with Ethylene Oxide

Designation of synthesis products X_nE_m *	Origin of acid	Surface tension (in dynes/cm) of solutions of 0.01% (I) and 0.1% (II) concentration at boundary with				Contact angle of 0.10% solution	Foam nos. ** of 0.10% soln. (in ml)
		Air		Vaeline Oil			
		I	II	I	II		
X_6E_{13}	Secondary products of Oxo Synthesis	64.2	49.7	—	—	73	40
X_7E_{13}		61.5	46.5	30.2	18.8	—	0
X_8E_{15}		51.3	38.5	—	—	—	50
$X_{10-17}E_9$	From oxidized paraffin (factory sample)	61.6	41.1	24.0	9.0	67	150
$X_{18}E_{20}$	Chemically pure sample	69.0	40.7	21.6	10.9	—	130
AsE_5	From T_1 fuel	55.6	36.9	20.0	—	55	200

* X_n is an acid with an average of n carbon atoms in the chain. E_m represents m molecules of ethylene oxide per 1 mole acid; As is Asidol.

** Foam unstable

Aqueous solutions of polyoxyethylene ethers of aliphatic alcohols are characterized by low surface tension at the air interface and low contact angles, especially if there is little branching in the carbon chain.

Condensation products of acids with ethylene oxide. The condensation products of Oxo process fatty acids, stearic acid, acids obtained by oxidation of paraffins, and naphthenic acids ("asidols") with ethylene oxide were synthesized.

The physicochemical properties of these substances indicate that their surface activity is relatively low (Table 5). However, the condensation product of asidol with ethylene oxide is more active than analogous products derived from fatty acids.

Relatively small amounts of ethylene oxide are sufficient for the formation of water-soluble surface-active substances from naphthenic acids.

A characteristic property of solutions of surface-active substances synthesized from fatty acids is the almost complete absence of foaming. Exploratory laboratory experiments showed that these solutions may in some instances be used as antifoaming agents.

SUMMARY

1. Investigations of nonionic surface-active agents have shown that oxyethylated alkyl phenols obtained from technical products are similar to the commercial product OP-7 in their surface-active properties.

2. It is shown that oxyethylated C_{10-14} alcohols obtained by the Oxo synthesis have effective wetting properties.

Received August 4, 1955

PRODUCTION OF ADHESIVE UREA-FORMALDEHYDE RESINS

R.Z. Temkina

Chemical Laboratory of the Central Scientific Research Institute for Plywood and Furniture

The ability of urea to condense with formaldehyde is widely used in technology for the production of resins for various purposes. The use of urea-formaldehyde resins as adhesives in plywood production is based on their fairly high adhesive power and the possibility of their conversion into an infusible and insoluble state both by heating and at normal temperatures. The qualities required in adhesive urea-formaldehyde resins do not essentially differ from the qualities required, for example, in adhesive melamine-formaldehyde and urea-melamine-formaldehyde resins [1]. The advantage of urea-formaldehyde resins lies in the availability of the raw materials and in their more rapid hardening in comparison with phenol-formaldehyde resins of the resole type.

The condensation reaction of urea with formaldehyde has been studied in greatest detail in relation to the needs of the plastics and coatings industries. Since adhesive urea-formaldehyde resins differ substantially from resins used for coatings and molded articles in the plastics industry, the conditions for the production of adhesive resins differ from the conditions for the production of carbamide resins.

In the present investigation a study was made of the conditions for carrying out the condensation reaction of urea with formaldehyde in order to produce rapidly hardening resins for wood bonding.

The condensation products of urea with formadehyde which are usually obtained are unsuitable as adhesives for wood because of their high impregnating power and low viscosity. The method chosen for production of resins with the required properties was the method of partial dehydration of the resinous products under reduced pressure [3, 4], used in the production of phenol-formaldehyde and carbamide resins. No information is available in the literature on the temperature and extent of dehydration of low-viscosity resinous products under vacuum required to produce adhesive resins. For this reason, the conditions for the vacuum drying of urea-formaldehyde condensation products intended for use as adhesive resins were also studied.

EXPERIMENTAL*

On the basis of the results of studies of the condensation of urea with formaldehyde [5-8] for the production of molded articles, the two-stage condensation method was chosen for the present work; this ensures an excess of formaldehyde in the first stage of the reaction and a decrease in the formaldehyde content toward the end of the process by further additions of urea during the second condensation stage. The condensation of urea with formaldehyde was carried out first in a weakly alkaline and then in a weakly acid medium. The molar ratio of urea to formaldehyde was kept at 1:1.65. The catalysts used were such cheap and easily available substances as caustic soda and ammonium chloride. The experiments on the preparation of resinous condensation products of urea with formaldehyde were carried out at various temperatures (from 60 to 90°).

The course of the condensation reaction was followed by determinations of the pH of the reaction medium and of its free formaldehyde contents. The pH was determined colorimetrically by means of a universal indicator. The formaldehyde content was determined by the iodine and the sulfite methods [9]. The usual method was used for determination of the solids in the synthesized products. The viscosity of the condensation products was determined by the GIPI-4 viscosimeter mark VZ-4. The adhesive properties of the condensation products were also studied.

* T.V. Yachina assisted in the experimental work.

Effect of pH of the medium on the properties of the condensation products of urea and formaldehyde. Of all the conditions which have a decisive influence on the properties of the condensation products of urea and formaldehyde, the reaction of the medium is the most important. The literature contains reports on the use of alkaline, acid, and neutral media for the condensation reaction of urea with formaldehyde [10]. However, in the methods most widely used in industry first a neutral or alkaline medium followed by an acid medium, or first an acid followed by a neutral medium, are used. The products obtained at different pH values have different properties, and it was therefore necessary to determine the necessary pH conditions for the production of adhesive resins with the required properties.

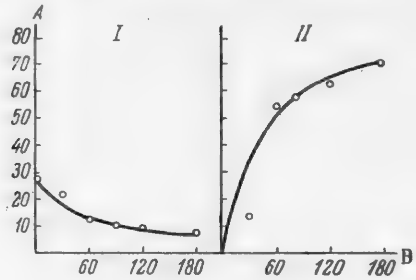

Fig. 1. Influence of an acid medium on variations of the formaldehyde content. A) Formaldehyde content (%), B) condensation time (min.). I) Free CH_2O in the condensation products, II) combined CH_2O (as % of original).

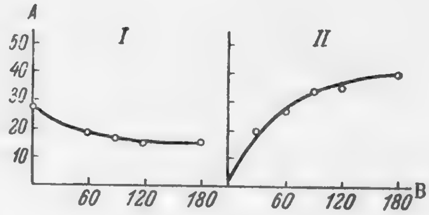

Fig. 2. Influence of an alkaline medium on variations of the formaldehyde content. A) Formaldehyde content (%), B) condensation time (min.). I) Free CH_2O in the condensation products, II) combined CH_2O (as % of original).

The formalin, containing 37.2% formaldehyde, had pH = 3. Its condensation with urea was commenced in our experiments after the pH had been adjusted in the initial stage to the following values by means of 40% caustic soda solution: 1) pH = 5; 2) pH ≈ 9-10 and 3) pH = 7.5. In the last case, the pH of the medium in the second stage of condensation was adjusted to 6.0 by addition of ammonium chloride. The reaction temperature was maintained at 80° in all the experiments.

The products obtained when the condensation is performed in an acid medium have an acid reaction, are sparingly soluble in water, unstable, and rapidly gelatinize on keeping. The substances obtained in an alkaline medium are partially soluble in water, are pastelike masses after vacuum drying, and thicken rapidly even after brief storage. Condensation of urea with formaldehyde carried out in a medium of pH 7.5-6 leads to formation of resinlike substances, partially soluble in water, which become syrupy after dehydration; they are more stable than the substances formed in acid and alkaline media.

Figures 1, 2, and 3 give kinetic data on the condensation reaction of urea with formaldehyde at various values of pH of the medium.

Figures 1,2, and 3 show that the binding of formaldehyde by urea proceeds at different rates with different pH values of the medium. The reaction between the starting substances is particularly rapid in an acid medium (pH = 5) and is much slower in an alkaline medium (pH = 9-10). When the reaction is carried out in a medium of variable pH (pH from 7.5 to 6.0) the rate at which the formaldehyde is combined is lowest at the beginning, while the medium is first weakly alkaline and then neutral. From the moment when the acidity of the solution increases to pH = 6.0, the amount of reacting formaldehyde increases rapidly, reaching 52% at the end of 3 hours of heating. In the same time, 72% of the original formaldehyde reacts during condensation in an acid medium, and 39% in an alkaline medium.

The results of these experiments showed that for production of adhesive resins the most suitable procedure is to condense urea with formaldehyde at variable pH: first in a weakly alkaline medium (pH = = 7.5-8) and then in a weakly acid medium (pH = 6.0). All the subsequent experiments were performed in these conditions.

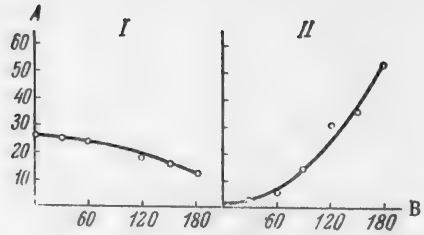

Fig. 3. Influence of a medium of variable acidity (pH = 7.5—6.0) on variations of the formaldehyde content. A) Formaldehyde content (in %) , B) condensation time (min.). I) Free CH_2O in the condensation products, II) combined CH_2O (as % of original).

Influence of the reaction temperature on the pH of the medium and on the solubility of the condensation products of urea and formaldehyde. To determine the influence of temperature on the kinetics of the condensation reaction and on the properties of the reaction products, the reaction of urea with formaldehyde was carried out at temperatures of 60, 70, 80, and 90°. The results of the experiments are given in the Table and in Fig. 4. Fig. 4 shows the variation of free and combined formaldehyde contents in the reaction medium at various temperatures.

Properties of Condensates Obtained at Different Temperatures of Reaction of Urea with Formaldehyde

Reaction temperature (°C)	Time before commencement of resinification (from the moment when pH is established at 6)	pH of condensate (at the end of 3 hours)	Solubility of final products in water
60	No resinification	6.0	Completely soluble
70	30 minutes	6.0	
80	10-15 minutes	6.0	Partially soluble
90	5 minutes	5.5	Low solubility

Influence of the method of introducing urea into the reaction. The properties of the reaction products of urea with formaldehyde are also influenced by the method of introducing the urea.

Experiments were performed in which urea was introduced in one, two, and three stages during the condensation with formaldehyde.

The results of the experiments are given in Fig. 5; these show that while resins containing 11.7% free formaldehyde are obtained when the urea is added in one step, when the same amount of urea is added in 2 and 3 steps the free formaldehyde content decreases to 11. 13 and 10.77% respectively.

Production of vacuumized adhesive resins. The flask containing the urea-formaldehyde condensation products was heated on a water bath the temperature of which was kept constant (60°). Water was distilled off under a residual pressure of 30-40 mm Hg, and the amount of water removed varied between 270 and 316 ml (from 1.3 kg of resin) in different experiments. After removal of the water the contents of the flask were cooled to room temperature.

The resins obtained after vacuum drying at 60° were homogeneous syrupy liquids, which did not separate out into layers, with different viscosities, which did not exceed 13-15 seconds after vacuum drying and cooling (irrespective of the amount of water removed) . The viscosity of the vacuumized resins reached a completely definite value of 60 to 120 seconds only after 10-12 hours.

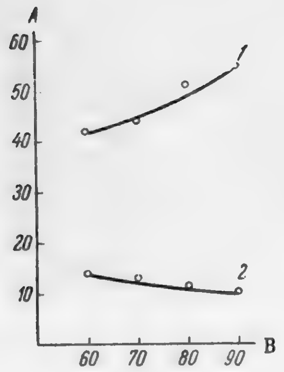

Fig. 4. Variation of the contents of free and combined CH_2O with the reaction temperature. A) Formaldehyde content (%), B) temperature (°C). I) Combined CH_2O, II) free CH_2O.

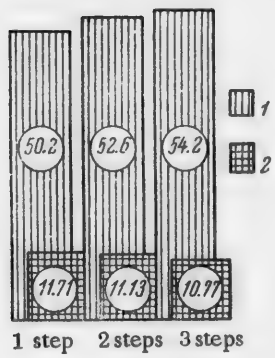

Fig. 5. Variation of the contents of free and combined CH_2O with various methods of adding the urea. 1) Combined CH_2O, 2) free CH_2O.

Tests of the resins obtained showed that products with viscosities of 90 seconds and over can be applied to wood surfaces by means of the usual rollers for the purpose. Studies of the conditions for the production of such resins showed that the vacuumizing should be continued for about 2 hours at 60° (until resins of 60-62% concentration are obtained) to yield resins with viscosities of 90 seconds and over.

The adhesive urea-formaldehyde resins obtained after vacuum drying (at 60-65°) have the following characteristics: pH = 6.7 —7.0; viscosity from the efflux time of 100 ml, 90-210 seconds; free formaldehyde content 1.2 to 3.5%; solids 60± 3% . The adhesive properties conform to the specifications for adhesives for the production of plywood stable to cold water.

The urea - formaldehyde resin has been given the code designation "TsNIIFM M-60".

SUMMARY

1. Urea-formaldehyde condensation products can be used with good results as adhesives for wood if they are prepared under the following conditions: molar ratio of urea to formaldehyde 1:1.65, condensation temperature 80°, duration of the condensation reaction 3 hours, pH of the medium 7.5-8.0 in the first stage and 6.0 in the second stage, dehydration of the resins at the end of the condensation reaction under a residual pressure of 40 mm Hg, distillation temperature 60-70°, distillation continued until resins of 60% concentration are obtained.

2. The pH of the medium influences not only the course of the condensation reaction, but also the consistency of the resins and their stability on keeping. The best resins have pH = 6-7.

3. Introduction of urea into the reaction mixture in several steps increases the amount of formaldehyde reacting with it; the greater the number of steps in which a given amount of urea is added, the more formaldehyde reacts with it.

LITERATURE CITED

[1] R.Z. Temkina, J. Appl, Chem., 27, 98 (1954).

[2] R.Z. Temkina, J. Appl. Chem., 27, 1313 (1954);

[3] I. P. Mikheev, Production of Phenol-Aldehyde Resins, State Chem. Press (1946).

[4] C. Ellis, Chemistry of Synthetic Resins, II, 2, State United Sci.- Tech. Press, Moscow (1938).

[5] A.A. Vansheidt and Z. K. Naumova, Symposium, Plastics, 3 (1939).

[6] G.S. Petrov, Carbamide Resins and Molding Compositions, Moscow Chem. Tech. Inst. Press. Moscow (1940).

[7] G.S. Petrov, B.N. Rutovsky, I.P. Losev, Technology of Synthetic Resins and Plastics, State Chem. Press, Moscow—Leningrad (1946).

[8] Pollak and Ripper, German Patent 437535 (1926).

[9] K. Andrianov, D. Kardashev, Practical Work on Synthetic Resins and Plastics, State Chem. Press (1946).

[10] J. Scheiber, Chemistry and Technology of Synthetic Resins, State Chem. Press, Moscow—Leningrad (1949).

Received September 5, 1955.

BRIEF COMMUNICATIONS

DETERMINATION OF NITROGEN IN COMPLEX COMPOUNDS

A. A. Grinberg and L. K. Simonova

Chair of General and Inorganic Chemistry, the Lensoviet Technological Institute, Leningrad, and Chair of Inorganic and Analytical Chemistry, the V. M. Molotov Technological Institute, Leningrad

An earlier communication [1] dealt with a new method for determination of nitrogen in stable ammines of platinum and cobalt.*

Later we began to use this method for determination of nitrogen in other complex compounds also. Compounds containing various amines in addition to ammonia were the first to be tested.

The total nitrogen in diammine-dimethylamine-platochloride, triammine-ethylamine-platochloride, and diammine-diethylamine-platochloride was successfully determined.

	Weight of substance (g):	0.0596, 0.0642, 0.0781.
	Found %:	N 15.33, 15.24, 15.32.
$[Pt(NH_3)_2m_2]Cl_2$.	Calculated %:	N 15.46.
	Weight of substance (g):	0.0631, 0.0549.
	Found %:	N 15.31, 15.39.
$[Pt(NH_3)_3Et]Cl_2$.	Calculated %:	N 15.46.
	Weight of substance (g):	0.0672, 0.0712.
	Found %:	N 14.21, 14.28.
$[Pt(NH_3)_2Et_2]Cl_2$.	Calculated %:	N 14.33.

Despite the high boiling point of benzylamine it proved possible to determine the total nitrogen in such a complex compound as diammine-dibenzylamine-platochloride.

	Weight of substance (g):	0.0684, 0.0598.
	Found %:	N 10.74, 10.78.
$[Pt(C_6H_5CH_2NH_2)_2(NH_3)_2]Cl_2$.	Calculated %:	N 10.90.

The explanation is that benzylamine readily distills with steam.

The total nitrogen in compounds containing amines which do not have this property could not be determined. For example, only $^3/_4$ of the total nitrogen in triammine-ethanolamine-platochloride, and only a half of the total nitrogen contained in dichloro-ammine-ethanolamine platinum and in diammine-diethanolamine-platochloride, could be determined.

* The method is based on reduction of the complex-former by ferrous sulfate in an alkaline medium followed by distillation of ammonia.

Weight of substance (g): 0.0539, 0.0612.
Found %: N 11.09, 11.07.
$[PtEtm(NH_3)_3]Cl_2$. Calculated %: N (from ammonia) 11.11.

Weight of substance (g): 0.0703, 0.0666.
Found %: N 4.06, 4.03.
$[PtEtmNH_3Cl_2]$. Calculated %: N (from ammonia) 4.07.

Weight of substance (g): 0.0623, 0.0636.
Found %: N 6.60, 6.62.
$[Pt(Etm)_2(NH_3)_2]Cl_2$. Calculated %: N (from ammonia) 6.65.

Thus, by combining our proposed method with total nitrogen determination by the Dumas method, it is possible to determine the nitrogen in ethanolamine and ammonia separately in the same complex compound.

The same applies to determination of nitrogen in complex compounds containing the CNS^- group in addition to ammonia, such as diammine-dithiocyano platinum.

Weight of substance (g): 0.1189, 0.1012.
Found %: N 7.91, 7.98
$[Pt(NH_3)_2(CNS)_2]$. Calculated %: N (from ammonia) 7.81.

In this case only the ammonia nitrogen is determined by our method. The nitrogen in the thiocyanate group can be determined with the aid of the Dumas method.

To investigate the applicability of this method to the determination of nitrogen in complex compounds containing nitrate and nitro groups, ordinary salts of nitric and nitrous acids were first tested.

It was found that in the conditions of this method, with the use of ferrous sulfate in an alkaline medium as reducing agent, nitrogen of sodium nitrate is not reduced to ammonia, while nitrite nitrogen is partially converted into ammonia and trapped by sulfuric acid on distillation.

Quantitative determination of nitrite nitrogen cannot be achieved by this method, as reduction of N^{+3} to N^{-3} proceeds by way of formation of a number of intermediate products. Some of these products (such as NO, and N_2O) are not absorbed by sulfuric acid solution and are removed from the reaction zone. Therefore low values for the nitrogen contents were obtained in all the determinations.

Weight of substance (g): 0.1185, 0.1230, 0.1012.
Found %: N 15.2, 16.25, 15.5.
$NaNO_2$. Calculated %: N 20.3.

In this case nitrogen losses were 10% of the total. It is very likely that in more harsh conditions and with a more suitable reducing agent a quantitative yield of ammonia might be obtained.

Nitrogen determination in a complex compound containing a nitro group also gave a low result.

This is illustrated by analytical data for potassium dibromodinitroplatinate.

Weight of substance (g): 0.0712, 0.0696.
Found %: N 4.48, 4.29.
$K_2[Pt(NO_2)_2Br_2]$. Calculated %: N 5.33.

The fact that nitrogen in the NO_3^- group is not reduced at all in the conditions of the proposed method makes it possible to determine ammonia nitrogen separately in complex compounds in presence of the nitro group.

This is illustrated by the analysis of acetylacetono-diammine-platochloride, a complex compound synthesized for the first time by A. A. Grinberg and I. N. Chapursky.

Weight of substance (g): 0.1006, 0.0925.
Found %: N 7.12, 7.21.
$[Pt(NH_3)_2Ac]NO_3$. Calculated %: N (from ammonia) 7.17.

SUMMARY

1. It is shown that nitrogen in complex compounds containing different amines can be determined by reduction of the complex-former by ferrous sulfate in an alkaline medium followed by distillation of ammonia.

2. It is shown that nitrogen can be determined separately in complex compounds containing ethanolamine and thiocyanate and nitrate groups together with ammonia and volatile amines.

LITERATURE CITED

[1] A. A. Grinberg and L. K. Simonova, J. Appl. Chem., 26, 10, 1080 (1953).*

Received June 15, 1956

* Original Russian pagination. See C. B. Translation.

INFLUENCE OF SMALL QUANTITIES OF CERTAIN ADDITIVES ON THE CEMENTING PROPERTIES OF γ-DICALCIUM SILICATE (γ-C_2S)

P. P. Budnikov and R. D. Azelitskaya

Calcium orthosilicate (Ca_2SiO_4) is a most important mineral in cement clinker. An interesting characteristic of this mineral is that it can exist in four modifications: α-, α'-, β- and γ-C_2S, all four of which have different densities, optical properties, behave differently when mixed with water, etc.

The stable form of calcium orthosilicate at ordinary temperatures is γ-Ca_2SiO_4. The other modifications are converted one into another at the appropriate temperatures.

It has been established that the metastable β-form persists at ordinary temperatures in presence of certain substances known as stabilizers. Stabilizers include borates, salts of the type A_nXO_4, excess CaO, and certain other compounds containing ions of greater radius than Ca^{++} [1].

Thilo and Funk [1] have established that compounds of alkali metals can serve as active stabilizers for β-Ca_2SiO_4: "Na_2CO_3, NaOH, and Na_2SO_4 [active in amounts < 0.2 molar % (~0.1 % by weight)] while < 3 % NaCl has no stabilizing effect on the β-form. Sodium compounds are incorporated into the Ca_2SiO_4 lattice only on heating to 1000° and over. The corresponding potassium compounds have the same action as the sodium compounds, but twice the amounts are required."

This effect of alkali metal compounds appears to us to be of great interest, and suggested a study of the influence of these compounds in the same amounts on the cementing properties of γ-Ca_2SiO_4.

It is reported in the literature that the γ-form is not capable of hydraulic hardening [2]. However, the results of our investigation [3], given below, suggest that the pure form of γ-C_2S nevertheless has cementing properties. It is very probable that the presence of small amounts of compounds formed during burning decrease the capacity of γ-C_2S for hydraulic hardening. This hypothesis may be based on the report by Thilo and Funk [1] that γ-C_2S is highly sensitive to very small quantities of various compounds.

The γ-C_2S used in our investigation was synthesized from chemically pure $CaCO_3$ and SiO_2, obtained from finely ground and washed Volsk sand. After burning, the γ-C_2S contained 0.13% free CaO, determined by the glycerate method [4].

The strength tests were made on small specimens 2 × 2 × 2 cm, pressed at 400 kg/cm², made from a 1 : 2 mixture with Volsk sand. The Volsk sand fraction used passed through a sieve with 256 holes/cm² and was retained by a sieve with 900 holes/cm². The paste was moistened with 10% water for pressing. The specimens were kept in moist surroundings. The additives were introduced into the mixture of γ-C_2S and sand during preparation of the specimens.

4 cubes were made for each test period. The γ-Ca_2SiO_4 was ground to pass completely through a sieve with 4900 holes/cm².

The results of the investigation of the influence of alkali salts on the strength of γ-Ca_2SiO_4 are shown in the Table.

The explanation for the low strength of pure γ-Ca_2S is that it was made from SiO_2 obtained by grinding and washing of Volsk sand. The washing was probably not thorough enough, and impurities which partially

stabilized the β-Ca_2SiO_4 remained in the sand. It has been shown by our investigations that a mixture of γ- and β-Ca_2SiO_4 has extremely low strength.

Amount of salt added to γ-$CaSiO_4$ (in %)	Compressive strength (kg/cm^2)		
	3 days	7 days	28 days
0.1 $CaCO_3$	1	1	3
0.5 $CaCO_3$	1	1	2
0.5 K_2CO_3	1	2	4
0.1 K_2CO_3	1	1	2
0.5 $CaSO_4$	1	2	3
0.1 $CaSO_4$	3	3	7
0.1 K_2SO_4	2	2	6
0.5 K_2SO_4	3	3	5
0.1 $CaCl_2$	3	3	6
0.5 $CaCl_2$	3	4	7
0.1 KCl	3	3	8
0.5 KCl	3	4	6
	4	4	5

At the same time, additions of small amounts of certain salts have a positive effect on the strength of even such an inactive compound as the one used in this case.

It may be concluded from the results in the table that potassium and calcium sulfates and chlorides have a positive effect on the strength of γ-Ca_2SiO_4. The carbonates of these cations, however, have no influence on the strength increase of γ-Ca_2SiO_4.

This result is interesting from several points of view. First, it indicates the active role of the anionic group in the hardening of γ-Ca_2SiO_4. Second, of the three anions studied, CO_3'', SO_4'', and Cl', the first is not active but the other two are. Small amounts of the anionic groups SO_4'' and Cl' added to γ-Ca_2SiO_4 may produce an average strength increase of 200% in the latter.

This effect may be explained by the fact that the anionic groups SO_4'' and Cl' are surface-active.

This is in full agreement with the modern theory of surface-active substances, advanced by Rebinder, Logginov [5], and others, according to which inorganic electrolytes may act as accelerators of the hardening process. These authors state that "the adsorption action of electrolytes of this type is confined to the formation of an electric double layer, in which the anions are adsorbed on the surface of the grains of cement, lime, or gypsum, while the cations constitute the diffuse layer." Probably the action of such surface-active additives is related to the adsorption of anions on the surface of the cement grains or, as in the present instance, on the surface of the γ-Ca_2SiO_4 mineral.

With reference to the paper by Thilo nd Funk [1] cited earlier, it may be assumed that in the stabilization of β-Ca_2SiO_4 by alkali metal compounds the latter play the role of surface-active agents.

LITERATURE CITED

[1] E. Thilo, H. Funk, Z. anorg. allg. Ch., 273, 1-2, 28-40 (1953).

[2] V. N. Yung, Fundamentals of Cement Technology, Industrial Construction Press (1951).

[3] P. P. Budnikov and R. D. Azelitskaya, Proc. Acad. Sci. USSR, 108, 3, 515 (1956).

[4] Yu. M. Butt, Manual of Cement Technology, Industrial Construction Press (1953).

[5] P. A. Rebinder and G. I. Logginov, Herald Acad. Sci. USSR 10 (1951).

Received December 12, 1955

ABSORPTION OF WATER FROM MOIST GAS BY CALCIUM CARBIDE

M.M. Shelechnik

The problem of absorption of water vapor from moist gases by calcium carbide is of great practical importance in addition to its purely scientific interest. This may be illustrated by the following examples.

Calcium carbide is the principal material used for production of acetylene. Airtight packages cannot always be used for its transport and storage. Contact between the carbide and the surrounding moist air is inevitable during production processes. The duration of the contact determines the amount of acetylene lost.

The drying of acetylene by calcium carbide is a progressive technological process. The drying is then, in a sense, a continuation of the production of acetylene, as the carbide reacts with moisture to give additional acetylene.

It can be shown that the reaction between water vapor and calcium carbide is important in a number of other industrial processes.

With unrestricted access of water to the calcium carbide surface, the hydrolysis rate at a given temperature is a function of the surface area of the lumps. The duration of the process is determined by the original lump size.

With carbide of 8/15 granulation, the decomposition is completed in 10-12 minutes [1].

When lumps of calcium carbide are kept in stationary moist air, they become coated fairly rapidly with a layer of lime. This coating is partially destroyed by the action of the evolving acetylene, and the lime partially crumbles off.

The carbide continuously increases in weight (Figure 1). This continues until the weight becomes constant, corresponding to the stoichiometric proportions

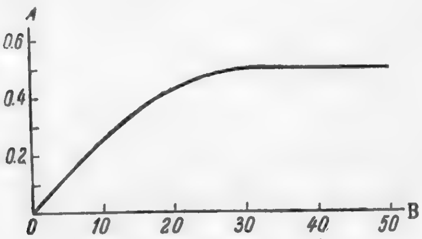

Fig. 1. Increase of the weight of carbide of 2/ 8 granulation with time, at 21.5° dry bulb and 15° wet bulb thermometer readings.
A) Weight increase of a 3.7187 g carbide sample (in g), B) time (hours).

$$\underset{64}{CaC_2} + \underset{36}{2H_2O} = \underset{74}{Ca(OH)_2} + \underset{26}{C_2H_2}.$$

The duration of this process depends not only on the lump size but also on the humidity of the air. For carbide of 8/15 granulation the decomposition is complete in 8-9 days at 21° dry bulb and 15° wet bulb temperatures.

For contact to occur between water and calcium carbide, the water vapor must first diffuse in the inert gas medium and then through the layer of lime formed on the carbide surface. We shall now derive the equation for moisture transfer [2].

The diffusion of water vapor in the gas medium is determined by the rate of mass transfer through the boundary layer. This rate is given by the following formula:

$$\frac{dG}{d\tau} = K_W F (H - H_0), \tag{1}$$

where G is the amount of water (in g) absorbed from the air by a lump of carbide of surface area F cm^2, τ is the time (in hours), K_W is the mass transfer coefficient (for water vapor) from moist air to the surface of the lime (in g/ $cm^2 \cdot$ hour), H is the moisture content of the air in g/g), H_0 is the moisture content of the air at the surface of the carbide lumps (in g/ g).

The rate of penetration of moisture through the crust of lime may be represented by the following equation:

$$\frac{dG}{d\tau} = \frac{D_W}{\delta} F (C - C_0), \tag{2}$$

where D_W is the coefficient of diffusion of moisture through the lime layer (in g/ cm$\cdot$hour), δ is the thickness of the lime layer (in cm), C is the moisture content of the lime at the air interface (in g/ g), and C_0 is the moisture content of the lime at the carbide interface (in g/ g).

It is known that any material in prolonged contact with moist air attains a constant moisture content, which is usually expressed in terms of the relative humidity of the contacting air

$$C = \frac{\beta H_0}{H'},$$

where β is the equilibrium moisture content coefficient of the lime, and H' is the humidity of air saturated in the given conditions.

The lime formed at the calcium carbide surface contains no moisture, and therefore $C_0 = 0$.

The thickness of the lime layer as a function of the amount of vapor absorbed is given by the equation

$$\delta = \frac{2.05 \cdot G}{1.2 \cdot F} = 1.71 \frac{G}{F},$$

where $2.05 = \frac{74}{36}$ is the amount of lime formed by the absorption of 1 g of water, and 1.2 is the density of lime (in g/cc).

Substituting these expressions into Formula (2), we have

$$\frac{dG}{d\tau} = \frac{D_W F^2 \beta H_0}{1.71 \cdot GH'}. \tag{3}$$

In steady state conditions, the amounts of substance passing in a given time interval through different parts of the system are equal. By equating the expressions (1) and (3) and eliminating H_0, we have

$$\frac{dG}{d\tau} = \frac{HF}{\frac{1}{K_W} + \frac{1.71 \cdot G \cdot H'}{D_W \beta F}}. \tag{4}$$

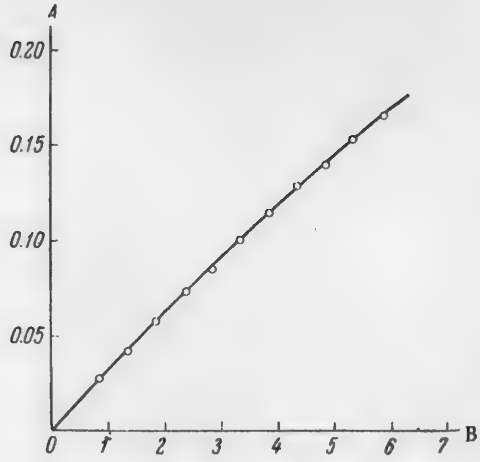

Fig. 2. Experimental verification of Formula (6). A) Weight increase (in g) of a carbide sample of 8/15 granulation at 17° dry bulb and 13.5° wet bulb thermometer readings, B) time (hours). The straight line represents results calculated from Formula (6); the circles represent experimental data.

Integration of this last expression gives the amount of moisture absorbed as a function of time

$$G = \frac{\beta D_W F}{1.71\, K_W \cdot H'} \left(\sqrt{1 + \frac{3.42 H \cdot H' K_W^2 \tau}{\beta D_W}} - 1 \right) \quad (5)$$

By multiplying G by the appropriate factor calculated from the stoichiometric proportions we can determine the amount of calcium carbide decomposed or the amounts of acetylene or lime formed.

The weight increase of the calcium carbide lumps is found by multiplication of the value of G from Formula (5) by 0.28, found from the stoichiometric proportions, and substitution of β by the value for lime. = 0.05.

$$\Delta g = 0.0082 \frac{D_W F}{K_W H'} \left(\sqrt{1 + \frac{68.50 H \cdot H' K_W^2 \tau}{D_W}} - 1 \right) \quad (6)$$

Experimental verification of Formula (6) showed that this relationship is in good agreement with the experimental results during the first 5-8 hours of the process, which corresponds to approximately 20% of the total moisture which the carbide can absorb. After 15 hours the weight increase is 10-12% less than the value given by Formula (6).

Figure 2 shows the weight increase for five lumps of calcium carbide. The average lump weight q is 1.2009 g.

Comparative data for the weight increase of 3.7187 g of calcium carbide of 2/8 granulation at dry and wet bulb temperatures of 21.5° and 15° respectively, are given below.

Time (hours)	Calculated weight increase (g)	Experimental weight increase (g)
1	0.0364	0.0366
2	0.0707	0.0704
3	0.1020	0.1018
4	0.1320	0.1303
5	0.1590	0.1590
6	0.1850	0.1797
22.5	0.5190	0.4568

For calculation of the dependence of the mass transfer coefficient K_W on the characteristic dimensions of the system, the relationship $Nu = C(Gr \cdot Pr)^m$ [3] was used. Experimental data (Fig. 2) yielded the expression $K_W = 0.5811\, g^{-1/12}$ and the diffusion coefficient of moisture through the lime layer $D_W = 0.0187$ g/cm·hour. For an average lump weight q = 0.2860 g we have the following relationship between the weight increase and time

$$\Delta g = 0.393\,(\sqrt{1 + 0.195\tau} - 1).$$

The reason for the approximate nature of the results obtained (Formula 5) lies in the assumption that the carbide and lime coating surfaces are equal. This assumption corresponds to the start of the process. Subsequently the carbide surface contracts and tends to zero, while the external surface of the lumps increases by approximately 50%. To take this into account would complicate the formulas and make them unsuitable for practical purposes. For calculations of the course of decomposition over prolonged time intervals, Formula (5) should be replaced by the semiempirical relationship

$$G = AF\sqrt{\frac{\Pi}{\Pi'} D_W \tau}, \tag{7}$$

where A is a constant, determined experimentally.

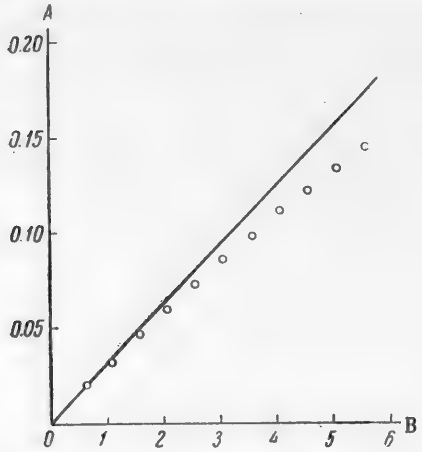

Fig. 3. Experimental verification of Equation (8). A) Weight increase (in g) of carbide sample, B) time (hours). The straight line represents results calculated from Formula (8); the circles represent experimental data.

The weight increase relationship (Figure 2) is approximately linear, and therefore the state of the carbide (amount of absorbed moisture) has little influence on the course of the process. The principal factor is the resistance of the gas boundary layer. If the duration of the process is not long (2-3 hours), the resistance of the lime layer may be neglected. The transfer Equation (4) is then simplified:

$$\frac{dG}{d\tau} \approx K_W HF.$$

The amount of absorbed moisture becomes

$$G \approx K_W HF\tau. \tag{8}$$

Figure 3. shows the increase in the weight of carbide, calculated from Equation (8). The circles represent the experimental data.

SUMMARY

1. Despite the formation of a coating of lime, the absorption of moisture from gases by calcium carbide is fairly rapid. In the first 6 hours, carbide absorbs ~ 10% of its own weight of moisture from still air.

2. Formulas have been derived for calculating the rate of moisture absorption in free convection conditions during the initial stages of the process. It is shown that the resistance to the diffusion of moisture in the air is predominant during this period.

LITERATURE CITED

[1] I.I. Strizhevsky, A.S. Zaitseva, M.M. Shelechnik, Welding Ind. 3 (1951).

[2] D.A. Frank-Kamenetsky, Diffusion and Heat Transfer in Chemical Kinetics, Acad. Sci. USSR Press, 55 (1947).

[3] M.A. Mikheev, Fundamentals of Heat Transfer, State Power Press, 84 (1947).

Received August 5, 1955

COMMUNICATION II. KINETICS OF REGENERATION OF THE ABSORBENT SOLUTION IN SULFUR REMOVAL BY THE POTASH PROCESS

I. G. Plit

The Dnepropetrovsk Institute of Chemical Technology

It was established by us earlier [1] that a two-stage scheme for regeneration of the absorbent solution is more rational in sulfur removal by the potash process. In the first stage, when the solution is boiled under a vacuum of 670-700 mm Hg (temperature 54-55°), the main reaction is decomposition of hydrosulfide, while in the second stage bicarbonate is decomposed and carbon dioxide liberated.

The present communication contains the results of an investigation of the influence of the main factors on the kinetics of the regeneration process during the first stage. As previously [1], the solution was analyzed after the experiment and the degree of regeneration in terms of hydrosulfide was calculated from the change of salt concentrations. The average boiling temperature in all the experiments was 54-55°, and the temperature of the escaping vapor was 20°.

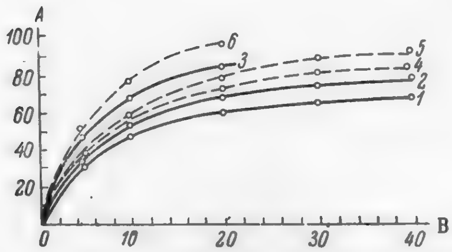

Fig. 1. Effect of the boiling time on the rate of decomposition of hydrosulfide. A) Degree of decomposition of KHS (in %), B) Duration of boiling (min.). Ratio K = $KHCO_3$/KHS and boiling rate respectively: 1) 1, 4.41; 2) 1, 6.45; 3) 1, 14.9; 4) 1.57, 4.61; 5) 1.57, 6.45; 6) 1.57, 14.1.

In the first series of experiments the effect of the boiling time on the rate of hydrosulfide decomposition was studied. A solution of the following composition (in g-equiv./liter) was used for the regeneration: K_2CO_3 0.83, $KHCO_3$ 0.25, KHS 0.25, $(H_2S)_{aq.}$ 0.176, with initial ratio K = $KHCO_3$/KHS = 1.

The results of these experiments are given in Fig. 1. The first group of experiments (Fig. 1) was performed at a constant solution boiling rate Q = 4.41 kcal /liter·min, in the boiling time range from 5 to 40 minutes inclusive.

The nature of the resultant curve shows that, despite the increase in the degree of regeneration, the rate of the process does not remain constant but decreases with duration of the boiling.

Because of the high contents of $KHCO_3$ and KHS in the original solution at the initial stage of the process, the hydrogen sulfide vapor pressure over the solution

$$P_{H_2S} = KRT \frac{C_{HCO_3^-}}{C_{CO_3^{--}}} C_{HS^-} \tag{1}$$

is high, and very rapid evolution of most of the hydrogen sulfide occurs during this period. The vapor pressure subsequently decreases because of the decreasing concentrations of the salts in solution, and the process becomes less rapid, approximately according to a parabolic law.

The evolution of the remaining hydrogen sulfide from the solution will therefore occur relatively slowly and will require considerable time, and therefore a considerable expenditure of heat. Because of this, to achieve more complete evolution of hydrogen sulfide from solutions in industrial conditions, the appropriate course is not to increase the boiling time but to use factors which would produce a considerable increase of the rate of the process with a short boiling time.

One such factor is the boiling rate. This is demonstrated by the curves in Fig. 1, which correspond to the solution boiling rates: Q = 4.41, 6.45 and Q = 14.9 kcal /liter· min. A comparison of these curves shows that a threefold increase of the solution boiling rate increases the degree of decomposition of the hydrosulfide by a factor of 1.4 and halves the time.

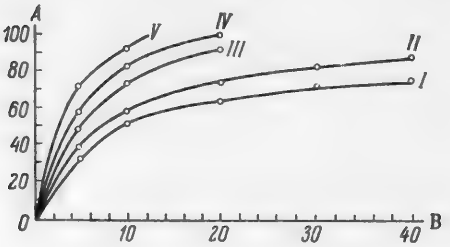

Fig. 2. Effect of hydrosulfide concentration in solution on its decomposition. A) Degree of decomposition of KHS (in %), B) Duration of boiling (min.). Ratio: K = $KHCO_3$/KHS and boiling rate respectively: I) 1, 4.94; II) 1, 6.91 (n = 0.75); III) 1.11, 15.2; IV) 1.8, 15.2; V) 2.63, 15.2.

This is confirmed by results in the regeneration of solutions with other ratios of salt concentrations. This is indicated by the broken curves, representing the boiling of a solution with the following initial salt concentrations (in g-equiv./liter): K_2CO_3 0.72, $KHCO_3$ 0.88, KHS 0.56, $H_2S_{aq.}$ 0.18 and the ratio K = $KHCO_3$/KHS = 1.57.

The experiments were performed at different boiling rates: Q = 4.61, 6.45 and 14.1 kcal /liter· min. The general relationship noted above is retained: the rate of the process increases with boiling rate.

The boiling rate is by no means the only factor which influences the process. Analysis of Equation (1) shows that the ratio K = $KHCO_3$/KHS and the hydrosulfide concentration in the solution can also have this effect. This is confirmed by experiments with different salt concentrations and ranges of the $KHCO_3$/KHS ratio.

Curves I and II in Fig. 2 represent the regeneration of solutions with different absolute contents of hydrosulfide, but with the same ratio $KHCO_3$/KHS = 1. Curve I corresponds to 0.75 g-equkv. of KHS per liter, and curve II, to 0.47 mole/liter.

A comparison of these results with those in Fig. 1, in which the respective boiling rates are the same, and the KHS content is 0.25 mole/liter, shows that the degree of recovery depends on the hydrosulfide concentration. However, the increase is very slight. An increase of the hydrosulfide concentration from 0.25 to 0.47 mole/liter, with a boiling time of 10 minutes, increases the degree of regeneration from 47.8 to 50.5%, and at a content of 0.75 mole/liter, from 51.2 to 53%.

A curious feature is that in these experiments the favorable influence of KHS concentration decreases somewhat with increase of boiling rate. Thus, in experiments with boiling rate Q = 4.41-4.9 kcal/liter·min. the increase in the degree of regeneration was 2.7 %, while in experiments with the higher KHS content of 0.75 mole/liter, but at Q = 6.91-6.45 kcal /liter·min. the degree of regeneration increased by only 2.1%.

Increase of the $KHCO_3$/KHS ratio in the solution has an entirely different effect. Excess bicarbonate greatly accelerates the regeneration process. This is confirmed by Curves III, IV, and V, for solutions with equal KHS contents boiled at the same rate, but with different $KHCO_3$/KHS ratios from 1.11 to 2.63.

Thus, the role of carbon dioxide in the absorption and regeneration process is different. While it somewhat retards the absorption of hydrogen sulfide, during regeneration it assists fairly intensively the liberation of hydrogen sulfide into the vapor phase. Therefore there is no sound basis for the tendency to plan the absorption in isolation from the rest of the process. The problem must be solved in conjunction with the regeneration cycle. The optimum conditions for the absorption cycle, which ultimately determine the amount of carbon dioxide absorbed must be chosen in relation to the required degree of gas purification and to the rate of the regeneration process which technological considerations demand.

Since the duration of boiling in industrial conditions cannot be great, we have represented our experimental results in the form of an empirical equation, which is valid for solution boiling times of up to ten minutes:

$$a = 8.15 \cdot t^{0.68} \cdot K^{0.24} \cdot 10^{0.0168\left(Q + \frac{20n}{t}\right)}, \qquad (2)$$

where a is the degree of decomposition of the hydrosulfide (in %), t is the boiling time (minutes), Q is the boiling rate in kcal /liter•min., n is the hydrosulfide content in the solution (in mole/liter) and K is the ratio $KHCO_3/KHS$ (in mole/mole or g-equiv./g-equiv.).

In the conditions of our experiments the error in the degree of decomposition of KHS calculated by this equation does not exceed 1-1.5%. In general this equation may be recommended, if not for quantitative calculations, then at least for qualitative analysis of the influence of the factors studied on the kinetics of the regeneration process. Such analysis indicates that the optimum conditions of the regeneration process in the first stage are provided by rapid boiling with the highest possible $KHCO_3/KHS$ ratio in the solution. The ease of regeneration is higher for increasingly spent solutions. Therefore an excessive increase of excess absorbent in the absorption process is not desirable from the regeneration aspect.

SUMMARY

A study of the influence of the principal factors on the process kinetics in the first stage of a two-stage solution regeneration scheme has shown that the optimum conditions are obtained at a high boiling rate with the greatest possible excess of $KHCO_3$ and KHS content in the solution.

LITERATURE CITED

[1] I. G. Plit, J. Appl. Chem., 29, 11, 1644 (1956).*

Received July 3, 1955

* Original Russian pagination. See C. B. Translation.

ISOLATION OF CAMPHENE FROM SOLUTIONS IN PINENE WITH RETENTION OF ITS OPTICAL ACTIVITY

G. A. Rudakov and M. M. Shestaeva

Central Scientific Research Institute for Wood Chemistry

In investigations of mixtures of terpenes it is often necessary to determine the optical rotation of their components. It then becomes necessary to isolate from the mixture certain amounts of the individual terpenes in a state of high purity by a method which excludes their racemization.

The problem is usually successfully solved by fractional distillation over sufficiently efficient columns, but in the presence of terpenes with very similar boiling points it is often more convenient to solve the problem by other methods, specific for each individual case.

Unfortunately, such methods are available for far from all mixtures of terpenes with similar boiling points which are found in practice. In particular, no reliable and relatively simple methods for isolation of pure camphene from solutions in pinene, with retention of its optical activity, have been described in the literature. However, pinene and camphene occur together in many natural products and in products obtained in artificial treatments of terpenes, while their boiling points (the b.p. of pinene is 155.9° at 756 mm [1], and the b.p. of camphene is 158.5° at 748 mm [2]) are so close together that their separation with the use of the columns generally used in analytical work, with 25-30 theoretical plates (TP) involves considerable difficulties. Usually not less than two consecutive distillations have to be performed to obtain pure camphene, and because of the low yields of camphene due to the formation of intermediate fractions, large amounts of the original material, often not available, must be used.

In addition to fractional distillation, freezing [3, 4] has been proposed as a method for isolation of camphene from solutions in pinene, but this process is complicated by the existence of a eutectic mixture containing 30% camphene [5] and, according to our observations, by formation of mixed crystals.

Other physical methods which have been proposed for the separation of pinene and camphene (extraction by oxygen-containing solvents [6], and diffusion through porous membranes [7]) have not been widely adopted, probably because of their complexity.

Chemical methods for the isolation of camphene are very few. The Aschan method, based on isomerization of pinene into monocyclic terpenes by the action of 60% sulfuric acid [8] followed by isolation of camphene by fractional distillation, is not suitable for the present purpose, as 60% sulfuric acid racemizes camphene. The method of Balbiano and Paolini [9], which consists of selective oxidation of pinene by mercuric acetate solutions [2], was successfully used by Kondakov [10] for isolation of camphene from solution in pinene, but it was not clear whether camphene was racemized during this method of its isolation.

The purpose of the present investigation was the selection or special development of a relatively simple method for the isolation of pure camphene from solutions in pinene, with retention of its optical activity, with the use of relatively small amounts of starting material.

For this purpose comparative tests were performed on fractional distillation, the Balbiano and Paolini method, a method based on selective oxidation of pinene by alkaline permanganate solution, and a method for the isolation of camphene in the form of a so-called canal compound with thiourea. The basis for the method of selective oxidation of pinene by alkaline permanganate solution was our observation that pinene

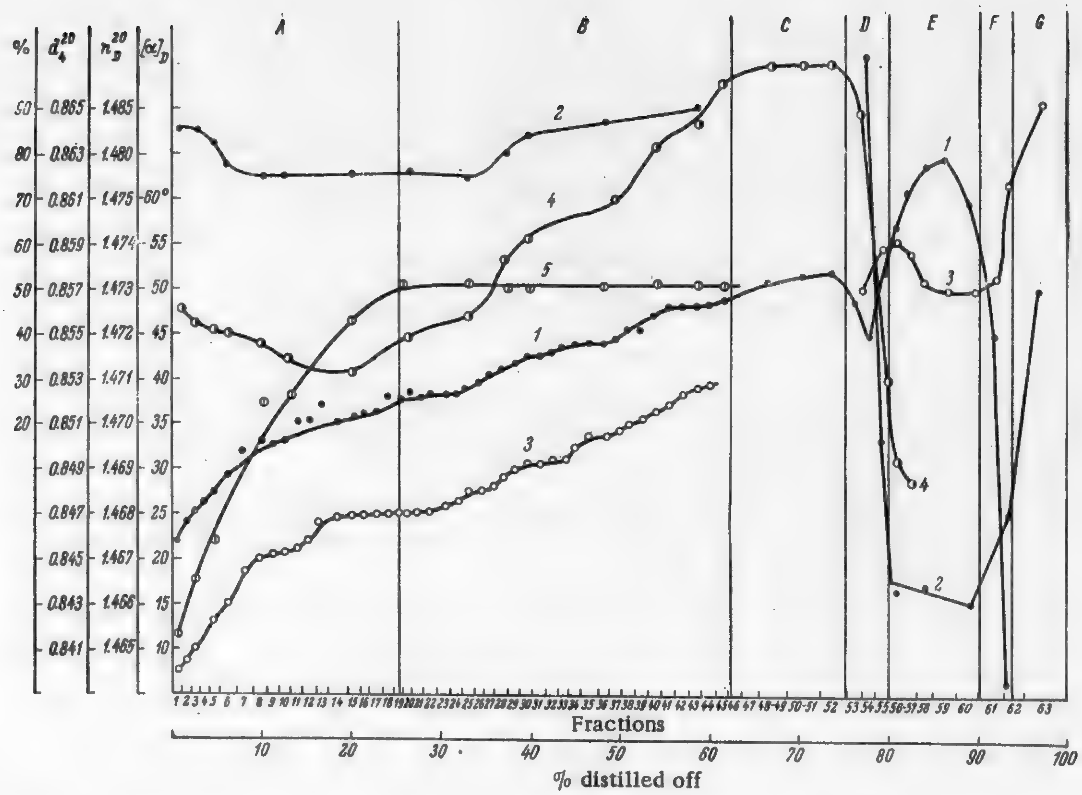

Fig. 1. Isolation of camphene from the products of catalytic isomerization of α-pinene containing unreacted pinene, with a column of 30 TP. 1) $[\alpha]_D$, 2) d_4^{20}, 3) n_D^{20}, 4) camphene + tricyclene + + fenchenes (in %) [12], 5) $[\alpha]_D$ for the sum of camphene + tricyclene + fenchenes (in pinene), calculated from the Biot formula [12]. A) α-pinene + tricyclene + camphene + fenchenes, B) α-pinene + + camphene, C) crude camphene (fractions 48-52, f.p. + 39°) D) camphene + d-β-pinene [13], E) limonene + α-terpinene, F) limonene + γ-terpinene, G) terpinolene.

and camphene are oxidized at appreciably different rates by this reagent, and the isolation of camphene in the form of a canal compound with thiourea was based on the work of Schlenk [11], who reported the formation of a crystalline compound of camphene with thiourea.

EXPERIMENTAL

Starting materials. The starting material was the isomerization product of α-pinene (n_D^{20} 1.4654, d_4^{20} 0.8580, $[\alpha]_D$ + 30.3°) obtained by heating the latter with titanic acid [12]. It contained 31% α-pinene, 45% camphene and tricyclene, about 2% fenchenes (including cyclofenchene) and 22% monocyclic terpenes. 2600 g of the isomerization product was subjected to vacuum distillation at 80 mm over a column of about 25-30 TP. The distillation results are shown in Fig. 1. The yield of crude camphene with f.p. + 39° was 22% of the original amount (fractions 48-52).

For the subsequent isolation of pure camphene by fractional distillation, crude camphene fractions 48-52 with f.p. + 39° were used and for isolation of camphene by chemical methods, a mixture of fractions 21-43 (group B) was used, containing 46% pinene and 54% camphene, n_D^{20} 1.4696, d_4^{20} 0.8659, $[\alpha]_D$ + 43.1°.

Fractional distillation of pure camphene was carried out at p = 80 mm Hg over a column of about 30 TP. 15% camphene (of the total charge) was isolated with f.p. +47.8°, which may be considered to be pure [14]. Thus by two consecutive rectifications it was possible to isolate 3.3% of the pure camphene present in the original isomerization product (in the calculation the small amount of tricyclene was reckoned as camphene), while all the remaining camphene was spread over the intermediate fractions. The results in isolation of camphene by the fractional distillation method are given in the table.

Results Obtained in the Isolation of Camphene from Products Containing Pinene

Experiment number *	Method of isolating camphene	Amount of starting material used (in g)	Yield %	Properties of camphene obtained			
				Freezing point	n_D^{54}	d_4^{54}	$[\alpha]_D$ **
1	Single fractional distillation	2600	22	+39°	1.4555	0.8388	+52.7°
2	Twofold fractional distillation	2600	3.3	+47.8	1.4560	0.8408	+55.5
3	Method of Balbiano & Paolini	60	27	+49	1.4562	0.8421	+55.4
4	Threefold precipation with thiourea	50	45	+41.5	1.4554	0.8404	+52.2
5	Sixfold precipation with thiourea	50	17	+48	1.4560	0.8409	+53.6
6	Selective oxidation by $KMnO_4$	120	90	+32	1.4552	—	+52.2
7	Ditto, with subsequent rectification	120	11	+47.3	1.4558	0.8428	+54.8
8	Ditto, with subsequent rectifications and corrections	120	11	+47.8	—	—	+55.2

* The starting material for Experiments 1 and 2 was the isomerization product obtained from pinene by heating with titanic acid, containing 31% pinene and 45% camphene; the starting material for Experiments 3-8 was a 54% solution of camphene in pinene.
** In benzene, c ~ 35.

Isolation of camphene by the Balbiano and Paolini method. To 60 g of a solution of camphene in pinene (fractions 21-43), a solution of 420 g of mercuric acetate in 1700 ml water was added. The mixture was mechanically shaken for two weeks and then kept for 6 months exposed to sunlight. The white curdy precipitate, with a slight gray tinge owing to reduction of mercury salts, was filtered off, washed, and suspended in 1 liter of 2% HCl. The suspension was saturated with H_2S, and NaOH was then added to an alkaline reaction. The liberated camphene was distilled in steam and, for final purification, distilled from a Favorsky flask. The yields and physical constants of the camphene obtained are given in the table.

Isolation of camphene in the form of a compound with thiourea. Experiments carried out in the conditions described by Schlenk [11] did not give satisfactory results: the camphene yield was low, and the separation was not complete enough. The following method was therefore used for isolation of camphene.

To 50 g of camphene solution in pinene (fractions 21-43), 130 g methanol and 120 g thiourea were added, and the reaction mixture was then heated under reflux. A completely homogeneous solution could not be obtained; the liquid separated out into two layers. The precipitate deposited on cooling to −10° was separated off by suction, dissolved on warming in 130 g methanol, and again precipitated by cooling. After the third freezing the canal compound was decomposed by water. The resultant camphene was distilled in steam. As it was found to be insufficiently pure, 15 g methanol and 15 g thiourea were added to 12.8 g camphene and three consecutive crystallizations were again performed. The properties and yields of the camphene obtained are given in the table. The data show that the resultant camphene still contained small amounts of impurities. The final purification of camphene in this case should probably be effected by fractional distillation.

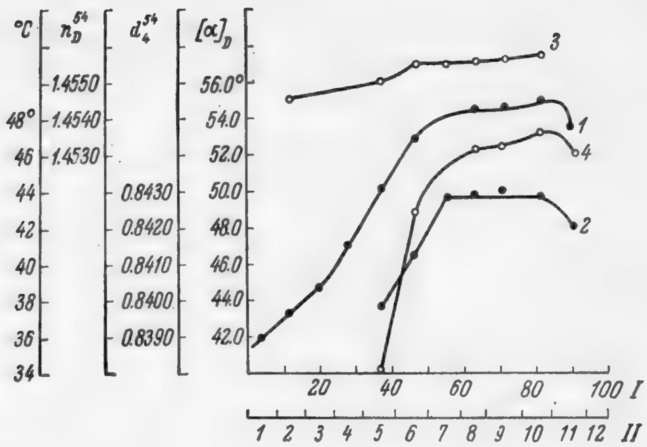

Fig. 2. Fractional distillation of camphene obtained by selective oxidation of a solution of camphene in pinene by alkaline permanganate solution. I) Amount distilled off (in %), II) Fraction numbers. 1) $[\alpha]_D$ (in benzene, c ~ 35); 2) d_4^{54}, 3) n_D^{54}, 4) freezing point.

Isolation of camphene by selective oxidation of the solvent pinene by permanganate. Preliminary experiments showed that pinene is oxidized almost exclusively on oxidation of a solution of camphene in pinene by 8% alkaline permangante solution at temperatures not exceeding 30°. At a definite stage in the reaction camphene separates out in the form of crystals still containing a certain amount of pinene. After this point the camphene begins to be oxidized fairly rapidly and therefore the reaction should be stopped and the final purification of the camphene carried out with the aid of an efficient fractionating column.

120 g of the original solution of camphene in pinene was oxidized by potassium permangante in the conditions described. Crude camphene was distilled in steam from the reaction products and then subjected to fractional distillation over a column of approximately 50 TP. The distillation results are given in Fig. 2.

The purest camphene was obtained from the 10th fraction: f.p. 47.3° and $[\alpha]_D$ + 54.8° (in benzene, c = 35). The specific rotation of this camphene is 1.2% lower than the specific rotation of camphene obtained by fractional distillation of the isomerization product, which can be attributed to the presence of small amounts of impurities, as indicated by its somewhat lower freezing point. Extrapolation of the optical rotation to the value corresponding to f.p. +47.8°, the freezing point of camphene obtained by fractional distillation of the isomerization product (Fig. 2), gives $[\alpha]_D$ + 55.2°, which practically coincides with $[\alpha]_D$ for camphene obtained by fractional distillation of the isomerization product. The properties and yields of camphene obtained by this method are given in the Table.

SUMMARY

Pure camphene can be isolated from solutions in pinene with complete retention of its optical activity by chemical methods: the method of Balbiano and Paolini, a method based on selective oxidation of pinene by permangante, and isolation of camphene in the form of a canal compound with thiourea. The Balbiano and Paolini method yields pure camphene directly, but is very lengthy; the other two methods involve subsequent purification of resultant camphene by a single fractional distillation, but are nevertheless more rapid.

All three methods can be successfully used with a much lower consumption of material than the isolation of camphene by fractional distillation of the original solutions of camphene in pinene over columns with about 30 TP.

LITERATURE CITED

[1] J. E. Hawkins, G. T. Armstrong, J. Am. Chem. Soc., 76, 3756 (1954).

[2] G. A. Rudakov, S. Ya. Korotov, J. Appl. Chem. 10, 312 (1937); M. D. Tilicheev, Physicochemical Properties of Individual Hydrocarbons, State United Sci-Tech. Press, 350 (1952).

[3] S. S. Nametkin, L. G. Bogacheva, J. Russ. Phys. Chem. Soc., 62, 1335 (1930).

[4] G. Austerweil, L. Peufaillit, German Patent 402995 (1922); Zbl., I, 299 (1925).*

[5] G. Austerweil, C. r., 178, 1174 (1924).**

[6] G. Austerweil, L. Peufaillit, German Patent 400253 (1922); Zbl. I, 299 (1925).

[7] G. Austerweil, L. Peufaillit, German Patent 428860 (1922); Zbl., II, 1100 (1926).

[8] O. Aschan Naphtenverbindungen, Terpene und Campheraten. Berlin, 203 (1929).

[9] L. Balbiano, V. Paolini, Ber., 35, 2995 (1902); 36, 3576 (1903).

[10] I. L. Kondakov, Parf. mod., 19, 212 (1926); Zbl., 1, 193 (1927).

[11] W. Schlenk, Lieb. Ann., 573, 142 (1951).

[12] G. A. Rudakov, Z. S. Khomenko, M. M. Shestayeva, J. Gen. Chem., 24, 549 (1954).***

[13] G. A. Rudakov, M. M. Shestayeva, J. Gen. Chem., 25, 627 (1955).***

[14] G. A. Rudakov, M. M. Shestayeva, J. Gen. Chem., 26, 2362 (1956).***

Received November 21, 1955

* Zbl. = Chem. Zentr.

** C.r. = Compt. rend.

*** Original Russian pagination. See C. B. Translation.

HIGH-TEMPERATURE THERMAL DECOMPOSITION OF PEAT DUST IN A CURRENT OF STEAM

V.G.Kashirsky, N.B.Lobacheva, and A.R.Yakoreva

The development of peat chemistry and chemical technology makes this fuel a very important form of chemical raw material.

The use of peat fuel for the production of high-calorific domestic gas and of gas mixtures for industrial organic synthesis has become of considerable interest.

Ivanovsky [1] has demonstrated the possibility of obtaining high-calorific gas by coking of peat together with cracking of pitch. Bogdanov [2] has described the potentialities of the use of peat coke in water gas generators for the production of synthesis gas mixtures. Kotkovsky and Markevich [3] have shown that gaseous products of the heat treatment and gasification of coke are suitable for ammonia synthesis.

The development of simple and efficient methods of gas production from cut peat, which is the cheapest to obtain, is of great importance. One such method is the thermal decomposition of the fuel, previously ground to a dustlike state, in conditions which ensure a high yield of gaseous pyrolysis products.

Chukhanov [4], and also Kashurichev and Chukhanov [5] report that upon rapid heating of the organic matter of peat its decomposition occurs mainly at the final temperature of the process, with formation of simple compounds, which are the most stable at that temperature. The high-temperature thermal conversion of dustlike and finely granular peat can be efficiently carried out in flow systems in reactors with combined transfer of heat to the fuel particles both from outside through the reactor walls, and from previously superheated conveying gas or steam.

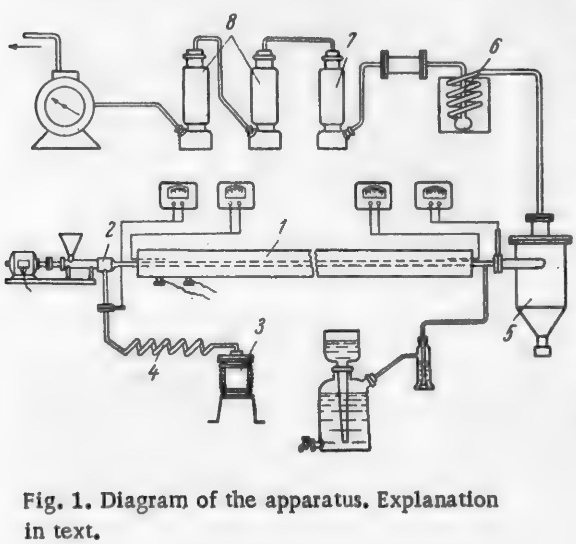

Fig. 1. Diagram of the apparatus. Explanation in text.

Wicke and Fetting [6] and other workers [7,8] who studied heat transfer between a hot surface and a turbulent dust—gas stream established that the coefficient of heat transfer from the wall to the stream can reach values of 200 to 1300 kcal / m^2 · hour· deg. Thus, the transfer of heat from the heating gases to the dust–gas stream is much more rapid than the transfer of heat into a layer of fuel lumps, so that high speed heating can be used for the thermal conversion of dustlike fuel.

We have studied the thermal decomposition of lowland peat dust under laboratory conditions, in a current of steam in an externally heated reactor. The composition and calorific value of this peat are given below.

W	Ash	C	H	N	S	Q (kcal/kg)
15.56	10.66	51.61	4.82	3.41	0.3	4061.9

The main part of the laboratory apparatus, shown diagrammatically in Figure 1, is a reaction tube 1, 3 meters long and 15 mm internal diameter. The peat dust was driven through the reactor by a stream of superheated steam, entering the mixer 2 from the steam generator 3 through the superheater 4.

The reaction tube is followed successively by a cyclone dust precipitator 5, a coil condenser 6, a tower 7 containing $CaCl_2$, adsorbers 8 containing active carbon for trapping gasoline, and a gas flow meter.

The peat dust feed rate was 10-12 g/minute in all the experiments, with a steam flow rate of 6-7 g/minute. The steam was superheated to 440-460° before the dust feed device. The experiments were performed in series of 3-4 experiments each, with reactor wall temperatures of 700, 800, 900, and 1000°.

The time spent by the fuel particles in the reaction tube was measured in fractions of a second in all the experiments. The particles were heated in the reaction tube at a rate of hundreds of degrees per second, while the temperature of the dust—gas stream at the exit from the reaction tube reached 520, 600, 700, 780°, in each series of experiments.

After each series of experiments average samples of gas, coke, and unreacted steam condensate were taken and analyzed.

TABLE 1

Yield and Composition of Gas Formed in the Thermal Decomposition of Peat Dust

Reactor temperature (°C)	Stream temperature (°C)	Gas yield (in normal liters/g)		Gas composition (in volume %)							γ - (in g/normal liter)	Unsaturated compounds		
		Dry peat	Organic matter	H_2S	CO_2	C_mH_n	CO	H_2	C_nH_{2n+2}	N_2		Isobutylene	Butylene propylene	Ethylene
700	520	293	330	0.6	26.0	10.3	22.7	30.0	5.9	4.5	1.101	13.0	24.0	63.0
800	600	470	540	0.5	21.2	9.1	22.5	36.6	5.4	4.7	0.970	8.0	18.0	74.0
900	700	840	942	0.2	17.4	5.2	22.7	42.6	4.9	7.0	0.861	7.6	10.4	81.0
1000	780	1230	1375	0.14	16.2	2.2	22.3	49.4	3.7	6.06	0.775	—	6.0	94.0

The yield and composition of the pyrolysis gas are given in Table 1. Figure 2 shows the dependence of the absolute yields of the individual components of the gaseous mixture on the gasification temperature.

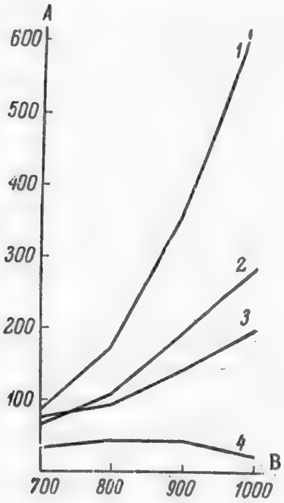

Fig. 2. Dynamics of the formation of the pyrolysis gas components. A) Yields of pyrolysis gas components (in normal liters/kg dry peat), B) reactor temperature (°C).
1) H_2; 2) CO; 3) CO_2; 4) $C_m H_n$.

Comparison of the results of our experiments with previously published data [1,9] shows that, in the temperature range studied, the gaseous products of pyrolysis of peat dust have higher contents of hydrogen, carbon monoxide, and unsaturated hydrocarbons, with lower contents of methane and carbon dioxide. The increase of the gas yield is due not only to a change in the mechanism of the thermal decomposition of the organic matter in the fuel particles and decomposition of pitch as the result of the rapid heating, but also to participation of steam in the gas formation processes.

Figure 2 shows that when the temperature of the dust—gas stream is above 700°, carbon of the coke particles is rapidly oxidized by steam with formation of hydrogen and carbon oxides. As a result of the vigorous reaction between superheated steam and the coke particles, the total content of free and bound hydrogen in the gas formed at a stream temperature of about 780° is 40% greater than the amount of hydrogen introduced into the reactor with the fuel.

The observed vigorous oxidation of dustlike coke by steam is caused by the highly developed contact surface, and also by the fact that, as a result of chemical degradation of the molecules of organic matter and the rupture of chemical bonds, the reformed carbon structure has the maximum degree of disorder [10], which increases the reactivity of the coke particles.

The highest absolute yield of gaseous olefins was found in the stream temperature range of 600-700°, when their weight content in the gas reached 8.1-13.9%. At stream temperatures above 700° about 1% of gasoline, calculated on the dry peat, was formed. The gasoline had d_4^{20} between 0.8626 and 0.8775, and n_D^{20} in the range 1.4980—1.5050. Aromatization of the gasoline was observed with increase of the decomposition temperature.

Table 2 shows the composition of the aqueous condensate collected in the receiver 6.

The high ammonia content in the aqueous condensate suggests the possibility of its industrial utilization. Increase of the decomposition temperature results in decomposition of the acids and phenols, and their contents in the condensate decrease.

The composition of the coke dust is given in Table 3.

Despite the increased ash content, the calorific power of the peat coke dust does not fall below 4000 kcal / kg in the conditions studied, so that it can be utilized as an effective fuel.

TABLE 2

Composition of Aqueous Condensate

Stream temperature (° C)	NH_3 (in g/liter)	Volatile phenols (in mg/liter)	Fatty acids, calculated as CH_3COOH (in mg/liter)	Oxidizability by $KMnO_4$ (in mg/liter)
520	12.85	2280	2968	5234
600	19.44	3040	2343	4342
700	34.58	2179	1770	2364
780	13.42	785	624	1277

TABLE 3

Composition (%) and Calorific Power of Peat Coke Dust

Reactor temperature (° C)	Stream temperature (° C)	Ash	C	H	S_{total}	Q (in kcal /kg)
700	520	23.30	59.35	2.82	0.42	5394
800	600	25.90	57.60	2.47	0.53	5149
900	700	33.46	50.73	1.71	1.00	4173
1000	780	43.38	46.39	1.33	1.22	3987

SUMMARY

An investigation of the thermal decomposition of peat dust in a stream of superheated steam in a stream temperature range of 520-780° showed that the yield and composition of the gas, and the composition of the peat coke and aqueous condensate, depend on the temperature conditions of the pyrolysis process. Laboratory investigations have demonstrated that thermal decomposition of peat dust in a current of steam, with high-speed heating of the particles, may be used for the production of gas for chemical purposes or for fuel.

LITERATURE CITED

[1] E.E.Ivanovsky, Peat Coking with Cracking of the Pitch, Ukrainian Sci.-Tech.Press, 106 (1935).

[2] N. N. Bogdanov, Proc. April Session, Acad. Sci. Belorussian SSR, 1945, Minsk (1947).

[3] A.P. Kotkovsky and S.V. Markevich, Bull. Acad. Sci. Belorussian SSR, 5, 123 (1954).

[4] Z.F. Chukhanov, Bull. Acad. Sci. USSR, Div. Tech. Sci., 8,7 (1954).

[5] A.P. Kashurichev, Z.F. Chukhanov, Proc. Acad. Sci. USSR, 101, 1, 115 (1955).

[6] E. Wicke, F. Fetting, Chemie Ingeneur Technik, 26, 6, 301 (1954).

[7] W.M. Dow, M. Iakob, Chem. Engng. Progr.,47, 42,637 (1951).

[8] M.Lewa, M. Grummer, Chem. Engng. Progr.,48, 6, 307 (1952).

[9] N.N.Bogdanov, Semicoking and Gasification of Peat, State Power Press, 48, 110, 113 (1947).

[10] V.I. Kasatochkin, Bull. Acad. Sci. USSR, Div. Tech. Sci., 10, 1401 (1953).

Received October 24, 1955.

JOURNAL OF APPLIED CHEMISTRY OF THE U.S.S.R. IN ENGLISH TRANSLATION

January, 1957

TABLE OF CONTENTS

TABLE OF CONTENTS (continued)

RUSSIAN AND GERMAN CRYSTALLOGRAPHY RESEARCH

IN COMPLETE ENGLISH TRANSLATION

THE GROWTH OF CRYSTALS—A Conference on the Growth of Crystals held by the Acad. Sciences, USSR, March, 1956, published in Russian June, 1957. Major Soviet contribution in this field. 43 important papers, 291 pages. Table of Contents on request.

Contents:

Introduction
I. General Questions
II. Theory
III. Experimental Research
IV. Growing of Single Crystals, Apparatus and Methods
V. Miscellaneous

only $15.00

SOVIET RESEARCH IN CRYSTALLOGRAPHY—Collection No. 5. Approx. 300–350 articles selected from all Russian chemical journals translated by Consultants Bureau, 1949–1955, comprising an estimated 1300 pages. To be published Feb. 1958. Single papers $7.50 each—Table of Contents on request. Price: $200.00

Contents—still tentative:

I. Structure determination, and structural change
II. Compound formation, and reaction studies in complex systems
III. Transformation, solubility, and phase diagrams
IV. Metals systems and their reactions
V. Experimental techniques and research methods
VI. Structure-sensitive properties
VII. Crystal growth and forms
VIII. General and theoretical papers

SPLITTING OF TERMS IN CRYSTALS, by Hans A. Bethe. The first publication in English of this important paper, originally published in German in 1929. Translated by Wendell Furry, who says of this work, "A classic in the field, by one of the world's most important theoretical physicists—of great interest to students of solid-state physics." **70 pages. $3.00**

All Consultants Bureau translations by *bilingual scientists.* Books are staple bound in durable paper covers; includes all diagrammatic and tabular material integral with the text; text is clearly reproduced by multilith process from IBM "cold type".

CONSULTANTS BUREAU, INC.

227 WEST 17th STREET, NEW YORK 11, N.Y.—U.S.A.

Telephone: ALgonquin 5-0713 • Cable Address: CONBUREAU, NEW YORK

Chemistry Collection No. 2

SOVIET RESEARCH IN

GLASS and CERAMICS

(1949-1955)

One hundred and forty six reports, in complete English translation, with all tabular material and diagrams integral with the text. Selection and Preface by W. G. Lawrence, Chmn., Dept. of Ceramic Research, State University of New York College of Ceramics at Alfred University.

The complete collection . . . $150.00

The one hundred and forty six reports included in this collection originally appeared in the Soviet Journals of General and Applied Chemistry and the Bulletin of the Academy of Sciences of the USSR, beginning with 1949. The collection comprises over 900 pages, more than 400,000 words of recent research on glass and ceramics by Soviet scientists, in complete English translation.

The Collection is divided into sections, which may be purchased separately, as follows:

Basic Science: (70 reports)	$ 90.00
Glass; glazes and enamels (32 reports)	40.00
Refractories (12 reports)	20.00
Cements, limes and plasters (28 reports)	35.00
Miscellaneous (4 reports)	7.50

CONSULTANTS BUREAU, INC.

227 WEST 17th STREET, NEW YORK 11, N. Y. — U.S.A.

Telephone: ALgonquin 5-0713 • Cable Address: CONBUREAU, NEW YORK